UNIVERSITY OF CALIFORNIA
RIVERSIDE

The Role of *LATERAL ORGAN FUSION1* (*LOF1*) in Shoot Architecture

A Dissertation submitted in partial satisfaction
of the requirements for the degree of

Doctor of Philosophy

in

Plant Biology

by

Elizabeth Maria Luscher

June 2020

Dissertation Committee:
Dr. Patricia Springer, Chairperson
Dr. Linda Walling
Dr. Jaimie Van Norman

The Dissertation of Elizabeth Maria Luscher is approved:

_____

_____

_____

Committee Chairperson

University of California, Riverside

Acknowledgements

Thank you to Dr. Patricia Springer for mentoring me for 7 years, providing guidance on my experiments, and teaching me about many aspects of plant development.

Thanks to all of my dissertation committee members – Dr. Patricia Springer, Dr. Linda Walling, and Dr. Jaimie Van Norman – for supporting me in my research and giving valuable feedback on dissertation. I would like to give a special thanks to Dr. Linda Walling for convincing me to come back to graduate school and continue my Ph.D. I thank Dr. Jaimie Van Norman for use of her laboratory's Leica SP8 microscope and for helping me to learn to use the microscope. I also thank Jess Toth and Jason Goff from the Van Norman laboratory for helping me to learn to use the microscope and answering when I had questions.

Thank you to Laura McGeehan for always checking up on me and monitoring my progress as a student.

I would like to thank Dr. Michael Prigge for the *phb-13 er-2* and *phb-13 phv-11 cna-2 er-2* seeds, and I would like to thank Dr. Miltos Tsiantis for the pEGAD *pPHB:PHB:GFP* plasmid.

Thank you to Taulima Nua and Zoe Yeoh for performing many of the RT-PCRs, T-DNA insertion site sequencing, and phenotyping of the mutants in Chapter 1. I also thank Taulima Nua performing many of the crosses required for Chapter 1 and Chapter 3.

Thank you to all members of the Springer lab both past and present. Our conversations about science were invaluable to designing and troubleshooting the experiments in my dissertation.

Thank you to my grandmother, Clara Ellert, for always talking to me on the phone and encouraging me throughout my time in graduate school. Thank you to my grandfather, Dr. Frederick Ellert, for teaching me the value of education from a young age. Thank you to both of my grandfathers for making my undergraduate education at Ohio State University possible.

Thank you to my mom, Judith Luscher, for always being proud of me and willing to talk whenever I needed it.

Thank you to my dad, Dr. Anthony Luscher, for supporting me throughout graduate school, always encouraging me to be the best that I can be and having high expectations.

Thank you to Jarrod West for supporting me in every way possible for many years and believing in me.

Dedication

This dissertation is dedicated to the following people:

Clara Ellert & Dr. Frederick Ellert

Maria Luscher & Frederick Luscher

Dr. Biao Ding

ABSTRACT OF THE DISSERTATION

The Role of *LATERAL ORGAN FUSION1* (*LOF1*) in Shoot Architecture

by

Elizabeth Maria Luscher

Doctor of Philosophy, Graduate Program in Plant Biology
University of California, Riverside, June 2020
Dr. Patricia Springer, Chairperson

Lateral organs form from the shoot apical meristem (SAM) and are separated from the SAM by the boundary region, an area of restricted growth. In *Arabidopsis*, the MYB-domain transcription factor LATERAL ORGAN FUSION1 (LOF1) is expressed in organ boundaries. LOF1 functions in organ separation and meristem formation. The focus of this dissertation is to characterize the molecular function of *LOF1*. In Chapter 1, proteins that interact with LOF1 were identified. These include transcription factors with documented roles in a variety of plant processes, including development, the shade-avoidance response, plastid DNA repair, and other environmental responses. Because many of the LOF1 interactors identified were localized to either the plastid or mitochondria and were involved in response to abiotic stress, we investigated the subcellular localization of LOF1-GFP in response to abiotic stress conditions in the root in Chapter 2. Simulated drought, exposure to high light conditions, and the presence of reactive oxygen species (ROS) did not change the subcellular localization of LOF1-GFP. In Chapter 3, a dominant mutation in PHABULOSA (PHB), a transcription factor

involved in meristem regulation and leaf polarity, was found to be a genetic suppressor of the *lof1-1* mutation. Our results suggest PHB and LOF1 do not regulate one another at the transcriptional level. Observations of plant architecture in *lof1-1* and *phb-13* loss-of-function mutants and transgenic plants expressing *PHB* under its native promoter revealed complex interactions between LOF1 and PHB to promote accessory bud formation and overall plant architecture.

Table of Contents

List of Figures

List of Tables

Introduction

Shoot apical meristem (SAM) Structure and Function

The shoot apical meristem (SAM), originally discovered by Kaspar Wolff in 1759 (Cutter, 1965), is a domed structure located near the apex of the plant. The SAM contains a population of stem cells and will give rise to all above ground organs of the plant. The root apical meristem (RAM), located underground, contains stem cells that will form the primary root tissues (Weigel and Jürgens, 2002). In contrast to animals, plants develop the majority of their organs post-embryonically (Walbot, 1985; Steeves and Sussex, 1989), meaning plants are continually generating new organs.

Organ primordia first develop as small bumps at the periphery of the SAM. Stem cells must divide in order to replenish cells daughter cells that are incorporated into organ primordia. The SAM consists of several zones important for development (Evans and Barton, 2002). Stem cells are located at the top of the dome in a region called the central zone, which consists of approximately 35-40 cells in *Arabidopsis thaliana*. The progeny of the stem cells are displaced outwards into the peripheral zone, which surrounds the central zone, and continue dividing. Stem cell progeny also divide and are displaced downwards into rib meristem, located underneath the central zone (Soyars *et al.*, 2016).

The SAM is comprised of distinct cell layers (Satina *et al.*, 1940; Szymkowiak and Sussex, 1996). The tunica, the outer layer or layers of the meristem, covers the inner cells of the corpus. In *Arabidopsis*, the epidermal layer (L1) and subepidermal layer (L2) make up the tunica and are maintained by anticlinal cell divisions. The L3 layer, which makes up the corpus, consists of cells interior to the L2. Cells of the L3 undergo divisions

in various different orientations (Gaillochet *et al.*, 2015; Truskina and Vernoux, 2018). Organ primordia arise from all three layers of the meristem (L1, L2, and L3). In differentiating organs, the L1 layer gives rise to cells that will become the epidermis, the L2 layer gives rise to the subepidermal layers of organs, and the L3 layer gives rise to interior portions of organs and stems, such as vasculature and pith (Satina and Blakeslee, 1941; Medford, 1992). In monocots, there are only two layers – L1 (tunica) and L2 (corpus). The L1 layer forms the epidermis and the L2 layer forms all internal tissues (Wang *et al.*, 2018). Because organ primordia are derived from all meristematic cell layers in monocots and dicots, these layers must communicate effectively with one another throughout organ development.

A negative feedback loop functions to control and maintain the population of stem cells in the SAM. WUSCHEL (WUS), a homeobox transcription factor, functions non-cell autonomously to positively regulate stem cell identity (Laux *et al.*, 1996). WUS accomplishes this by activating *CLAVATA3* (*CLV3*) expression in the central zone. CLV3 is a small ligand, which binds to its receptor CLAVATA1 (CLV1) (Clark *et al.*, 1993; Kayes and Clark, 1998; Otsuga *et al.*, 2001). CLV1/CLV3 action results in repression of *WUS* expression. Therefore, loss-of-function *wus* and *clv3* exhibit opposite phenotypes – failure to maintain the meristem and enlargement of the meristem, respectively. This maintenance of stem cells lends to the ability of plants to have indeterminate meristems for long periods of time (Fletcher *et al.*, 1999; Perales and Reddy, 2012).

SAM identity is determined by several genetic factors. This was first discovered in a mutant that ectopically expresses *KNOTTED1* (*KN1*) in maize, resulting in knot-like

structures on leaf blades, consisting of meristem-like tissues (Freeling and Hake, 1985; Vollbrecht *et al.*, 1991). When the wild-type expression pattern of *KNOTTED1* was observed, it was revealed to be expressed in the meristem but excluded from the lateral organs (Smith *et al.*, 1992). In certain genetic backgrounds, loss-of-function mutants of *kn1* do not establish or maintain a meristem (Vollbrecht *et al.*, 2000). Taken together, these observations suggest that *KN1* functions in the meristem to prevent meristematic cells from differentiating.

KNOX (KNOTTED-LIKE HOMEBOX) family proteins in *Arabidopsis thaliana* are related to KN1. The most well studied KNOX family gene is *SHOOTMERISTEMLESS* (*STM*). Similar to *kn1* mutants, *stm* loss-of-function mutants also fail to maintain their meristems due to meristematic cells differentiating without being replenished (Barton and Poethig, 1993; Long *et al.*, 1996). Another KNOX family gene, *KNOTTED-LIKE FROM Arabidopsis Thaliana 1* (*KNAT1*), was found to have a similar phenotype to *KN1* in maize when ectopically overexpressed in *Arabidopsis* leaves (Lincoln *et al.*, 1994; Chuck *et al.*, 1996). *KNAT1* was later found to correspond to *BREVIPEDICELLUS* (*BP*), which has functions in regulating shoot architecture (Douglas *et al.*, 2002; Venglat *et al.*, 2002).

ASYMMETRIC LEAVES1 (AS1), a MYB domain containing protein, and ASYMMETRIC LEAVES2 (AS2), an LBD- (LATERAL ORGAN BOUNDARIES DOMAIN) containing protein are expressed in organ primordia (Byrne *et al.*, 2000; Semiarti *et al.*, 2001). In the developing primordia, AS1, AS2, and HIRA, a chromatin remodeling factor, form a complex to restrict the expression of *KNOX* genes (Lin *et al.*,

2003; Phelps-Durr *et al.*, 2005; Guo *et al.*, 2008). In contrast, in the SAM where *STM* and other *KNOX* genes are expressed, *AS1* is negatively regulated by STM, allowing for *KNOX* gene expression (Byrne *et al.*, 2002; Guo *et al.*, 2008). Therefore, genes expressed in the meristem and genes expressed in the developing primordia act antagonistically to regulate one another (Rast and Simon, 2008).

The notion that *AS1* and *AS2* have a role in primordia development is not solely based on gene expression pattern data. *as1* and *as2* loss-of-function mutants are characterized by lobed and irregularly shaped leaves with aberrant outgrowths along the petiole (Semiarti *et al.*, 2001; Byrne *et al.*, 2002; Machida *et al.*, 2015). *AS1* in *Arabidopsis* is the ortholog of *Rough sheath2* (*Rs2*) in maize, and *Arabidopsis AS2* is the ortholog of *Indeterminate gametophyte1* (*Ig1*) in maize (Schneeberger *et al.*, 1998; Evans, 2007). *Rs2* loss-of-function mutants have twisted leaves with an uneven surface, while *Ig1* mutants have been reported to contain leaves with irregular flaps of tissue on the leaf surface and distortion of some leaf tissues (Schneeberger *et al.*, 1998; Evans, 2007). These data indicate that the function of *Arabidopsis AS1* and *AS1* orthologs in maize are at least partially conserved in leaf primordia development.

Boundary Region Features and Roles

The boundary region is located between the SAM and the developing primordia. Cells in the boundary region are smaller and divide less frequently than surrounding cells as shown by several different studies. Control of entry into and exit from the cell cycle is tightly regulated in both plants and animals (Edgar and Lehner, 1996). Level of G-cyclins

in animals helps control entry into the cell cycle. Plant D-cyclins were found to be similar to animal G-cyclins (Soni *et al.*, 1995; Meijer and Murray, 2000). In *Antirrhinum* meristems, it was found that *cyclin D3b* expression was not present in a zone at the base of floral organ primordia near the stem. The authors believe this could be a developmental boundary to separate the floral organs from the stem (Gaudin *et al.*, 2000). The decrease of *cyclin D3b* expression in the boundary region suggests that fewer cells in this region are entering into the cell cycle, indicating that this is an area of few cell divisions. To examine cell divisions in the tomato apex, samples were treated with colchicine to arrest cells in mitosis, allowing cell divisions in the meristem, boundary, and developing primordia to be quantified over time (Hussey, 1971). This experiment revealed that there were fewer cell divisions in the boundary region than in either the meristem or primordia. In addition, the cells in the boundary region also had smaller cell volume, consistent with the boundary being a region of limited growth. The overexpression of boundary-specific transcription factors has resulted in overall smaller plants (Shuai *et al.*, 2002; Lee *et al.*, 2009), which suggests that boundary genes function to limit growth. As the plant develops, boundary regions are maintained, such that they become areas in the plant body where organs meet.

A primary function of the boundary region is to physically separate the developing primordia from the meristematic stem cells. Without proper boundary formation, the organs remain attached, resulting in a fusion. In addition, some boundary regions play an important role in plant architecture. One such region is the paraclade junction. The primary inflorescence stem gives rise to axillary branches. A single leaf –

termed the cauline leaf – subtends each axillary branch. In between the cauline leaf and axillary branch is the accessory bud, which functions to grow out into a branch if the axillary branch is damaged or the tip of the inflorescence is removed. The area where the primary inflorescence, axillary branch, and cauline leaf meet is called the paraclade junction. The pedicel-stem junction is another example of a boundary region within the plant body.

There is some evidence that boundaries are needed for meristem formation. Loss-of-function mutants of boundary genes sometimes result in loss of meristem maintenance, impacting either the SAM, axillary, or accessory meristems (Aida *et al.*, 1997; Greb *et al.*, 2003; Lee *et al.*, 2009). Axillary meristems form in the axil of a leaf and gives rise to an bud that has potential to form an axillary shoot (Wang *et al.*, 2018). In *Arabidopsis*, the axillary bud in the cauline-leaf axil grows out into the axillary branch. Accessory meristems form later in development. Accessory meristems are defined as groups of meristems subtended by the same leaf (Bell, 1991). *Arabidopsis* plants are thought to form one accessory bud per paraclade junction in the majority of paraclade junctions. On occasion, a paraclade junction will fail to form an accessory bud (Raman *et al.*, 2008; Yang *et al.*, 2012; Wang *et al.*, 2014; Shi *et al.*, 2016). However, there have been documented cases where most paraclade junctions on each individual plant do not form accessory buds (Stirnberg *et al.*, 2002). This suggests the existence of an environmental component to accessory bud formation.

Boundary Genes

1. *CUP-SHAPED COTYLEDON* (*CUC*) genes encode a family of three NAC [NO APICAL MERISTEM (NAM), ATAF, CUC] transcription factors that are expressed in the boundary beginning during embryo development, where they are thought to activate *STM* expression (Aida *et al.*, 1997; Takada *et al.*, 2001). *cuc* single loss-of-function mutants have subtle phenotypes. However, double mutants have fused cotyledons, shaped much like a cup, for which the family is named (Aida *et al.*, 1999). *cuc* double mutants with this phenotype also do not have SAM activity after embryogenesis, and no true leaves are formed (Aida *et al.*, 1997; Hibara *et al.*, 2006). This suggests that *CUC* genes function in organ separation and meristem maintenance.

mir164 is a microRNA that post-transcriptionally regulates *CUC* genes. Overexpression of mir164 leads to lower levels of *CUC1* and *CUC2*, but does not reduce levels of *CUC3* (Vroeman *et al.*, 2003; Laufs *et al.*, 2004), indicating that *mir164* may regulate two of the three *CUC* family members. Plants overexpressing *mir164* have fused cotyledons and petioles, much like double loss-of-function *cuc* mutants (Laufs *et al.*, 2004). Expressing a *miR164*-resistant version of *CUC1* under the *CUC1* promoter caused alterations in embryonic development, reduction in number of leaf petioles, cotyledon orientation defects, misshapen rosette leaves, and change in number of floral organs (Mallory *et al.*, 2004). The post-transcriptional regulation of *CUC* genes by *mir164* indicates that precise control of *CUC* gene expression levels and patterns are important for development.

Orthologs of *CUC* genes have been reported in multiple plant species, with many demonstrated to have similar functions. In snapdragon (*Antirrhinum majus)*, a mutation in the gene *CUPULIFORMIS* (*CUP*) leads to the dramatic phenotype of fusions in almost all above ground organs, including leaves, stems, cotyledons, and floral organs during embryonic, vegetative, and reproductive development (Weir *et al.*, 2004; Rebocho *et al.*, 2017). *cup* mutants typically lack branch formation in the leaf axils, suggesting that *cup* mutants may have a defect in axillary meristem formation or outgrowth, although the specific cause for lack of branches has not been investigated [suggested in (Hibara *et al.*, 2006)]. Mutations in *NO APICAL MERISTEM* (*NAM*) in *Petunia* led to fusion of cotyledons and some floral organs. There were also severe defects in the primary apical meristem (Souer *et al.*, 1996). Co-suppression of *NAM* and its homologs *NAM HOMOLOG-1* (*NH-1*) and *NAM HOMOLOG-3* (*NH-3*) resulted in fusions in lateral organs during vegetative development (Souer *et al.*, 1998). Plants lacking a functional copy of *GOBLET* (*GOB*) in tomato (*Solanum lycopersicum*) terminate after producing two fused cotyledons, but occasionally they recover and produce leaves that are simpler than wild-type tomato leaves (Brand *et al.*, 2007). Plants containing a *mir164*-resistant version of *GOB* (*Gob4-d*), in which *GOB* contains a mutation that does not allow for complementary pairing with *miR164*, have higher degrees of leaf lobing and secondary leaflet fusions, resulting in fewer leaflets. Tomato plants with overexpression of *miR164* lack secondary leaflets (Berger *et al.*, 2009), which suggests that *GOB* is involved in leaf complexity in tomato and that *miR164* regulation of *CUC/NAM* is conserved. In the cases of *Arabidopsis*, snapdragon, *Petunia*, and tomato, *CUC*/*NAM* genes were expressed in all

boundaries between organ primordia and meristems from early embryogenesis to floral development (Cheng *et al.*, 2012). These studies confirm that *CUC*/*NAM* genes play an important role in organ separation and primary meristem formation and exhibit some level of functional redundancy among family members.

2. *LATERAL SUPPRESSOR* (*LAS*) is boundary expressed and encodes a GRAS-domain transcription factor in *Arabidopsis* (Greb *et al.*, 2003). *LAS* is expressed in developing leaf primordia, close to the stem. This marks the region where an axillary meristem will form. *las* mutants fail to form axillary meristems in leaf axils during vegetative development and have axillary shoots fused to the primary stem (Greb *et al.*, 2003). Formation of axillary buds during reproductive development in *las* mutant plants is unperturbed, indicating *LAS* functions in axillary meristem formation during vegetative development. The *LAS* ortholog in tomato, *LATERAL SUPRESSOR* (*LS*), appears to have a similar function, where plants without functional *LS* do not form axillary meristems (Schumacher *et al.*, 1999). These data indicate that *LAS* functions in axillary meristem formation during vegetative development, and *LAS* function could be conserved.

3. REGULATOR OF AXILLARY MERISTEMS 1 (RAX1) is a R2R3 MYB domain transcription factor that regulates axillary meristem formation. The *Arabidopsis* genome encodes two other *RAX* homologs, *RAX2* and *RAX3*. All three genes function partially redundantly in axillary meristem formation. *RAX1* expression is detected first in the boundary between the meristem and initiating leaf primordia and marks the site of future axillary meristem formation (Keller *et al.*, 2006; Müller *et al.*, 2006). *rax1-3* loss-of-function single mutants had reduced numbers of axillary buds in rosette-leaf axils early in

development, when grown in short-day conditions. However, the number of axillary buds was increased towards the top of the rosette (Müller *et al.*, 2006). *rax1-2* loss-of-function mutants, isolated in the Ws-2 background, have a branching defect, where mutants produce fewer paraclades from both rosette- and cauline-leaf axils (Keller *et al.*, 2006). *rax-1D*, a dominant mutation in the Columbia background, was isolated though an activation tagging experiment. Effects were dosage dependent. *rax-1D*/+ plants were slightly dwarfed with compact leaves. They produced fewer rosette branches but more paraclade junctions compared to wild-type plants. *rax-1D* homozygous mutant plants were much smaller than *rax-1D*/+ plants, and the meristem terminated after producing six to ten leaves. However, after a period of time *rax-1D* homozygous plants recovered and were able to produce a few rosette branches (Keller *et al.*, 2006). Therefore, *RAX* genes positively regulate the formation of lateral meristems during the vegetative phase and early reproductive phase.

RAX1 is thought to act through *CUC* genes, as *cuc1 rax1* double loss-of-function mutants are enhanced in branching defects compared to single *rax1* mutants, and *CUC* transcripts are lower in the *rax1-2* loss-of-function mutant (Keller *et al.*, 2006). *RAX1* functions with the bHLH transcription factor REGULATOR OF AXILLARY MERISTEM FORMATION (ROX). *rax1 rox1* double mutants have enhanced *rax1* branching phenotypes, and expression patterns of *RAX1* and *ROX1* overlap (Yang *et al.*, 2012). *RAX1* is transcriptionally regulated by the WRKY transcription factor EXCESSIVE BRANCHES 1 (EXB1) in a positive manner. Plants with gain-of-function version of *EXB1*(*exb1-d*) have excessive axillary meristem initiations and appear bushy.

This phenotype is partially rescued by mutations in *RAX* genes (Guo *et al.*, 2015), indicating that *RAX* function is required for the *exb1-d* excess branching phenotype. *RAX1* may be involved in regulating axillary meristem formation through multiple pathways.

The *RAX* ortholog in tomato, *BLIND* (*BL*), was shown to be involved in the initiation of lateral meristems during vegetative and reproductive development. RNA interference (RNAi) was used to knock down levels of *BL*, which resulted in plants with reduced number of lateral shoots and flowers per inflorescence. Most plants also showed premature termination of the primary axis (Schmitz *et al.*, 2002). Therefore, *BL* in tomato is involved in the process of lateral meristem initiation, much like *RAX1* in *Arabidopsis*. This is indicative of a conserved function between *RAX1* in *Arabidopsis* and *BL* in tomato.

4. *JAGGED LATERAL ORGANS* (*JLO*) encodes an LBD-family transcription factor expressed in the boundary between the meristem and lateral organs at the embryo stage, root meristems, and boundaries between meristems and developing organs in the shoot (Borghi *et al.*, 2007; Rast and Simon, 2012). Loss of *JLO* function results in ectopic expression of *KNOX* genes. JLO acts in a trimeric protein complex with ASYMMETRIC LEAVES 2 (AS2; another LBD protein) and ASYMMETRIC LEAVES 1 (AS1) to suppress *BREVIPEDICELLUS* (*BP*) expression in lateral organs (Rast and Simon, 2012). In addition, JLO and AS2 also regulate *PINFORMED* (*PIN*) genes (*PIN1*, *PIN3*, *PIN4*, and *PIN7*) and auxin transport beginning in embryogenesis (Rast and Simon, 2012), thus demonstrating that *JLO* plays a role in auxin signaling. JLO was shown to be involved in

degrading the AUX/IAA protein BODENLOS (BDL). In *jlo* mutants, which have higher levels of BDL, root meristem development is compromised (Rast-Somssich *et al.*, 2017). JLO therefore sensitizes the root to auxin to allow for root meristematic development. Recently, the SUMO modification of JLO was found to have a role in controlling secondary cell wall formation (Liu *et al.*, 2019).

5. KNOTTED-like HOMEOBOX 6 (KNAT6) is a KNOTTED-like family member that is boundary expressed and contributes redundantly with STM in maintenance of the SAM and organ separation (Belles-Boix *et al.*, 2006). *knat6* mutants have no abnormal phenotypes. However, mutations in *knat6* enhance meristem maintenance defects caused by the weak *stm-2* allele. *knat6 stm-2* double mutant seedlings also have fusion between cotyledons and a severe meristem maintenance defect (Belles-Boix *et al.*, 2006). *CUC3* expression, which is normally seen in the boundaries of cotyledon margins and the boundary between the SAM and cotyledons (Vroeman *et al.*, 2003), is impacted in *stm-2 knat6-1* mutants. In the double mutant, *GUS* expression in the *CUC3* enhancer-trap line was very weak or absent, although expression was normal in *stm-2* and *knat6-1* single mutants (Belles-Boix *et al.*, 2006). These results reveal a role for *KNAT6* in meristem maintenance. Because the *knat6 stm-2* phenotype is similar to *cuc* double mutants, *KNAT6:GUS* activity was investigated in *cuc1 cuc2* mutants. *KNAT6* expression was reduced in *cuc1 cuc2* mutants, indicating *CUC1* and *CUC2* are redundant and required for *KNAT6* expression (Belles-Boix *et al.*, 2006). *KNAT6* contributes to SAM maintenance and organ separation though the *STM*/*CUC* pathway.

KNAT6 is involved with two additional genes, *PENNYWISE* (*PNY*) and *BREVIPEDICELLUS* (*BP*, also known as *KNAT1*), in inflorescence development (Ragni *et al.*, 2008). *PNY*, which encodes a member of the BELL/BELLRINGER/REPLUMLESS family of transcription factors, contributes to SAM maintenance with *STM* (Byrne *et al.*, 2003). *pny* mutants are characterized by defects in phyllotaxy, short stature, and loss of apical dominance (Roeder *et al.*, 2003; Smith and Hake, 2003; Bhatt *et al.*, 2004). *BP* plays a role in inflorescence growth, and *bp* loss-of-function mutants have reduced internode and petiole growth, downward bending siliques, and bending at nodes (Venglat *et al.*, 2002; Douglas *et al.*, 2002; Smith and Hake, 2003). A mutation in *knat6,* when combined either with a mutation in *bp* or *pny*, results in a partial rescue of the mutant phenotype, indicating *KNAT6* may function with *BP* and *PNY* in inflorescence development (Belles-Boix *et al.*, 2006; Ragni *et al.*, 2008). *KNAT2*, the most closely related family member to *KNAT6*, was found to be involved as well, performing a partially redundant role with *KNAT6. KNAT6* and *KNAT2* expression domains were enlarged in *bp pny* double mutants (Ragni *et al.*, 2008). Therefore, BP and PNY restrict *KNAT6* and *KNAT2* expression to promote inflorescence development. Later, it was found that BP interacts with chromatin remodeling factor BRAHMA (BRM) to regulate *KNAT6* and *KNAT2* levels (Zhao *et al.*, 2015). This suggests that a nucleosome or chromatin remodeling step is part of *KNAT6* and *KNAT2* genetic regulation.

6. *LATERAL ORGAN BOUNDARIES* (*LOB*) is the founding member of the *LATERAL ORGAN BOUNDARIES DOMAIN* (*LBD*) family of genes that are conserved in plants.

There are 43 LOB-domain containing proteins in total in *Arabidopsis* (Shuai *et al.*, 2002). *LOB* is expressed in organ boundaries at the base of all lateral organs formed by the SAM and also at the base of lateral roots (Shuai *et al.*, 2002). Loss-of-function *lob* mutants exhibit an organ fusion in the paraclade junction between the cauline leaf and the axillary branch (Bell *et al.*, 2012). This fusion may be the only *lob* loss-of-function phenotype because of LBD functional redundancy. Overexpression of *LOB* leads to plants with smaller rosette leaves and petioles (Shuai *et al.*, 2002). These phenotypes suggest that LOB may be involved in the regulation of cell growth in the boundary as well as organ separation.

LOB is involved in a feedback loop with brassinosteroids (BRs), and *PHYB ACTIVATION TAGGED SUPPRESSOR* (*BAS1)*, a BR-inactivating enzyme, in order to limit growth in boundary regions (Bell *et al.*, 2012). BRs comprise a class of plant hormones that are responsible for a wide variety of developmental processes, such as vascular differentiation, cell expansion, and reproductive development. BRs are not transported long distances in the plant and are thought to be synthesized locally [reviewed in (Hategan *et al.*, 2011; Nolan *et al.*, 2020)]. BR is a positive regulator of *LOB* expression and *BAS1* is a direct target of LOB transcriptional activation. BAS1 functions to catabolize BR, thus LOB and BR form a feedback loop to limit accumulation of BR in boundaries. Expressing *BAS1* under the *LOB* promoter suppresses the organ fusion observed in the *lob* mutant (Bell *et al.*, 2012). This suggests that BR hyperaccumulation is the cause of the fusion phenotype in the *lob* mutant.

Since the discovery of *LOB*, LBDs have been implicated in a wide variety of developmental processes, such as callus induction, lateral root formation, anthocyanin biosynthesis, and plant defense in *Arabidopsis* (Okushima *et al.*, 2007; Rubin *et al.*, 2009; Thatcher *et al.*, 2012; Xu *et al.*, 2018), highlighting the importance of LBD proteins in a multitude of plant functions.

7. *LATERAL ORGAN FUSION1* (*LOF1*/AtMYB117) and *LATERAL ORGAN FUSION2* (*LOF2*/AtMYB105) encode MYB transcription factors (MYB subgroup 21), which contain a conserved DNA-binding MYB domain and an FxDFL motif of unknown function (Stracke *et al.*, 2001). *LOF1* is expressed at the base of floral organs, pedicel-stem junctions, the adaxial side of rosette leaf bases, and junctions between the inflorescence meristem and flower primordia (Lee *et al.*, 2009). *LOF1* is expressed in the paraclade junction between the axillary branch and primary stem and between the cauline leaf and axillary branch (Lee *et al.*, 2009). *lof1-1* mutants with abolished expression in the paraclade junction have a fusion between the axillary branch and cauline leaf. They also do not form accessory buds. Based on expression of the *pSTM:GUS* reporter, no meristematic tissue is present in *lof1-1* paraclade junctions (Lee *et al.*, 2009). The lack of accessory bud and the fusion between the axillary branch and cauline leaf in *lof1-1* paraclade junctions suggests that *LOF1* is involved in accessory meristem formation and organ separation. *LOF1* has also been implicated in fruit and ovule development (Gomez *et al.*, 2011).

pLOF2:GUS expressing plants revealed that *LOF2* is expressed in a similar pattern as *LOF1* in organ boundaries. However, *LOF2* is expressed broadly in floral

primordia. *lof2* loss-of-function mutants do not have a detectable abnormal phenotype, but *lof1 lof2* loss-of-function double mutants display an enhanced phenotype compared to the *lof1-1* single mutant. Flower pedicel and primary inflorescence fusions and decurrent strands between the cauline leaf and primary stem are common in double mutants (Lee *et al.*, 2009). Decurrent strands, or strands of tissue from one organ that remain attached to another organ, can be signs of boundary region defects (Emery *et al.*, 2003; Lee *et al.*, 2009; Colling *et al.*, 2015). In addition, *lof1 lof2* double mutants also displayed some vasculature polarity defects, but no additional polarity defects were apparent. Thus, *LOF1* and *LOF2* function with partially redundancy in organ separation (Lee *et al.*, 2009).

The *lof1-1* mutant phenotype is enhanced by *cuc2* or *cuc3* mutations. *lof1-1 cuc2* and *lof1-1 cuc3* plants appeared the same as individual *lof1-1*, *cuc2*, and *cuc3* single mutants during vegetative growth but exhibited more severe fusions in the paraclade junction than *lof1* single mutants. In addition, pedicel-stem and primary stem to axillary branch fusions were present in double mutants. *lof1-1 cuc2* and *lof1-1 cuc3* double mutants displayed meristematic defects as well; axillary meristems on the primary inflorescence were sometimes replaced by a single flower, and second order cauline-leaf axils were bare or contained a solitary flower. The *lof1-1* mutant was additionally found to enhance the weak *stm-10* allele, which fails to maintain a SAM and meristem termination occurs after 2-3 true leaves are produced. *stm-10* mutants eventually produce more leaves from axillary meristems and are able to bolt. *lof1-1 stm-10* mutants were more severe than *stm-10* alone, displaying more rosette leaf fusions, and the SAM terminated earlier than in *stm-10* single mutants. Some *lof1-1 stm-10* mutants resembled

the *stm-1* null mutant, which does not initiate a SAM (Barton and Poethig, 1993; Lee *et al.*, 2009). This indicates *LOF1* is involved in SAM maintenance and not just accessory bud formation.

TRIFOLIATE (*TF*) in tomato encodes an MYB transcription factor closely related to *LOF1* and *LOF2* in *Arabidopsis*. *TF* was found to be expressed in axillary meristems, leaflets, the boundary zone between rachis and leaflets, adaxial regions of leaf primordia, and broadly in the vegetative SAM (Naz *et al.*, 2013). *tf* mutant plants have fewer axillary stems and less leaf complexity when compared to wild-type tomato. Tomato plants overexpressing *TF* have the opposite phenotype (Naz *et al.*, 2013). Therefore, *TF* in tomato plays a role in leaflet initiation and formation of axillary meristems.

As previously discussed, *GOB* is a *CUC* ortholog in tomato, and loss-of-function *gob* mutants have simpler leaves (Brand *et al.*, 2007). CUCs and GOB are NAC transcription factors and LOFs and TF are MYB transcription factors. Expression data suggests *CUC*s, *GOB*, *LOF*s, and *TF* are all boundary expressed, while mutant analysis indicates these genes are involved in boundary specification (Aida *et al.*, 1999; Hibara *et al.*, 2006; Brand *et al.*, 2007; Lee *et al.*, 2009; Naz *et al.*, 2013) This suggests a link between boundary specification and leaf complexity in species that contain compound leaves.

8. TAXIMIN, a novel signaling peptide, was discovered in the mid-2010's in the medicinal tree *Taxus baccata*. TAXIMIN1 (TAX1) in *Arabidopsis* is a cysteine-rich signaling peptide that is part of the TAXIMIN (TAX) family, which is conserved in plants (Colling *et al.*, 2015). *35S:TAX1*-expressing *Arabidopsis* plants were delayed in

development, small in size, and exhibited alterations in silique shape. Interestingly, *35S:TAX1*-expressing plants also exhibited fusions of the axillary branch and cauline leaf as well as the primary stem and cauline leaf. The primary stem and cauline leaf fusion results in a decurrent strand (Colling *et al.*, 2015). This phenotype resembles that of the *lof1-1* loss-of-function mutant (Lee *et al.*, 2009). However, *TAX1* expression was not changed in *lof1 lof2* mutants and conversely *LOF1* expression was not changed in *35S:TAX1* expressing plants (Colling *et al.*, 2015). This suggests that *TAX1* and *LOF1* function in separate pathways for organ separation. Later, it was confirmed that *TAX1* is not transcriptionally activated or repressed by LOF1, and it was found that *TAX1* overexpressing plants are hypersensitive to light (Colling *et al.*, 2016).

Role of Hormones in the SAM and Boundary Region

Cytokinins (CKs) are plant hormones that positively regulate cell division (Skoog and Miller, 1957). CK is present throughout the SAM, the highest concentration being in the very top of the meristem close to the stem cell niche (Shani *et al.*, 2006). Analysis of triple-mutant plants that have loss-of-function in three CK receptors *HISTIDINE KINASE 2* (*AHK2*), *AHK3* and *AHK4/CRE1/WOODEN LEG* (*WOL*), show reduced meristem size, decreased leaf initiation rate, and defects in lateral organs (Nishimura *et al.*, 2004; Riefler *et al.*, 2006). Additionally, when an enzyme that degrades CK, cytokinin oxidase, was misexpressed in tobacco and *Arabidopsis*, plants had the same defects as seen in the triple mutant of CK receptors, and the meristem occasionally terminated (Werner *et al.*, 2001, 2003). Therefore, CK response is needed for meristem function. Further, it was

discovered that one of the ways that *KNOX* genes, such as *STM*, maintain meristem indeterminacy is through the activation of CK (Jasinski *et al.*, 2005; Yanai *et al.*, 2005). Type A *Arabidopsis* response regulators (ARRs) are negative regulators of CK signaling (Hwang *et al.*, 2012). WUS negatively regulates some *ARRs* (*ARR5*, *ARR6*, *ARR7*, and *ARR15*) by binding their promoters directly. This is biologically relevant because overexpression of a constitutively active ARR led to meristem termination (Leibfried *et al.*, 2005).

Gibberellins (GAs) are a type of plant hormone that regulates various developmental processes, such as stem elongation, germination, flowering, and fruit senescence (Daviere and Achard, 2013). GAs accumulate in the incipient primordia and assist in promoting differentiation. KNOX proteins negatively regulate GA biosynthesis directly (Sakamoto *et al.*, 2001; Hay *et al.*, 2002). STM positively regulates GA2-oxidase, which deactivates GA. Thus, it appears that it is important to keep GA out of the meristem, in order to prevent meristem differentiation (Chen *et al.*, 2004). In plants with constitutively active GA and reduced CK activity, meristem termination and cotyledon fusion were observed (Jasinski *et al.*, 2005). Thus, GA and CK act together in promoting meristem maintenance and specifying the boundary between SAM and primordia. Ratios of CK and GA appear important for development, and the two hormones mutually antagonize one another by negatively regulating each other's activity.

Auxins were the first major plant hormones to be discovered and are incredibly important for plant development and growth [reviewed in (Mockaitis and Estelle, 2008)]. An area of high auxin concentration, known as an auxin maximum, marks the site of the

incipient lateral organ primordia before outgrowth (Swarup and Bennett, 2003). Auxin can be transported long or short distances within the plant body. Auxin transport is directional or polar. The direction of auxin transport is dependent on the auxin efflux carriers known as PIN- FORMED (PIN) proteins. Specifically, the oriented placement of PINs on the plasma membrane controls the direction of auxin flow (Adamowski and Friml, 2015). This was discovered when a mutation in the *Arabidopsis PIN1* gene caused a naked "pin" inflorescence to form that was completely devoid of organs (Gälweiler *et al.*, 1998; Vernoux *et al.*, 2000). Exogenous application of auxin to the peripheral SAM of the *pin1* mutant causes organ formation at the site of application (Reinhardt *et al.*, 2000). Double mutants of *pin1* and *pinoid* (*pid*), another auxin transport facilitator, sometimes failed to produce cotyledons. It was observed the *STM* and *CUC* gene expression is present in the incipient primordia of the cotyledons in the embryo of the *pin1 pid* double mutants. Cotyledon formation was restored when *cuc1* was additionally mutated and partially restored when *stm* was mutated (Furutani *et al.*, 2004). This highlights a role for auxin transport in preventing *KNOX* and *CUC* gene expression in developing organ primordia. Auxin has antagonistic interactions with CK as auxin has been shown to downregulate CK (Miyawaki *et al.*, 2004). In summary, in the SAM there is a high CK:auxin ratio and low GA. In emerging primordia, there is a low CK:auxin ratio and high GA. These hormone ratios help to specify the SAM, incipient primordia, and boundary between them.

As mentioned previously, LOB and BR form a feedback loop to limit BR accumulation in the boundary. Additionally, *LOB* is not the only boundary expressed

gene known to be involved with BR. BRASSINOZOLE-RESISTANT1 (BZR1), a transcription factor downstream of BR signaling that modulates BR-response gene expression, represses *CUC3* by directly binding to the *CUC3* promoter (Gendron *et al.*, 2012). *CUC2* and *CUC3* positively regulate *LOF1* expression in the boundary region (Gendron *et al.*, 2012). Thus, modulation of BR in the boundary has the ability to affect multiple boundary genes, either directly or indirectly.

Leaf Polarity in Plants

Polarity at its most simple is any asymmetry along one or more axes. This occurs at the molecular, cellular, tissue, organ, and whole plant levels (Sachs, 1991). It is thought that polarity is set up early in development and must represent a coordination of events between many cells (Sachs, 1991). For example, polarity in plant embryo development begins even before the first zygotic division, as apical-basal polarity is evident within the egg cell itself (Schulz and Jensen, 1968; Mansfield and Briarty, 1991). The first cell division of the zygote forms a small apical cell that gives rise to most of the embryo, and a larger basal cell, that forms the suspensor and part of the root in most species (quiescent center and columella stem cells in *Arabidopsis)* (Laux *et al.*, 2004).

The establishment of polarity is equally important in leaves as in the plant as a whole. For example, the leaf blade must develop a thick cuticle and rows of tightly packed palisade mesophyll cells on top of the blade for photosynthesis to be efficient. Additionally, stomata form primarily on the bottom of the leaf blade in order for transpiration to occur without the plant being susceptible to water deficit (Husbands *et*

al., 2009). A simple leaf has three axes of polarity: proximodistal (tip-base), adaxial-abaxial (upper-lower), and lateral (midvein-margin). The upper and lower side of the leaf blade is known as the adaxial and abaxial side of the leaf, respectively (Reinhardt and Kuhlemeier, 2002).

Proximodistal Leaf Polarity: Leaves are known to mature from tip to base (basipetally) in a wave. Mutants that completely fail to elaborate proximo-distal patterning have not been found, but genes involved in proximo-distal patterning have been identified. One such gene is *BLADE ON PETIOLE* (*BOP*) in *Arabidopsis*. *bop* mutants have blade displaced proximally on the petiole, creating a proximal (petiole) to distal (blade) change (Norberg *et al.*, 2005; Ha *et al.*, 2007). The BOP1/BOP2 complex directly regulates AS2 and in *bop* mutants, AS2 activity is reduced, and therefore KNOX activity is increased (Jun *et al.*, 2010). This suggests one function of BOP proteins is to repress meristematic gene expression in the leaf indirectly through AS2.

Maize leaves consist of a proximal sheath wrapped around the hollow culm and a flat, distal blade that captures light for photosynthesis. The ligule is a fringe of tissue that extends adaxially where the blade and sheath meet and is thought to function to keep dirt and fungal spores from entering the culm. Two auricles, wedge-shaped appendages that aid in leaf bending, are located next to the ligule on the mediolateral plane near the culm [review in (Foster *et al.*, 2004)]. As mentioned earlier, *AS1* in *Arabidopsis* is the ortholog of *Rs2* in maize, *AS2* in *Arabidopsis* is the ortholog of *Ig1* (Schneeberger *et al.*, 1998; Evans, 2007), and some *as1* and *as2* loss-of-function mutants have leaflets that are generated from asymmetric positions on the petiole (Semiarti *et al.*, 2001; Byrne *et al.*,

2002; Machida *et al.*, 2015). *Rs2* mutants have sheath extending distally, resulting in a new sheath-blade boundary that causes ectopic ligule and auricle tissue that bleed into the blade (Schneeberger *et al.*, 1998). This represents a shift of the ligule and auricle into the blade and sheath – a defect in proximo-distal polarity. *ig1* mutants had leaf flaps on the adaxial midrib of the blade and sheath, distortion of the ligular region, and although rare, knots of sheath tissue present on the leaf blade (Kermicle, 1971; Evans, 2007). This is similarly a change in proximo-distal polarity. It was also found that AS1 and AS2 interact with one another and positively regulates transcription factors involved in adaxial-abaxial leaf polarity (Fu *et al.*, 2007), mentioned in the next section. Taken together, this indicates *Rs2* in maize and *AS1* and/or *AS2* in *Arabidopsis* could be involved in the patterning of one or more axes in leaf polarity in addition to their role in leaf primordia development.

Adaxial-Abaxial Leaf Polarity: Maintaining adaxial-abaxial polarity in a flat and long structure is difficult, and there are a large number of transcription factors that play a role in this process (Moon and Hake, 2011). It has also been demonstrated in classical experiments that using a surgical incision to physically separate incipient primordia from the meristem results in loss of adaxial-abaxial polarity (Sussex, 1951, 1954), suggesting that a signal from the meristem is required for adaxial/abaxial patterning. Loss of adaxial-abaxial polarity results in leaves that are radially symmetric and contain no discernable leaf blade [reviewed (Bowman *et al.*, 2002)].

Genetic analysis has revealed mutants with defects in adaxial-abaxial leaf patterning. In *Antirrhinum majus* (snapdragon), loss-of-function mutations in the MYB

transcription factor *PHANTASTICA* (*PHAN*) led to abaxialized radial or partially radial leaves, among other phenotypes (Waites and Hudson, 1995; Waites *et al.*, 1998). The adaxial side of *phan* mutant leaves has patches of adaxial and abaxial tissue and lamina-like outgrowths at the adaxial and abaxial boundaries. These observations led to the hypothesis that both adaxial and abaxial domains are needed for blade outgrowth (Waites and Hudson, 1995). Orthologs of *PHAN* encode MYB transcription factors known as the ARP family [*ASYMMETRIC LEAVES 1* (*AS1*); *ROUGH SHEATH2* (*RS2*); and *PHAN*]. The *ARP* genes are expressed in young leaf primordia and are thought to play roles in adaxial identity. *as1* (*Arabidopsis*) mutants exhibit a low frequency of abaxialized phenotypes (Xu *et al.*, 2003). *rs2* (maize) mutants sometimes contain semi-bladeless leaves. However, adaxial-abaxial polarity appears to be maintained in these mutant leaves regardless (Schneeberger *et al.*, 1998; Timmermans *et al.*, 1999; Tsiantis *et al.*, 1999).

In *Arabidopsis*, two genes encoding homeodomain-leucine zipper (HD-Zip) class III transcription factors, *PHABULOSA* (*PHB*) and *PHAVOLUTA* (*PHV*), were found to be involved in leaf polarity. *PHB* and *PHV* are adaxial determinants because gain-of-function mutants lack abaxial cell fate and display radial symmetry (McConnell and Barton, 1998; McConnell *et al.*, 2001). In wild-type plants, *PHB* and *PHV* transcript accumulates only in the adaxial domain, and transcript accumulation was absent in the abaxial domain. In the dominant mutants, *PHB* and *PHV* transcript accumulation was observed throughout the leaf blade in both the adaxial and abaxial domains (McConnell *et al.*, 2001). The dominant mutations disrupt a miRNA-binding site conserved in the HD-Zip III family members, suggesting a mechanism for the gain-of-function phenotype.

HD-Zip class III transcription factors are post-transcriptionally regulated by *miRNA165/166* (which precursors accumulate on the abaxial side of the leaf) (Yao *et al.*, 2009; Miyashima *et al.*, 2013). Therefore, although HD-Zip III transcription factors are expressed in the developing primordia in both the adaxial and abaxial domains, the transcripts only accumulate in the adaxial region due to miRNA regulation (Rhoades *et al.*, 2002; Emery *et al.*, 2003; Tang *et al.*, 2003).

A related HD-Zip III, *REVOLUTA* (*REV)* was found to function with *PHB* and *PHV* in specifying adaxial cell fate (Otsuga *et al.*, 2001; Emery *et al.*, 2003). The single knock-out mutants *phb* and *phv* are reported to appear wild-type, presumably because HD-Zip class III genes exhibit functional redundancy (Emery *et al.*, 2003; Prigge *et al.*, 2005). *rev-6* knock-out mutants have reduced lateral meristem formation in the leaf axils of rosette and cauline leaves. Occasionally, the axils of affected leaves develop a filamentous structure of leaf in place of a lateral meristem. The floral meristem is also affected in some flowers, where the inner organs failed to form due to the defective meristem (Otsuga *et al.*, 2001). However, loss of *PHB*, *PHV*, and *REV* function results in the apical portion of the embryo being replaced by a radially symmetric apical structure. Due to seedling lethality, leaf phenotypes of loss-of-function *phb phv rev* triple mutants cannot be assessed. While *phb-13 phv-11* double mutants appear wild-type, *phb-13 rev-6* double mutants sometimes have a meristem that terminates in a pin structure before true leaves are produced, have one cotyledon, or have no cotyledons (Prigge *et al.*, 2005). In addition, *phv-11 rev-6* double mutants display the same meristematic phenotypes as *phb-13 rev-6* in low numbers. In both *phb-13 rev-6* and *phv-11 rev-6* mutants, there are leaf

polarity defects. Trumpet-shaped leaves, mirror-image leaf duplications, and occasional radial cotyledons are observed in both genotypes. These results support the fact that many adaxial determinants have additional roles in meristem maintenance, such that adaxial fate is tied to the fate of the meristem (Prigge *et al.*, 2005).

The *KANADI* (*KAN*) abaxial determinants were first discovered as genes involved in polarity establishment in carpels (Eshed *et al.*, 1999). The *KAN* gene family encodes GARP-domain transcription factors that are expressed abaxially (Izhaki and Bowman, 2007). There are four *KAN* genes in *Arabidopsis* (*KAN1*, *KAN2*, *KAN3*, and *KAN4*). Single *kan* mutants do not have an abnormal leaf polarity phenotype, whereas double or triple mutants show varying degrees of adaxialization. Misexpression of *KAN1* or *KAN2* throughout the leaf causes abaxialization and leaf radialization (Eshed *et al.*, 1999). These expression patterns and mutant analysis indicate *KAN*s are abaxial identity determinants. In *kan1 kan2 kan3* triple mutants, *HD-Zip III* genes are expressed throughout the radially symmetric leaves (Eshed *et al.*, 2004). Also, ectopically overexpressing *KAN* genes through the entire primordia leads to loss of *HD-Zip III* expression (Kerstetter *et al.*, 2001). Further, in *phb phv rev* triple mutants, the abaxialized leaf phenotype is suppressed by additional mutations in *KAN* genes (Izhaki and Bowman, 2007). Therefore, KANADI and HD-Zip III transcription factors act in mutual antagonism to one another.

AS2 and *KANADIs* additionally exhibit mutual antagonism. KAN proteins were found to bind to a *cis*-element in the *AS2* promoter, leading to downregulation of *AS2* expression in the abaxial domain (Wu *et al.*, 2008). In turn, *KAN* expression is

upregulated in the *as2* mutant, suggesting that AS2 is a negative regulator of *KAN* (Lin *et al.*, 2003). In summary, *KANADI*s and adaxial identity genes often mutually repress one another at one or more levels of regulation.

AUXIN RESPONSE FACTOR3/ETTIN (*ARF3*) and *ARF4* have also been implicated in abaxial leaf identity. Single loss-of-function mutations in *ARF3* or *ARF4* do not cause leaf polarity defects, however, loss-of-function of both *ARF3* and *ARF4* results in leaves that curl upwards and have ectopic outgrowths of tissue on the abaxial side (Pekker *et al.*, 2005). *ARF3* and *ARF4* are post-transcriptionally regulated by a *trans*-acting small-interfering RNA (tasi-RNA) derived from *TAS3* transcripts, which limits *ARF3* and *ARF4* transcript accumulation to the abaxial domain, although *ARF3* and *ARF4* are expressed throughout the primordia (Allen *et al.*, 2005; Fahlgren *et al.*, 2006; Hunter *et al.*, 2006). Therefore, ARF3 and ARF4 proteins only accumulates abaxially (Chitwood *et al.*, 2009). While *TAS3* is expressed on the adaxial side, tasi-ARFs show movement towards the abaxial side, forming a gradient (Nogueira *et al.*, 2007; Chitwood *et al.*, 2009; Schwab *et al.*, 2009). Thus, there are two small RNA gradients - a tasi-ARF gradient beginning at the adaxial epidermis of the leaf and a *mirRNA165/166* gradient beginning at the abaxial epidermis – are critical for leaf polarity. These two opposing small RNA gradients have been shown to be important for development as they act as a buffer against fluctuations in target gene expression (Skopelitis *et al.*, 2012, 2017).

YABBY genes, which encode proteins with zinc-finger and helix-loop-helix domains, have been proposed to be involved in blade outgrowth. There are six *YABBY* genes in total in *Arabidopsis: YABBY2* (*YAB2*), *YABBY3* (*YAB3*), *YABBY5* (*YAB5*),

CRABS CLAW (*CRC*), *INNER NO OUTER* (*INO*), and *FILAMENTOUS FLOWER* (*FIL*) (Siegfried *et al.*, 1999; Villanueva *et al.*, 1999). *CRC* and *INO* are only expressed in floral organs, but the remaining *YABBY* genes are expressed abaxially in developing lateral organs (Sawa *et al.*, 1999). Single loss-of-function mutations in *YABBY* genes have no abnormal leaf phenotype. However, quadruple *yabby* mutants have varying loss of lamina expansion, from patches of lamina expansion to complete radialization of the leaf blade. A global expression analysis in a quadruple *yabby* mutant indicates that adaxial-abaxial polarity is established but not maintained in these mutants (Sarojam *et al.*, 2010). Double mutant *fil yab3* plants exhibit ectopic meristems on adaxial surfaces of cotyledons and leaf blades. Further, KNOX homeobox genes *STM*, *BP*, and *KNAT2* are upregulated in *fil yab3* leaves (Kumaran *et al.*, 2002). This suggests that *YAB* genes function to downregulate *KNOX* homeobox genes so that meristem function is restricted to the SAM. Thus, *YABBY* genes are involved in both suppressing meristematic genes in the shoot system and promoting leaf blade outgrowth. Regarding known YABBY activities with abaxial determinants, *YABBY* gene induction upregulates *KAN1* and *ARF4* (Bonaccorso *et al.*, 2012); however, it is unclear if this was a direct or indirect effect.

It has been proposed for some time that lateral organs provide feedback to stem cells (Sussex, 1952). Mutants defective in one or more *YAB* genes leads to a size increase in the central SAM even though *YAB* genes are not expressed in the SAM (Goldshmidt *et al.*, 2008). Therefore, it was proposed that *YAB* genes are involved feedback regulation to effect SAM size using some type of mobile signal. Modeling experiments suggest a *YAB*-derived signal is transported to the boundary, where another secondary messenger is

transported to the SAM to relay the signal (Shi *et al.*, 2018). The model also supports that stem cells are associated with low auxin levels, and high auxin levels negatively affect SAM size (Shi *et al.*, 2018). It is unclear if the signal is auxin or a component downstream of auxin signaling.

The primary plant hormone auxin is involved in lamina outgrowth. Auxin is synthesized and undergoes polar transport throughout the plant, creating areas of high auxin concentration where growth and development are actively occurring (Bowman and Floyd, 2008; Vanneste and Friml, 2009). During primordia development, an auxin maximum becomes concentrated at the tip – or distal end – of the primordia (Benkova *et al.*, 2003; Reinhardt *et al.*, 2005). Later, auxin is evenly distributed from the margins to both sides of the midvein to promote lamina outgrowth (Aloni *et al.*, 2003; Scanlon, 2003; Zgurski *et al.*, 2005). The polar auxin efflux carrier protein PIN-FORMED1 (PIN1) is ectopically localized in the *kan* triple mutant plants (Izhaki and Bowman, 2007), and uneven auxin distribution occurs in *as1* and *as2* mutants that have asymmetrical lamina outgrowth (Zgurski *et al.*, 2005). Therefore, auxin is linked to both lamina outgrowth and known adaxial-abaxial polarity determinants.

Midvein-Margin Leaf Polarity: Little is known about midvein-margin leaf patterning in plants except that it is established early in development (Freeling, 1992). In maize leaf primordia, recruitment of founder cells occurs in two mediolateral compartments. The central domain consists of the midrib and distal leaf tip, and the lateral domain consists of the leaf domain extending from the central compartment to the leaf margin. This includes the margins of the lower portion of the leaf blade and the

entire sheath (Scanlon *et al.*, 1996). Two genes in maize, *Narrow sheath2* (*Ns1*) and *Narrow sheath2* (*Ns2*), encode WUSCHEL HOMEOBOX (WOX) proteins required for recruitment of founder cells into the lateral region of the initiating primordia. *Ns* mutants have a deletion of a lateral compartment that includes the leaf margins (Scanlon and Freeling, 1997; Scanlon, 2000). The central domain is not affected in *Ns* mutants.

Ns1 and *Ns2* are orthologous to *PRESSED FLOWERS* (*PRS*)/*WOX3* in *Arabidopsis*. *PRS* is expressed in the lateral foci of the peripheral zone of the SAM, which is similar to the expression pattern of *Ns1* and *Ns2* in maize. The *prs* mutant phenotype is subtle with plants lacking stipules, which are small outgrowths at the base of leaves (Matsumoto and Okada, 2001; Nardmann *et al.*, 2004); stipules are produced from cells of the lateral compartment in *Arabidopsis* (Nakata *et al.*, 2012). *YABBY* genes positively regulate *PRS*, which is expressed at the leaf margin in order to promote blade outgrowth (Nakata *et al.*, 2012). When a mutation in *prs* is combined with a mutation in *wox1*, another *WOX* gene family member in *Arabidopsis*, a narrow leaf phenotype is observed (Vandenbussche *et al.*, 2009; Nakata *et al.*, 2012). This evidence suggests that *Ns* and *PRS*/*WOX3* orthologs are conserved in regulating lateral organ development although species-specific functions have evolved.

Contributions of this dissertation

This dissertation focuses on characterization of the role of *LOF1* in plant development and during abiotic stress. In Chapter 1, I show that LOF1 interacts with a number of transcription factors including, HB4, WHY3, MYB32, and LRB2, in a yeast-

two hybrid assay. This interaction appears specific, as LOF1 does not interact with closely related family members HAT3 and WHY1 in yeast. In Chapter 2, I investigated the subcellular localization of LOF1 during abiotic stress conditions. While none of the tested abiotic stress conditions appeared to cause LOF1 to change subcellular localization from the nucleus, this may mean that some of the putative chloroplast-localized interactors move to the nucleus under certain conditions. In Chapter 3, I show that the leaf polarity gene *PHB* is a genetic suppressor of *lof1-1*. *LOF1* promotes paraclade junction and accessory bud formation, while *PHB* and a subset of other *HD-Zip III* genes repress formation of both paraclade junctions and accessory buds. *LOF1* and *PHB* not only function together in accessory bud formation but impact overall plant architecture.

References

Adamowski M, Friml J. 2015. PIN-dependent auxin transport: Action, regulation, and evolution. Plant Cell **27**, 20–32.

Aida M, Ishida T, Fukaki H, Fujisawa H, Tasaka M. 1997. Genes involved in organ separation in *Arabidopsis*: An analysis of the c*up-shaped cotyledon* mutant. Plant Cell **9**, 841–857.

Aida M, Ishida T, Tasaka M. 1999. Shoot apical meristem and cotyledon formation during Arabidopsis embryogenesis: Interaction among the *CUP-SHAPED COTYLEDON* and *SHOOT MERISTEMLESS* genes. Development **126**, 1563–1570.

Allen E, Xie Z, Gustafson AM, Carrington JC. 2005. microRNA-directed phasing during *trans*-acting siRNA biogenesis in plants. Cell **121**, 207–221.

Aloni R, Schwalm K, Langhans M, Ullrich CI. 2003. Gradual shifts in sites of free-auxin production during leaf-primordium development and their role in vascular differentiation and leaf morphogenesis in *Arabidopsis*. Planta **216**, 841–853.

Barton MK, Poethig RS. 1993. Formation of the shoot apical meristem in *Arabidopsis thaliana*: An analysis of development in the wild type and in the *shoot meristemless* mutant. Development **119**, 823–831.

Bell AD. 1991. Plant Form: an Illustrated Guide to Flowering Plant Morphology.

Bell EM, Lin W, Husbands AY, Yu L, Jaganatha V, Jablonska B, Mangeon A, Neff MM, Girke T, Springer PS. 2012. *Arabidopsis* lateral organ boundaries negatively regulates brassinosteroid accumulation to limit growth in organ boundaries. Proceedings of the National Academy of Sciences USA **109**, 21146–21151.

Belles-Boix E, Hamant O, Witiak SM, Morin H, Traas J, Pautot V. 2006. *KNAT6*: An *Arabidopsis* homeobox gene involved in meristem activity and organ separation. Plant Cell **18**, 1900–1907.

Benkova E, Michniewicz M, Sauer M, Teichmann T, Seifertova D, Jürgens G, Friml J. 2003. Local, efflux-dependent auxin gradients as a common module for plant organ formation. Cell **115**, 591–602.

Berger Y, Harpaz-Saad S, Brand A, Melnik H, Sirding N, Alvarez JP, Zinder M, Samach A, Eshed Y, Ori N. 2009. The NAC-domain transcription factor GOBLET specifies leaflet boundaries in compound tomato leaves. Development **136**, 823–832.

Bhatt AM, Etchells JP, Canales C, Lagodienko A, Dickinson H. 2004. VAAMANA - A BEL1-like homeodomain protein, interacts with KNOX proteins BP and STM and regulates inflorescence stem growth in *Arabidopsis*. Gene **328**, 103–111.

Bonaccorso O, Lee JE, Puah L, Scutt CP, Golz JF. 2012. FILAMENTOUS FLOWER controls lateral organ development by acting as both an activator and a repressor. BMC Plant Biology **12**, 1–15.

Borghi L, Bureau M, Simon R. 2007. *Arabidopsis JAGGED LATERAL ORGANS* is expressed in boundaries and coordinates *KNOX* and *PIN* activity. Plant Cell **19**, 1795–1808.

Bowman JL, Eshed Y, Baum SF. 2002. Establishment of polarity in angiosperm lateral organs. Trends in Genetics **18**, 134–141.

Bowman JL, Floyd SK. 2008. Patterning and polarity in seed plant shoots. Annual Review of Plant Biology **59**, 67–88.

Brand A, Shirding N, Shleizer S, Ori N. 2007. Meristem maintenance and compound-leaf patterning utilize common genetic mechanisms in tomato. Planta **226**, 941–951.

Byrne ME, Curtis M, Arroyo JM, Dunham M, Martienssen RA, Barley R, Hudson A. 2000. *Asymmetric leaves1* mediates leaf patterning and stem cell function in *Arabidopsis*. Nature **408**, 967–971.

Byrne ME, Groover AT, Fontana JR, Martienssen RA. 2003. Phyllotactic pattern and stem cell fate are determined by the *Arabidopsis* homeobox gene *BELLRINGER*. Development **130**, 3941–3950.

Byrne ME, Simorowski J, Martienssen RA. 2002. *ASYMMETRIC LEAVES1* reveals *knox* gene redundancy in *Arabidopsis*. Development **129**, 1957–65.

Chen H, Banerjee AK, Hannapel DJ. 2004. The tandem complex of BEL and KNOX partners is required for transcriptional repression of *ga20ox1*. Plant Journal **38**, 276–284.

Cheng X, Peng J, Ma J, Tang Y, Chen R, Mysore KS, Wen J. 2012. *NO APICAL MERISTEM* (*MtNAM*) regulates floral organ identity and lateral organ separation in *Medicago truncatula*. New Phytologist **195**, 71–84.

Chitwood DH, Nogueira FTS, Howell MD, Montgomery TA, Carrington JC, Timmermans MCP. 2009. Pattern formation via small RNA mobility. Genes & Development **23**, 549–554.

Chuck G, Lincoln C, Hake S. 1996. *KNAT1* induces lobed leaves with ectopic meristems when overexpressed in Arabidopsis. Plant Cell **8**, 1277–1289.

Clark SE, Running MP, Meyerowitz EM. 1993. *CLAVATA1*, a regulator of meristem and flower development in *Arabidopsis*. Development **119**, 397–418.

Colling J, Pollier J, Bossche R Vanden, Makunga NP, Pauwels L, Goossens A. 2016. Hypersensitivity of Arabidopsis *TAXIMIN1* overexpression lines to light stress is correlated with decreased sinapoyl malate abundance and countered by the antibiotic cefotaxime. Plant Signaling & Behavior **11**, 1–4.

Colling J, Tohge T, De Clercq R, Brunoud G, Vernoux T, Fernie AR, Makunga NP, Goossens A, Pauwels L. 2015. Overexpression of the *Arabidopsis thaliana* signalling peptide TAXIMIN1 affects lateral organ development. Journal of Experimental Botany **66**, 5337–5349.

Cutter EG. 1965. Recent experimental studies of the shoot apex and shoot morphogenesis. The Botanical Review **31**, 7–113.

Daviere JM, Achard P. 2013. Gibberellin signaling in plants. Development **140**, 1147–1151.

Douglas SJ, Chuck G, Dengler RE, Pelecanda L, Riggs CD. 2002. *KNAT1* and *ERECTA* regulate inflorescence architecture in Arabidopsis. Plant Cell **14**, 547–558.

Edgar BA, Lehner CF. 1996. Developmental control of cell cycle regulators: A fly's perspective. Science **274**, 1646–1652.

Emery JF, Floyd SK, Alvarez J, Eshed Y, Hawker NP, Izhaki A, Baum SF, Bowman JL. 2003. Radial patterning of *Arabidopsis* shoots by class III HD-ZIP and KANADI genes. Current Biology **13**, 1768–1774.

Eshed Y, Baum SF, Bowman JL. 1999. Distinct mechanisms promote polarity establishment in carpels of *Arabidopsis*. Cell **99**, 199–209.

Eshed Y, Izhaki A, Baum SF, Floyd SK, Bowman JL. 2004. Asymmetric leaf development and blade expansion in *Arabidopsis* are mediated by KANADI and YABBY activities. Development **131**, 2997–3006.

Evans MMS. 2007. The *indeterminate gametophyte1* gene of maize encodes a LOB domain protein required for embryo sac and leaf development. Plant Cell **19**, 46–62.

Evans MMS, Barton MK. 2002. Genetics of angiosperm shoot apical meristem development. Annual Review of Plant Physiology and Plant Molecular Biology **48**, 673–701.

Fahlgren N, Montgomery TA, Howell MD, Allen E, Dvorak SK, Alexander AL, Carrington JC. 2006. Regulation of *AUXIN RESPONSE FACTOR3* by *TAS3* ta-siRNA affects developmental timing and patterning in *Arabidopsis*. Current Biology **16**, 939–944.

Fletcher JC, Brand U, Running MP, Simon R, Meyerowitz EM. 1999. Signaling of cell fate decisions by *CLAVATA3* in *Arabidopsis* shoot meristems. Science **283**, 1911–1914.

Foster T, Hay A, Johnston R, Hake S. 2004. The establishment of axial patterning in the maize leaf. Development **131**, 3921–3929.

Freeling M. 1992. A conceptual framework for maize leaf development. Developmental Biology **153**, 44–58.

Freeling M, Hake S. 1985. Developmental genetics of mutants that specify knotted leaves in maize. Genetics **111**, 617–634.

Fu Y, Xu L, Xu B, Yang L, Ling Q, Wang H, Huang H. 2007. Genetic interactions between leaf polarity-controlling genes and *ASYMMETRIC LEAVES1* and *2* in *Arabidopsis* leaf patterning. Plant and Cell Physiology **48**, 724–735.

Furutani M, Vernoux T, Traas J, Kato T, Tasaka M, Aida M. 2004. *PIN-FORMED1* and *PINOID* regulate boundary formation and cotyledon development in *Arabidopsis* embryogenesis. Development **131**, 5021–5030.

Gaillochet C, Daum G, Lohmann JU. 2015. O cell, where art thou? The mechanisms of shoot meristem patterning. Current Opinion in Plant Biology **23**, 91–97.

Gälweiler L, Guan CH, Muller A, Wisman E, Mengen K, Yephremov A, Palme K. 1998. Regulation of polar auxin transport by AtPIN1 in *Arabidopsis* vascular tissue. Science **282**, 2226–2230.

Gaudin V, Lunness PA, Fobert PR, Towers M, Riou-Khamlichi C, Murray JAH, Coen E, Doonan JH. 2000. The expression of *D-cyclin* genes defines distinct developmental zones in snapdragon apical meristems and is locally regulated by the *Cycloidea* gene. Plant Physiology **122**, 1137–1148.

Gendron JM, Liu J-S, Fan M, Bai M-Y, Wenkel S, Springer PS, Barton MK, Wang Z-Y. 2012. Brassinosteroids regulate organ boundary formation in the shoot apical meristem of *Arabidopsis*. Proceedings of the National Academy of Sciences USA **109**, 21152–21157.

Goldshmidt A, Alvarez JP, Bowman JL, Eshed Y. 2008. Signals derived from *YABBY* gene activities in organ primordia regulate growth and partitioning of *Arabidopsis* shoot apical meristems. Plant Cell **20**, 1217–1230.

Gomez MD, Urbez C, Perez-Amador MA, Carbonell J. 2011. Characterization of *constricted fruit* (*ctf*) mutant uncovers a role for *AtMYB117/LOF1* in ovule and fruit development in *Arabidopsis thaliana*. PLoS ONE **6**, 1–10.

Greb T, Clarenz O, Schafer E, Herrero R, Schmitz G, Theres K. 2003. Molecular analysis of the *LATERAL SUPPRESSOR* gene in *Arabidopsis*. Genes & Development **17**, 1175–1187.

Guo M, Thomas J, Collins G, Timmermans MCP. 2008. Direct repression of *KNOX* loci by the ASYMMETRIC LEAVES1 complex of *Arabidopsis*. Plant Cell **20**, 48–58.

Guo D, Zhang J, Wang X, Han X, Wei B, Wang J, Li B, Yu H, Huang Q, Gu H, Qu LJ, Qin G. 2015. The WRKY transcription factor WRKY71/EXB1 controls shoot branching by transcriptionally regulating *RAX* genes in Arabidopsis. Plant Cell **27**, 3112–3127.

Ha CM, Jun JH, Nam HG, Fletcher JC. 2007. *BLADE-ON-PETIOLE1* and *2* control *Arabidopsis* lateral organ fate through regulation of LOB domain and adaxial-abaxial polarity genes. Plant Cell **19**, 1809–1825.

Hategan L, Godza B, Szekeres M. 2011. Regulation of brassinosteroid metabolism. Brassinosteroids: A Class of Plant Hormone. 57-82.

Hay A, Kaur H, Phillips A, Hedden P, Hake S, Tsiantis M. 2002. The gibberellin pathway mediates KNOTTED1-type homeobox function in plants with different body plans. Current Biology **12**, 1557–1565.

Hibara K, Karim MR, Takada S, Taoka K, Furutani M, Aida M, Tasaka M. 2006. *Arabidopsis CUP-SHAPED COTYLEDON3* regulates postembryonic shoot meristem and organ boundary formation. Plant Cell **18**, 2946–2957.

Hunter C, Willmann MR, Wu G, Yoshikawa M, De la Luz Gutierrez-Nava M, Poethig SR. 2006. Trans-acting siRNA-mediated repression of ETTIN and ARF4 regulates heteroblasty in *Arabidopsis*. Development **133**, 2973–2981.

Husbands AY, Chitwood DH, Plavskin Y, Timmermans MCP. 2009. Signals and prepatterns: New insights into organ polarity in plants. Genes & Development **23**, 1986–1997.

Hussey G. 1971. Cell division and expansion and resultant tissue tensions in the shoot apex during the formation of a leaf primordium in the tomato. Journal of Experimental Botany **22**, 702–714.

Hwang I, Sheen J, Müller B. 2012. Cytokinin signaling networks. Annual Review of Plant Biology **63**, 353–380.

Izhaki A, Bowman JL. 2007. KANADI and class III HD-Zip gene families regulate embryo patterning and modulate auxin flow during embryogenesis in *Arabidopsis*. Plant Cell **19**, 495–508.

Jasinski S, Piazza P, Craft J, Hay A, Woolley L, Rieu I, Phillips A, Hedden P, Tsiantis M. 2005. KNOX action in *Arabidopsis* is mediated by coordinate regulation of cytokinin and gibberellin activities. Current Biology **15**, 1560–1565.

Jun JH, Ha CM, Fletcher JC. 2010. BLADE-ON-PETIOLE1 coordinates organ determinacy and axial polarity in *Arabidopsis* by directly activating ASYMMETRIC LEAVES2. Plant Cell **22**, 62–76.

Kayes JM, Clark SE. 1998. *CLAVATA2*, a regulator of meristem and organ development in *Arabidopsis*. Development **125**, 3843–51.

Keller T, Abbott J, Moritz T, Doerner P. 2006. *Arabidopsis REGULATOR OF AXILLARY MERISTEMS1* controls a leaf axil stem cell niche and modulates vegetative development. Plant Cell **18**, 598–611.

Kermicle JL. 1971. Pleiotropic effects on seed development of the *indeterminate gametophyte* gene in maize. American Journal of Botany **58**, 1–7.

Kerstetter RA, Bollman K, Taylor RA, Bomblies K, Poethig RS. 2001. *KANADI* regulates organ polarity in *Arabidopsis*. Nature **411**, 706–709.

Kumaran MK, Bowman JL, Sundaresan V. 2002. *YABBY* polarity genes mediate the repression of *KNOX* homeobox genes in Arabidopsis. Plant Cell **14**, 2761–2770.

Laufs P, Peaucelle A, Morin H, Traas J. 2004. MicroRNA regulation of the CUC genes is required for boundary size control in *Arabidopsis* meristems. Development **131**, 4311–4322.

Laux T, Mayer KF, Berger J, Jürgens G. 1996. The *WUSCHEL* gene is required for shoot and floral meristem integrity in *Arabidopsis*. Development **122**, 87–96.

Laux T, Würschum T, Breuninger H. 2004. Genetic regulation of embryonic pattern formation. Plant Cell **16**, 190–202.

Lee D-K, Geisler M, Springer PS. 2009. *LATERAL ORGAN FUSION1* and *LATERAL ORGAN FUSION2* function in lateral organ separation and axillary meristem formation in *Arabidopsis*. Development **136**, 2423–2432.

Leibfried A, To JPC, Busch W, Stehling S, Kehle A, Demar M, Kieber JJ, Lohmann JU. 2005. WUSCHEL controls meristem function by direct regulation of cytokinin-inducible response regulators. Nature **438**, 1172–1175.

Lin W, Shuai B, Springer PS. 2003. The *Arabidopsis LATERAL ORGAN BOUNDARIES*-domain gene *ASYMMETRIC LEAVES2* functions in the repression of *KNOX* gene expression and in adaxial-abaxial patterning. Plant Cell **15**, 2241–2252.

Lincoln C, Long J, Yamaguchi J, Serikawa K, Hake S. 1994. A *knotted1*-like homeobox gene in *Arabidopsis* is expressed in the vegetative meristem and dramatically alters leaf morphology when overexpressed in transgenic plants. Plant Cell **6**, 1859–1876.

Liu C, Yu H, Li L. 2019. SUMO modification of LBD30 by SIZ1 regulates secondary cell wall formation in *Arabidopsis thaliana*. PLoS Genetics **15**, 1–19.

Long JA, Moan EI, Medford JI, Barton MK. 1996. A member of the KNOTTED class of homeodomain proteins encoded by the *STM* gene of *Arabidopsis*. Nature **379**, 66–69.

Machida C, Nakagawa A, Kojima S, Takahashi H, Machida Y. 2015. The complex of ASYMMETRIC LEAVES (AS) proteins plays a central role in antagonistic interactions of genes for leaf polarity specification in *Arabidopsis*. WIREs Developmental Biology **4**, 655–671.

Mallory AC, Dugas DV, Bartel DP, Bartel B. 2004. MicroRNA regulation of NAC-domain targets is required for proper formation and separation of adjacent embryonic, vegatative, and floral organs. Current Biology **14**, 1035–1046.

Mansfield SG, Briarty LG. 1991. Early embryogenesis in *Arabidopsis thaliana* II. The developing embryo. Canadian Journal of Botany **69**, 461–476.

Matsumoto N, Okada K. 2001. A homeobox gene, *PRESSED FLOWER*, regulates lateral axis-dependent development of *Arabidopsis* flowers. Genes & Development **15**, 3355–3364.

McConnell JR, Barton MK. 1998. Leaf polarity and meristem formation in *Arabidopsis*. Development **125**, 2935–2942.

McConnell JR, Emery J, Eshed Y, Bao N, Bowman J, Barton MK. 2001. Role of *PHABULOSA* and *PHAVOLUTA* in determining radial patterning in shoots. Nature **411**, 709–713.

Medford JI. 1992. Vegetative apical meristems. Plant Cell **4**, 1029–1039.

Meijer M, Murray JAH. 2000. The role and regulation of D-type cyclins in the plant cell cycle. Plant Molecular Biology **43**, 621–633.

Miyashima S, Honda M, Hashimoto K, Tatematsu K, Hashimoto T, Sato-Nara K, Okada K, Nakajima K. 2013. A comprehensive expression analysis of the Arabidopsis *MICRORNA165/6* gene family during embryogenesis reveals a conserved role in meristem specification and a non-cell-autonomous function. Plant and Cell Physiology **54**, 375–384.

Miyawaki K, Matsumoto-Kitano M, Kakimoto T. 2004. Expression of cytokinin biosynthetic isopentenyltransferase genes in *Arabidopsis*: Tissue specificity and regulation by auxin, cytokinin, and nitrate. Plant Journal **37**, 128–138.

Mockaitis K, Estelle M. 2008. Auxin receptors and plant development: A new signaling paradigm. Annual Review of Cell and Developmental Biology **24**, 55–80.

Moon J, Hake S. 2011. How a leaf gets its shape. Current Opinion in Plant Biology **14**, 24–30.

Müller D, Schmitz G, Theres K. 2006. *Blind* homologous *R2R3 MYB* genes control the pattern of lateral meristem initiation in *Arabidopsis*. Plant Cell **18**, 586–597.

Nakata M, Matsumoto N, Tsugeki R, Rikirsch E, Laux T, Okada K. 2012. Roles of the middle domain–specific *WUSCHEL-RELATED HOMEOBOX* genes in early development of leaves in *Arabidopsis*. Plant Cell **24**, 519–535.

Nardmann J, Ji J, Werr W, Scanlon MJ. 2004. The maize duplicate genes *narrow sheath1* and *narrow sheath2* encode a conserved homeobox gene function in a lateral domain of shoot apical meristems. Development **131**, 2827–2839.

Naz AA, Raman S, Martinez CC, Sinha NR, Schmitz G, Theres K. 2013. *Trifoliate* encodes an MYB transcription factor that modulates leaf and shoot architecture in tomato. Proceedings of the National Academy of Sciences USA **110**, 2401–2406.

Nishimura C, Ohashi Y, Sato S, Kato T, Tabata S, Ueguchi C. 2004. Histidine kinase homologs that act as cytokinin receptors possess overlapping functions in the regulation of shoot and root growth in Arabidopsis. Plant Cell **16**, 1365–1377.

Nogueira FTS, Madi S, Chitwood DH, Juarez MT, Timmermans MCP. 2007. Two small regulatory RNAs establish opposing fates of a developmental axis. Genes & Development **21**, 750–755.

Nolan TM, Vukasinovic N, Liu D, Russinova E, Yin Y. 2020. Brassinosteroids: Multidimensional regulators of plant growth, development, and stress responses. Plant Cell **32**, 295-318.

Norberg M, Holmlund M, Nilsson O. 2005. The *BLADE ON PETIOLE* genes act redundantly to control the growth and development of lateral organs. Development **132**, 2203–2213.

Okushima Y, Fukaki H, Onoda M, Theologis A, Tasaka M. 2007. ARF7 and ARF19 regulate lateral root formation via direct activation of *LBD*/*ASL* genes in *Arabidopsis*. Plant Cell **19**, 118–130.

Otsuga D, DeGuzman B, Prigge MJ, Drews GN, Clark SE. 2001. *REVOLUTA* regulates meristem initiation at lateral positions. Plant Journal **25**, 223–236.

Pekker I, Alvarez JP, Eshed Y. 2005. Auxin response factors mediate *Arabidopsis* organ asymmetry via modulation of KANADI Activity. Plant Cell **17**, 2899–2910.

Perales M, Reddy GV. 2012. Stem cell maintenance in shoot apical meristems. Current Opinion in Plant Biology **15**, 10–16.

Phelps-Durr TL, Thomas J, Vahab P, Timmermans MCP. 2005. Maize rough sheath2 and its *Arabidopsis* orthologue ASYMMETRIC LEAVES1 Interact with HIRA, a predicted histone chaperone, to maintain *knox* gene silencing and determinacy during organogenesis. Plant Cell **17**, 2886–2898.

Prigge MJ, Otsuga D, Alonso JM, Ecker JR, Drews GN, Clark SE. 2005. Class III homeodomain-leucine zipper gene family members have overlapping, antagonistic, and distinct roles in Arabidopsis development. Plant Cell **17**, 61–76.

Ragni L, Belles-Boix E, Günl M, Pautot V. 2008. Interaction of *KNAT6* and *KNAT2* with *BREVIPEDICELLUS* and *PENNYWISE* in *Arabidopsis* Inflorescences. Plant Cell **20**, 888–900.

Raman S, Greb T, Peaucelle A, Blein T, Laufs P, Theres K. 2008. Interplay of miR164, *CUP-SHAPED COTYLEDON* genes and *LATERAL SUPPRESSOR* controls axillary meristem formation in *Arabidopsis thaliana*. Plant Journal **55**, 65–76.

Rast-Somssich MI, Zádníková P, Schmid S, Kieffer M, Kepinski S, Simon R. 2017. The *Arabidopsis JAGGED LATERAL ORGANS* (*JLO*) gene sensitizes plants to auxin. Journal of Experimental Botany **68**, 2741–2755.

Rast MI, Simon R. 2008. The meristem-to-organ boundary: More than an extremity of anything. Current Opinion in Genetics & Development **18**, 287–294.

Rast MI, Simon R. 2012. *Arabidopsis JAGGED LATERAL ORGANS* acts with *ASYMMETRIC LEAVES2* to coordinate *KNOX* and *PIN* expression in shoot and root meristems. Plant Cell **24**, 2917–2933.

Rebocho AB, Kennaway JR, Bangham JA, Coen E. 2017. Formation and shaping of the *Antirrhinum* flower through modulation of the *CUP* boundary gene. Current Biology **27**, 2610-2622.

Reinhardt D, Kuhlemeier C. 2002. Plant architecture. EMBO Reports **3**, 846–851.

Reinhardt D, Mandel T, Kuhlemeier C. 2000. Auxin regulates the initiation and radial position of plant lateral organs. Plant Cell **12**, 507–518.

Reinhardt D, Pesce E-R, Stieger P, Mandel T, Baltensperger K, Bennett M, Traas J, Friml J, Kuhlemeier C. 2005. Regulation of phyllotaxis by polar auxin transport. Nature **426**, 255–260.

Rhoades MW, Reinhart BJ, Lim LP, Burge CB, Bartel B, Bartel DP. 2002. Prediction of plant microRNA targets. Cell **110**, 513–520.

Riefler M, Novak O, Strnad M, Schmülling T. 2006. *Arabidopsis* cytokinin receptor mutant reveal functions in shoot growth, leaf senescence, seed size, germination, root development, and cytokinin metabolism. Plant Cell **18**, 40–54.

Roeder AHK, Ferrandiz C, Yanofsky MF. 2003. The role of the REPLUMLESS homeodomain protein in patterning the *Arabidopsis* fruit. Current Biology **13**, 1630–1635.

Rubin G, Tohge T, Matsuda F, Saito K, Scheible WR. 2009. Members of the *LBD* family of transcription factors repress anthocyanin synthesis and affect additional nitrogen responses in *Arabidopsis*. Plant Cell **21**, 3567–3584.

Sachs T. 1991. Cell polarity and tissue patterning in plants. Development **112**, 83–93.

Sakamoto T, Kamiya N, Ueguchi-Tanaka M, Iwahori S, Matsuoka M. 2001. KNOX homeodomain protein directly suppresses the expression of a gibberellin biosynthetic gene in the tobacco shoot apical meristem. Genes & Development **15**, 581–590.

Sarojam R, Sappl PG, Goldshmidt A, Efroni I, Floyd SK, Eshed Y, Bowman JL. 2010. Differentiating Arabidopsis shoots from leaves by combined YABBY activities. Plant Cell **22**, 2113–2130.

Satina S, Blakeslee AF. 1941. Periclinal chimeras in Datura stramonium in relation to development of leaf and flower. American Journal of Botany **28**, 862–871.

Satina S, Blakeslee AF, Avery A. 1940. Demonstration of the three germ layers in the shoot apex of Datura by means of induced polyploidy in periclinal chimeras. American Journal of Botany **27**, 895–905.

Sawa S, Watanabe K, Goto K, Liu YG, Shibata D, Kanaya E, Morita EH, Okada K. 1999. *FILAMENTOUS FLOWER*, a meristem and organ identity gene of *Arabidopsis*, encodes a protein with a zinc finger and HMG-related domains. Genes & Development **13**, 1079–1088.

Scanlon MJ. 2000. NARROW SHEATH1 functions from two meristematic foci during founder-cell recruitment in maize leaf development. Development **127**, 4573–4585.

Scanlon MJ. 2003. The polar auxin transport inhibitor N-1-naphthylphthalamic acid disrupts leaf inhibition, KNOX protein regulation, and formation of leaf margins in maize. Plant Physiology **133**, 597–605.

Scanlon MJ, Freeling M. 1997. Clonal sectors reveal that a specific meristematic domain is not utilized in the maize mutant *narrow sheath*. Developmental Biology **182**, 52–66.

Scanlon MJ, Schneeberger RG, Freeling M. 1996. The maize mutant *narrow sheath* fails to establish leaf margin identity in a meristematic domain. Development **122**, 1683–1691.

Schmitz G, Tillmann E, Carriero F, Fiore C, Cellini F, Theres K. 2002. The tomato *Blind* gene encodes a MYB transcription factor that controls the formation of lateral meristems. Proceedings of the National Academy of Sciences USA **99**, 1064–1069.

Schneeberger R, Freeling M, Tsiantis M, Langdale JA. 1998. The *rough sheath2* gene negatively regulates homeobox gene expression during maize leaf development. Development **125**, 2857–2865

Schulz R, Jensen WA. 1968. Capsella embryognesis: The egg, zygote, and young embryo. American Journal of Botany **55**, 807–819.

Schumacher K, Schmitt T, Rossberg M, Schmitz G, Theres K. 1999. The *Lateral suppressor* (*Ls*) gene of tomato encodes a new member of the VHIID protein family. Proceedings of the National Academy of Sciences USA **96**, 290–295.

Schwab R, Maizel A, Ruiz-Ferrer V, Garcia D, Bayer M, Crespi M, Voinnet O, Martienssen RA. 2009. Endogenous tasiRNAs mediate non-cell autonomous effects on gene regulation in *Arabidopsis thaliana*. PLoS ONE **4**, 4–9.

Semiarti E, Ueno Y, Tsukaya H, Iwakawa H, Machida C, Machida Y. 2001. The *ASYMMETRIC LEAVES2* gene of *Arabidopsis thaliana* regulates formation of a symmetric lamina, establishment of venation and repression of meristem-related homeobox genes in leaves. Development **128**, 1771–83.

Shani E, Yanai O, Ori N. 2006. The role of hormones in shoot apical meristem function. Current Opinion in Plant Biology **9**, 484–489.

Shi B, Guo X, Wang Y, Xiong Y, Wang J, Hayashi K, Lei J. 2018. Feedback from lateral organs controls shoot apical meristem growth by modulating auxin transport. Developmental Cell **44**, 204–216.

Shi B, Zhang C, Tian C, Wang J, Wang Q, Xu T, Xu Y, Ohno C, Sablowski R, Heisler MG, Theres K, Wang Y, Jiao Y. 2016. Two-step regulation of a meristematic cell population acting in shoot branching in *Arabidopsis*. PLoS Genetics **12**, 1–20.

Shuai B, Reynaga-Pena CG, Springer PS. 2002. The *LATERAL ORGAN BOUNDARIES* gene defines a novel, plant-specific gene family. Plant Physiology **129**, 747–761.

Siegfried KR, Eshed Y, Baum SF, Otsuga D, Drews GN, Bowman JL. 1999. Members of the *YABBY* gene family specify abaxial cell fate in *Arabidopsis*. Development **126**, 4117–4128.

Skoog F, Miller CO. 1957. Chemical regulation of growth and organ formation in plant tissues cultured in vitro. Syposium of the Society of Experimental Biology **11**, 118–130.

Skopelitis DS, Benkovics AH, Husbands AY, Timmermans MCP. 2017. Boundary formation through a direct threshold-based readout of mobile small RNA gradients. Developmental Cell **43**, 265-273.

Skopelitis DS, Husbands AY, Timmermans MCP. 2012. Plant small RNAs as morphogens. Current Opinion in Cell Biology **24**, 217–224.

Smith LG, Greene B, Veit B, Hake S. 1992. A dominant mutation in the maize homeobox gene, *Knotted-1*, causes its ectopic expression in leaf cells with altered fates. Development **116**, 21–30.

Smith HMS, Hake S. 2003. The interaction of two homeobox genes *BREVIPEDICELLUS* and *PENNYWISE*, regulates internode patterning in the Arabidopsis inflorescence. Plant Cell **15**, 1717–1727.

Soni R, Carmichael JP, Shah ZH, Murray JA. 1995. A family of cyclin D homologs from plants differentially controlled by growth regulators and containing the conserved retinoblastoma protein interaction motif. Plant Cell **7**, 85–103.

Souer E, Van Houwelingen A, Bliek M, Kloos D, Mol J, Koes R. 1998. Co-suppression of *nam* and homologous gene leads to a reduction in axillary meristem formation and increased leaf and stem size in *Petunia*: A possible role for NAC domain genes in plant development. Flowering Newsletter **26**, 36–46.

Souer E, Van Houwelingen A, Kloos D, Mol J, Koes R. 1996. The *No Apical Meristem* gene of Petunia is required for pattern formation in embryos and flowers and is expressed at meristem and primordia boundaries. Cell **85**, 159–170.

Soyars CL, James SR, Nimchuk ZL. 2016. Ready, aim, shoot: Stem cell regulation of the shoot apical meristem. Current Opinion in Plant Biology **29**, 163–168.

Steeves TA, Sussex IM. 1989. Patterns in Plant Development.

Stirnberg P, Van de Sande K, Leyser HMO. 2002. *MAX1* and *MAX2* control shoot lateral branching in *Arabidopsis*. Development **129**, 1131–1141.

Stracke R, Werber M, Weisshaar B. 2001. The *R2-R3-MYB* gene family in *Arabidopsis thaliana*. Cell Signaling & Gene Regulation **4**, 447–456.

Sussex IM. 1951. Experiments on the cause of dorsiventrality in leaves. Nature **167**, 651–652.

Sussex IM. 1952. Regeneration of the potato shoot apex. Nature **170**, 755–757.

Sussex IM. 1954. Experiments on the cause of dorsiventrality in leaves. Nature **174**, 351–352.

Swarup R, Bennett M. 2003. Auxin transport: The fountain of life in plants? Developmental Cell **5**, 824–826.

Szymkowiak EJ, Sussex IM. 1996. What chimeras can tell us. Annual Review of Plant Physiology and Plant Molecular Biology **47**, 351–376.

Takada S, Hibara K, Ishida T, Tasaka M. 2001. The *CUP-SHAPED COTYLEDON1* gene of *Arabidopsis* regulates shoot apical meristem formation. Development **128**, 1127–1135.

Tang G, Reinhart BJ, Bartel DP, Zamore PD. 2003. A biochemical framework for RNA silencing in plants. Genes & Development **17**, 49–63.

Thatcher LF, Powell JJ, Aitken EAB, Kazan K, Manners JM. 2012. The lateral organ boundaries domain transcription factor LBD20 functions in Fusarium wilt susceptibility and jasmonate signaling in Arabidopsis. Plant Physiology **160**, 407–418.

Timmermans MCP, Hudson A, Becraft PW, Nelson T. 1999. ROUGH SHEATH2: A MYB protein that represses *KNOX* homeobox genes in maize lateral organ primordia. Science **284**, 151–153.

Truskina J, Vernoux T. 2018. The growth of a stable stationary structure: Coordinating cell behavior and patterning at the shoot apical meristem. Current Opinion in Plant Biology **41**, 83–88.

Tsiantis M, Schneeberger R, Golz JF, Freeling M, Langdale JA. 1999. The maize *rough sheath2* gene and leaf development programs in monocot and dicot plants. Science **284**, 154–156.

Vandenbussche M, Horstman A, Zethof J, Koes R, Rijpkema AS, Gerats T. 2009. Differential recruitment of WOX transcription factors for lateral development and organ fusion in *Petunia* and *Arabidopsis*. Plant Cell **21**, 2269–2283.

Vanneste S, Friml J. 2009. Auxin: A trigger for change in plant development. Cell **136**, 1005–1016.

Venglat SP, Dumonceaux T, Rozwadowski K, Parnell L, Babic V, Keller W, Martienssen R, Selvaraj G, Datla R. 2002. The homeobox gene *BREVIPEDICELLUS* is a key regulator of inflorescence architecture in *Arabidopsis*. Proceedings of the National Academy of Sciences USA **99**, 4730–4735.

Vernoux T, Kronenberger J, Grandjean O, Laufs P, Traas J. 2000. *PIN-FORMED 1* regulates cell fate at the periphery of the shoot apical meristem. Development **127**, 5157–5165.

Villanueva JM, Broadhvest J, Hauser BA, Meister RJ, Schneitz K, Gasser CS. 1999. I*NNER NO OUTER* regulates abaxial-adaxial patterning in *Arabidopsis* ovules. Genes *&* Development **13**, 3160–3169.

Vollbrecht E, Reiser L, Hake S. 2000. Shoot meristem size is dependent on inbred background and presence of the maize homeobox gene, *knotted1*. Development **127**, 3161–3172.

Vollbrecht E, Veit B, Sinha N, Hake S. 1991. The developmental gene *Knotted-1* is a member of a maize homeobox gene family. Nature **350**, 241–243.

Vroeman CW, Mordhorst AP, Albrecht C, Kwaaitaal MACJ, De Vries SC. 2003. The *CUP-SHAPED COTYLEDON3* gene is required for boundary and shoot meristem formation in *Arabidopsis*. Plant Cell **15**, 1563–1577.

Waites R, Hudson A. 1995. *Phantastica*: A gene required for dorsoventrality of leaves in *Antirrhinum majus*. Development **121**, 2143–2154.

Waites R, Selvadurai HRN, Oliver IR, Hudson A. 1998. The *PHANTASTICA* gene encodes a MYB transcription factor involved in growth and dorsoventrality of lateral organs in *Antirrhinum*. Cell **93**, 779–789.

Walbot V. 1985. On the life strategies of plants and animals. Trends in Genetics **1**, 165–169.

Wang B, Smith SM, Li J. 2018. Genetic regulation of shoot architecture. Annual Review of Plant Biology **69**, 437-468.

Wang Y, Wang J, Shi B, Yu T, Qi J, Meyerowitz EM, Jiao Y. 2014. The stem cell niche in leaf axils is established by auxin and cytokinin in *Arabidopsis*. Plant Cell **26**, 2055–2067.

Weigel D, Jürgens G. 2002. Stem cells that make stems. Nature **415**, 751–754.

Weir I, Lu J, Cook H, Causier B, Schwarz-Sommer Z, Davies B. 2004. *CUPULIFORMIS* establishes lateral organ boundaries in *Antirrhinum*. Development **131**, 915–922.

Werner T, Motyka V, Laucou V, Smets R, Van Onckelen H, Schmülling T. 2003. Cytokinin-deficient transgenic *Arabidopsis* plants show multiple developmental alterations indicating opposite functions of cytokinins in the regulation of shoot and root meristem activity. Plant Cell **15**, 2532–2550.

Werner T, Motyka V, Strnad M, Schmulling T. 2001. Regulation of plant growth by cytokinin. Proceedings of the National Academy of Sciences USA **98**, 10487–10492.

Wu G, Lin WC, Huang T, Poethig RS, Springer PS, Kerstetter RA. 2008. KANADI1 regulates adaxial-abaxial polarity in *Arabidopsis* by directly repressing the transcription of *ASYMMETRIC LEAVES2*. Proceedings of the National Academy of Sciences USA **105**, 16392–16397.

Xu C, Cao H, Zhang Q, Wang H, Xin W, Xu E, Zhang S, Yu R, Yu D, Hu Y. 2018. Control of auxin-induced callus formation by bZIP59-LBD complex in *Arabidopsis* regeneration. Nature Plants **4**, 108–115.

Xu L, Xu Y, Dong A, Sun Y, Pi L, Xu Y, Huang H. 2003. Novel *as1* and *as2* defects in leaf adaxial-abaxial polarity reveal the requirement for *ASYMMETRIC LEAVES1* and *2* and *ERECTA* functions in specifying leaf adaxial identity. Development **130**, 4097–4107.

Yanai O, Shani E, Dolezal K, Tarkowski P, Sablowski R, Sandberg G, Samach A, Ori N. 2005. *Arabidopsis* KNOXI proteins activate cytokinin biosynthesis. Current Biology **15**, 1566–1571.

Yang F, Wang Q, Schmitz G, Müller D, Theres K. 2012. The bHLH protein ROX acts in concert with RAX1 and LAS to modulate axillary meristem formation in *Arabidopsis*. Plant Journal **71**, 61–70.

Yao X, Wang H, Li H, Yuan Z, Li F, Yang L, Huang H. 2009. Two types of cis-acting elements control the abaxial epidermis-specific transcription of the *MIR165a* and *MIR166a* genes. FEBS Letters **583**, 3711–3717.

Zgurski JM, Sharma R, Bolokoski DA, Schultz EA. 2005. Asymmetric auxin response precedes asymmetric growth and differentiation of *asymmetric leaf1* and *asymmetric leaf2 Arabidopsis leaves*. Plant Cell **17**, 77–91.

Zhao M, Yang S, Chen CY, Li C, Shan W, Lu W, Cui Y, Liu X, Wu K. 2015. *Arabidopsis* BREVIPEDICELLUS interacts with the SWI2/SNF2 chromatin remodeling ATPase BRAHMA to regulate *KNAT2* and *KNAT6* expression in control of inflorescence architecture. PLoS Genetics **11**, 1–21.

Chapter 1

Identification and Characterization of Protein Interactors of LATERAL ORGAN FUSION1 (LOF1)

Abstract

The boundary region separates the emerging lateral organ from the meristem. *LATERAL ORGAN FUSION1* (*LOF1*) encodes a MYB-domain transcription factor expressed in boundary regions. *LOF1* is expressed at the paraclade junction between the axillary branch and cauline leaf, the primary stem and axillary branch, and other boundaries. *lof1-1* loss-of-function mutants display organ fusion between the cauline leaf and axillary branch and lack accessory meristems. These phenotypes suggest that LOF1 functions in meristem maintenance and organ separation. In order to identify additional proteins that are important for organ separation and meristem maintenance or other aspects of plant development, we identified proteins that interact with LOF1 in a yeast two-hybrid screen. The isolated proteins have a pattern of involvement in photosynthesis, chloroplast development, or response/sensing of abiotic stress in the chloroplast and/or mitochondria. Several transcription factors were identified as putative LOF1 interactors (MYB32, LRB2, WHY3, and ATHB4). These proteins were of interest because transcription factors often act in complexes with other transcription factors. LOF1 interacted with WHY3 and ATHB4 in yeast but did not appear to interact with closely related proteins, WHY1 and HAT3, respectively. T-DNA insertional mutants of genes of interest were obtained and characterized. These mutants were crossed to the *lof1-1*

mutant to look for evidence of genetic interactions. Although many double mutants were analyzed at different developmental stages, we were not able to identify consistent double mutant phenotypes. In summary, LOF1 protein interactions are highly specific. LOF1 interacts with proteins involved in response to abiotic stress that are subcellularly localized to the plastid and/or mitochondria.

Introduction

All post-embryonic above-ground organs in plants are produced by the shoot apical meristem (SAM). Each organ arises first as a protrusion from the SAM that grows out and develops (Steeves and Sussex, 1989). The boundary region separates the developing organs from the meristem (Aida and Tasaka, 2006). The boundary region is characterized by lower rates of cell division and smaller cell volume compared to surrounding regions (Hussey, 1971; Callos and Medford, 1994). Plants that fail to properly separate meristematic stem cells and developing organs by forming a boundary region result in organ fusions (Aida, 1997; Aida *et al.*, 1999; Lee *et al.*, 2009; Bell *et al.*, 2012; Colling *et al.*, 2015). *LATERAL ORGAN FUSION1* (*LOF1*) encodes a MYB transcription factor expressed in cells at the base of floral organs, pedicel-stem junctions, adaxial side of the rosette leaf base, and junctions between inflorescence meristem and flower primordia (Lee *et al.*, 2009). *LOF1* is also expressed in the paraclade junction between the axillary branch and primary stem and between the cauline leaf and axillary branch (Lee *et al.*, 2009). Loss-of-function mutations in *lof1* result in fusion between the axillary branch and cauline leaf and loss of accessory bud formation (Lee *et al.*, 2009).

Loss-of-function mutations of *lof2*, a closely related gene, do not cause any abnormal phenotypes. However, *lof1lof2* double mutants have flower pedicel and primary inflorescence fusions and decurrent strands between the cauline leaf and primary stem (Lee *et al.*, 2009). Therefore, *LOF1* and *LOF2* function partially redundantly in organ separation.

Transcription factors modulate target genes either by activation or repression of transcription. MYB-(myeloblastosis) domain containing proteins are transcription factors. The MYB domain binds DNA directly, and MYB domains are highly conserved (Dubos *et al.*, 2010). This domain consists of four or fewer amino acid repeats (approximately 52 amino acids in length) that form three alpha helices. The second and third helices form a helix-turn-helix structure with a hydrophobic core (Ogata *et al.*, 1994). The third helix makes contact with and binds DNA (Jia *et al.*, 2004). MYB proteins contain three types of repeats – named R1, R2, and R3 – and are divided into classes depending on which repeats are present and their arrangement in each protein. LOF1 and LOF2 are part of subgroup 21 of R2R3 MYB family of transcription factors, which contains a FxDFL motif of unknown function in the C-termini (Stracke *et al.*, 2001). The R2R3 class of proteins is widely expanded in plants compared to animals, leading to the theory that R2R3 proteins in plants play an important role in plant-specific processes (Martin and Paz-Ares, 1997).

MYB proteins are known to act in transcription factor complexes. A WD-repeat/bHLH/MYB complex acts as a regulator to modulate anthocyanin accumulation (Payne *et al.*, 2000; Ramsay and Glover, 2005). Anthocyanins are a class of flavonoids

that protect against UV radiation, regulate pigmentation in flowers to attract pollinators, and function against insect and pathogen attack (Vogt *et al.*, 1994; Winkel-Shirley, 2002; Gould, 2004; Lepiniec *et al.*, 2006). Anthocyanin accumulation is stimulated by developmental signals and different environmental stresses (Loreti *et al.*, 2008; Shan *et al.*, 2009). In the WD-repeat/bHLH/MYB complex, the WD-repeat protein TRANSPARENT TESTA GLABRA1 (TTG1) recruits basic-helix-loop-helix (bHLH) transcription factors and the R2R3 MYB transcription factors (MYB75, MYB90, MYB113, and MYB114) (Zimmermann *et al.*, 2004; Gonzalez *et al.*, 2008; Rowan *et al.*, 2009). This complex upregulates the expression of anthocyanin biosynthesis genes, such as *DIHYDROFLAVONOL REDUCTASE* (*DFR*) (Shirley *et al.*, 1995; Gonzalez *et al.*, 2008). Another variation of the WD-repeat/bHLH/MYB complex, consisting of TTG1, GLABRA3 (GL3), and MYB23, mediates the development of trichomes (Walker *et al.*, 1999; Zhao *et al.*, 2008). This suggests interactions between MYB and bHLH are utilized for multiple plant processes.

The binding of R2R3-MYB transcription factors to other proteins can modulate their activities (Dubos *et al.*, 2010). BRs (brassinosteroids) comprise a class of plant hormones that are responsible for a wide variety of developmental processes, such as vascular differentiation, cell expansion, and reproductive development [reviewed in (Nolan *et al.*, 2020)]. BES1/BZR1 (BRI1-ETHYLMETHANE SULFONATE SUPPRESSOR1/ BRASSINAZOLE-RESISTANT1) is a transcription factor downstream of the BR signaling cascade that regulates transcription of BR response genes. MYB30 and BES1 interact to promote target gene expression of a specific subset of genes that

cannot be regulated without MYB30 (He *et al.*, 2002; Li *et al.*, 2009). Thus, the binding of MYB30 to BES1 allows BES1 to activate additional BR-response genes. MYB proteins are not only involved in BR signaling but are known to interact with at least one component of the auxin signaling pathway. MYB77 was shown to interact with AUXIN RESPONSE FACTOR (ARF) proteins to regulate expression of auxin response genes and modulate lateral root development (Shin *et al.*, 2007). Therefore, MYBs may participate in modulation of gene expression in response to plant hormones.

MYB proteins also interact with components of the light signaling pathway. LONG AFTER FAR-RED LIGHT (LAF1)/MYB18 interacts with LONG HYPOTCOTYL IN FAR RED1 (HFR1), a bHLH protein, to positively regulate of red light signaling and inhibit hypocotyl growth (Yang *et al.*, 2009). BLUE INSENSITIVE TRAIT1 (BIT1)/REGULATOR OF AXILLARY MERSITEM2 (RAX2)/MYB38 controls expression of blue-light dependent genes. In the light, CRYPTOCHROME1 (CRY1) - a UV-A and blue-light photoreceptor – interacts with and stabilizes BIT1. In the dark, BIT1 is degraded after interaction with CONSTITUTIVE PHOTOMORPHOGENIC1 (COP1) (Hong *et al.*, 2008). *BIT1*/*RAX2* is also one of three *RAX* genes that positively regulate axillary meristem formation (Keller *et al.*, 2006; Müller *et al.*, 2006). These data suggest MYBs are important components in both red and blue light signaling.

Because MYBs are known to act in complexes with other transcription factors, we performed a yeast two-hybrid screen to identify proteins that interact with LOF1. Many of the proteins isolated in the screen are involved in response to abiotic stress and/or are

predicted to be subcellularly localized to the chloroplast or mitochondria. Focusing specifically on transcription factors, we identified several interactors of interest. One MYB protein of interest, MYB32, is part of subgroup 4 of R2-R3 MYB transcription factors (Stracke *et al.*, 2001). *MYB32* is expressed in the leaves, developing lateral roots, and anthers. *MYB32* is involved in pollen development, and genetic lesions in *MYB32* result in 50% defective, "donut" shaped pollen (Preston *et al.*, 2004). Little else is known about *MYB32*. Another protein of interest that was identified multiple times in the screen is WHIRLY3 (WHY3), a transcription factor that is subcellularly localized in both the chloroplast and nucleus (Krause *et al.*, 2005; Grabowski *et al.*, 2008). WHY3 functions in plastid DNA repair (Maréchal *et al.*, 2009). The third interactor of interest is ARABIDOPSIS THALIANA HOMEOBOX4 (ATHB4), an HD-Zip class II transcription factor that functions in the shade avoidance response, cotyledon development, and meristem maintenance (Sorin *et al.*, 2009; Turchi *et al.*, 2013). Our final LOF1 interactor of interest in this study is LIGHT-RESPONSIVE BRIC-A-BRAC/TRAMTRACK/BROAD2 (LRB2) – a negative regulator of photomorphogenesis in response to red light. LRB2 plays a role in the degradation of PHYB and PHYD (Christians *et al.*, 2012; Ni *et al.*, 2014). In order to evaluate genetic interactions between *LOF1* and genes that encode for our proteins of interest, double mutants were examined.

Results

Yeast Two-Hybrid Assay to Identify LOF1-Interacting Proteins

Transcription factors in plants often work together in complexes to regulate gene expression (Smaczniak *et al.*, 2012; Xu *et al.*, 2015); therefore, LOF1 might interact with other transcription factors to fulfill its function. To identify undiscovered LOF1 interactors, ~570,000 interactions were screened using the Matchmaker® Gold Yeast Two-Hybrid System (Clontech). The full-length *LOF1* coding region was cloned into pGBKT7, generating a translational fusion between LOF1 and the GAL4 DNA-binding domain (BD). GAL4 is a yeast transcription factor used in the expression of galactose-induced genes. The library used in the screen was made from cDNA isolated from RNA extracted from inflorescence tips of wild-type and *ap1cal* mutant *Arabidopsis* (Kempin *et al.*, 1995). The library was cloned into pGADT7, which allowed the library proteins to be translationally fused to the GAL4 activation domain (AD). We chose this library for the screen because it is enriched in tissue that contains regions in the plant where *LOF1* is expressed; thus, the tissue was theoretically rich in LOF1-interacting proteins. Appropriate tests to check if BD-LOF1 alone could activate reporter gene expression were carried out. After the transformation, yeast cells were plated on minimal media (SD) lacking tryptophan (for selection of BD-LOF1 plasmid), leucine (for selection of AD library plasmid), histidine and adenine (to select for expression of reporter genes). 3-amino-triazole (3-AT), which competitively inhibits the product of the histidine biosynthetic gene *HISTIDINE3* (*HIS3*) in yeast, was added to the plates for stringency in yeast growth. For example, increasing the 3-AT concentration in the media raises the

minimum amount of *HIS3* gene expression necessary for yeast to grow. Colonies that grew in the primary screen were re-streaked on plates a second time to confirm their positive phenotype and to ensure they arose from single cells. Colonies surviving from the screen were additionally plated on SD -Trp/-Leu and Aureobasidin A (A) (to select for the expression of reporter genes). Aureobasidin A is a fungicide that kills wild-type yeast at low concentrations, and Matchmaker Gold© yeast contain the *AUR1-C* reporter gene that confers resistance to Aureobasidin A. In total, 143 yeast colonies grew on both types of selective media plates.

To determine the number of redundant isolates, colonies were grown in SD -Leu medium. Under these conditions, the AD plasmids were retained and the BD-LOF1 plasmid was expected to be lost, due to lack of selective pressure. Yeast was pelleted and AD plasmids were extracted. Plasmids were used in PCR reactions with primers flanking the cDNA insertion site of the library plasmid. Based on the size of the PCR products derived from the insertions, nine of the yeast colonies appeared to contain more than one AD-library plasmid with the highest number in one colony being four (data not shown).

To confirm that isolated plasmids contained protein fusions that interacted with LOF1, each plasmid was retransformed into yeast containing BD-LOF1. Yeast from these colonies were grown up in SD -Leu to select for the AD-library plasmid. After growth, plasmids were extracted from the yeast cells, transformed into *E. coli*, and selected on plates containing ampicillin. Positive *E. coli* colonies were grown up and plasmids were extracted. Individual plasmids isolated from the screen were retransformed yeast that already contained the full-length LOF1 in pGBKT7 plasmid. Transformed

yeast were grown on both SD -Trp -Leu (to select for the BD and AD plasmids), SD -Trp -Leu -Ade -His +3-AT and SD -Trp/-Leu + A (to select for protein-protein interactions). In instances when multiple AD plasmids were present, it was necessary to determine which AD plasmid allowed yeast growth on selective media. The yeast plasmid DNA extract was transformed into *E. coli* and plated on media with ampicillin to select for colonies with AD-library plasmids. *E. coli* colonies recovered from this screen were used in a colony PCR reaction to amplify the cDNA insertion. The size of the PCR products allowed at least one colony containing each individual AD-library plasmid isolated from the original yeast colony to be identified. Subsequently, each representative *E. coli* colony was grown up and AD plasmids were extracted. The plasmids were then transformed into yeast containing full-length BD-LOF1 in pGBKT7 plasmids. Transformed yeast were plated on SD -Trp/-Leu to select for transformants. At least one colony from each transformation was streaked out before patching on selective media. Patching on selective media (SD -Trp/-Leu/-Ade/-His + 3-AT) allowed determination of which library plasmids isolated from the *E. coli* colonies allowed yeast growth, and identified the putative LOF1 interactor, which was further characterized.

A total of 68 clones were identified that contained cDNAs encoding AD fusion proteins that potentially interacted with LOF1. *E. coli* cultures containing the AD plasmids from these 68 colonies were grown up, and plasmids were isolated. AD plasmid insertions were sequenced. Of the 68, 16 colonies contained cDNA sequences that were out of frame with the AD. Seven of the out-of-frame colonies contained *ZINC FINGER HOMEODOMAIN1* (*ZFHD1*)/*ARABIDOPSIS THALIANA HOMEOBOX PROTEIN29*

(*ATHB29*) (AT1G69600), which encodes a homeodomain transcription factor induced by drought, salinity, and abscisic acid (ABA) (Tran *et al.*, 2007). All seven clones were in the same frame – shifted one basepair in the 3' direction of the original *ZFHD1* coding sequence. This frameshift produces a 37 amino acid protein of the following sequence: VFQTTTTTSKLSSHRRRTNCHRRNGCLLQRVFEKPRG. This protein does not contain any common protein motifs according to available databases. Since *ZFHD1* clones were obtained many times in the yeast two-hybrid assay, we considered the possibility that *ZFHD1* is translated in frame. To address this, *ZFHD1* was cloned into the pGADT7 vector, in frame with the AD. We were not able to recover yeast cells containing this plasmid; therefore, it appears that *AD-ZFHD1* is toxic to the Matchmaker Gold strain yeast. It remains to be determined if ZFHD1 and LOF1 interact in yeast.

After sequencing and grouping clones representative of the same cDNA together, 42 unique coding sequences remained (Table 1.1). A large number of these putative LOF1-interacting proteins have been implicated in abiotic stress responses or association with the chloroplast and/or mitochondria (Chapter 2). Four LOF1 interactors were obtained multiple times in the yeast two-hybrid screen. RGS-HXK1 INTERACTING PROTEIN 1 (RHIP1) (At4G26410) was isolated six times, the most frequent of any clone (Table 1.1). *RHIP1* is reported to be involved in glucose-regulated gene expression (Huang *et al.*, 2015). Glucose acts as a metabolite and signaling molecule to affect plant growth and development (Sheen, 2014). In *Arabidopsis*, glucose is sensed in three different ways - a G-protein coupled pathway involving *REGULATOR OF G-PROTEIN SIGNALING 1* (*RGS1*), the *HEXOKINASE 1* (*HXK1*) pathway, and the *SNF1-RELATED*

KINASE1/TARGET of RAPAMYCIN (*SnRK1/TOR*) pathway (Smeekens *et al.*, 2010; Urano *et al.*, 2012). Out of these three glucose-sensing pathways, RHIP1 interacts with important proteins in two of the pathways - RGS1 and HXK1 (Huang *et al.*, 2015). RHIP1 serves as a physical scaffold for RGS1 and HXK1 to integrate sugar-sensing pathways (Huang *et al.*, 2015). *rhip1* mutants display developmental defects. *rhip1-1* and *rhip1-2* mutants have longer roots in seedlings and larger inflorescences in adult plants compared to control plants. *rhip1-2* are also more sensitive to 6% glucose compared to control plants (Huang *et al.*, 2015).

FERREDOXIN 2 (FD2) (At1G60950), an iron-sulfur containing protein that acts as an electron acceptor for photosystem I (PSI) during photosynthesis in the chloroplast (Arnon, 1988; Somers *et al.*, 1990), was obtained three times in the screen (Table 1.1). FD2 is also an integral part of the ferredoxin-thioredoxin reductase (FTR)/thioredoxin (TRX) and NADPH-dependent thioredoxin reductase (NTRC) redox hubs in the chloroplast, providing reducing power (Leister *et al.*, 2019). Loss-of-function mutants of *fd2* in *Arabidopsis* accumulate high levels of reactive oxygen species (ROS) in the chloroplast (Voss *et al.*, 2008). Additionally, *fd2* loss-of-function mutants are better acclimated than wild-type controls to long-term, high-light conditions (Liu *et al.*, 2013). It was reported that *fd2* knock-out mutants in *Arabidopsis* were more susceptible to infection by *Pseudomonas syringae* and *Golovinomyes cichoracearum* (Wang *et al.*, 2018). Thus, *FD2* plays a role in plant defense and response to abiotic stress conditions.

At2G41600, a mitochondrial glycoprotein of which little is known, was isolated three times in the assay. Lastly, *WHIRLY 3* (*WHY3*), which is discussed below, was obtained twice (Table 1.1).

Four transcription factors of interest were selected for further analysis (Table 1.1): MYB DOMAIN PROTEIN 32 (MYB32), HOMEOBOX LEUCINE ZIPPER PROTEIN 4 (HB4), LIGHT-REPONSE BTB 2 (LRB2), and WHIRLY 3 (WHY3) (Table 1.2). In summary, LOF1 interacts in yeast with a number of proteins that appear to be localized to the chloroplast and/or mitochondria as well as those involved in response to abiotic stress. LOF1 also interacts with a number of other proteins that function as transcription factors.

Investigation of Interaction of LOF1 with WHY1 and HAT3

Two of the interactors of interest – ATHB4 and WHY3 – function redundantly with other related proteins. *ATHB4* is functionally redundant with *HOMEOBOX ARABIDOPSIS THALIANA3* (*HAT3*) (Bou-Torrent *et al.*, 2012; Turchi *et al.*, 2013), and *WHY3* is functionally redundant with *WHIRLY1* (*WHY1*) (Maréchal *et al.*, 2009; Xiong *et al.*, 2009) (Table 1.2). ATHB4 and HAT3 are encoded by paralogous genes and share 93% protein identity (Ciarbelli *et al.*, 2008)**;** WHY1 and WHY3 share 94% protein identity (Cappadocia *et al.*, 2010). Therefore, we tested for potential interaction between LOF1 and WHY1 or HAT3 using a yeast two-hybrid assay. First, *WHY1* and *HAT3* were separately cloned into AD library plasmids. Then, *WHY1* pGADT7 and *HAT3* pGADT7 were transformed into Matchmaker Gold strain yeast containing full-length LOF1 in

pGBKT7. Yeast were plated on SD -Trp -Leu (to select for the BD-LOF1 and AD plasmids, respectively) as well as SD -Trp/-Leu/-Ade/-His + 3-AT (to select for protein-protein interactions). Transformants grew on selective media for the BD-LOF1 and the AD plasmids but did not grow on selective media for expression of reporter genes (protein-protein interactions) (Figure 1.1). Lack of growth on selective media suggests that WHY1 and HAT3 do not interact with LOF1. These data suggest LOF1 interaction is specific to WHY3 and ATHB4 and, despite the highly conserved amino acid sequences, LOF1 does not interact with closely related proteins WHY1 and HAT3. These findings indicate that LOF1 interactions are very specific.

Characterization of *MYB32*, *LRB2*, *WHY3*, *WHY1*, *ATHB4*, and *HAT3* Mutants

If the proteins of interest (Table 1.2) interact with LOF1 *in planta*, then we might find evidence of genetic interactions. To obtain examine possible genetic interactions between LOF1 and interacting proteins, plants with mutant alleles of the genes encoding the interactors of interest were obtained. We also examined mutants in WHY3 and ATHB4, to look for evidence of genetic interactions. For *MYB32*, we obtained seeds for one T-DNA insertion mutant (Alonso *et al.*, 2003). *atmyb32-2* (SALK_132874) was reported to contain a T-DNA insertion in exon 1 and represent a knockout mutation (Preston *et al.*, 2004). However, no T-DNA insertion could be confirmed in the plants from the provided seed. When the previous generation of seed was obtained from the same source, no T-DNA insertion could be confirmed from that stock either. It is possible

that due to the aberrant pollen phenotype (Preston *et al.*, 2004), the T-DNA insertion was lost during seed propagation. For this reason, *MYB32* was not further studied.

Three T-DNA insertion mutants were available for *LRB2 – lrb2-1* (SALK_001013), *lrb2-2* (SALK_044446), and *lrb2-3* (SALK_100118) (Christians *et al.*, 2012). All three alleles were previously described as knockouts (Christians *et al.*, 2012; Hu *et al.*, 2014). *lrb2-1* was reported to have a T-DNA insertion in intron two, but we could not find this insertion in the plants grown from stock seeds. Because the provided T-DNA insertion site from the ABRC is only accurate within ~300 base pairs, we sequenced the insertion site of the *lrb2-2* and *lrb2-3* T-DNA alleles from the left border. To locate the exact site of the T-DNA insertion, PCR was performed with primers located inside *LRB2* and on the left border of the T-DNA. The insertion site of *lrb2-3* was after base pair 2376 in the published genomic sequence and after base pair 1206 in the genomic sequence for *lrb2-2*, respectively (Figure 1.2 A). To determine if *lrb2-2* and *lrb2-3* were null alleles, RT-PCR amplifying sequences downstream of the T-DNA insertion site was performed on *lrb2-2* and *lrb2-3* as well as wild-type controls. For both alleles, no *LRB2* transcript was detected, while *LRB2* transcript was detected for wild-type controls (Figure 1.2 B; 1.2 C). This evidence is consistent with *lrb2-2* and *lrb2-3* being null alleles, as previously suggested (Christians *et al.*, 2012; Hu *et al.*, 2014).

One T-DNA insertion allele was obtained for *WHY3*, *why3-1* (SALK_005345C) (Alonso *et al.*, 2003). This allele has not been previously analyzed. RT-PCR analysis demonstrated that the T-DNA insertion in *why3-1*, predicted to be in the 5’ UTR, does

not appear to impact transcript levels of *WHY3* compared to wild-type control plants (data not shown).

A second *why3* allele, *KO3* [Seattle TILLING Project; (Maréchal *et al.*, 2009)], has a mutation that changes a TGG codon to a TGA stop codon in the third exon of *WHY3*, leading to a truncated protein of 87 amino acids (Maréchal *et al.*, 2009) (Figure 1.3 A). This single base pair change was confirmed in the *KO3* mutants by allele-specific PCR. Previous data suggests that some WHY3 protein is still present in *KO3* mutant plants, but in *why3 why1* double mutants WHY1 and WHY3 proteins are undetectable (Maréchal *et al.*, 2009). *WHY3* RT-PCR using primers that anneal after the *KO3* mutation revealed that *KO3* plants had low levels of *WHY3* compared to the wild-type control (Figure 1.3 B). Any protein translated from the *KO3 WHY3* sequence is presumed to be non-functional due to a previous study that showed any WHY3 protein present in *KO3* plants could no longer bind DNA (Maréchal *et al.*, 2009). This suggests that *KO3* is at least a knock-down allele of *WHY3*.

For *WHY1*, *KO-1*/*why1-1* (SALK_023713), *KO-2*/*why1-2* (SALK_147680), and *why1-3* (CS65558) were obtained (Yoo *et al.*, 2007). *KO-1* and *why1-3* were reported to have insertion sites in the first intron. The *KO-2* T-DNA insertion site was reported in the second exon. After sequencing, it was revealed that *KO-2*/*why1-2* and *why1-3* had the same T-DNA insertion site located 297 base pairs into the published genomic sequence in the first exon (Figure1.4 A). *KO-1* had a T-DNA insertion site after base pair 271 of the genomic sequence, also in the first exon (Figure 1.4 A). *WHY1* RT-PCR experiments showed that *KO-2*/*why1-2* had reduced transcript levels when compared to wild-type

controls (Figure 1.4 B), and *KO-1* had no detectable *WHY1* transcript (Figure1.4 C). This suggests that *KO-2*/*why1-2* are knock-down alleles and *KO-1* is a null allele of *WHY1*.

Two T-DNA mutants were obtained for *ATHB4*: *athbb4-1* (SALK_104843) and *athb4-2* (SALK_121097). We could not locate a T-DNA insertion in *athb4-1* seed (Sorin *et al.*, 2009). Sequencing confirmed the presence of a T-DNA insertion in *athb4-2*, after base pair 43 of the published genomic sequence, in the 5' UTR (Figure 1.5 A). RT-PCR of *HB4* showed that *athb4-2* had lower transcript levels when compared to wild-type controls (Figure 1.5 B). This suggests that *athb4-2* is a knock-down allele of *ATHB4*.

Four T-DNA insertion alleles were obtained from the ABRC for *HAT3*: *hat3-1* (SALK_105877), *hat3-2* (SALK_083383), *hat3-3* (SALK_014055C), and *hat3-4* (SALK_105885). *hat3-3* had already been described as a null allele of *HAT3* (Turchi *et al.*, 2013). Sequencing of the T-DNA insertion sites showed that the insertion in *hat3-4* was after base pair 17 of the published genomic sequence, in the 5' UTR. *hat3-1* and *hat3-2* had the same T-DNA insertion location as *hat3-4* (Figure 1.6 A). The *hat3-3* T-DNA was located after base pair 395 of the genomic sequence in the first exon. RT-PCR showed that *hat3-2* had reduced transcript levels compared to wild-type controls, and *hat3-3* had no detectable transcript levels compared to wild-type controls (Figure 1.6 B). This suggests that *hat3-2* (and presumably also *hat3-1*) is a knock-down allele, and suggests that *hat3-3* is a knock-out allele of *HAT3*. RT-PCR of *HAT3* for *hat3-4* compared to wild-type controls revealed that *hat3-4* had reduced transcript levels (Figure 1.6 C). Therefore, *hat3-4* is a knock-down allele of *HAT3*.

First, phenotypes of the verified homozygous single mutants were evaluated and then crossed to *lof1-1* mutant plants to obtain homozygous double mutants. At least thirty plants of each genotype were evaluated at both the two-week (seedling) and 6-week (mature) time periods after germination for overall phenotypes as well as organ fusions. We also examined root phenotypes in seedlings. We did not see any enhancement or suppression of the *lof1-1* phenotype in these double mutants, nor were any new abnormal phenotypes observed.

We also examined published phenotypes for mutants of our genes of interest. *why1why3* double mutants were reported to have yellow, variegated leaves at a low frequency (about 5%) (Maréchal *et al.*, 2009). However, we were not able to observe a variegated phenotype in our double mutants that persisted throughout development. *athb4 hat3* double mutants were reported to have narrow cotyledons and meristem termination at a low frequency (Turchi *et al.*, 2013). We did not observe these phenotypes in our plants. *lrb2* mutants were previously published to have a slight red-light sensitivity phenotype (Christians *et al.*, 2012); this phenotype was not assessed in our study. Lastly, we did not examine triple mutants (*athb4 hat3 lof1-1* and *why1 why3 lof1-1*) due to time constraints. Because LOF1 interacts with ATHB4 and WHY3 in yeast but does not interact with HAT3 and WHY1, there may be no enhancement or suppression of phenotypes in triple mutants verses double mutants.

Discussion

LOF1-Interactors Respond to Abiotic Stress and are Localized to the Plastid and/or Mitochondria

To understand more about the specific role of LOF1 as a transcription factor involved in organ separation and meristem maintenance (Lee *et al.*, 2009), we identified and characterized putative interacting proteins. Here, we demonstrate that LOF1 interacts in yeast with other proteins that have reported functions in response to abiotic stress and localize to the plastid and/or mitochondria (Table 1.1). The yeast two-hybrid screen revealed 43 LOF1-interacting proteins. Although the yeast two-hybrid library used in the screen was enriched in cell types that express *LOF1*, the specific expression domain of *LOF1* comprised only a fraction of those cells (Lee *et al.*, 2009). Consequently, the library more highly represents cells that do not express *LOF1*. Therefore, some of the interactors recovered from this screen could represent false positives as proteins might be present in the library that are not typically expressed in the same cell types or subcellular compartments as LOF1. Thus, these proteins do not actually interact with LOF1 in *Arabidopsis* due to spatial (or temporal/developmental) separation. On the contrary, it is also possible that all of the interactors recovered from the assay are true interactors of LOF1 and that LOF1 has diverse and yet unidentified functions.

For all of the T-DNA insertion alleles in this study, the T-DNA insertion sites were sequenced only from the left border. Thus, there is the potential in each allele that there are two or more copies of the T-DNA insertion at the same locus or that the entire T-DNA, including the right border, did not insert at this locus. It is also possible that

partial duplications and/or inversions of the T-DNA sequence occurred but were not detected.

Of the 43 putative LOF1-interactors identified, we chose to focus further on several transcription factors: WHY3, ATHB4, and LRB2.

WHY Proteins Regulate Transcription in the Nucleus, Modulate Plastid DNA Repair, and are Sensitive to Redox Changes

WHY3 was isolated multiple times in the LOF1 yeast-two-hybrid screen and is involved in plastid DNA repair and gene regulation (Maréchal *et al.*, 2009; Xiong *et al.*, 2009). However, WHY proteins were originally discovered for their role in plant defense response and ability to regulate defense by binding to pathogenesis-related gene promoters in potato (*Solanum tuberosum*) and *Arabidopsis* (Desveaux *et al.*, 2000, 2004). Thus, these proteins act as transcription factors for plant defense response genes. WHY1 and WHY3 also bind to an upstream regulatory region of *AtKP1*, a kinesin-like gene, which leads to transcriptional repression (Xiong *et al.*, 2009). This indicates that more than one WHY protein may regulate some genes, and WHY proteins may be involved in transcriptional regulation for a variety of plant responses.

WHY1 binds both single and double-stranded DNA and RNA in maize (*Zea mays*) chloroplasts (Prikryl *et al.*, 2008). WHY proteins form tetramers arranged in a "pinwheel" or "whirligig" pattern in which single-stranded DNA can be interwoven; these interactions have low sequence specificity (Desveaux *et al.*, 2002; Cappadocia *et al.*, 2010, 2012). WHY proteins are named for this property. One interesting and peculiar

aspect of WHY proteins is their ability to localize to two distinctly different subcellular regions within a cell. In barley (*Hordeum vulgare*), it was found that WHIRLY1 (WHY1) localizes to plastids and the nucleus within the same cell (Grabowski *et al.*, 2008). Earlier, GFP fusion experiments in *Arabidopsis* showed that WHY1 and WHY3 localize to the chloroplast, while WHY2 localizes to the mitochondria (Krause *et al.*, 2005). WHY proteins could perform different roles in different subcellular regions of the cell and/or be involved in plastid-to-nucleus retrograde signaling.

As previously, mentioned WHY1 and WHY3 play roles in plastid DNA repair. DNA repair in higher plants occurs by several different pathways, such as Nucleotide Excision Repair (NER), Base Excision Repair (BER), and Double-Strand Break Repair (DSB) (Kimura and Sakaguchi, 2006). DNA repair mechanisms are necessary due to the constant exposure of DNA in plants to UV radiation from sunlight, chemical substances in the environment, and errors that occur during DNA replication. Furthermore, biotic stresses and secondary metabolism in plants produce ROS, which can cause cellular components, like DNA, to be damaged (Britt, 1999). Plastid and mitochondrial DNA can be damaged in the same way as genomic DNA, and WHY proteins help minimize DNA damage by repressing a DNA repair mechanism called the microhomology-mediated break-induced replication (MMBIR), which can lead to plastid DNA rearrangements (Maréchal *et al.*, 2009; Cappadocia *et al.*, 2010). In *why1why3* double mutant *Arabidopsis* plants, rearranged plastid DNA could be amplified by PCR, but it could not in wild-type plants (Maréchal *et al.*, 2009). This indicates that WHY1 and WHY3 aid in the correct repair of damaged plastid DNA.

Most double loss-of-function *why1 why3* mutant plants have no abnormal phenotype. However, about 5% of plants have a variegated leaf phenotype (Maréchal *et al.*, 2009). The variegated phenotype of *why1 why3* plants led the authors to believe WHY proteins may be involved in chloroplast biogenesis, chloroplast development, or attuning photosynthesis to environmental changes (Maréchal *et al.*, 2009). While WHY involvement in plastid DNA repair mechanisms explained the mutant phenotype, some thought there was more to the story. More recently, it was discovered that WHY1 interacts with light-harvesting protein complex I (LHCA1) and affects expression of genes encoding photosystem I (PSI) (Huang *et al.*, 2017). In barley, *WHY1* RNAi mutants had more chlorophyll but less sucrose than wild-type plants (Comadira *et al.*, 2015), suggesting that photosynthesis is affected and is less efficient in these mutants, not just chloroplast development alone. It was additionally reported that WHY3 is a redox affected protein because it was found in the thiol-disulfide redox proteome of the chloroplast (Ströher and Dietz, 2008). Because of documented WHY protein involvement in detecting plastid DNA damage and sensitivity to redox state combined with subcellular localization in both the plastid and nucleus, it has been suggested that WHY proteins may be involved in plastid-to-nucleus retrograde signaling in order to maintain plastid function in differing environmental conditions, and thus, they are important for communication between the plastid and nucleus [suggested in (Krause *et al.*, 2009; Guan *et al.*, 2018)]. WHY protein involvement in plastid-to-nucleus retrograde signaling will be discussed in detail in Chapter 2.

A *why1* mutant that was not examined in this dissertation, *KO1* (SALK_099937), was previously crossed to *KO3* (*why3-2*). The *KO1*/*why3-2* double mutant has no detectable levels of WHY1 or WHY3 protein (Maréchal *et al.*, 2009). Unfortunately, *KO1* (SALK_099937) was no longer available from stock resources. Therefore, we examined different T-DNA insertion alleles of *WHY1*, including *KO-1*/*why1-1* and *KO-2*/*why1-2*. Our growth conditions may differ from those reported when variegated leaf phenotype of the *KO1*/*why3-2* double mutant was described (Maréchal *et al.*, 2009). This would explain why we could not recapitulate the phenotype.

WHY1 and *WHY3* have similar expression patterns and are expressed in young leaves (including petioles), and expression levels decrease as development continues (Klepikova *et al.*, 2016). *WHY1* and *WHY3* are also expressed in pedicels, the primary inflorescence, and seeds during germination (Winter *et al.*, 2007; Klepikova *et al.*, 2016). One study noted *WHY1* expression in barley is highest in immature cells at the leaf base, while protein levels are highest near the center of the leaf – where young chloroplasts are developing (Krupinska *et al.*, 2014). *WHY3* and *LOF1* expression overlaps at the base of young leaves (Lee *et al.*, 2009).

The petiole, the stalk that joins the leaf to the stem, is the site of bending for leaf positioning in *Arabidopsis*. Petioles move upwards (hyponasty) and elongate when the plant is exposed to shade, low light, or submergence (Smith and Whitelam, 1997; Cox *et al.*, 2003; Pierik *et al.*, 2004). In *Arabidopsis*, light quality and quantity are both important factors. Leaves become more horizontal as light intensity increases (Hangarter, 1997; Millenaar *et al.*, 2005). This response is typical of rosette species, but it is different

from non-rosette species, where leaves become more vertical as light intensity increases (King, 1997; Valladares and Pugnaire, 1999; Falster and Westoby, 2003). For example, high-light and submergence result in excess ROS production in rice (Bailey-Serres and Voesenek, 2008; Chan *et al.*, 2016). Since WHY proteins are hypothesized to act as retrograde signals and chloroplast redox sensors, WHY3 and LOF1 could interact during ROS-producing abiotic stress conditions to modulate genes that control petiole angle or petiole elongation. LOF1 may receive input from a number or proteins, which would explain LOF1 interaction with many plastid-localized proteins. To test this hypothesis, petiole angle and elongation should be examined among *why3* single mutants, *lof1-1* single mutants, and *why3 lof1-1* double mutants exposed to high light (or ROS directly). Change in petiole angle or elongation between single mutants and the double mutant would indicate WHY3 and LOF1 involvement in plant response to high light.

Another possibility is that accessory bud production is altered in response to high light (and/or ROS) in *Arabidopsis*, and could explain the WHY3 – LOF1 interaction to promote or repress expression of genes that function in accessory bud formation. Investigation of the impact of high-light exposure on accessory bud formation would benefit this study. Plants grown in high light for extended periods of time are bushier in appearance and have more branches (Tian *et al.*, 2017). However, it is not known if plants exposed to high-light conditions produce more accessory buds or if the increased branch number is a result of outgrowth of pre-existing accessory buds and rosette-leaf axil buds. If high-light exposure leads to production of more accessory buds, it would be worth investigating WHY3 and LOF1 involvement in this process.

In support of this hypothesis, links between shoot meristem activity and ROS balance have been speculated in the past. *FAR-RED ELONGATED HYPOCOTYL3* (*FHY3*) encodes a component of the red-light signaling network involved in response to high intensity far-red light (Allen *et al.*, 2005; Ma *et al.*, 2019). *fhy3* mutants showed conditional, stress-related symptoms and are assumed to have increased ROS production or decreased ROS tolerance. Mutants of *REVOLUTA* (*REV*) produce fewer axillary meristems in rosette leaf axils. The axillary meristem defect displayed by the *rev* single mutant was enhanced in *fhy3 rev* double mutants (Talbert *et al.*, 1995; Stirnberg *et al.*, 2012). Additionally, *Arabidopsis* mutants impaired in both thioredoxin and glutathione-mediated thiol reduction are not able to maintain floral meristems (Bashandy *et al.*, 2010). *MORE AXILLARY BRANCHES2* (*MAX2*) and *MORE AXILLARY BRANCHES1* (*MAX1*) encode proteins involved in strigolactone signaling (Stirnberg *et al.*, 2002, 2007; Challis *et al.*, 2013). *max1* and *max2* single mutants have increased branching (accessory buds grow out) and increased ROS tolerance. Additionally, *max1 max2* double mutants have meristem fasciation (Stirnberg *et al.*, 2002, 2012; Hye *et al.*, 2004). The connection between ROS-tolerant phenotypes and meristematic activity should be further explored.

ATHB4 is Involved in Shade Avoidance, Meristem Maintenance, and Leaf Polarity

Another LOF1 interactor isolated in the yeast two-hybrid screen was ATHB4, a protein known to be involved in shade avoidance (Sorin *et al.*, 2009). In plants, growing in crowded environments can limit the amount of light for photosynthesis. A plant shaded by another plant will activate a response called the shade avoidance syndrome (SAS), a

set of responses to obtain adequate light for photosynthesis. SAS includes hypocotyl elongation, stem elongation, changes in flowering time, leaf expansion, and changes in leaf angle. Since photosynthesis absorbs red light (R) and transmits far red light (FR), a low R:FR ratio leads to SAS. R:FR ratio is sensed by phytochrome receptors, which have two photoconvertible forms that exist together in the same cells: an active FR-absorbing form (Pfr) and an inactive R-absorbing form (Pr). Low R:FR displaces the equilibrium towards the inactive Pr, while high R:FR displaces the equilibrium towards the active Pfr form. The active forms of phytochromes (Pfr) interact with PHYTOCHROME INTERACTING FACTORS (PIFs), which are basic helix-loop-helix (bHLH) transcription factors that modulate the expression of *PHYTOCHROME RAPIDLY REGULATED* (*PAR*) genes. *PAR* genes are responsible for activating SAS (Franklin, 2008; Martínez-García *et al.*, 2010; Leivar and Quail, 2011; Casal, 2013).

The family of ten HD-Zip class II transcription factors are involved in SAS. Expression of five members - *ARABIDOPSIS THALIANA HOMEOBOX2* (*ATHB2*), *ARABIDOPSIS THALIANA HOMEOBOX4* (*ATHB4*), *HOMEOBOX ARABIDOPSIS THALIANA1* (*HAT1*), *HOMEOBOX ARABIDOPSIS THALIANA2* (*HAT2*), and *HOMEOBOX ARABIDOPSIS THALIANA3* (*HAT3*) - are upregulated by low R:FR light (Sessa *et al.*, 2005; Ciarbelli *et al.*, 2008). However, this regulation could be indirect for *HAT2* because *HAT2* expression is induced by auxin, and the auxin pathway is upregulated in rich far-red light conditions (Devlin *et al.*, 2003). These five HD-Zip II proteins are divided phylogenetically into two clades – gamma and delta. The gamma clade is made up of ATHB2, HAT1, and HAT2, while the delta clade is made up of

HAT3 and ATHB4 (Ciarbelli *et al.*, 2008). In *Arabidopsis*, plants overexpressing *ATHB2* in low R:FR light show reduced hypocotyl elongation and increased leaf expansion compared to control plants (Steindler *et al.*, 1999). When *HAT2* was overexpressed, plants had long petioles, epinastic cotyledons, and small leaves (Sawa *et al.*, 2002). In *HAT3* overexpression lines, hypocotyl elongation is enhanced in high R:FR light (Ruberti *et al.*, 2012). The HD-Zip II family gamma and delta clades are thought to act redundantly as SAS positive regulators. However, there is one exception to this pattern – ATHB4. Both loss- and gain-of-function *athb4* mutants led to reduced hypocotyl elongation when compared to control plants. This led to the suggestion that ATHB4 is a SAS complex regulator instead of either a positive or negative regulator of SAS (Sorin *et al.*, 2009). This indicates that ATHB4 may have a unique role in SAS regulation not shared by other HD-Zip II proteins.

The most closely related *HD-Zip II* to *ATHB4* is *HAT3* (Ciarbelli *et al.*, 2008). *ATHB4* and *HAT3* have roles in cotyledon development and meristem maintenance. Loss-of-function double mutant *athb4hat3* plants additionally have cotyledons with polarity defects, meristem termination, and occasional fused cotyledons. When combined with a loss-of-function mutation in an *HD-Zip III* gene (*rev-5* or *phb-13*), these defects are more severe and embryo development is also impaired (Turchi *et al.*, 2013). Overexpression of *HAT3* leads to leaves that curl upwards (Bou-Torrent *et al.*, 2012), a leaf polarity phenotype. Thus, *ATHB4* and *HAT3* along with *HD-Zip III* genes are important for cotyledon development, leaf polarity, and meristem maintenance. The fused cotyledons

observed in *athb4 hat3* are also an indication that *ATHB4* and *HAT3* may function in boundary specification.

The *athb4 hat3* double loss-of-function mutant was reported to have lancet-shaped cotyledons, meristem termination, and occasionally loss of one cotyledon; however, this was not observed in our growth conditions (Turchi *et al.*, 2013). This could be because we examined a different *athb4* allele than this previous study. Turchi *et al* also reported no abnormal phenotypes for *athb4-1*, a knockout allele (Sorin *et al.*, 2009). Unfortunately, we could not recover the *athb4-1* T-DNA insertion in plants grown from seeds obtained from the stock center and therefore, we used *athb4-2*, a knock-down allele, instead.

ATHB4 has two separate molecular activities. The HD-Zip binds DNA, and the ethylene-responsive element binding factor-associated amphiphilic repression (EAR) region is associated with protein-protein interactions. Both activities are required for HB4's role in leaf polarity, whereas the DNA-binding region is not needed for regulating a response to seedling proximity or SAS (Gallemí *et al.*, 2017). The EAR motif may also be a transcriptional repression domain (Kagale *et al.*, 2010). More recently, it was found that low R:FR ratio leads to early exit from cell proliferation in the leaf, and this process requires *ATHB4* and *ATHB2* (Carabelli *et al.*, 2018); therefore, *ATHB4* may be one of the genes directly responsible for the narrow-leaf phenotype observed in shaded *Arabidopsis* plants.

HAT3 and *ATHB4* expression patterns align well with their functions in SAS and cotyledon development. *HAT3* and *ATHB4* are expressed adaxially in developing leaves

and cotyledons as well as in the SAM. In older leaves, *HAT3* and *ATHB4* are expressed in the vasculature (Turchi *et al.*, 2013). *ATHB4* is expressed in the inflorescence meristem and in carpels (Winter *et al.*, 2007; Klepikova *et al.*, 2016). Therefore, *ATHB4* and *LOF1* expression patterns overlap at the base of developing leaves (Lee *et al.*, 2009).

Wild-type *Arabidopsis* plants produce fewer buds in rosette-leaf axils in low R:FR light (Finlayson *et al.*, 2010). Plants need to limit outward growth in shaded environments so energy can be maximized for vertical growth (Teichmann and Muhr, 2015). This would be most relevant during reproductive growth in *Arabidopsis* as rosette species do not undergo much internode elongation in the vegetative phase (Ballaré, 1999; Vandenbussche *et al.*, 2003). Therefore, a similar pathway to the rosette-leaf axil bud limiting mechanism in low R:FR light may exist for accessory buds. We already know that accessory bud formation is highly environmentally sensitive, especially to light (discussed further in Chapter 3). As a SAS complex regulator, ATHB4 may interact with LOF1 to promote transcription of genes that promote or inhibit accessory bud formation in response to light conditions.

ATHB4 and LOF1 may instead interact to transcribe genes involved in petiole movement as part of the shade avoidance response. As a rosette species, *Arabidopsis* is particularly vulnerable to shading. Leaf positioning is utilized to escape shading (Ballaré, 1999; Vandenbussche *et al.*, 2003). This is supported by previous evidence that *LOF1* is impacted by light and affects leaf angle. The degree of *lof1* fusion is highly environmentally sensitive, and severe *lof1* fusions cause the axillary branch and cauline leaf to bend downwards. Thus, *LOF1* levels impact cauline leaf angle. We also know that

lof1-1 mutants are more severe in short-day conditions (Lee *et al.*, 2009). To determine if ATHB4 and LOF1 are involved in petiole movement during SAS, *lof1* and *athb4* null mutants, as well as *lof1 athb4* double mutants, should be grown in low R:FR conditions. If rosette petiole and cauline leaf angles are enhanced or suppressed in double mutants, this would implicate LOF1 in the shade avoidance response.

It should be noted that the *ATHB4* clone isolated from the yeast two-hybrid screen lacked the sequence in the 5' region that codes for the first three amino acids in the N-terminal portion of ATHB4. In contrast, I tested for interaction between LOF1 and the full-length HAT3 protein. Although one study found that the N-terminal domains of ATHB4 and HAT3 shared substantial identity (Ciarbelli *et al.*, 2008), they were not completely identical in amino acid sequence. Therefore, the fact that LOF1 interacted with ATHB4 and not HAT3 in yeast could be due or partially due to these differences.

LRB2 Modulates Response to Red Light with PHYB and PHYD

The final protein of interest, LIGHT-RESPONSIVE BRIC-A-BRAC/TRAMTRACK/BROAD2 (LRB2), is involved in protein degradation. The breakdown of short-lived proteins is an important feature of regulatory pathways. In eukaryotes, much of this turnover is mediated by the ubiquitin/26S proteasome system (UPS) (Kerscher *et al.*, 2006). In this system, ubiquitin (Ub) is covalently attached to proteins set for degradation through the E1-E2-E3 conjugation system. These poly-Ub additions are recognized by the 26S proteasome, a large protein complex responsible for unfolding and destroying ubiquitinated proteins. The specificity of the UPS system lies in

the E3 Ub protein ligases, which recognize the structural motifs in the target protein (Smalle and Vierstra, 2004). The multi-subunit Cullin-RING ligases (CRLs) are a highly diverse class of E3s, which consist of a Cullin (CUL) backbone and E2-Ub-docking RING Box1 (RBX1) (Hua and Vierstra, 2011). One subtype of CRL is the Bric-a-Brac/Tramtrack/Broad complex (BTB) E3s (Furukawa *et al.*, 2003). It has been noted that BTBs regulate developmentally important processes, such as leaf and flower morphogenesis, abscisic acid signaling, and organogenesis (Hepworth *et al.*, 2005; Cheng *et al.*, 2007; Lechner *et al.*, 2011).

While *LRB3* is likely a pseudogene, *LRB2* is closely related to *LRB1* and both act as BTB E3 complexes to negatively regulate photomorphogenesis in response to red light (Christians *et al.*, 2012). *lrb2* mutants display slightly compacted rosette leaves when grown in short-day conditions and show a slight red-light sensitivity (Christians *et al.*, 2012). *lrb1 lrb2* double mutants are markedly red-light hypersensitive and show a severe phenotype when grown in white light – dwarf rosette leaves, shorter petioles, and late flowering (Christians *et al.*, 2012). *lrb1 lrb2* double mutants do not accumulate PHYA like many red-light hypersensitive mutants. Instead, levels of PHYB and PHYD proteins are abnormally high (mRNA levels are normal). The *lrb1lrb2* red-light hypersensitive phenotype can be reversed by eliminating PHYB or PHYD (Christians *et al.*, 2012). This implies that LRB1 and LRB2 are involved in light-dependent turnover of phyB and phyD and act as negative regulators of photomorphogenesis. More recently, a potential mechanism of how LRB1 and LRB2 degrade PHYB was discovered. Light-induced PIF3 phosphorylation stimulates recruitment of LRB1 and LRB2 proteins to the PIF3-PHYB

complex. The LRBs then promote degradation of both PIF3 and PHYB in order to mediate red-light signaling (Ni *et al.*, 2014). This is presumed to be indirect as LRB1 and LRB2 do not interact with PHYB or PHYD (Christians *et al.*, 2012).

LRB1 and LRB2 were found to play a role in flowering. FLOWERING LOCUS T (FT) is a florigenic mobile signal produced in the leaves in response to photoperiod. The signal is transported to the shoot apical meristem (SAM), where it promotes meristem transition from vegetative to floral (Corbesier *et al.*, 2007). *FT* expression is directly repressed in juvenile plants by the MADS box transcription factor FLOWERING LOCUS C (FLC) (Michaels and Amasino, 1999; Searle *et al.*, 2006; Jang *et al.*, 2009). Therefore, *FLC* must be repressed in order for flowering to occur. FRIGIDA (FRI) is a major activator of FLC (Napp-Zinn, 1987; Michaels and Amasino, 1999; Choi *et al.*, 2011), and FRI degradation occurs after vernalization – the induction of flowering by a period of exposure to cold temperatures [reviewed in (Zhu *et al.*, 2015)]. It was reported that both LRBs interact with FRIGIDA (FRI) directly to cause FRI degradation and thus flowering (Hu *et al.*, 2014). This led to the hypothesis that red-light signaling through LRBs may play a role in regulating FRI degradation and thus, the control of flowering during vernalization (Wiersma and Christians, 2015).

LRB1 and LRB2 are broadly expressed in a variety of tissues throughout all stages of development in *Arabidopsis*. Expression does not seem to be dramatically up or downregulated by most environmental conditions (Christians *et al.*, 2012). Therefore, *LRB2* expression is presumed to overlap with that of *LOF1* (Lee et al, 2009).

LRB2 and LOF1 could interact to regulate petiole angle during response to red light, and this may or may not involve turnover of PHYB. PHYB was found to be the most important phytochrome in regulating leaf inclination in both cucumber and *Arabidopsis* (Ballare *et al.*, 1995; Mullen *et al.*, 2006). *Arabidopsis phyB* mutants were reported to be impaired in the detection of R:FR ratios and have fewer branches (Shen *et al.*, 2007). To investigate this possibility, *lof1-1 lrb2* mutants would need to be exposed to red light and examined for enhancement or suppression of the *lrb2* single mutant phenotype (Christians *et al.*, 2012). Petiole growth and angle would be examined in single and double mutants. Enhancement or suppression of petiole growth or change in petiole angle in *lof1-1 lrb2* double mutants compared to single mutants would indicate LOF1 modulates petiole growth with LRB2. To determine potential involvement of PHYB, levels of PHYB would be assessed in *lrb2* and *lof1-1* single and *lof1-1 lrb2* double mutants. If *lof1-1 lrb2* contained higher or lower levels of PHYB then *lrb2*, this would indicate LOF1 contributes to PHYB turnover.

Alternatively, LOF1 could also be involved with LRB function in flowering and vernalization. This is supported by the fact that FRIGIDA-LIKE1 (FRI1) was isolated as a LOF1-interactor in the screen (Table 1.1). Because all plants were grown at a constant temperature, any impacts on vernalization in mutants would not be observed in these studies.

A remaining experiment is to examine potential LOF1 and LRB1 interaction. LRB1 was not isolated in the screen (Table 1.1), and the *lrb1* mutant did not have any abnormal phenotypes (Christians *et al.*, 2012). Therefore, we did not examine *lrb1*

mutants in this study. In our analysis of the *lof1-1 lrb2* double mutants, no discernable phenotypes were seen when grown in white light (data not shown); this is in contrast to the *lrb1 lrb2* mutants, which are smaller and have reduced petiole growth (Christians *et al.*, 2012). In the future, analysis of the *lrb1 lrb2 lof1-1* triple mutant may be valuable. The triple mutant may have an enhanced or suppressed phenotype in white light compared to *lrb1 lrb2* double mutants if LRB1 and LOF1 interact. If this is the case, LRB1, LRB2, and LOF1 may function together in modulation of petiole angle.

Conclusion

In a yeast two-hybrid screen, LOF1 was found to interact with a number of proteins that are predicted to have a subcellular localization in the chloroplast and/or mitochondria. WHY1, LRB2, and ATHB4 were identified as LOF1-interacting proteins of interest and were further characterized. Interestingly, proteins thought to be functionally redundant to WHY1 and ATHB4, WHY3 and HAT3, respectively, did not interact with LOF1 in yeast. Due to the high amino acid sequence identity between WHY1 and WHY3, as well as ATHB4 and HAT3, LOF1 protein-protein interactions appear highly specific. After obtaining mutants of genes encoding LOF1-interacting proteins and crossing these mutants to *lof1-1*, no enhancement or suppression of *lof1-1* mutant phenotypes could be observed. Furthermore, no new phenotypes were observed in the single mutants of genes encoding interacting proteins or in the double mutants after crossing to *lof1-1*. Because many of the LOF1-interacting proteins are involved in abiotic stress response, the possibility remains that the single and double mutants were not

exposed to environmental conditions or stressors that would allow an altered phenotype to be observed.

Materials and Methods

Yeast Two-Hybrid Screen

LOF1 cDNA was amplified from Col-0 cDNA using the primers listed in Table 1.3 and cloned into pCR4 using TOPO^{TM} TA Cloning Kit (Thermo Fisher Scientific). Then, *LOF1* pCR4 was cut with *BamHI* and *NdeI* and ligated into pGBKT7 (Clontech). The resulting BD-LOF1fusion was transformed into yeast strain Matchmaker Gold (Clontech) using the lithium acetate transformation protocol from The Yeast Protocols Handbook (Clontech), with some modifications. After transformation, the yeast cells were resuspended in 1 mL YPD media instead of TE buffer as recommended. The expression of the BD-LOF1 fusion protein was verified in yeast via Western blot (data not shown) before use in the yeast two-hybrid screen. The yeast two-hybrid library was made from cDNA isolated from RNA extracted from inflorescence tips of Columbia and *ap1cal1* mutants (Kempin *et al.*, 1995). The pGBKT7-53 BD-DNA and pGADT7-T AD plasmids (Clontech) were used as a control for positive interaction. A yeast strain containing full-length BD-LOF1 and pGADT7 empty was used as a negative control.

Potential interactors were screened on selective media, which included SD -Trp/-Leu/-Ade/-His +3-AT (3-Amino-1,2,4-triazole) and SD -Trp/-Leu + Aureobasidin A. A concentration of 7.5 mM 3-AT and a concentration of 7.5 μg/mL Aureobasidin A were used, respectively, on selective plates. The primary screen was done by plating yeast on

selective media containing SD -Trp/-Leu/-Ade/-His +3-AT for a period of one week. Colonies were picked and patched onto SD -Trp/-Leu + Aureobasidin A for a second screen. Plasmids were extracted from yeast using an adapted Zymolyase-based yeast DNA miniprep protocol from the Amsbio website (http://www.amsbio.com/protocols/Zymolyase_Protocols.pdf). Yeast was first pelleted from liquid culture and then resuspended in 250 µl Zymolyase (lyticase) solution (1.2 M sorbitol/ 10 mM tris pH 8.0/ 10 mM $CaCl_2$/ 1% beta mercaptoethanol/ 0.7 mg/ml Zymolyase). After incubation at 37ºC for thirty minutes, 200 µl lysis solution (50 mM tris pH 8.0/ 50 mM EDTA/ 1.2% SDS) was added. After mixing, 150 µl KAc solution was added to the tube (60 mL 5M potassium acetate/ 11.5 mL glacial acetic acid/ 28.5 mL water). After mixing again, DNA was precipitated with isopropanol and spun down in a microcentrifuge for ten minutes. DNA was washed with 95% ethanol, let dry, and resuspended in TE buffer (100 µl). A similar protocol is published here (Singh and Weil, 2002).

cDNA sequences in library plasmids were amplified with primers flanking the insertion (Table 1.3) in order to determine insertion size and number of AD plasmids per yeast colony. The insertions in the recovered plasmids were sent for sequencing by the UCR Core Genomics Facility with T7 primer (Table 1.3).

Yeast Two-Hybrid of Proteins Functionally Redundant with LOF1 Interactors

HAT3 and *WHY1* were amplified from Col-0 cDNA using primers that span the start and stop codons and introduced a 5' *NcoI* restriction site and a 3' *ClaI* restriction site

(Table 1.3). Amplicons were cloned into pMiniT using the PCR Cloning Kit (NEB). *HAT3* pMiniT and *WHY1* pMiniT were transformed into K12 ER2925 *E. coli* (NEB) that lacks *dam* methylation. After sequencing to confirm the integrity of the clones (UCR Core Facility), *HAT3* pMiniT and *WHY1* pMiniT were extracted from *E. coli* using Qiaprep Spin Miniprep Kit (Qiagen) and digested with *NcoI* and *ClaI*. The *HAT3* and *WHY1* products of restriction digest were ligated into pGADT7 (Clontech) that had been digested with the same enzymes. The resulting AD-WHY1 and AD-HAT3 plasmids were transformed into yeast containing full-length BD-LOF1 using the protocol from The Yeast Protocols Handbook (Clontech). Yeast containing AD-WHY3 or AD-ATHB4 and full-length BD-LOF1 were used as positive controls. Yeast containing full-length BD-LOF1 and the empty vector was used as a negative control. Yeast containing both BD-LOF1 and the individual AD fusion were spotted on SD -Trp/-Leu (non-selective media) and SD -Trp/-Leu/-His/-Ade + 3-AT (selective media) at the same concentrations, determined by OD600 of yeast in liquid media. Yeast were grown on plates containing selective media for several days at 30ºC before observation. Yeast were grown on non-selective media for two days before observation.

ZFHD1 was amplified from Col-0 cDNA using primers spanning the coding region (Table 1.3) and cloned into pMiniT using the PCR Cloning Kit (NEB). *ZFHD1* was cloned from pMiniT into pGADT7 using *XhoI* and *NdeI* restriction sites, and the resulting AD-*ZFHD1* fusion was transformed into *E. coli*. Attempts to introduce *ZFHD1* pGADT7 into Matchmaker Gold© strain yeast were unsuccessful, suggesting the possibility that it was toxic to yeast.

Plant Materials and Growth Conditions

Arabidopsis thaliana Columbia (Col-0) was used as wild type in all experiments.

Soil Method: Seeds were first treated at -80ºC overnight. They were then sterilized with 95% ethanol and allowed to dry before being sown on Sunshine LC1 mix with Osmocote 14-14-14 (150g/bag) and Marathon (225g/bag) added to soil. Plants were grown at 18-23ºC in 16-hour light/8-hour dark cycles.

Plate Method: Seeds were sterilized with 95% ethanol for 5 minutes, treated with 20% bleach/0.01% Tween 20 for 5 minutes, and rinsed five times with sterile water. Seeds were sown on Murashige and Skoog (MS) media (pH 5.7) (Murashige and Skoog, 1962) with added 1% sucrose. They were stratified at 4ºC in the dark for 48 hours before being transferred to a growth chamber with 120 μM/m^2s white light with a 16-hour light/ 8-hour dark cycle. The temperature was a constant 22ºC.

The *lof1-1* mutant used was as previously described (Lee *et al.*, 2009). The *KO3* mutant was as previously described (Maréchal *et al.*, 2009). The *KO-1*/*why1-1* and *KO-2*/*why1-2* mutants were also previously described (Yoo *et al.*, 2007). *why1-3* seeds were obtained from the ABRC (Alonso *et al.*, 2003). *lrb2-1*, *lrb2-2*, and *lrb2-3* T-DNA insertion alleles were previously described (Christians *et al.*, 2012). The *athb4-2* seeds were previously described (Sorin *et al.*, 2009). The *hat3-1*, *hat3-2*, and *hat3-4* seeds were from the ABRC (Alonso *et al.*, 2003). The *hat3-3* allele was previously described (Turchi *et al.*, 2013).

Transcript Analysis

To characterize T-DNA insertion alleles for our genes of interest, total RNA was extracted from mutant and Col-0 control plants using TRIZOL® reagent (Invitrogen) and precipitated by 100% isopropanol. Pellets were rinsed with 75% ethanol. RNA (1-2 ug) was used for cDNA synthesis using SuperScript III Reverse Transcriptase (Invitrogen) or SuperScript IV Reverse Transcriptase (Thermo Fisher Scientific) according to manufacturer protocols. *ACTIN2* (*ACT2*) primers were used to equalize cDNA for RT-PCR (Table 1.3) using 22 cycles of amplification. Sequences for primers used in RT-PCR of *LRB2*, *WHY3*, *WHY1*, *ATHB4*, and *HAT3* are listed in Table 1.3. Cycle number used for RT-PCR of specific genes is given in the following Figures 1.2, 1.3, 1.4, 1.5 and 1.6.

Sequencing T-DNA Insertion Sites

PCR was performed with one primer on the T-DNA left border and one in the gene of interest. PCR products were checked on a 1% agarose gel and cleaned with MiniElute PCR Purification Kit (Qiagen). Products were then sent for sequencing at the UCR Core Facility with LBb1.3 primer (Table 1.3). Gene diagrams (Figures 1.2 A, 1.3 A, 1.4 A, 1.5 A, and 1.6 A) created using the http://wormweb.org/exonintron website for representation of intron-exon gene structure.

Phenotypic Analysis of Mutants

To cross mutants of interest to *lof1-1*, plants used as female parent were emasculated using forceps and a stereomicroscope. Two days later, pollen from male

parents was applied to the stigmas of the female parent flowers. Siliques were allowed to mature and were collected when dry. F1 plants resulting from crosses were confirmed by genotyping. Genotyping primers are listed in Table 1.3. In the F2 generation, WT plants, single mutants of interest, *lof1-1* mutants, and double mutant plants were obtained and confirmed by genotyping. At least thirty plants of each genotype in the F3 generation (all from the same F1 plant) were planted and compared to one another for analysis at both two-weeks old (on plates) and six-weeks old (on soil).

Triple mutants (*athb4 hat3 lof1-1* and *why3 why1 lof1-1*) were obtained by crossing *athb4 lof1-1* to *hat3 lof1-1* and *why3 why1* to *why1 lof1-1*, respectively. Crosses were confirmed by genotyping in the F1 generation. Primers used for genotyping are listed in Table 1.3.

References

Aida M. 1997. Genes involved in organ separation in *Arabidopsis*: An analysis of the *cup-shaped cotyledon* mutant. Plant Cell **9**, 841–857.

Aida M, Ishida T, Tasaka M. 1999. Shoot apical meristem and cotyledon formation during *Arabidopsis* embryogenesis: Interaction among the *CUP-SHAPED COTYLEDON* and *SHOOT MERISTEMLESS* genes. Development **126**, 1563–1570.

Aida M, Tasaka M. 2006. Genetic control of shoot organ boundaries. Current Opinion in Plant Biology **9**, 72–77.

Allen T, Koustenis A, Theodorou G, Somers DE, Kay SA, Whitelam GC, Devlin PF. 2006. *Arabidopsis* FHY3 specifcally gates phytochrome signaling to the circadian clock. Plant Cell **18**, 2506-2516.

Alonso JM, Stepanova AN, Leisse TJ, Kim CJ, Chen H, Shinn P, Stevenson DK, Zimmerman J, Barajas P, Cheuk R, Gadrinab C, Heller C, Jeske A, Koesema E, Meyers CC, Parker H, Prednis L, Ansari Y, Choy N, Deen H, Geralt M, Hazari N, Hom E, Karnes M, Mulholland C, Ndubaku R, Schmidt I, Guzman P, Aguilar-Henonin L, Schmid M, Weigel D, Carter DE, Marchand T, Risseeuw E, Brogden D, Zeko A, Crosby WL, Berry CC, Ecker JR. 2003. Genome-wide insertional mutagenesis of *Arabidopsis thaliana*. Science **301**, 653–657.

Arnon DI. 1988. The discovery of ferredoxin: the photosynthetic path. Trends in Biochemical Sciences **13**, 30–33.

Bailey-Serres J, Voesenek LACJ. 2008. Flooding stress: Acclimations and genetic diversity. Annual Review of Plant Biology **59**, 313–339.

Ballaré CL. 1999. Keeping up with the neighbours: Phytochrome sensing and other signalling mechanisms. Trends in Plant Science **4**, 97–102.

Ballare CL, Scopel AL, Roush ML, Radosevich SR. 1995. How plants find light in patchy canopies. A comparison between wild-type and phytochrome-B-deficient mutant plants of cucumber. Functional Ecology **9**, 859–868.

Bashandy T, Guilleminot J, Vernoux T, Caparros-Ruiz D, Ljung K, Meyer Y, Reichheld JP. 2010. Interplay between the NADP-linked thioredoxin and glutathione systems in *Arabidopsis* auxin signaling. Plant Cell **22**, 376–391.

Bell EM, Lin W, Husbands AY, Yu L, Jaganatha V, Jablonska B, Mangeon A, Neff MM, Girke T, Springer PS. 2012. *Arabidopsis* lateral organ boundaries negatively regulates brassinosteroid accumulation to limit growth in organ boundaries. Proceedings of the National Academy of Sciences USA **109**, 21146–21151.

Bou-Torrent J, Salla-Martret M, Brandt R, Musielak T, Palauqui JC, Martínez-García JF, Wenkel S. 2012. ATHB4 and HAT3, two class II HD-ZIP transcription factors, control leaf development in Arabidopsis. Plant Signaling and Behavior **7,** 1-6.

Britt AB. 1999. Molecular genetics of DNA repair in higher plants. Trends in Plant Science **4**, 20–25.

Callos JD, Medford JI. 1994. Organ positions and pattern formation in the shoot apex. Plant Journal **6**, 1–7.

Cappadocia L, Maréchal A, Parent JS, Lepage É, Sygusch J, Brisson N. 2010. Crystal structures of DNA-whirly complexes and their role in *Arabidopsis* organelle genome repair. Plant Cell **22**, 1849–1867.

Cappadocia L, Parent JS, Zampini É, Lepage É, Sygusch J, Brisson N. 2012. A conserved lysine residue of plant Whirly proteins is necessary for higher order protein assembly and protection against DNA damage. Nucleic Acids Research **40**, 258–269.

Carabelli M, Possenti M, Sessa G, Ruzza V, Morelli G, Ruberti I. 2018. Arabidopsis HD-Zip II proteins regulate the exit from proliferation during leaf development in canopy shade. Journal of Experimental Botany **69**, 5419–5431.

Casal JJ. 2013. Photoreceptor signaling networks in plant responses to shade. Annual Review of Plant Biology **64**, 403–427.

Challis RJ, Hepworth J, Mouchel C, Waites R, Leyser O. 2013. A role for *MORE AXILLARY GROWTH1* (*MAX1*) in evolutionary diversity in strigolactone signaling upstream of *MAX2*. Plant Physiology **161**, 1885–1902.

Chan KX, Phua SY, Crisp P, McQuinn R, Pogson BJ. 2016. Learning the languages of the chloroplast: Retrograde signaling and beyond. Annual Review of Plant Biology **67**, 25–53.

Cheng Y, Qin G, Dai X, Zhao Y. 2007. NPY1, a BTB-NPH3-like protein, plays a critical role in auxin-regulated organogenesis in *Arabidopsis*. Proceedings of the National Academy of Sciences USA **104**, 18825–18829.

Choi K, Kim J, Hwang HJ, Kim S, Park C, Kim SY, Lee I. 2011. The FRIGIDA complex activates transcription of FLC, a strong flowering repressor in *Arabidopsis*, by recruiting chromatin modification factors. Plant Cell **23**, 289–303.

Christians MJ, Gingerich DJ, Hua Z, Lauer TD, Vierstra RD. 2012. The light-response BTB1 and BTB2 proteins assemble nuclear ubiquitin ligases that modify phytochrome B and D signaling in Arabidopsis. Plant Physiology **160**, 118–134.

Ciarbelli AR, Ciolfi A, Salvucci S, Ruzza V, Possenti M, Carabelli M, Fruscalzo A, Sessa G, Morelli G, Ruberti I. 2008. The Arabidopsis homeodomain-leucine zipper II gene family: Diversity and redundancy. Plant Molecular Biology **68**, 465–478.

Colling J, Tohge T, De Clercq R, Brunoud G, Vernoux T, Fernie AR, Makunga NP, Goossens A, Pauwels L. 2015. Overexpression of the *Arabidopsis thaliana* signalling peptide TAXIMIN1 affects lateral organ development. Journal of Experimental Botany **66**, 5337–5349.

Comadira G, Rasool B, Kaprinska B, García BM, Morris J, Verrall SR, Bayer M, Hedley PE, Hancock RD, Foyer CH. 2015. WHIRLY1 functions in the control of responses to nitrogen deficiency but not aphid infestation in barley. Plant Physiology **168**, 1140–1151.

Corbesier L, Vincent C, Jang S, Fornara F, Fan Q, Searle I, Giakountis A, Farrona S, Gissot L, Turnbull C, Coupland G. 2007. FT protein movement contributes to long-distance signaling in floral induction of *Arabidopsis*. Science **316**, 1030–1033.

Cox MCH, Millenaar FF, De Jong Van Berkel YEM, Peeters AJM, Voesenek LACJ. 2003. Plant movement. Submergence-induced petiole elongation in *Rumex palustris* depends on hyponastic growth. Plant Physiology **132**, 282–291.

Desveaux D, Allard J, Brisson N, Sygusch J. 2002. A new family of plant transcription factors displays a novel ssDNA-binding surface. Nature Structural Biology **9**, 512–517.

Desveaux D, Despres C, Joyeux A, Subramaniam R, Brisson N. 2000. PBF-2 is a novel single-stranded DNA binding factor implicated in *PR-10a* gene activation in potato. Plant Cell **12**, 1477–1489.

Desveaux D, Subramaniam R, Després C, Mess JN, Lévesque C, Fobert PR, Dangl JL, Brisson N. 2004. A 'Whirly' transcription factor is required for salicylic acid-dependent disease resistance in *Arabidopsis*. Developmental Cell **6**, 229–240.

Devlin PF, Yanovsky MJ, Kay SA. 2003. A genomic analysis of the shade avoidance response in Arabidopsis. Plant Physiology **133**, 1617–1629.

Dubos C, Stracke R, Grotewold E, Weisshaar B, Martin C, Lepiniec L. 2010. MYB transcription factors in *Arabidopsis*. Trends in Plant Science **15**, 573–581.

Falster DS, Westoby M. 2003. Leaf size and angle vary widely across species: What consequences for light interception? New Phytologist **158**, 509–525.

Finlayson SA, Krishnareddy SR, Kebrom TH, Casal JJ. 2010. Phytochrome regulation of branching in Arabidopsis. Plant Physiology **152**, 1914–1927.

Franklin KA. 2008. Shade avoidance. New Phytologist **179**, 930–944.

Furukawa M, He YJ, Borchers C, Xiong Y. 2003. Targeting of protein ubiquitination by BTB-Cullin 3-Roc1 ubiquitin ligases. Nature Cell Biology **5**, 1001–1007.

Gallemí M, Molina-Contreras MJ, Paulišić S, Salla-Martret M, Sorin C, Godoy M, Franco-Zorrilla JM, Solano R, Martínez-García JF. 2017. A non-DNA-binding activity for the ATHB4 transcription factor in the control of vegetation proximity. New Phytologist **216**, 798–813.

Gonzalez A, Zhao M, Leavitt JM, Lloyd AM. 2008. Regulation of the anthocyanin biosynthetic pathway by the TTG1/bHLH/Myb transcriptional complex in Arabidopsis seedlings. Plant Journal **53**, 814–827.

Gould KS. 2004. Nature's Swiss army knife: The diverse protective roles of anthocyanins in leaves. Journal of Biomedicine and Biotechnology **5**, 314–320.

Grabowski E, Miao Y, Mulisch M, Krupinska K. 2008. Single-stranded DNA-binding protein Whirly1 in barley leaves is located in plastids and the nucleus of the same cell. Plant Physiology **147**, 1800–1804.

Guan Z, Wang W, Yu X, Lin W, Miao Y. 2018. Comparative proteomic analysis of coregulation of CIPK14 and WHIRLY1/3 mediated pale yellowing of leaves in *Arabidopsis*. International Journal of Molecular Sciences **19**, 1-22.

Hangarter RP. 1997. Gravity, light and plant form. Plant, Cell and Environment **20**, 796–800.

He JX, Gendron JM, Yang Y, Li J, Wang ZY. 2002. The GSK3-like kinase BIN2 phosphorylates and destabilizes BZR1, a positive regulator of the brassinosteroid signaling pathway in *Arabidopsis*. Proceedings of the National Academy of Sciences USA **99**, 10185–10190.

Hepworth SR, Zhang Y, Mckim S, Li X, Haughn GW. 2005. BLADE-ON-PETIOLE–dependent signaling controls leaf and floral patterning in Arabidopsis. Plant Cell **17**, 1434–1448.

Hong SH, Kim HJ, Ryu JS, Choi H, Jeong S, Shin J, Choi G, Nam HG. 2008. CRY1 inhibits COP1-mediated degradation of BIT1, a MYB transcription factor, to activate blue light-dependent gene expression in Arabidopsis. Plant Journal **55**, 361–371.

Hooper CM, Castleden IR, Tanz SK, Aryamanesh N, Millar AH. 2017. SUBA4: The interactive data analysis cantre for Arabidopsis subcellular protein locations. Nucleic Acids Research **45**, 1064-1074.

Hu X, Kong X, Wang C, Ma L, Zhao J, Wei J, Zhang X, Loake GJ, Zhang T, Huang J, Yang Y. 2014. Proteasome-mediated degradation of FRIGIDA modulates flowering time in *Arabidopsis* during vernalization. Plant Cell **26**, 4763–4781.

Hua Z, Vierstra RD. 2011. The Cullin-RING ubiquitin-protein ligases. Annual Review of Plant Biology **62**, 299–334.

Huang D, Lin W, Deng B, Ren Y, Miao Y. 2017. Dual-located WHIRLY1 interacting with LHCA1 alters photochemical activities of photosystem I and is involved in light adaptation in Arabidopsis. International Journal of Molecular Sciences **18**, 1–18.

Huang JP, Tunc-Ozdemir M, Chang Y, Jones AM. 2015. Cooperative control between AtRGS1 and AtHXK1 in a WD40-repeat protein pathway in *Arabidopsis thaliana*. Frontiers in Plant Science **6**, 1–11.

Hussey G. 1971. Cell division and expansion and resultant tissue tensions in the shoot apex during the formation of a leaf primordium in the tomato. Journal of Experimental Botany **22**, 702–714.

Isemer R, Krause K, Grabe N, Kitahata N, Asami T, Krupinska K. 2012. Plastid located WHIRLY1 enhances the responsiveness of *Arabidopsis* seedlings toward abscisic acid. Frontier in Plant Science **3**, 1-11.

Jang S, Torti S, Coupland G. 2009. Genetic and spatial interactions between *FT*, *TSF* and *SVP* during the early stages of floral induction in Arabidopsis. Plant Journal **60**, 614–625.

Jia L, Clegg MT, Jiang T. 2004. Evolutionary dynamics of the DNA-binding domains in putative R2R3-MYB genes identified from rice subspecies *indica* and *japonica* genomes. Plant Physiology **134**, 575–585.

Kagale S, Links MG, Rozwadowski K. 2010. Genome-wide analysis of ethylene-responsive element binding factor-associated amphiphilic repression motif-containing transcriptional regulators in Arabidopsis. Plant Physiology **152**, 1109–1134.

Keller T, Abbott J, Moritz T, Doerner P. 2006. *Arabidopsis REGULATOR OF AXILLARY MERISTEMS1* controls a leaf axil stem cell niche and modulates vegetative development. Plant Cell **18**, 598–611.

Kempin SA, Savidge B, Yanofsky MF. 1995. Molecular basis of the cauliflower phenotype in Arabidopsis. Science **267**, 522–525.

Kerscher O, Felberbaum R, Hochstrasser M. 2006. Modification of proteins by ubiquitin and ubiquitin-like proteins. Annual Review of Cell and Developmental Biology **22**, 159–180.

Kimura S, Sakaguchi K. 2006. DNA repair in plants. Chemical Reviews **106**, 753–766.

King DA. 1997. The functional significance of leaf angle in *Eucalyptus*. Australian Journal of Botany **45**, 619–639.

Klepikova AV, Kasianov AS, Gerasimov ES, Logacheva MD, Penin AA. 2016. A high resolution map of the *Arabidopsis thaliana* developmental transcriptome based on RNA-seq profiling. Plant Journal **88**, 1058–1070.

Krause K, Herrmann U, Fuss J, Miao Y, Krupinska K. 2009. Whirly proteins as communicators between plant organelles and the nucleus? Endocytobiosis and Cell Research **19**, 51–62.

Krause K, Kilbienski I, Mulisch M, Rödiger A, Schäfer A, Krupinska K. 2005. DNA-binding proteins of the Whirly family in *Arabidopsis thaliana* are targeted to the organelles. FEBS Letters **579**, 3707–3712.

Krupinska K, Oetke S, Desel C, Mulisch M, Schäfer A, Hollmann J, Kumlehn J, Hensel G. 2014. WHIRLY1 is a major organizer of chloroplast nucleoids. Frontiers in Plant Science **5**, 1–11.

Lechner E, Leonhardt N, Eisler H, Parmentier Y, Alioua M, Jacquet H, Leung J, Genschik P. 2011. MATH/BTB CRL3 receptors target the homeodomain-leucine zipper ATHB6 to modulate abscisic acid signaling. Developmental Cell **21**, 1116–1128.

Lee D-K, Geisler M, Springer PS. 2009. *LATERAL ORGAN FUSION1* and *LATERAL ORGAN FUSION2* function in lateral organ separation and axillary meristem formation in *Arabidopsis*. Development **136**, 2423–2432.

Leister, D. 2019. Piecing the puzzle together: The central role of reactive oxygen species and redox hubs in chloroplast retrograde signaling. Antioxidants and Redox Signaling **9**, 1206-1219.

Leivar P, Quail PH. 2011. PIFs: Pivotal components in a cellular signaling hub. Trends in Plant Science **16**, 19–28.

Lepiniec L, Debeaujon I, Routaboul J-M, Baudry A, Pourcel L, Nesi N, Caboche M. 2006. Genetics and biochemistry of seed flavonoids. Annual Review of Plant Biology **57**, 405–430.

Li L, Yu X, Thompson A, Guo M, Yoshida S, Asami T, Chory J, Yin Y. 2009. Arabidopsis MYB30 is a direct target of BES1 and cooperates with BES1 to regulate brassinosteroid-induced gene expression. Plant Journal **58**, 275–286.

Liu J, Huang S, Sun M, Liu S, Liu Y, Wang W, Zhang X, Wang H, Hua W. 2012. An improved allele-specific PCR primer design method for SNP marker analysis and its application. Plant Methods **8**, 1-9.

Liu J, Wang P, Liu B, Feng D, Zhang J, Su J, Zhang Y, Wang JF, Wang H Bin. 2013. A deficiency in chloroplastic ferredoxin 2 facilitates effective photosynthetic capacity during long-term high light acclimation in *Arabidopsis thaliana*. Plant Journal **76**, 861–874.

Loreti E, Povero G, Novi G, Solfanelli C, Alpi A, Perata P. 2008. Gibberellins, jasmonate and abscisic acid modulate the sucrose-induced expression of anthocyanin biosynthetic genes in *Arabidopsis*. New Phytologist **179**, 1004–1016.

Ma L, Li Y, Li X, Xu D, Lin X, Liu M, Li G, Qin X. 2019. FAR-RED ELONGATED HYPOCOTYLS3 negatively regulates shade avoidance responses in *Arabidopsis*. Plant, Cell and Environment **42**, 3280–3292.

Maréchal A, Parent J-S, Véronneau-Lafortune F, Joyeux A, Lang BF, Brisson N. 2009. Whirly proteins maintain plastid genome stability in *Arabidopsis*. Proceedings of the National Academy of Sciences USA **106**, 14693–14698.

Martin C, Paz-Ares J. 1997. MYB transcription factors in plants. Trends in Genetics **13**, 67–73.

Martínez-García JF, Galstyan A, Salla-Martret M, Cifuentes-Esquivel N, Gallemí M, Bou-Torrent J. 2010. Regulatory components of shade avoidance syndrome. Advances in Botanical Research **53**, 65–116.

Michaels SD, Amasino RM. 1999. *FLOWERING LOCUS C* encodes a novel MADS domain protein that acts as a repressor of flowering. Plant Cell **11**, 949–956.

Millenaar FF, Cox MCH, De Jong Van Berkel YEM, Welschen RAM, Pierik R, Voesenek LAJC, Peeters AJM. 2005. Ethylene-induced differential growth of petioles in Arabidopsis. Analyzing natural variation, response kinetics, and regulation. Plant Physiology **137**, 998–1008.

Mullen JL, Weinig C, Hangarter RP. 2006. Shade avoidance and the regulation of leaf inclination in *Arabidopsis*. Plant, Cell and Environment **29**, 1099–1106.

Müller D, Schmitz G, Theres K. 2006. *Blind* homologous *R2R3 MYB* genes control the pattern of lateral meristem initiation in *Arabidopsis*. Plant Cell **18**, 586–597.

Murashige T, Skoog F. 1962. A revised medium for rapid growth and bio assays with tobacco tissue cultures. Physiologia Plantarum **15**, 473–497.

Napp-Zinn K. 1987. Vernalization-environmental and genetic regulation. Manipulation of Flowering London: Butterworths, 123–132.

Ni W, Xu SL, Tepperman JM, Stanley DJ, Maltby DA, Gross JD, Burlingame AL, Wang ZY, Quail PH. 2014. A mutually assured destruction mechanism attenuates light signaling in *Arabidopsis*. Science **344**, 1160–1164.

Nolan TM, Vukasinovic N, Liu D, Russinova E, Yin Y. 2020. Brassinosteroids: Multidimensional regulators of plant growth, development, and stress responses. Plant Cell **32**, 295-318.

Ogata K, Morikawa S, Nakamura H, Sekikawa A, Inoue T, Kanai H, Sarai A, Ishii S, Nishimura Y. 1994. Solution structure of a specific DNA complex of the Myb DNA-binding domain with cooperative recognition helices. Cell **79**, 639–648.

Payne CT, Zhang F, Lloyd AM. 2000. *GL3* encodes a bHLH protein that regulates trichome development in Arabidopsis through interaction with GL1 and TTG1. Genetics **156**, 1349–1362.

Pierik R, Whitelam GC, Voesenek LACJ, De Kroon H, Visser EJW. 2004. Canopy studies on ethylene-insensitive tobacco identify ethylene as a novel element in blue light and plant-plant signalling. Plant Journal **38**, 310–319.

Preston J, Wheeler J, Heazlewood J, Li SF, Parish RW. 2004. AtMYB32 is required for normal pollen development in *Arabidopsis thaliana*. Plant Journal **40**, 979–995.

Prikryl J, Watkins KP, Friso G, Van Wijk KJ, Barkan A. 2008. A member of the Whirly family is a multifunctional RNA- and DNA-binding protein that is essential for chloroplast biogenesis. Nucleic Acids Research **36**, 5152–5165.

Ramsay NA, Glover BJ. 2005. MYB-bHLH-WD40 protein complex and the evolution of cellular diversity. Trends in Plant Science **10**, 63–70.

Rowan DD, Cao M, Lin-Wang K, Cooney JM, Jensen DJ, Austin PT, Hunt MB, Norling C, Hellens RP, Schaffer RJ, Allan AC. 2009. Environmental regulation of leaf colour in red *35S:PAP1 Arabidopsis thaliana*. New Phytologist **182**, 102–115.

Ruberti I, Sessa G, Ciolfi A, Possenti M, Carabelli M, Morelli G. 2012. Plant adaptation to dynamically changing environment: The shade avoidance response. Biotechnology Advances **30**, 1047–1058.

Sawa S, Ohgishi M, Goda H, Higuchi K, Shimada Y, Yoshida S, Koshiba T. 2002. The *HAT2* gene, a member of the HD-Zip gene family, isolated as an auxin inducible gene by DNA microarray screening, affects auxin response in *Arabidopsis*. Plant Journal **32**, 1011–1022.

Searle I, He Y, Turck F, Vincent C, Fornara F, Krober S, Amasino RA, Coupland G. 2006. The transcription factor FLC confers a flowering response to vernalization by repressing meristem competance and systemic singaling in *Arabidopsis*. Genes & Development **20**, 898–912.

Sessa G, Carabelli M, Sassi M, Ciolfi A, Possenti M, Mittempergher F, Becker J, Morelli G, Ruberti I. 2005. A dynamic balance between gene activation and repression regulates the shade avoidance response in *Arabidopsis*. Genes & Development **19**, 2811–2815.

Shan X, Zhang Y, Peng W, Wang Z, Xie D. 2009. Molecular mechanism for jasmonate-induction of anthocyanin accumulation in *Arabidopsis*. Journal of Experimental Botany **60**, 3849–3860.

Sheen J. 2014. Master regulators in plant glucose signaling networks. Journal of Plant Biology **57**, 67–79.

Shen H, Luong P, Huq E. 2007. The F-box protein MAX2 functions as a positive regulator of photomorphogenesis in Arabidopsis. Plant Physiology **145**, 1471–1483.

Shin R, Burch AY, Huppert KA, Tiwari SB, Murphy AS, Guilfoyle TJ, Schachtman DP. 2007. The *Arabidopsis* transcription factor MYB77 modulates auxin signal transduction. Plant Cell **19**, 2440–2453.

Shirley B, Kubasek WL, Storz G, Bruggemann E, Koorneef M, Ausubel FM, Goodman HM. 1995. Analysis of *Arabidopsis* mutants deficient in flavonoid biosynthesis. Plant Journal **8**, 659–671.

Singh MV, Weil PA. 2002. A method for plasmid purification directly from yeast. Analytical Biochemistry **307**, 13-17.

Smaczniak C, Immink RGH, Muiño JM, Blanvillain R, Busscher M, Busscher-Lange J, Dinh QD, Liu S, Westphal A, Boeren S, Parcy F, Xu L, Carles CC, Angenent GC, Kaufmann K. 2012. Characterization of MADS-domain transcription factor complexes in *Arabidopsis* flower development. Proceedings of the National Academy of Sciences USA **109**, 1560–1565.

Smalle J, Vierstra RD. 2004. The ubiquitin 26S proteasome proteolytic pathway. Annual Review of Plant Biology **55**, 555–590.

Smeekens S, Ma J, Hanson J, Rolland F. 2010. Sugar signals and molecular networks controlling plant growth. Current Opinion in Plant Biology **13**, 273–278.

Smith H, Whitelam GC. 1997. The shade avoidance syndrome: Multiple responses mediated by multiple phytochromes. Plant, Cell and Environment **20**, 840–844.

Somers DE, Caspar T, Quail PH. 1990. Isolation and characterization of a ferredoxin gene from *Arabidopsis thaliana*. Plant Physiology **93**, 572–577.

Sorin C, Salla-Martret M, Bou-Torrent J, Roig-Villanova I, Martínez-García JF. 2009. ATHB4, a regulator of shade avoidance, modulates hormone response in Arabidopsis seedlings. Plant Journal **59**, 266–277.

Steeves TA, Sussex IM. 1989. Patterns in Plant Development.

Steindler C, Matteucci A, Sessa G, Weimar T, Ohgishi M, Aoyama T, Morelli G, Ruberti I. 1999. Shade avoidance responses are mediated by the ATHB-2 HD-Zip protein, a negative regulator of gene expression. Development **126**, 4235–4245.

Stirnberg P, Furner IJ, Ottoline Leyser HM. 2007. MAX2 participates in an SCF complex which acts locally at the node to suppress shoot branching. Plant Journal **50**, 80–94.

Stirnberg P, Van de Sande K, Leyser HMO. 2002. *MAX1* and *MAX2* control shoot lateral branching in *Arabidopsis*. Development **129**, 1131–1141.

Stirnberg P, Zhao S, Williamson L, Ward S, Leyser O. 2012. *FHY3* promotes shoot branching and stress tolerance in Arabidopsis in an *AXR1*-dependent manner. Plant Journal **71**, 907–920.

Stracke R, Werber M, Weisshaar B. 2001. The *R2-R3-MYB* gene family in *Arabidopsis thaliana*. Cell Signaling & Gene Regulation **4**, 447–456.

Ströher E, Dietz KJ. 2008. The dynamic thiol-disulphide redox proteome of the *Arabidopsis thaliana* chloroplast as revealed by differential electrophoretic mobility. Physiologia Plantarum **133**, 566–583.

Talbert PB, Adler HT, Parks DW, Comai L. 1995. The *REVOLUTA* gene is necessary for apical meristem development and for limiting cell divisions in the leaves and stems of *Arabidopsis thaliana*. Development **121**, 2723–2735.

Teichmann T, Muhr M. 2015. Shaping plant architecture. Frontiers in Plant Science **6**, 1–18.

Tian Y, Sacharz J, Ware MA, Zhang H, Ruban AV. 2017. Effects of periodic photoinhibitory light exposure on physiology and productivity of Arabidopsis plants grown under low light. Journal of Experimental Botany **68**, 4249–4262.

Tran LSP, Nakashima K, Sakuma Y, Osakabe Y, Qin F, Simpson SD, Maruyama K, Fujita Y, Shinozaki K, Yamaguchi-Shinozaki K. 2007. Co-expression of the stress-inducible zinc finger homeodomain ZFHD1 and NAC transcription factors enhances expression of the *ERD1* gene in Arabidopsis. Plant Journal **49**, 46–63.

Turchi L, Carabelli M, Ruzza V, Possenti M, Sassi M, Peñalosa A, Sessa G, Salvi S, Forte V, Morelli G, Ruberti I. 2013. *Arabidopsis* HD-Zip II transcription factors control apical embryo development and meristem function. Development **140**, 2118–2129.

Urano D, Phan N, Jones JC, Yang J, Huang J, Grigston J, Taylor JP, Jones AM. 2012. Endocytosis of the seven-transmembrane RGS1 protein activates G-protein-coupled signalling in *Arabidopsis*. Nature Cell Biology **14**, 1079–1088.

Valladares F, Pugnaire FI. 1999. Tradeoffs between irradiance capture and avoidance in semi-arid environments assessed with a crown architecture model. Annals of Botany **83**, 459–469.

Vandenbussche F, Vriezen WH, Smalle J, Laarhoven LJJ, Harren FJM, Van Der Straeten D. 2003. Ethylene and auxin control the Arabidopsis response to decreased light intensity. Plant Physiology **133**, 517–527.

Vogt T, Pollak P, Tarlyn N, Taylor LP. 1994. Pollination or wound-induced kaempferol accumulation in petunia stigmas enhances seed production. Plant Cell **6**, 11–23.

Voss I, Koelmann M, Wojtera J, Holtgrefe S, Kitzmann C, Backhausen JE, Scheibe R. 2008. Knockout of major leaf ferredoxin reveals new redox-regulatory adaptations in *Arabidopsis thaliana*. Physiologia Plantarum **133**, 584–598.

Walker AR, Davison PA, Bolognesi-Winfield AC, James CM, Srinivasan N, Blundell TL, Esch JJ, David Marks M, Gray JC. 1999. The *TRANSPARENT TESTA GLABRA1* locus, which regulates trichome differentiation and anthocyanin biosynthesis in Arabidopsis, encodes a WD40 repeat protein. Plant Cell **11**, 1337–1349.

Wang M, Rui L, Yan H, Shu H, Zhao W, Lin JE, Zhang K, Blakeslee JJ, Mackey D, Tang D, Wei Z, Wang G-L. 2018. The major leaf ferredoxin Fd2 regulates plant innate immunity in Arabidopsis. Molecular Plant Pathology **19**, 1377–1390.

Wiersma C, Christians M. 2015. Modification of LRB complex members in *Arabidopsis thaliana*. Student Summer Scholars **157**, 1-10.

Winkel-Shirley B. 2002. Biosynthesis of flavonoids and effects of stress. Current Opinion in Plant Biology **5**, 218–223.

Winter D, Vinegar B, Nahal H, Ammar R, Wilson G V., Provart NJ. 2007. An 'electronic fluorescent pictograph' browser for exploring and analyzing large-scale biological data sets. PLoS ONE **2**, 1–12.

Woo HR, Kim JH, Nam HG, Lim PO. 2004. The delayed leaf senescence mutants of *Arabidopsis*, *ore1*, *ore3*, and *ore9* are tolerant to oxidative stress. Plant and Cell Physiology **45**, 923–932.

Xiong JY, Lai CX, Qu Z, Yang XY, Qin XH, Liu GQ. 2009. Recruitment of AtWHY1 and AtWHY3 by a distal element upstream of the kinesin gene *AtKP1* to mediate transcriptional repression. Plant Molecular Biology **71**, 437–449.

Xu W, Dubos C, Lepiniec L. 2015. Transcriptional control of flavonoid biosynthesis by MYB-bHLH-WDR complexes. Trends in Plant Science **20**, 176–185.

Yang SW, Jang I-C, Henriques R, Chua N-H. 2009. FAR-RED ELONGATED HYPOCOTYL1 and FHY1-LIKE associate with the *Arabidopsis* transcription factors LAF1 and HFR1 to transmit phytochrome A signals for inhibition of hypocotyl elongation. Plant Cell **21**, 1341–1359.

Yoo HH, Kwon C, Lee MM, Chung IK. 2007. Single-stranded DNA binding factor AtWHY1 modulates telomere length homeostasis in Arabidopsis. Plant Journal **49**, 442–451.

Zhao M, Morohashi K, Hatlestad G, Grotewold E, Lloyd A. 2008. The TTG1-bHLH-MYB complex controls trichome cell fate and patterning through direct targeting of regulatory loci. Development **135**, 1991–1999.

Zhu D, Rosa S, Dean C. 2015. Nuclear organization changes and the epigenetic silencing of *FLC* during vernalization. Journal of Molecular Biology **427**, 659–669.

Zimmermann IM, Heim MA, Weisshaar B, Uhrig JF. 2004. Comprehensive identification of *Arabidopsis thaliana* MYB transcription factors interacting with R/B-like BHLH proteins. Plant Journal **40**, 22–34.

Figure 1.1 LOF1-BD interaction with proteins of interest. Yeast two-hybrid assay contained BD-LOF1 and the indicated AD fusion proteins were dotted on -WL or -WLAH +3-AT selective media and grown for 48 hours. W = tryptophan; L = leucine; A = adenine; H = histidine; 3-AT = 3-amino-1, 2, 4-triazole.

Prey	-WL	-WLAH +3AT
HB4-AD		
HAT3-AD		
WHY1-AD		
WHY3-BD		
AD		

Figure 1.2 *LRB2* schematic representation and transcript levels in *lrb2* mutants. A) Schematic representation of *LRB2* gene. Gene is drawn in the 5' to 3' direction. Boxes represent exons. Lines represent introns. Unfilled boxes represent the 5' UTR and 3' UTR. Blue triangles represent T-DNA insertion sites. Red arrows represent primers used in RT-PCR. The scale bar is 100 base pairs in length. B) Semi-quantitative RT-PCR was used to measure transcript levels of *LRB2* in *lrb2-2* and wild-type controls. RNA was isolated from pooled shoots of 14-day-old seedlings. C) Semi-quantitative RT-PCR was used to measure transcript levels of *LRB2* of *lrb2-3*/SALK_100118 and wild-type controls. RNA was isolated from unopened floral buds of adult plants. Cycle numbers are given in parentheses to the right of gel lanes.

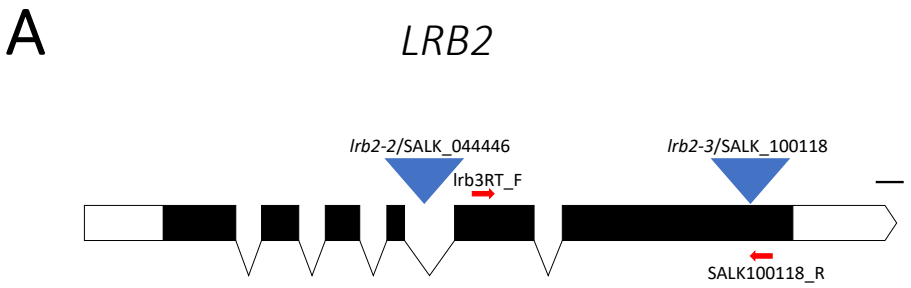
A
LRB2
lrb2-2/SALK_044446
lrb3RT_F
lrb2-3/SALK_100118
SALK100118_R
B
lrb2-2/SALK_044446
Columbia WT
LRB2
(28)
ACT2
(22)
C
Columbia WT
lrb2-3/SALK_100118
LRB2
(29)
ACT2
(22)

Figure 1.3 *WHY3* schematic representation and transcript levels in *why3*/*KO3* mutants. A) Schematic representation of *WHY3* gene. Gene diagram uses the same symbols as in Figure 1.2. Gene is drawn in the 5' to 3' direction. Scale bar is 100 base pairs in length. B) Semi-quantitative RT-PCR of *WHY3* in *KO3* allele and wild-type control plants. RNA was isolated from unopened floral buds of six-week-old plants. Cycle numbers are given in parentheses to the right of gel lanes.

A

WHY3

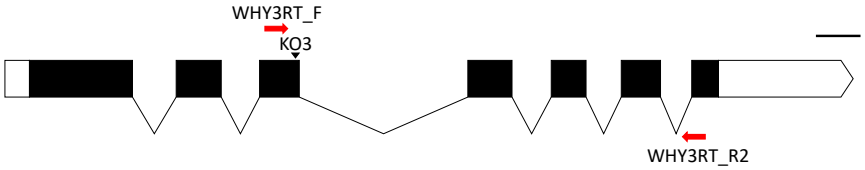

B

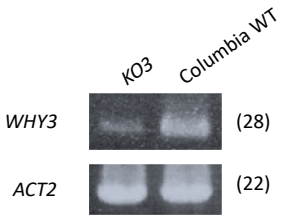

Figure 1.4 *WHY1* schematic representation and transcript levels in *why1* mutants. A) Schematic representation of *WHY1* gene. Gene diagram uses the same symbols as in Figure 1.2. Gene is drawn in the 5' to 3' direction. The scale bar is 100 base pairs in length. B and C) Semi-quantitative RT-PCR of *WHY1* transcript levels between *KO-1/why1-1*/SALK_023713 and wild-type control plants in B and between *why1-3*/CS65558 and wild-type control plants in C. RNA was isolated from pooled shoots of 14-day old seedlings. Cycle numbers are given in parentheses to the right of gel lanes.

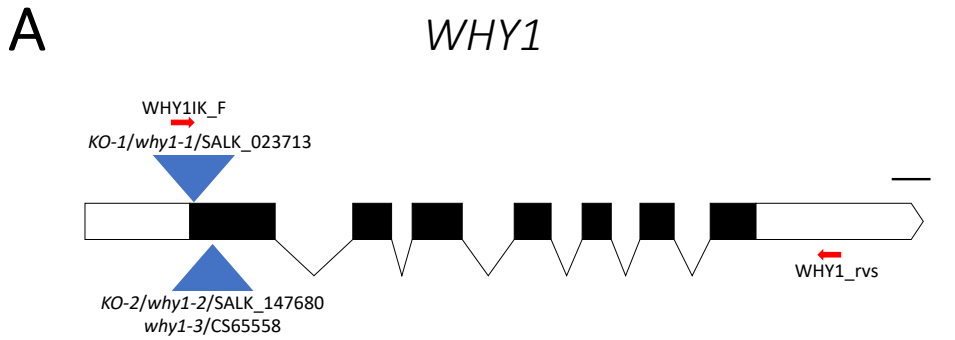
A
WHY1
WHY1IK_F
KO-1/why1-1/SALK_023713
WHY1_rvs
KO-2/why1-2/SALK_147680
why1-3/CS65558
B
KO-1/why1-1/SALK_023713
Columbia WT
WHY1
(30)
ACT2
(22)
C
Columbia WT
why1-3/CS65558
WHY1
(27)
ACT2
(22)

Figure 1.5 *ATHB4* schematic representation and transcript levels in *athb4* mutants. A) Schematic representation of *ATHB4* gene. Gene diagram uses the same symbols as in Figure 1.2. Gene is drawn in the 5' to 3' direction. The scale bar is 100 base pairs in length. B) Semi-quantitative RT-PCR of *ATHB4* transcript levels between *athb4-2*/SALK_121097 and wild-type control plants. RNA was isolated from pooled shoot tissue from 14-day old seedlings. Cycle numbers are given in parentheses to the right of gel lanes.

A

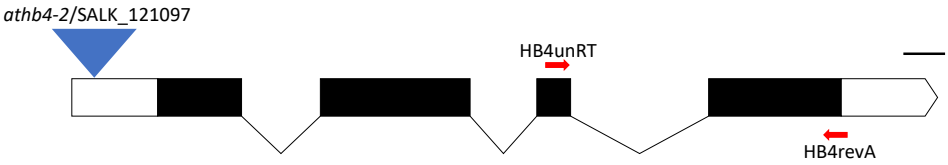
ATHB4
athb4-2/SALK_121097
HB4unRT
HB4revA

B

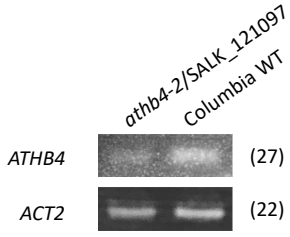
athb4-2/SALK_121097
Columbia WT
ATHB4
(27)
ACT2
(22)

Figure 1.6 *HAT3* schematic representation and transcript levels in *hat3* mutants. A) Schematic representation of *HAT3* gene. Gene diagram uses the same symbols as in Figure 1.2. Gene is drawn in the 5' to 3' direction. The scale bar is 100 base pairs in length. B and C) Semi-quantitative RT-PCR of *HAT3* in *hat3-2*/SALK_083383, *hat3-3*/SALK_014055C, and wild-type controls in B and in *hat3-4*/SALK_105885 and wild-type controls in C. RNA was isolated from shoot tissue from 14-day old seedlings. Cycle numbers are given in parentheses to the right of gel lanes.

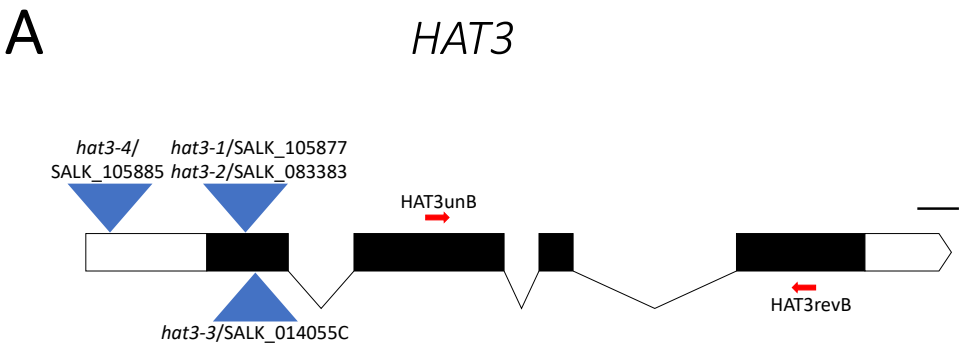
A
HAT3
hat3-4/
SALK_105885
hat3-1/SALK_105877
hat3-2/SALK_083383
HAT3unB
HAT3revB
hat3-3/SALK_014055C
B
hat3-2/SALK_083383
hat3-3/SALK_014055C
Columbia WT
HAT3
(27)
ACT2
(22)
C
Columbia WT
hat3-4/SALK_105885
HAT3
(27)
ACT2
(22)

Table 1.1 LOF1-interacting proteins identified in the yeast two-hybrid assay. Number of times each LOF1 interactor was isolated in the yeast two-hybrid assay is shown. Interactors are listed in order of chromosome number and location. Predicted subcellular localization assessed from SUBA4 and available data (Hooper *et al.,* 2017).

Locus	Gene Abbreviation	Protein Name/Family	Putative Function	Times Obtained	Predicted Localization
At4G26410	*RHIP1*	RGS-HXK1 INTERACTING PROTEIN 1	Regulating glucose-regulated gene expression	6	nucleus, mitochondria
At1G60950	*FD2*	FERREDOXIN 2	major leaf ferredoxin	3	chloroplast
At2G41600	N/A	N/A	mitochondrial glycoprotein	3	mitochondria
At2G02740	*WHY3*	WHIRLY 3	DNA repair, defense response, regulation of transcription	2	nucleus, chloroplast
At1G06390	*ATGSK1*	GSK/SHAGGY-LIKE PROTEIN KINASE 1	Response to osmotic stress, brassinosteroid signaling, protein phosphorylation	1	cytosol, plasma membrane
At1G07210	*RPS18*	RIBOSOMAL PROTEIN S18	ribosomal protein, translation	1	chloroplast, mitochondria
At1G11430	*MORF9*	MULTIPLE ORGANELLAR RNA EDITING FACTOR 9	RNA editing in chloroplasts, cytidine to uridine editing	1	chloroplast
At1G12840	*ATVHA-C/DET3*	ARABIDOPSIS VACUOLAR ATP SYNTHASE SUBUNIT C/DE-ETIOLATED 3	vacuolar H(+)-ATPase, proton transmembrane transportlignin biosynthesis, unidimensional cell growth	1	many

At1G13440	*GAPC2*	GLYCERALDEHYDE-3-PHOSPHATE DEHYDROGENASE C-2	defense response, oxidation-reduction process, gluconeogenesis, glycolytic process	1	many
At1G17830	N/A	hypothetical protein, DUF789	Unknown	1	nucleus
At1G31930	*XLG3*	EXTRA-LARGE GTP-BINDING PROTEIN 3	root development and morphogenesis, response to sugars, gravitropism, response to ABA	1	nucleus, G-protein complex
At1G49240	*ACT8*	ACTIN 8	cell division, root hair cell tip growth	1	many
At1G56280	*DI19*	DROUGHT-INDUCED 19	response to drought, positive regulation of transcription	1	nucleus
At1G66200	*GLN1;2*	GLUTAMINE SYNTHETASE 1;2	glutamine biosynthesis, nitrate assimilation	1	apoplast, chloroplast, cytosol, mitochondria, vacuole
At1G73820	*SSU72*	suppressor of sua7 2 (yeast)	vernalization, mRNA processing, CTD phosphatase	1	chloroplast, nucleus
At1G79010	N/A	alpha-helical ferredoxin	mitochondrial electron transport, aerobic respiration	1	mitochondria
At2G20330	N/A	transducin/WD40 repeat-like superfamily	douvle-stranded DNA break processing, regulation of histone H2B ubiquitination	1	nucleus, E3 ubiquitin ligase complex
At2G26400	*ARD3*	ACIREDUCTONE DIOOXYGENASE 3	methionine metabolic process, oxidation-reduction process	1	cytosol, nucleus, plasma membrane

At2G44910	*ATHB4*	ARABIDOPSIS HOMEOBOX-LEUCINE ZIPPER PROTEIN 4	shadeavoidance response, leaf development, response to red light	1	nucleus
At3G46940	*DUT1*	DUTP-PYROPHOSPHATASE-LIKE 1	DNA repair, dUTP catabolic process	1	cytosol
At3G47650	*BDS2*	BUNDLE SHEATH DEFECTIVE 2, DNAJ/Hsp40 cysteine-rich domain superfamily	chaperone-mediated protein folding, chloroplast ribulose biphosphate carboxylase complex assembly	1	chloroplast, cytosol
At3G54826	*ZR3*	ZINC RIBBON 3, Zim17-type zinc finger	protein folding, protein stabilization, protein import in mitocondria	1	mitochondria
At3G55700	N/A	UDP-glycosyltransferase superfamily protein	UDP-glycosyltransferase, glycosyl group transfer	1	nucleus, intracellular membrane-bound organelle
At3G60450	N/A	phosphoglycerate mutase family protein	Unknown	1	cytosol, nucleus
At3G61600	*LRB2*	LIGHT-RESPONSIVE BTB 2, POZ/BTB containing G-protein	protein ubiquitylation, response to red light	1	nucleus, cytoplasm
At4G14746	N/A	neurogenic notch-like protein	Unknown	1	membrane
At4G20890	*TUB9*	TUBULIN 9, TUBULIN BETA-9 CHAIN	microtubule cytoskeleton organization, cell cycle	1	plasma membrane, cytosol

At4G29840	*MTO2/TS*	METHIONINE OVER-ACCUMULATOR 2/ THREONINE SYNTHASE	threonine biosynthesis	1	chloroplast, mitochondria
At4G34990	*MYB32*	MYB DOMAIN PROTEIN 32	pollen development, salt stress response, regulation of transcription	1	nucleus
At5G14970	N/A	seed maturation-like protein	Unknown	1	Unknown
At5G11450	*PPD5*	PSBP DOMAIN PROTEIN 5, PsbP family	Mog1/PcbP/DUF1795-like photosystem II reaction center, photosynthesis, axillary bud formation	1	chloroplast, mitochondria
At5G16320	*FRL1*	FRIGIDA LIKE 1	vernalization, cell differentiation, flower development	1	nucleus
At5G17930	N/A	MIF4G/MA3 domain containing protein	ribosomal small subunit biogenesis	1	nucleus
At5G22640	*EMB1211/TIC100*	EMBRYO DEFECTIVE 1211/TRANSLOCON AT THE INNER ENVELOPE OF CHLOROPLASTS 100, MORN motif protein	embryo development, chloroplast biogenesis, protein import into chloroplast	1	chloroplast, nucleus
At5G46420	N/A	16s rRNA processing RimM family	rRNA processing, UDP-N-acetylglucosamine biosynthesis	1	chloroplast, ribosome
At5G51110	*RAF2*	RUBISCO ASSEMBLY FACTOR 2	rubisco assembly, ABA stress response, salt stress response, tetrahydrobiopterin biosynthesis, chloroplast ribulose biphosphate carboxylase complex assembly	1	chloroplast, nucleus, plasma membrane

At5G58290	*RPT3*	REGULATORY PARTICLE TRIPLE-A ATPASE 3, 26S proteome AAA-ATPASE subunit	protein catabolism, positive regulation of RNA polymerase II transcriptional pre-initiation complex assembly, light-dependent hypocotyl elongation	1	cell wall, cytosol, chloroplast, nucleus
At5G58220	*ALNS/ TTL*	ALLANTOIN SYNTHASE/ TRANSTHYRETIN-LIKE PROTEIN	allatoin synthase, brassinosteroid signaling, regulation of growth by extracellular stimulus, purine nucleobase metabolic process	1	cytosol, peroxisome, extracellular region
At5G58330	*NADP-MDH*	NADP-DEPENDENT MALATE DEHYDROGENASE, lactate/malate dehydrogenase family	hydrogen peroxide signaling, response to redox state, tricarboxylic acid cycle	1	chloroplast, mitochondria, apoplast
At5G62690	*TUB2*	TUBULIN BETA CHAIN 2, tubulin beta-2/beta-3 chain	microtubule cytoskeleton organization, mitotic cell cycle	1	many
At5G62700	*TUB3*	TUBULIN BETA CHAIN 3, tubulin beta-2/beta-3 chain	microtubule cytoskeleton organization, mitotic cell cycle	1	Golgi, cell wall, cytoplasm
At5G65260	N/A	RNA-binding (RRM/RBD/RNP motifs) family protein	Unknown	1	cytoplasm, nucleus

Table 1.2 LOF1-interacting proteins of interest and functionally redundant proteins.

Interactor of Interest	Putative Functionally Redundant Protein
MYB32	None
LRB2	None
ATHB4	HAT3
WHY3	WHY1

Table 1.3 List of oligonucleotide sequences. Primers designed using the following reference are indicated (Liu *et al.*, 2012).

Primer	Sequence (5' --> 3')	Tm	Use	Source
myb117y2h_R	GGATCCTCACGCCGTCCCCAAGCCAA	82.5	Cloning of *LOF1* full length	
LOF1NdeI_F	CATATGTTTATAACGGAAAAACAAGTGTGG	64.4	Cloning of *LOF1* full length	
ADLD_R2	GCACGATGCACAGTTGAAGT	56.1	PCR of Y2H library plasmid inserts	
ADLD_F2	TGAAGATACCCCACCAAACC	54.6	PCR of Y2H library plasmid inserts	
3'AD LD Insert Screening	GTGAACTTGCGGGGTTTTTCAGTATCTACGAT	61.5	PCR of Y2H library plasmid inserts	Clontech
5'AD LD Insert Screening	CTATTCGATGATGAAGATACCCCACCAAACCC	61.4	PCR of Y2H library plasmid inserts	Clontech
BD_R	CGTTTTAAAACCTAAGAGTC	45.6	PCR to check Y2H BD plasmid	Clontech
BD_F	TCATCGGAAGAGAGTAGT	45.8	PCR to check Y2H BD plasmid	Clontech
T7	GTAATACGACTCACTATAGGGC	56.2	Sequencing Y2H library inserts	
ZFHD1_R	ATCGATCAAGAAGATGAAGAC	49.7	Cloning of *ZFHD1*	
ZFHD1_F	CATATGGATTTGTCTTCCA	46.9	Cloning of *ZFHD1*	
ZFHD1seq_R	GTGGGACTCGGCATAAACTC	55.6	Sequencing of *ZFHD1* clone	
HAT3_ClaI_R	ATCGATCTAATGAGAACCAGCAGCAGGT	61.1	Cloning of *HAT3*	
HAT3_NcoI_F	CCATGGGGATGAGTGAAAGAGATGATG	58.9	Cloning of *HAT3*	
WHY1_ClaI_R	ATCGATCATCTATTCCATTCATAGTC	52.3	Cloning of *WHY1*	
WHY1_NcoI_F	CCATGGGGATGTCGCAACTCTTATCGACT	63.1	Cloning of *WHY1*	

Hat3_R	ACCATGGTTGAAAAGGGATG	53.1	Genotyping of *HAT3*	
Hat3_F	GCATATGCTGCATGTGTGATG	54.8	Genotyping of *HAT3*	
HB41_R	GGGTTCACGGGGTAACTCTAG	56.8	Genotyping of *HB4*	
HB41_F	TCTGAAACATAGATCCGAAGT	50.8	Genotyping of *HB4*	
pMYB117_F2	GGCAGTCCACAGCAAAATCGAATATCG	73.7	Genotyping of *LOF1*	(Lee *et al.,* 2009)
pMYB117_R	CCCGGGTGAACCGCTACATCTCCAAGAG	78.4	Genotyping of *LOF1*	(Lee *et al.,* 2009)
QLOF1_R	GCATCAGCCTCTCCTCTTCTT	54.4	Genotyping of *LOF1*	
WHY1yk_R2	CAAAGAACACAAGTAAAC	43.5	Genotyping of *WHY1*	(Yoo *et al.,* 2007)
WHY1yk_F2	CTCTGAGTGTGTAAAGGA	48.0	Genotyping of *WHY1*	(Yoo *et al.,* 2007)
SALK100118_F	AGCCTAGCCTCCGAAGAATC	56.4	Genotyping of *LRB2*	
SALK100118_R	ACTGCTTTCCCTCCTGTGAA	56.3	RT-PCR and genotyping of *LRB2*	
W138rev	GCCCAAGGCTAACTAGATTACCGAT	58.3	Genotyping of *WHY3*	(Márechal *et al.,* 2009)
KOWT2_F	TGGTGTTCGTCAATATGATGGG	55.0	Genotyping of *WHY3*	(Liu *et al.,* 2012)
KO3mu1_F	TGGTGTTCGTCAATATGATCGA	53.9	Genoyping of *why3/KO* mutants	(Liu *et al.,* 2012)
LBa1	TGGTTCACGTAGTGGGCCATCG	73.0	Genotyping of *lof1-1*	SALK Institute
LBb1.3	ATTTTGCCGATTTCGGAAC	51.5	Genotyping of SALK lines and T-DNA insert sequencing	SALK Institute
lrb2RT_F	TGCCTCTTGTATGAGGTACTGC	56.5	RT-PCR of *LRB2*	

ACT2-C	ACTCACCACCACGAACCAG	63.8	RT-PCR of *ACT2*	
ACT2-N	AAAATGGCCGATGGTGAGG	66.9	RT-PCR of *ACT2*	
HB4unRT	TCAGAACCGTAGGGCAAG	54.3	RT-PCR of *HB4*	(Turchi *et al.*, 2013)
HB4revA	CCCTAGCGACCTGATTTTTGCTGG	60.1	RT-PCR of *HB4*	(Turchi *et al.*, 2013)
WHY1_rvs	CAGACTGATGTTTTGAGATACAACC	53.9	RT-PCR of *WHY1*	(Isemer *et al.*, 2012)
WHY1IK_F	AGGGAACAAACACAAAGCGA	55.1	RT-PCR of *WHY1*	(Yoo *et al.*, 2007)
WHY3RT_F	TCTGGTGCGTTCAAGCTG	55.6	RT-PCR of *WHY3*	
WHY3RT_R2	AGCCTATAAGGTGCGGCAAG	57.5	RT-PCR of *WHY3*	
HAT3unB	CAGGTGCAGTTGGAGGAGGTAG	59.3	RT-PCR of *HAT3*	(Turchi *et al.*, 2013)
HAT3revB	GAGTAGTGGGAGGTTTCATGTGC	57.6	RT-PCR of *HAT3*	(Turchi *et al.*, 2013)

Chapter 2

The Subcellular Localization of LOF1-GFP in Response to Abiotic Stress

Abstract

Many plastid-localized proteins are encoded by the nucleus in the plant cell and therefore many plastid functions – such as division and DNA replication – are controlled by the nucleus. This is referred to as anterograde control. Conversely, the status of the plastid must be communicated to the nucleus. Retrograde signals relay plastid developmental status or functional states, such as stress, to the nucleus. Environmental stresses - such as excess light or water deficit - lead to the production of retrograde signals that inform the nucleus of plastid stress. Photosynthesis, the process by which plants use light and carbon dioxide to produce oxygen and glucose, takes place in the chloroplast of plant cells. Reactive oxygen species (ROS) produced in the chloroplast during abiotic stress have the potential to impair photosynthesis. ROS are thought to act as a retrograde signal. Additional possible retrograde signals have been proposed, such as tetrapyrroles, certain isoprenoids, and some transcription factors. Because retrograde signals move from the plastid to the nucleus for both the purpose of communicating information on plastid development and plastid functional state, plastid development is tightly linked to plastid functional state. *LATERAL ORGAN FUSION1* (*LOF1*) is expressed in organ boundaries and encodes an MYB transcription factor. A LOF1 yeast two-hybrid assay (Chapter 1) revealed that LOF1 interacts with proteins that are involved in abiotic stress responses and are localized to the chloroplast and/or mitochondria. At

least one protein isolated in the screen, WHIRLY3 (WHY3), was shown to be localized to both the nucleus and chloroplast (Table 1.1). Under our growth conditions, LOF1-GFP is localized to the nucleus in roots. When exposed to simulated drought, high light, or ROS (H_2O_2), LOF1-GFP did not appear to change subcellular localization and remained nuclear-localized under all stress conditions tested. Therefore, plastid- and/or mitochondria-localized proteins may change subcellular localization during conditions of abiotic stress to interact with LOF1 in the nucleus.

Introduction

The Chloroplast and Retrograde Signaling

The plastid in plants evolved from endosymbiosis events with ancient eukaryotic cells (Nott *et al.*, 2006). The unicellular, free-living, photosynthetic bacterium that would eventually evolve into the plastid was in control of its own gene expression. Over time, microbial genes were transferred to the host's genome or were lost due to their nonessential nature. The contemporary plastid genome in higher plants contains fewer than 100 genes. Most of the over 3000 polypeptides needed by the chloroplast are encoded by genes from the nuclear genome and post-translationally imported into the chloroplast (Abdallah *et al.*, 2000; Leister, 2003). Because so many chloroplast-targeted proteins are encoded by the nuclear genome, the nucleus has some control of chloroplast development and gene expression (Goldschmidt-Clermont, 1998; Leon *et al.*, 1998). This anterograde control the nucleus has upon chloroplast functions serves primarily to coordinate nucleus and chloroplast gene expression so that the proper stoichiometry of

chloroplast protein complexes is achieved (Jung and Chory, 2010). The chloroplast has retrograde control mechanisms as well, by which chloroplast development and functional states can regulate nuclear gene expression. An increasing number of identified retrograde signals involve response to abiotic stress factors after seedling establishment [reviewed in (De Souza *et al.*, 2017)].

Retrograde signaling was first observed about forty years ago when it was discovered that repression of protein synthesis in the plastid also disturbed cytosolic protein synthesis for nuclear-encoded genes (Bradbeer *et al.*, 1979). There are two types of retrograde signaling. Biogenic signaling is the signaling pathways involved in plastid development, and operational signaling is signaling involved in altering plastid homeostasis in response to environment cues (Pogson *et al.*, 2008). The chloroplast is thought to act like environmental sensor for the plant cell and plays a role in adaptation to abiotic and biotic stress (Chan *et al.*, 2016). Signals emanating from the chloroplast coordinate the activities of the nucleus and other organelles.

The chloroplast is essential for photosynthesis and the production of metabolites and hormones in plant cells. There are two stages to photosynthesis: the light-dependent reactions and the light-independent reactions (Pogson and Albrecht, 2011). In the light-dependent stage, the chloroplast captures light energy and converts it into chemical energy in the form of nicotinamide adenine dinucleotide phosphate (NADPH) and adenosine triphosphate (ATP) with oxygen as a byproduct. In the light-independent reaction, NADPH provides hydrogen and ATP provides energy for the formation of glucose. The light-dependent reactions take place on the chloroplast's thylakoid

membrane. The thylakoid membrane contains some of the most important protein complexes for photosynthesis: photosystem II (PSII), cytochrome b_6f (b_6f), photosystem I (PSI), and ATP synthase (Bishop, 1971; Haehnel, 1984). Electrons are transferred to and from different proteins on the thylakoid membranes via redox reactions in a process called the electron transport chain (ETC). A proton gradient inside the thylakoid lumen forms, creating a force that produces ATP. Disruption of the ETC creates retrograde signals (Krall *et al.*, 1961; Frenkel, 1995).

In order for chloroplast biogenesis and photosynthesis to occur, genes that encode chloroplast-localized proteins must be transcribed from both the nucleus and chloroplast. Chloroplast protein translation, import, and turnover are also essential. Communication between the chloroplast and nucleus is critical to this process. Often, mutations in genes involved in retrograde signaling or chloroplast development will both lead to a chlorotic or bleached leaf phenotype. Thus, chloroplast development is tightly linked with organellar signaling (Pogson *et al.*, 2015).

In plant cells, the process of photosynthesis produces reactive oxygen species (ROS). ROS take four major forms in plant cells: singlet oxygen ($^1O_2$), hydrogen peroxide (H_2O_2), superoxide anion (O_2^-), and hydroxyl radical (HO^-). Most ROS are produced from the partial reduction of atmospheric triplet oxygen ($^3O_2$) during light-dependent photosynthesis at PSI to form a superoxide anion (Baker, 1991; Cruz De Carvalho, 2008). The superoxide anion is then disproportionated to hydrogen peroxide by superoxide dismutase, or this can happen spontaneously. Hydrogen peroxide can sometimes then be reduced to a hydroxyl radical by PSII-bound metals when water is

incompletely reduced to hydrogen peroxide (Asada, 2006). More rarely ROS originates from PSII, where the excited triplet center chlorophyll interacts with oxygen to produce singlet oxygen (Pospíšil, 2009). These are the most common ways for ROS to form during photosynthesis; ROS form through other pathways in plant cells and in different organelles. Mitochondria, chloroplasts, and peroxisomes all generate a low level of ROS under normal environmental conditions that does not cause a plant stress response. ROS are not a problem to plant cells until levels become high (Pitzschke *et al.*, 2006)

Different abiotic stresses, such as high light, drought, and nutrient deprivation, all lead to increased ROS production by decreasing the maximum photosynthetic capacity of the chloroplast. ROS cause oxidative stress through the altering of redox reactions necessary for photosynthesis, putting strain on the ETC (Smirnoff, 1993; Li *et al.*, 2009; Moellering *et al.*, 2010). The high reactivity of ROS molecules causes oxidative damage to cellular components, such as lipids, proteins, and DNA, eventually leading to cell death if ROS species are not rapidly dissipated (Mittler, 2002). When exposed to high light for long periods of time, anthocyanin (a ROS scavenger) will accumulate in leaves, plants will become bushier and will often flower early (Fahnenstich *et al.*, 2008; Tian *et al.*, 2017). Leaf angle may change (Valladares and Pugnaire, 1999; Millenaar *et al.*, 2005), and brown lesions may form on leaves, eventually becoming necrotic (Halliwell, 2006; Heyneke *et al.*, 2013).

Plants have several ways of coping with ROS and high-light stress. One way is by moving the leaves or chloroplasts away from the light source. Chloroplasts will re-distribute to the anticlinal walls in palisade mesophyll cells during high light exposure.

Similarly, the leaves may become positioned more vertically: although most species are not able to move their leaves quickly enough to avoid damage (King, 1997; Wada, 2013). Another ROS-coping mechanism is non-photochemical quenching, which is achieved by the antenna of PSII discharging photons as heat. It is estimated that over half of the light absorbed by PSII is redirected in this manner. Non-photochemical quenching competes with fluorescence emission and, thus, photosynthesis (Ort, 2001; Niyogi and Truong, 2013). ROS can also be detoxified to less harmful substances, thereby inhibiting further oxidative damage. For example, ascorbate and glutathione are important reducing agents that function to eliminate ROS (Jiménez *et al.*, 1998; Asensi-Fabado and Munné-Bosch, 2010; Foyer and Noctor, 2011).

ROS, components of tetrapyrrole biosynthesis, some secondary metabolites, and certain transcription factors have been previously identified as retrograde signaling candidates (Singh *et al.*, 2015; De Salvo *et al.,* 2017). ROS are retrograde signaling candidates because changes in chloroplast redox status have long been associated with changes in nuclear gene expression (Leister, 2019). H_2O_2 is the most likely ROS species to be involved in retrograde signaling for several reasons. H_2O_2 is the most stable of the common ROS species and has the longest half-life (~1 ms), which allows it to move between subcellular compartments (Cruz De Carvalho, 2008). Transcriptomic analyses have revealed hundreds of H_2O_2-responsive genes in *Arabidopsis* (Ding *et al.*, 2010; Yun *et al.*, 2010). H_2O_2 is also known to mediate abscisic acid (ABA) signaling in response to drought stress (Neill et al, 2007; Wang et al, 2008). Singlet oxygen ($^1O_2$) is an unlikely retrograde signal candidate due to limited diffusion ability and extremely short half-life

(3-4 μs) combined with high reactivity (Kochevar, 2004; Krieger-Liszkay, 2005; Mullineaux *et al.*, 2006). However, β-cyclocitral (β-CC) is a $^1O_2$-oxidation product of carotenoids and induces expression of genes responsive to $^1O_2$ (Ramel *et al.*, 2012). β-CC has the ability to travel to the cytosol by diffusion and has been proposed to act as a $^1O_2$ messenger (Leister, 2012; Ramel *et al.*, 2012). Therefore, $^1O_2$ may generate a retrograde signal - β-CC. A role for the superoxide anion ($O_2^{\cdot-}$) in retrograde signaling has also been suggested; however, its' half-life is 2-4 μs, so it is unlikely to "be" the signal. The generation of $O_2^{\cdot-}$ in the absence of H_2O_2 revealed that there were some genes that were specifically responsive to $O_2^{\cdot-}$ signaling (Scarpeci *et al.*, 2008) suggesting a H_2O_2-independent and $O_2^{\cdot-}$-dependent mechanism of signaling.

Metabolites play a role in retrograde signaling. One metabolite and potential retrograde signal is 3'-phosphoadenosine-5'-phosphate (PAP). The PAP pathway is a highly conserved and ancient pathway that is thought to be critical for adaptation to land. PAP is generated in *Arabidopsis* from the secondary sulfur pathway (Marino *et al.*, 2016; Zhao *et al.,* 2019). PAP accumulates in the rosette leaves under excessive light conditions or drought and functions to activate stress-response genes (Estavillo *et al.,* 2011). Under standard conditions, PAP is maintained at low levels by SAL1, which degrades PAP into adenosine monophosphate (AMP) and inorganic phosphate (Pi) in both chloroplasts and mitochondria (Chen *et al.*, 2011; Estavillo *et al.*, 2011; Chan *et al.*, 2016). *SAL1* – also known as *FIERY1* (*FRY1*) - encodes a phosphatase-like protein with 3'(2'),5'-bisphosphate nucleotidase and inositol polyphosphate 1-phosphatase activities (Quintero et al, 1996). *sal1* mutants have delayed flowering, rounder rosette leaves, and shorter

petiole length (Xiong *et al.*, 2001, 2004; Rossel *et al.*, 2006; Gy *et al.*, 2007; Rodríguez *et al.*, 2010; Zhang *et al.*, 2011). In some cases, thicker leaves (Wilson *et al.*, 2009) and compromised apical dominance (Robles *et al.*, 2010) were observed. Elevated PAP levels in *sal1* mutants inhibit nuclear exoribonucleases (XRNs), such that RNA quality control mechanisms, microRNA biogenesis, and post-transcriptional gene silencing are perturbed (Zarkovic *et al.*, 2005; Gy *et al.*, 2007). Therefore, the SAL1-PAP retrograde pathway has been hypothesized to alter gene expression in response to high light or drought conditions.

Isoprenoids are a large group of plant metabolites that take part in a wide array of physiological processes, such as seed germination and photosynthesis. The plastidial methylerythritol phosphate (MEP) pathway is responsible for biosynthesis of isopentenyl diphosphate (IPP) and dimethylallyl diphosphate (DMAPP), which are essential building blocks of isoprenoids (Vranová *et al.*, 2013). The MEP pathway is tied to chloroplast development, such that MEP pathway deficiencies lead to chloroplast developmental defects. Thus, the MEP pathway is thought to be involved in retrograde signaling (Xiao *et al.*, 2013). Methylerythritol cyclodiphosphate (MEcPP) is produced by the MEP pathway in response to oxidative stress, wounding, high-light, or variety of other biotic and abiotic stress conditions (Xiao *et al.*, 2012). 4-hydroxy-3-methylbut-2-enyl diphosphate synthase (HDS) catalyzes the rate-limiting step in the MEP pathway (Rodríguez-Concepción, 2006). One *hds* mutant had elevated basal salicylic acid (SA) levels as well as increased resistance to the bacterial pathogen *Pseudomonas syringae pv. tomato* (*Pst*) (Gil *et al.*, 2005). Another *hds* mutant had altered levels of some stress-responsive nuclear-encoded

plastid proteins (Chehab *et al.*, 2008). Stress-induced MEcPP production also occurs in bacteria (Ostrovsky *et al.*, 1998). While the exact signaling mechanism by which MEcPP alters gene expression is unknown, MEcPP is proposed to function by altering chromatin structure (Xiao *et al.,* 2012; Xiao *et al.,* 2013). Collectively, MEcPP is not only an intermediate in the MEP pathway but also an evolutionarily conserved, global, stress-responsive metabolite.

Tetrapyrroles are another class of metabolites suggested to be involved in retrograde signaling pathways or be retrograde signals themselves. Tetrapyrroles are a class of chemical compounds featuring a four-pyrrole ring structure that play important biological roles in living organisms. For example, tetrapyrroles are involved in the biosynthesis of hemoglobin in animals and chlorophyll in plants (Tanaka and Tanaka, 2007). Seedlings grown on norflurazon (NF), a chemical inhibitor of carotenoid biosynthesis, experience photooxidative damage to plastids in normal light conditions (Oelmüller and Mohr, 1986). The mutants did not show signs of plastid photooxidative damage when grown on NF were identified and were involved with tetrapyrrole biosynthesis including: heme oxygenase, phytochromobilin synthase, and the H-subunit of Mg chelatase (Susek *et al.*, 1993; Mochizuki *et al.*, 2001). Mutations in these genes caused activated photosynthesis-associated nuclear-encoded genes implicating tetrapyrrole intermediates in retrograde signaling. This data however does not determine which tetrapyrrole is involved in retrograde signaling, and tetrapyrrole retrograde signals are considered controversial.

Transcription factors with dual subcellular localization in both the nucleus and plastid are strong candidates for involvement in retrograde signaling. HEMERA (HMR)/pTAC12 is dually localized in the plastid and nucleus in both *Arabidopsis* and maize (Chen *et al.*, 2010; Pfalz *et al.,* 2015). *hmr* mutants are unusual in that they are defective in PHY signaling, and PIFs do not degrade under standard light conditions (Qui *et al.,* 2015). HMR is an essential protein associated with the plastid-encoded plastid RNA polymerase (PEP) (Pfalz *et al.*, 2006). In the nucleus, HMR interacts with PIFs and PHYs to regulate hypocotyl growth upon exposure to light (Qiu *et al.*, 2015). HMR also regulates daytime temperature sensing with PHYB and PIF4 and interacts with PIF4 directly (Qiu *et al.,* 2019). A mechanism was discovered where HMR must first be targeted to the plastids, be processed into mature form, and then relocated to the nucleus (Nevarez *et al.,* 2017), indicating dual localization is important for HMR function.

Another transcription factor with similar dual localization is WHIRLY 1 (WHY1) (Table 1.2), a small protein involved in transcriptional activation of plant defense genes (Desveaux *et al.*, 2000, 2002, 2004). In barley, it was found that WHY1 localized to plastids and the nucleus in the same cell (Grabowski *et al.*, 2008). When transgenic *WHY1* was expressed from the plastid genome and translated in the chloroplasts, the protein was also found in the nucleus at the same molecular weight (Isemer *et al.*, 2012). Therefore, WHY1 is mobile and has a dual subcellular localization in both the chloroplast and the nucleus. In *Arabidopsis*, there are three *WHIRLY* genes (*WHY1*, *WHY2*, and *WHY3*). GFP fusion protein experiments have shown that WHY1 and WHY3 localize to the chloroplast, while WHY2 localizes to the mitochondria (Krause *et al.*, 2005). WHY

proteins are named for their ability to bind DNA in tetramers, forming a "pinwheel" or "whirligig" shape. WHY proteins can also bind single-stranded DNA, and there is low sequence specificity in the WHY-ssDNA interactions (Desveaux *et al.*, 2002; Cappadocia *et al.*, 2010, 2012).

WHY1 and WHY3 not only localize to the same organelle; they may be functionally redundant. WHY1 and WHY3 have the ability to act as transcription factors together. They were both found to bind and regulate *ARABIDOPSIS KINESIN-LIKE PROTEIN 1* (*AtKP1*), a kinesin-like gene (Xiong *et al.*, 2009), indicating that WHY3 also exhibits dual localization in the nucleus and chloroplast like WHY1. In *why1 why3* loss-of-function mutants, about 5% of the plants exhibit a yellow variegated leaf phenotype (Maréchal *et al.*, 2009). Also, rearranged plastid DNA could be amplified by PCR from *why1 why3* double mutant plants, while it could not be from wild-type control plants (Maréchal *et al.*, 2009). This combined with the fact that WHY1was found to bind both single- and double-stranded DNA in maize (*Zea mays*) chloroplasts (Prikryl *et al.*, 2008), suggests that both WHY1 and WHY3 have multiple potential targets. WHY1 and WHY3 repress an error-prone DNA repair mechanism in plastids called microhomology-mediated break-induced replication (MMBIR) (Maréchal *et al.*, 2009; Cappadocia *et al.*, 2010). Later, it was found that *PolI-like B* (*Pol1B*) is recruited to the DNA breaks for DNA repair by WHY1 and WHY3 in the plastids (Parent *et al.*, 2011).

WHY1 and WHY3 have been connected to photosynthesis and change in redox status of the chloroplast. WHY3 was found in the thiol-disulfide redox proteome of the chloroplast, making WHY3 a redox sensitive protein (Ströher and Dietz, 2008).

Furthermore, it was found that in plants treated with inhibitors of chloroplast and mitochondrial functions, *WHY1* and *WHY3* were upregulated (Karpinska *et al.*, 2017), meaning that *WHY1* and *WHY3* respond to perturbations in these organelles. It was reported that plants having reduced *WHY1* due to RNAi had higher chlorophyll content but less sucrose than wild-type plants, indicating that photosynthesis was less efficient in *WHY1* RNAi plants (Comadira *et al.*, 2015). More recently, it was found that WHY1 interacts with light-harvesting protein complex I (LHCA1) and has the ability to impact expression of genes encoding proteins that constitute PSI (Huang *et al.*, 2017). In summary, WHY1 and WHY3 appear tied to the redox status or photosynthetic status of the chloroplast. Taken together, these results suggest that WHY proteins may be involved in plastid-to-nucleus retrograde signaling in order to maintain plastid function in differing environmental conditions, and thus, they are important for communication between the plastid and nucleus [suggested in (Krause *et al.*, 2009; Foyer *et al.*, 2014; Guan *et al.*, 2018)].

One publication suggested that movement of WHY1 from the chloroplasts to the nucleus could be triggered by the redox state of the electron transport chain, specifically (Foyer *et al.*, 2014). WHY1 interacts with CALCINEURIN *B*-LIKE-INTERACTING PROTEIN KINASE 14 (CIPK14), an SNF1-like protein kinase. CIPK14 was found to phosphorylate WHY1 in the nucleus and could regulate WHY1 subcellular localization and distribution ratio between the chloroplasts and nucleus (Ren *et al.*, 2017).

The Shoot Apical Meristem (SAM) and Boundary Regions

Stem cells in plants reside at the shoot tip in a region called the shoot apical meristem (SAM). The SAM is shaped like a dome, and the stem cells are located at the top of the dome. Developing lateral organs, or primordia, form as protrusions from the SAM (Weigel and Jürgens, 2002; Braybrook and Kuhlemeier, 2010). The boundary region is located in the area between the SAM and developing lateral organs. Cells in the boundary region are smaller in volume and divide less frequently (Hussey, 1971; Gaudin *et al.*, 2000). The boundary region is thought to not only physically separate developing lateral organs from the meristem but also to relay signals between the two regions and possibly to perceive or respond to environmental cues (Sussex, 1954; Bowman *et al.*, 2002). If the boundary region does not form properly or is defective, organs can become fused to one another or to the meristem (Aida, 1997; Lee *et al.*, 2009; Bell *et al.*, 2012; Colling *et al.*, 2015). Meristem fate appears tied to the boundary region, such that some mutants of boundary-expressed genes have meristems that terminate or fail to form (Aida, 1997; Greb *et al.*, 2003; Hibara *et al.*, 2006; Lee *et al.*, 2009).

LATERAL ORGAN FUSION1 (LOF1) is a MYB transcription factor that was identified in an enhancer trap screen for genes that are expressed in the boundary regions of plants (Lee *et al.*, 2009). *LOF1* is expressed at the base of the rosette leaves, pedicel-stem junctions, base of floral organs, and in the paraclade junction – where the primary stem, axillary branch, and cauline leaf join. The paraclade junction also contains an accessory meristem that grows out into a new branch if the axillary branch is damaged or removed. *LOF1* does not appear to be expressed in the roots. *lof1-1* mutants have fusion

between the axillary branch and cauline leaf. The accessory bud is also absent in these mutants (Lee *et al.*, 2009). A closely related gene, *LATERAL ORGAN FUSION2* (*LOF2*), has a similar expression pattern. However, *LOF2* appears to be expressed more broadly than *LOF1*, and *lof2* mutants have a wild-type phenotype. *lof1 lof2* double mutants have more fusions than *lof1* single mutants alone, indicating the two genes function partially redundantly (Lee *et al.*, 2009).

LOF1 is thought to be a transcription factor. Therefore, one might expect LOF1 to be localized to the nucleus. Many of the proteins identified as LOF1 interactors from a yeast two-hybrid screen are proteins involved with the chloroplast and/or mitochondria. Many are associated with abiotic stress responses (Chapter 1; Table 1.1). One interactor from the yeast two-hybrid screen that was obtained multiple times is WHY3 (Table 1.2). Given the results from the yeast two-hybrid screen and previous knowledge on both WHY1 and WHY3, we decided to investigate whether LOF1 changes subcellular localization in the presence of abiotic stress conditions.

Results

LOF1-mCherry-GFP Subcellular Localization Under Standard Growth Conditions

In order to observe LOF1 subcellular localization under standard and abiotic-stress growth conditions, LOF1-mCherry-GFP fusion proteins, under control of an estradiol-inducible promoter, were stably transformed into the Col-0 accession of *Arabidopsis thaliana*. Because the *LOF1* expression pattern in the boundary region is in

close proximity to the meristem, imaging in the shoot apex is challenging. We therefore examined subcellular localization of LOF1-mCherry-GFP in the root meristematic zone.

Under our growth conditions, LOF1-mCherry-GFP was observed in the nuclei of root cells in meristematic and elongation zones following induction with β-estradiol for 24 hours (Figure 2.1 A). Whether or not the seedlings were incubated in light or dark conditions during the induction period did not impact LOF1-mCherry-GFP subcellular localization (Figure 2.1 A and B). A non-transgenic sibling of the LOF1-mCherry-GFP expressing transgenic plant did not show any detectable fluorescent signal when imaged (Figure 2.1 C).

As a negative control, a construct that expressed *GFP* using a β-estradiol inducible promoter was transformed into *Arabidopsis*. When grown in conditions of 24-hours standard light or 24-hours dark, GFP fluorescence showed no specific subcellular localization (Figure 2.2).

LOF1-mCherry-GFP Subcellular Localization Under High Light Conditions

Several LOF1-interacting proteins were predicted to be chloroplast-associated. Since the chloroplast is the primary organelle involved in photosynthesis, we assessed whether LOF1 subcellular localization was altered by light stress. As previously mentioned, high-light causes excess excitation at PS II, which can lead to production of singlet oxygen ($^1O_2$) from chlorophyll and at PS I lead to production of $O_2^{\cdot -}$ and H_2O_2 (Smirnoff, 1993; Li *et al.*, 2009; Moellering *et al.*, 2010; Ramel *et al.*, 2012).

Because different studies on high-light stress in *Arabidopsis* have uncovered differentially expressed genes or proteomic changes at different time points after exposure to high light stress, multiple time points of high-light stress exposure were used in this study. Most studies performed high-light stress for periods of times between 1 and 24 hours, so our experiments took this into account (Rossel *et al.*, 2002; Kimura *et al.*, 2003; Müller-Moulé *et al.*, 2004; Phee *et al.*, 2004; Vanderauwera *et al.*, 2005). A light intensity of about 1000 μmol photons $m^{-2}s^{-1}$ was used for high-light conditions due to previous data that even higher intensities would lead to damage and cell death in leaves (Szechyńska-Hebda and Karpiński, 2013). In roots, even short periods of standard light exposure cause stress and excess ROS production (Yokawa *et al.,* 2011). LOF1-mCherry-GFP expressing transgenic seedlings were exposed to 1, 2, 4, 6, 12, and 24-hours of high light. Images revealed that LOF1-mCherry-GFP subcellular localization remained in the nucleus after exposure to high light at all time points (Figure 2.3; 2.4). High light exposure of the tested time periods does not lead to change in subcellular localization of LOF1-mCherry-GFP in roots.

LOF1-mCherry-GFP Subcellular Localization in the Presence of Reactive Oxygen Species (ROS)

ROS are produced by plastids and other organelles during stress and have the ability to cause damage to photosynthetic machinery (De Souza *et al.*, 2018). To test LOF1 subcellular localization in the presence of ROS, we used H_2O_2 as the ROS species due to stability, half-life, and documented ability to move between subcellular

compartments (Mittler, 2002; Cruz De Carvalho, 2008). There is evidence that some genes that are differentially expressed following exposure to H_2O_2 are also differentially expressed under high-light exposure (Vanderauwera *et al.*, 2005).

Arabidopsis in cell culture and leaves exposed to 10 - 20 mM H_2O_2 exhibited differential gene expression compared to control plants (Desikan *et al.*, 2001; Balazadeh *et al.*, 2011). After observing the roots exposed to 10 mM and 20 mM of H_2O_2, it was revealed that all of the root meristematic zones were damaged by the H_2O_2 treatment and could not be used to determine LOF1 localization (data not shown). We then treated with a lower concentration of 1 mM H_2O_2, which allowed imaging of some roots. In an experiment looking at root growth after exposure to H_2O_2 concentrations ranging from 1 mM to 4 mM, concentrations of 2 mM or higher caused a root curvature phenotype and loss of gravitropism. Additionally, root growth was visibly impacted by H_2O_2 concentrations as low as 1 mM (Zhou *et al.*, 2018). Therefore, we explored concentrations of less than 1 mM H_2O_2, which were still expected to result in oxidative stress. Under conditions of exposure to 100 μM, 500 μM, and 1mM H_2O_2 for 24 hours, LOF1-mCherry-GFP was localized to the nucleus (Figure 2.5). These data suggest that LOF1-mCherry-GFP does not change subcellular localization in response to exposure to low concentrations of H_2O_2.

LOF1-mCherry-GFP Subcellular Localization Under Water Deficit

Because many genes affected by high-light conditions are also affected by water deficit (Kimura *et al.*, 2003), and genes with differential expression in water-deficit

conditions were found in the yeast two-hybrid screen (Chapter 1). LOF1-GFP protein localization in response to water deficit was tested. Polyethylene glycol (PEG) has been used to simulate water-deficit conditions in *Arabidopsis* and other plant species for some time (Sunkar, 2010). PEG is non-ionic and inert but is still able to influence water potential (Lagerwerff *et al.*, 1961).

After 24-hour treatment with PEG 6000 (Promega), Columbia plants showed an increase in *RD19*, *RESPONSE TO DEHYDRATION19* (AT4G39090), transcript levels compared to controls that did not have contact with PEG (Figure 2.6). *RD19* has been previously shown to be upregulated in response to water deficit (Koizumi *et al.*, 1993). This indicated that the PEG treatment was successful. After 24-hour exposure to 25% PEG 6000, LOF1-mCherry-GFP was localized to the nucleus (Figure 2.7). This indicates that water deficit (PEG exposure) does not change subcellular localization of LOF1-mCherry-GFP.

Discussion

LOF1 expression has not been detected in the root (Lee *et al.*, 2009). However, we decided to examine LOF1 subcellular localization in the root due to ease of viewing the meristematic zone and *LOF1*'s association with the meristem. It is much more difficult to view meristematic cells in the shoot, and shoot boundary regions in *Arabidopsis* are not easily accessible for viewing. Shoot meristems are covered by developing organ primordia that would need to be dissected away for transgene induction and imaging, while keeping the plant healthy enough for confocal microscopy. It is

possible that LOF1 subcellular localization does change in the shoot, where chloroplasts are photosynthetically active. Proplastids and etioplasts are present in roots and other dark-grown tissues, while differentiated chloroplasts are generally not present. The lack of differentiated chloroplasts may have prevented us from observing a subcellular localization change of LOF1. It is important to note that differentiated chloroplasts are not present in LOF1-expressing boundary cells either, but instead, these cells contain proplastids that are not photosynthetically active (Pyke, 2009; Jarvis and López-Juez, 2013).

Although high light, drought, and ROS stresses did not appear to change subcellular localization of LOF1-mCherry-GFP, it is possible that stress conditions we did not test, such as salt or cold, do alter LOF1 subcellular localization. We did not use constitutive *LOF1* overexpression lines because overexpression of boundary genes typically results in small, developmentally delayed plants that are prone to transgene silencing, and/or suffer from infertility. After many attempts, we were not able to recover *35S:LOF1* lines that had expression in the second generation after transformation. Therefore, an inducible overexpression scenario was chosen for *LOF1*.

At least one past experiment identified upregulation of several *APETALA2*/*ETHYLENE RESPONSE FACTOR* (*AP2*/*ERF*) transcripts in response to high-light treatment (800 μmol m^{-2} s^{-1}) within the first ten minutes after treatment. After one hour of time, no alterations in transcript levels could be detected (Vogel *et al.*, 2014). "Ultra-fast" responses to high-light treatment have been reported. After high-light treatments ranging from 15 seconds to three hours, it was revealed that 503 out of 731

transcripts induced by high light were induced in the time frame between 20 and 60 seconds (Kleine *et al.*, 2007; Suzuki *et al.*, 2015). Since we could not reliably obtain root images in under ten minutes of time after high-light treatment, it is possible that LOF1-mCherry-GFP does change subcellular localization, but the change happens too quickly to be observed in our experiments.

Our experiments examined the possible change in subcellular localization of LOF1-mCherry-GFP in response to abiotic stress. It is likely however, that a small change in the distribution of LOF1-mCherry-GFP protein would have been difficult to detect. For example, if 10% of total LOF1-mCherry-GFP protein moved from the nucleus to the chloroplast under abiotic stress conditions, it would likely not have been detected. Changes in levels of SUPEROXIDE DISMUTASE (SOD) isoforms in the cytoplasm, chloroplast, and mitochondria occur in response to soil drought in wheat (Huseynova *et al.,* 2014). This suggests that low percentage changes in subcellular localization of a specific protein do occur in response to abiotic stress.

Conclusion

Our results indicate that under our growth conditions LOF1 is present in the nucleus. When observing LOF1-mCherry-GFP subcellular localization in the conditions of water deficit, high light, and presence of ROS, we did not observe a change in LOF1-mCherry-GFP subcellular localization. This suggests that the LOF1 interactors obtained from the yeast two-hybrid assay may represent proteins with dual subcellular localization both in the nucleus and the plastid and/or mitochondria. This is supported by the fact that

WHY3, which has been confirmed to have localization in both the nucleus and chloroplast, was obtained multiple times in the LOF1 yeast two-hybrid screen (Chapter 1; Table 1.1). LOF1-interactors may change subcellular localization from the plastid and/or mitochondria to the nucleus during abiotic stress conditions and interact with LOF1 in the nucleus.

Materials and Methods

Plant Materials and Growth Conditions

Seeds were incubated with 95% ethanol for 5 minutes, treated with 20% bleach/0.01% Tween 20 for 5 minutes, and rinsed five times with sterile water. Seeds were then sown on 1X Murashige and Skoog (MS) media (pH 5.7) (Murashige and Skoog, 1962) with added 1% sucrose and 1% agar. They were stratified at 4 ºC in the dark for 48 hours before being transferred to a growth chamber with 120 μM/m^2s white light with a 16-hour light/ 8-hour dark cycle. The temperature was a constant 22 ºC.

Transcript Analysis

Col-0 seedlings were floated in solutions 25% PEG 6000 (Promega) dissolved in MS, 30% PEG 6000 dissolved in MS, or mock-treated with MS alone for a period of 24 hours. Unstressed seedlings growing on plates were used as a negative control. Total RNA was extracted from whole plants by TRIZOL® reagent (Invitrogen) and precipitated by 100% isopropanol. Pellets were cleaned with 75% ethanol. RNA (2 μg) was used for cDNA synthesis using SuperScript IV Reverse Transcriptase (Thermo Fisher Scientific) enzymes. *ACTIN2* (*ACT2*) primers were used to equalize cDNA for

RT-PCR (Table 2.1) using 22 cycles of amplification. *RD19* primers used in RT-PCR are listed in Table 2.1, and 22 cycles of amplification were used in *RD19* RT-PCR.

Abiotic Stress Conditions

For water-deficit stress conditions, five-day-old seedlings were floated in 25% PEG 6000 (Promega) dissolved in MS media [plus 80 μm β-estradiol (Sigma-Aldrich) for induction of expression of LOF1-mCherry-GFP] or mock-induced with MS media [plus 80 μm β-estradiol for mock induction] for a 24-hour period and then imaged. Seedlings were six days old at the time of imaging. Water potentials from -0.23 to -0.51 Mpa impose "moderate water stress" (Van Der Weele *et al.*, 2000), while 20% PEG imposes -5.11 Mpa, which is "severe stress" (Van Der Weele *et al.*, 2000; Xu *et al.*, 2013).

For ROS conditions, five-day-old seedlings were exposed to hydrogen peroxide (H_2O_2; Promega) for a period of 24 hours prior to imaging. H_2O_2 solutions were at concentrations of 100 μM, 500 μM, and 1000 μM. Control solution did not contain hydrogen peroxide. All solutions contained 80 μM β-estradiol for induction of LOF1-mCherry-GFP. H_2O_2 (30%; Fisher Scientific) was used to make 100 μM, 500 μM, and 1000 μM dilutions.

For all light conditions, five-day-old seedlings were floated in 80 μM β-estradiol (dissolved in distilled water) for a period of 24-hours. During this time, seedlings were exposed to 1, 2, 4, 6, 12, or 24-hours of high light. Control plates remained under "standard light" conditions for 24-hours and in dark (covered with foil) for 24 hours. LED light panels containing red, blue, and white LED lights were used. For "standard light" conditions, the white light was set at ~19.4 micromoles per meter squared per

second (μmol/m^2/s), the blue light at ~26.9 μmol/m^2/s, and the red light at ~59.4 μmol/m^2/s. Overall, the light reading was ~100 μmol/m^2/s for the "standard light" conditions. For the "high light" condition, the white light was set at ~116.5 μmol/m^2/s, the blue light at ~204.2 μmol/m^2/s, and the red light at ~680.6 μmol/m^2/s. Overall, the light reading for the "high light" conditions was about 1000 μmol/m^2/s. L1-1000 DataLogger (Li-COR) light meter was used to measure light readings. For the "dark" conditions, plates were covered in foil and left in the same room as plates exposed to "standard light" and "high light" conditions.

The β-estradiol (Sigma-Aldrich) for all conditions was dissolved in dimethylformamide (DMF) at a stock concentration of 0.4 M. As a negative control, transgenic plants harboring estradiol-inducible GFP were used for all experiments. The same estradiol inducible promoter construct was used for GFP as for LOF1-mCherry-GFP. The β-estradiol did not well penetrate into multiple cell layers of the root. The addition of wetting agents or surfactants did not allow β-estradiol to be visualized in more cell layers of the root (data not shown). Therefore, LOF1-mCherry-GFP is visible in the epidermis, outer lateral root cap cells, and outer columella root cap cells in images.

Plant Transformation

For transformation, binary vectors were transformed into GV3101 *Agrobacterium tumefaciens* GV3101 (Koncz *et al.*, 1992). Transformation of *Arabidopsis* was performed using the floral dip method (Clough and Bent, 1998).

Transgenic Populations

For the β-estradiol inducible GFP control, GFP was cloned via PCR from paBindGFP (Bleckmann et al, 2010) into pENTR using the pENTR/D-TOPO^{TM} Cloning Kit (ThermoFisher) (primers listed in Table 2.1). Then, cloned into pMDC7 (Curtis and Grossniklaus, 2003) using a Gateway cloning LR reaction (Invitrogen). First-generation transgenic populations (T1) were screened on MS plates supplemented with hygromycin (25 μg) for a period of 1.5 to 2 weeks before transplanting resistant seedlings to soil. Plants were kept in dark until germination. Resistant plants were genotyped to confirm presence of the transgene (Table 2.1). In confirmed transgenics, T2 seeds were plated on MS supplemented with hygromycin (25 μg). Segregation ratios of approximately 3:1 (resistant: susceptible) were used to identify T2 lines with one transgene locus.

Confocal Microscopy

Roots were stained with 10 μM propidium iodide (PI) dissolved in distilled water for 30-60 seconds. Roots were then visualized through laser scanning confocal microscopy on a Leica SP8 upright microscope (Van Norman lab, UCR). Root meristematic and elongation zones were viewed in the median longitudinal plane using LAS X software (Leica). Florescent signals were captured according to the following: GFP (excitation 488 nm, emission 492-530 nm) and PI (excitation 536 nm, emission 585-660 nm) [adapted from (Campos *et al.*, 2019)]. Lateral root cap cells in the meristematic zone slough off as the root grows (Kumpf and Nowack, 2015). This sloughing off results in cellular disruption that makes accurate visualization of LOF1-mCherry-GFP subcellular localization difficult. Therefore, images were taken of the elongation zone,

where sloughing off does not occur, in addition to the meristematic zone (Kumpf and Nowack, 2015). Images of the meristematic and elongation zone were taken from same root if possible.

References

Abdallah F, Salamini F, Leister D. 2000. A prediction of the size and evolutionary origin of the proteome of chloroplasts of *Arabidopsis*. Trends in Plant Science **5**, 141–142.

Aida M. 1997. Genes involved in organ separation in *Arabidopsis*: An analysis of the *cup-shaped cotyledon* mutant. Plant Cell **9**, 841–857.

Asada K. 2006. Production and scavenging of reactive oxygen species in chloroplasts and their functions. Plant Physiology **141**, 391–396.

Asensi-Fabado MA, Munné-Bosch S. 2010. Vitamins in plants: Occurrence, biosynthesis and antioxidant function. Trends in Plant Science **15**, 582–592.

Baker NR. 1991. A possible role for photosystem II in environmental perturbations of photosynthesis. Physiologia Plantarum **81**, 563–570.

Balazadeh S, Kwasniewski M, Caldana C, Mehrnia M, Zanor MI, Xue GP, Mueller-Roeber B. 2011. ORS1, an H_2O_2-responsive NAC transcription factor, controls senescence in *Arabidopsis thaliana*. Molecular Plant **4**, 346–360.

Bell EM, Lin W, Husbands AY, Yu L, Jaganatha V, Jablonska B, Mangeon A, Neff MM, Girke T, Springer PS. 2012. *Arabidopsis* lateral organ boundaries negatively regulates brassinosteroid accumulation to limit growth in organ boundaries. Proceedings of the National Academy of Sciences USA **109**, 21146–51.

Bishop N. 1971. Photosynthesis: The electron transport system of green plants. Annual Review of Biochemistry **40**, 197–226.

Bowman JL, Eshed Y, Baum SF. 2002. Establishment of polarity in angiosperm lateral organs. Trends in Genetics **18**, 134–141.

Bradbeer W, Atkinson Y, Borner T, Hagemann R. 1979. Cytoplasmic synthesis of plastid polypeptides may be controlled by plastid-synthesised RNA. Nature **279**, 816–817.

Braybrook SA, Kuhlemeier C. 2010. How a plant builds leaves. Plant Cell **22**, 1006–1018.

Campos R, Goff J, Rodriguez-Furlan C, Van Norman JM. 2019. The Arabidopsis receptor kinase IRK is polarized and represses specific cell divisions in roots. Developmental Cell **52**, 1–13.

Cappadocia L, Maréchal A, Parent JS, Lepage É, Sygusch J, Brisson N. 2010. Crystal structures of DNA-whirly complexes and their role in *Arabidopsis* organelle genome repair. Plant Cell **22**, 1849–1867.

Cappadocia L, Parent JS, Zampini É, Lepage É, Sygusch J, Brisson N. 2012. A conserved lysine residue of plant Whirly proteins is necessary for higher order protein assembly and protection against DNA damage. Nucleic Acids Research **40**, 258–269.

Chan KX, Crisp PA, Estavillo GM, Pogson BJ. 2010. Chloroplast-to-nucleus communication: Current knowledge, experimental strategies and relationship to drought stress signaling. Plant Signaling and Behavior **5**, 1575-1582.

Chan KX, Phua SY, Crisp P, McQuinn R, Pogson BJ. 2016. Learning the languages of the chloroplast: Retrograde signaling and beyond. Annual Review of Plant Biology **67**, 25–53.

Chehab EW, Kaspi R, Savchenko T, Rowe H, Negre-Zakharov F, Kliebenstein D, Dehesh K. 2008. Distinct roles of jasmonates and aldehydes in plant-defense responses. PLoS ONE **3**, 1–10.

Chen M, Galvão RM, Li M, Burger B, Bugea J, Bolado J, Chory J. 2010. *Arabidopsis* HEMERA/pTAC12 Initiates photomorphogenesis by phytochromes. Cell **141**, 1230–1240.

Chen H, Zhang B, Hicks LM, Xiong L. 2011. A nucleotide metabolite controls stress-responsive gene expression and plant development. PLoS ONE **6**, 1-14.

Clough SJ, Bent AF. 1998. Floral dip: A simplified method for *Agrobacterium*-mediated transformation of *Arabidopsis thaliana*. Plant Journal **16**, 735–743.

Colling J, Tohge T, De Clercq R, Brunoud G, Vernoux T, Fernie AR, Makunga NP, Goossens A, Pauwels L. 2015. Overexpression of the *Arabidopsis thaliana* signalling peptide TAXIMIN1 affects lateral organ development. Journal of Experimental Botany **66**, 5337–5349.

Comadira G, Rasool B, Kaprinska B, García BM, Morris J, Verrall SR, Bayer M, Hedley PE, Hancock RD, Foyer CH. 2015. WHIRLY1 functions in the control of responses to nitrogen deficiency but not aphid infestation in barley. Plant Physiology **168**, 1140–1151.

Cruz De Carvalho MH. 2008. Drought stress and reactive oxygen species: Production, scavenging and signaling. Plant Signaling and Behavior **3**, 156–165.

Curtis MD, Grossniklaus U. 2003. A gateway cloning vector set for high-throughput functional analysis of genes in planta. Plant Physiology **133**, 462–469.

Desikan R, Mackerness SA-H, Hancock JT, Neill SJ. 2001. Regulation of the Arabidopsis transcriptome by oxidative stress. Plant Physiology **127**, 159–172.

Desveaux D, Allard J, Brisson N, Sygusch J. 2002. A new family of plant transcription factors displays a novel ssDNA-binding surface. Nature Structural Biology **9**, 512–517.

Desveaux D, Despres C, Joyeux A, Subramaniam R, Brisson N. 2000. PBF-2 is a novel single-stranded DNA binding factor implicated in *PR-10a* gene activation in potato. Plant Cell **12**, 1477–1489.

Desveaux D, Subramaniam R, Després C, Mess JN, Lévesque C, Fobert PR, Dangl JL, Brisson N. 2004. A 'Whirly' transcription factor is required for salicylic acid-dependent disease resistance in *Arabidopsis*. Developmental Cell **6**, 229–240.

Ding M, Hou P, Shen X, Wang M, Deng S, Sun J, Xiao F, Wang R, Zhou X, Lu C, Zhang D, Zheng X, Hu Z, Chen S. 2010. Salt-induced expression of genes related to Na+/K+ and ROS homeostasis in leaves of salt-resistant and salt-sensitive poplar species. Plant Molecular Biology **73**, 251–269.

Estavillo GM, Crisp PA, Pornsiriwong W, Wirtz M, Collinge D, Carrie C, Giraud E, Whelan J, David P, Javot H, Brearlry C, Hell R, Marin E, Pogson BJ. 2011. Evidence for a SAL1-PAP chloroplast retrograde pathway that functions in drought and high light signaling in *Arabidopsis*. Plant Cell **23**, 3992–4012.

Fahnenstich H, Scarpeci TE, Valle EM, Flügge U-I, Maurino VG. 2008. Generation of hydrogen peroxide in chloroplasts of Arabidopsis overexpressing glycolate oxidase as an inducible system to study oxidative stress. Plant Physiology **148**, 719–729.

Foyer CH, Karpinska B, Krupinska K. 2014. The functions of WHIRLY1 and REDOXRESPONSIVE TRANSCRIPTION FACTOR 1 in cross tolerance responses in plants: A hypothesis. Philosophical Transactions of the Royal Society **369**, 1-8.

Foyer CH, Noctor G. 2011. Ascorbate and glutathione: The heart of the redox hub. Plant Physiology **155**, 2–18.

Frenkel AW. 1995. Photosynthetic phosphorylation. Photosynthesis Research **46**, 73–77.

Gaudin V, Lunness PA, Fobert PR, Towers M, Riou-Khamlichi C, Murray JAH, Coen E, Doonan JH. 2000. The expression of *D-cyclin* genes defines distinct developmental zones in snapdragon apical meristems and is locally regulated by the *Cycloidea* gene. Plant Physiology **122**, 1137–1148.

Gil MJ, Coego A, Mauch-Mani B, Jordá L, Vera P. 2005. The Arabidopsis *csb3* mutant reveals a regulatory link between salicylic acid-mediated disease resistance and the methyl-erythritol 4-phosphate pathway. Plant Journal **44**, 155–166.

Goldschmidt-Clermont M. 1998. Coordination of nuclear and chloroplast gene expression in plant cells. International Review of Cytology **177**, 115–180.

Grabowski E, Miao Y, Mulisch M, Krupinska K. 2008. Single-stranded DNA-binding protein Whirly1 in barley leaves is located in plastids and the nucleus of the same cell. Plant Physiology **147**, 1800–1804.

Greb T, Clarenz O, Schafer E, Herrero R, Schmitz G, Theres K. 2003. Molecular analysis of the *LATERAL SUPPRESSOR* gene in *Arabidopsis*. Genes & Development **17**, 1175–1187.

Guan Z, Wang W, Yu X, Lin W, Miao Y. 2018. Comparative proteomic analysis of coregulation of CIPK14 and WHIRLY1/3 mediated pale yellowing of leaves in *Arabidopsis*. International Journal of Molecular Sciences **19**, 1-22.

Gy I, Gasciolli V, Lauressergues D, Morel JB, Gombert J, Proux F, Proux C, Vaucheret H, Mallory AC. 2007. *Arabidopsis* FIERY1, XRN2, and XRN3 are endogenous RNA silencing suppressors. Plant Cell **19**, 3451–3461.

Haehnel W. 1984. Photosynthetic electron transport in higher plants. Annual Review of Plant Physiology **35**, 659–693.

Halliwell B. 2006. Reactive species and antioxidants. Redox biology is a fundamental theme of aerobic life. Plant Physiology **141**, 312–322.

Heyneke E, Luschin-Ebengreuth N, Krajcer I, Wolkinger V, Müller M, Zechmann B. 2013. Dynamic compartment specific changes in glutathione and ascorbate levels in *Arabidopsis plants* exposed to different light intensities. BMC Plant Biology **13**, 1–19.

Hibara K, Karim R, Takada S, Taoka K, Furutani M, Aida M, Tasaka M. 2006. *Arabidopsis CUP-SHAPED COTYLEDON3* regulates postembryonic shoot meristem and organ boundary formation. Plant Cell **18**, 2946–2957.

Huang D, Lin W, Deng B, Ren Y, Miao Y. 2017. Dual-located WHIRLY1 interacting with LHCA1 alters photochemical activities of photosystem I and is involved in light adaptation in Arabidopsis. International Journal of Molecular Sciences **18**, 1–18.

Huseynova IM, Aliyeva DR, Aliyev JA. 2014. Subcellular localization and responses of superoxide dismutase isoforms in local wheat varieties subjected to continuous soil drought. Plant Physiology and Biochemistry **81**, 54-60.

Hussey G. 1971. Cell division and expansion and resultant tissue tensions in the shoot apex during the formation of a leaf primordium in the tomato. Journal of Experimental Botany **22**, 702–714.

Isemer R, Krause K, Grabe N, Kitahata N, Asami T, Krupinska K. 2012. Plastid located WHIRLY1 enhances the responsiveness of *Arabidopsis* seedlings toward abscisic acid. Frontiers in Plant Science **3**, 1–11.

Jarvis P, López-Juez E. 2013. Biogenesis and homeostasis of chloroplasts and other plastids. Nature Reviews Molecular Cell Biology **14**, 787–802.

Jiménez A, Hernández JA, Pastori G, Del Rio LA, Sevilla F. 1998. Role of the ascorbate-glutathione cycle of mitochondria and peroxisomes in the senescence of pea leaves. Plant Physiology **118**, 1327–1335.

Jung HS, Chory J. 2010. Signaling between chloroplasts and the nucleus: Can a systems biology approach bring clarity to a complex and highly regulated pathway? Plant Physiology **152**, 453–459.

Karpinska B, Alomrani SO, Foyer CH. 2017. Inhibitor-induced oxidation of the nucleus and cytosol in *Arabidopsis thaliana*: Implications for organelle to nucleus retrograde signalling. Philosophical Transactions of the Royal Society **372**, 1-9.

Kimura M, Yamamoto YY, Seki M, Sakurai T, Sato M, Abe T, Yoshida S, Manabe K, Shinozaki K, Matsui M. 2003. Identification of *Arabidopsis* genes regulated by high light-stress using cDNA microarray. Photochemistry and Photobiology **77**, 226–233.

King DA. 1997. The functional significance of leaf angle in *Eucalyptus*. Australian Journal of Botany **45**, 619–639.

Kleine T, Kindgren P, Benedict C, Hendrickson L, Strand A. 2007. Genome-wide gene expression analysis reveals a critical role for CRYPTOCHROME1 in the response of Arabidopsis to high irradiance. Plant Physiology **144**, 1391–1406.

Kochevar IE. 2004. Singlet oxygen signaling: From intimate to global. Science STKE **2004**, 1–4.

Koizumi M, Yamaguchi-Shinozaki K, Tsuji H, Shinozaki K. 1993. Structure and expression of two genes that encode distinct drought-inducible cysteine proteinases in *Arabidopsis thaliana*. Gene **129**, 175–182.

Koncz C, Németh K, Rédei GP, Schell J. 1992. T-DNA insertional mutagenesis in *Arabidopsis*. Plant Molecular Biology **20**, 963–976.

Krall AR, Good NE, Mayne BC. 1961. Cyclic and non-cyclic photophosphorylation in chloroplasts distinguished by use of labeled oxygen. Plant Physiology **36**, 44–47.

Krause K, Herrmann U, Fuss J, Miao Y, Krupinska K. 2009. Whirly proteins as communicators between plant organelles and the nucleus? Endocytobiosis and Cell Research **19**, 51–62.

Krause K, Kilbienski I, Mulisch M, Rüdiger A, Schäfer A, Krupinska K. 2005. DNA-binding proteins of the Whirly family in *Arabidopsis thaliana* are targeted to the organelles. FEBS Letters **579**, 3707–3712.

Krieger-Liszkay A. 2005. Singlet oxygen production in photosynthesis. Journal of Experimental Botany **56**, 337–346.

Kumpf RP, Nowack MK. 2015. The root cap: A short story of life and death. Journal of Experimental Botany **66**, 5651–5662.

Lagerwerff JV, Ogata G, Eagle H. 1961. Control of osmotic pressure of culture solutions with polyethylene glycol. Science **133**, 1486–1487.

Lee D-K, Geisler M, Springer PS. 2009. *LATERAL ORGAN FUSION1* and *LATERAL ORGAN FUSION2* function in lateral organ separation and axillary meristem formation in *Arabidopsis*. Development **136**, 2423–2432.

Leister D. 2003. Chloroplast research in the genomic age. Trends in Genetics **19**, 47–56.

Leister D. 2012. Retrograde signaling in plants: From simple to complex scenarios. Frontiers in Plant Science **3**, 1–9.

Leister D. 2019. Piecing the puzzle together: The central role of reactive oxygen species and redox hubs in chloroplast retrograde signaling. Antioxidants and Redox Signaling **30**, 1206–1219.

Leon P, Arroyo A, Mackenzie S. 1998. Nuclear control of plastid and mitochondrial development in higher plants. Annual Review of Plant Physiology and Plant Molecular Biology **49**, 453–480.

Li Z, Wakao S, Fischer BB, Niyogi KK. 2009. Sensing and responding to excess light. Annual Review of Plant Biology **60**, 239–260.

Maréchal A, Parent J-S, Véronneau-Lafortune F, Joyeux A, Lang BF, Brisson N. 2009. Whirly proteins maintain plastid genome stability in *Arabidopsis*. Proceedings of the National Academy of Sciences USA **106**, 14693–14698.

Marino D, Ariz I, Lasa B, Santamaría E, Fernández-Irigoyen J, González-Murua C, Tejo PMA. 2016. Quantitative proteomics reveals the importance of nitrogen source to control glucosinolate metabolism in *Arabidopsis thaliana* and *Brassica oleracea*. Journal of Experimental Botany **67**, 3313–3323.

Millenaar FF, Cox MCH, De Jong Van Berkel YEM, Welschen RAM, Pierik R, Voesenek LAJC, Peeters AJM. 2005. Ethylene-induced differential growth of petioles in Arabidopsis. Analyzing natural variation, response kinetics, and regulation. Plant Physiology **137**, 998–1008.

Mittler R. 2002. Oxidative stress, antioxidants and stress tolerance. Trends in Plant Science **7**, 405–410.

Mochizuki N, Brusslan JA, Larkin R, Nagatani A, Chory J. 2001. *Arabidopsis genomes uncoupled 5* (*GUN5*) mutant reveals the involvement of MG-chelatase H subunit in plastid-to-nucleus signal transduction. Proceedings of the National Academy of Sciences USA **98**, 2053–2058.

Moellering ER, Muthan B, Benning C. 2010. Freezing tolerance in plants requires lipid remodeling at the outer chloroplast membrane. Science **330**, 226–228.

Müller-Moulé P, Golan T, Niyogi KK. 2004. Ascorbate-deficient mutants of Arabidopsis grow in high light despite chronic photooxidative stress. Plant Physiology **134**, 1163–1172.

Mullineaux PM, Karpinski S, Baker NR. 2006. Spatial dependence for hydrogen peroxide-directed signaling in light-stressed plants. Plant Physiology **141**, 346–350.

Murashige T, Skoog F. 1962. A revised medium for rapid growth and bio assays with tobacco tissue cultures. Physiologia Plantarum **15**, 473–497.

Nevarez AP, Qiu Y, Inoue H, Yoo CY, Benfey PN, Schnell DJ, Chen M. 2017. Mechanism of dual targeting of the phytochrome signaling component HEMERA/pTAC12 to plastids and the nucleus. Plant Physiology **173**, 1953-1966.

Niyogi KK, Truong TB. 2013. Evolution of flexible non-photochemical quenching mechanisms that regulate light harvesting in oxygenic photosynthesis. Current Opinion in Plant Biology **16**, 307–314.

Nott A, Jung H-S, Koussevitzky S, Chory J. 2006. Plastid-to-nucleus retrograde signaling. Annual Review of Plant Biology **57**, 739–759.

Oelmüller R, Mohr H. 1986. Photooxidative destruction of chloroplasts and its consequences for expression of nuclear genes. Planta **167**, 106–113.

Ort DR. 2001. When there is too much light. Plant Physiology **125**, 29–32.

Ostrovsky D, Diomina G, Lysak E, Matveeva E, Ogrel O, Trutko S. 1998. Effect of oxidative stress on the biosynthesis of 2-C-methyl-D- erythritol-2,4-cyclopyrophosphate and isoprenoids by several bacterial strains. Archives of Microbiology **171**, 69–72.

Parent JS, Lepage E, Brisson N. 2011. Divergent roles for the two polI-like organelle DNA polymerases of Arabidopsis. Plant Physiology **156**, 254–262.

Pfalz J, Liere K, Kandlbinder A, Dietz KJ, Oelmüller R. 2006. pTAC2, -6, and -12 are components of the transcriptionally active plastid chromosome that are required for plastid gene expression. Plant Cell **18**, 176–197.

Pfalz J, Holtzegel U, Barkan A, Weisheit W, Mittag M, Pfannschmidt T. 2015. ZmpTAC12 binds single-stranded nucleic acids and is essential for accumulation of the plastid-encoded polymerase complex in maize. New Phytologist **206**, 1024-1037.

Phee B-K, Cho J-H, Park S, Jung JH, Lee Y-H, Jeon J-S, Seong HB, Hahn T-R. 2004. Proteomic analysis of the response of *Arabidopsis* chloroplast proteins to high light stress. Proteomics **4**, 3560–3568.

Pitzschke A, Forzani C, Hirt H. 2006. Reactive oxygen species signaling in plants. Antioxidants and Redox Signaling **8**, 1757–1764.

Pogson BJ, Albrecht V. 2011. Genetic dissection of chloroplast biogenesis and development: An overview. Plant Physiology **155**, 1545–1551.

Pogson BJ, Ganguly D, Albrecht-Borth V. 2015. Insights into chloroplast biogenesis and development. Biochimica et Biophysica Acta **1847**, 1017–1024.

Pogson BJ, Woo NS, Förster B, Small ID. 2008. Plastid signalling to the nucleus and beyond. Trends in Plant Science **13**, 602–609.

Pospíšil P. 2009. Production of reactive oxygen species by photosystem II. Biochimica et Biophysica Acta **1787**, 1151–1160.

Prikryl J, Watkins KP, Friso G, Van Wijk KJ, Barkan A. 2008. A member of the Whirly family is a multifunctional RNA- and DNA-binding protein that is essential for chloroplast biogenesis. Nucleic Acids Research **36**, 5152–5165.

Pyke K. 2009. Plastid Biology.

Qiu Y, Li M, Pasoreck EK, Long L, Shi Y, Galvão RM, Chou CL, Wang H, Sun AY, Zhang YC, Jiang A, Chen M. 2015. HEMERA couples the proteolysis and transcriptional activity of PHYTOCHROME INTERACTING FACTORS in Arabidopsis photomorphogenesis. Plant Cell **27**, 1409–1427.

Qiu Y, Kim RJ-E, Moore CM, Chen M. 2019. Daytime temperature is sensed by phytochrome B in *Arabidopsis* through a transcriptional activator HEMERA. Nature Communications **140**, 1-13.

Ramel F, Birtic S, Ginies C, Soubigou-Taconnat L, Triantaphylidès C, Havaux M. 2012. Carotenoid oxidation products are stress signals that mediate gene responses to singlet oxygen in plants. Proceedings of the National Academy of Sciences USA **109**, 5535–5540.

Ren Y, Li Y, Jiang Y, Wu B, Miao Y. 2017. Phosphorylation of WHIRLY1 by CIPK14 shifts its localization and dual functions in *Arabidopsis*. Molecular Plant **10**, 749–763.

Robles P, Fleury D, Candela H, Cnops G, Alonso-Peral MM, Anami S, Falcone A, Caldana C, Willmitzer L, Ponce MR, Van Lijsebettens M, Micol JL. 2010. The *RON1*/*FRY1*/*SAL1* gene is required for leaf morphogenesis and venation patterning in Arabidopsis. Plant Physiology **152**, 1357–1372.

Rodríguez-Concepción M. 2006. Early steps in isoprenoid biosynthesis: Multilevel regulation of the supply of common precursors in plant cells. Phytochemistry Reviews **5**, 1–15.

Rodríguez VM, Chételat A, Majcherczyk P, Farmer EE. 2010. Chloroplastic phosphoadenosine phosphosulfate metabolism regulates basal levels of the prohormone jasmonic acid in Arabidopsis leaves. Plant Physiology **152**, 1335–1345.

Rossel JB, Walter PB, Hendrickson L, Chow WS, Poole A, Mullineaux PM, Pogson BJ. 2006. A mutation affecting *ASCORBATE PEROXIDASE 2* gene expression reveals a link between responses to high light and drought tolerance. Plant, Cell and Environment **29**, 269–281.

Rossel JB, Wilson IW, Pogson BJ. 2002. Global changes in gene expression in response to high light in Arabidopsis. Plant Physiology **130**, 1109–1120.

Scarpeci TE, Zanor MI, Carrillo N, Mueller-Roeber B, Valle EM. 2008. Generation of superoxide anion in chloroplasts of *Arabidopsis thaliana* during active photosynthesis: A focus on rapidly induced genes. Plant Molecular Biology **66**, 361–378.

Singh R, Singh S, Parihar P, VP Singh, Prasad SM. 2015. Retrograde signaling between plastid and nucleus: A review. Journal of Plant Physiology **181**, 55–66.

Smirnoff N. 1993. The role of active oxygen in the response of plants to water deficit and desiccation. New Phytologist **125**, 27–58.

De Souza A, Wang J-Z, Dehesh K. 2017. Retrograde signals: Integrators of interarganellar communication and orchestrators of plant development. Annual Review of Plant Biology **68**, 85-108.

Ströher E, Dietz KJ. 2008. The dynamic thiol-disulphide redox proteome of the *Arabidopsis thaliana* chloroplast as revealed by differential electrophoretic mobility. Physiologia Plantarum **133**, 566–583.

Sunkar R. 2010. Plant stress tolerance: Methods and protocols.

Susek RE, Ausubel FM, Chory J. 1993. Signal transduction mutants of Arabidopsis uncouple nuclear *CAB* and *RBCS* gene expression from chloroplast development. Cell **74**, 787–799.

Sussex IM. 1954. Experiments on the cause of dorsiventrality in leaves. Nature **174**, 351–352.

Suzuki N, Devireddy AR, Inupakutika MA, Baxter A, Miller G, Song L, Shulaev E, Azad RK, Shulaev V, Mittler R. 2015. Ultra-fast alterations in mRNA levels uncover multiple players in light stress acclimation in plants. Plant Journal **84**, 760–772.

Szechyńska-Hebda M, Karpiński S. 2013. Light intensity-dependent retrograde signalling in higher plants. Journal of Plant Physiology **170**, 1501–1516.

Tanaka R, Tanaka A. 2007. Tetrapyrrole biosynthesis in higher plants. Annual Review of Plant Biology **58**, 321–346.

Tian Y, Sacharz J, Ware MA, Zhang H, Ruban AV. 2017. Effects of periodic photoinhibitory light exposure on physiology and productivity of Arabidopsis plants grown under low light. Journal of Experimental Botany **68**, 4249–4262.

Valladares F, Pugnaire FI. 1999. Tradeoffs between irradiance capture and avoidance in semi-arid environments assessed with a crown architecture model. Annals of Botany **83**, 459–469.

Vanderauwera S, Zimmermann P, Rombauts S, Vandenabeele S, Langebartels C, Gruissem W, Inzé D, Van Breusegem F. 2005. Genome-wide analysis of hydrogen peroxide-regulated gene expression in Arabidopsis reveals a high light-induced transcriptional cluster involved in anthocyanin biosynthesis. Plant Physiology **139**, 806–821.

Vogel MO, Moore M, König K, Pecher P, Alsharafa K, Lee J, Dietz KJ. 2014. Fast retrograde signaling in response to high light involves metabolite export, MITOGEN-ACTIVATED PROTEIN KINASE6, and AP2/ERF transcription factors in *Arabidopsis*. Plant Cell **26**, 1151–1165.

Vranová E, Coman D, Gruissem W. 2013. Network analysis of the MVA and MEP Pathways for isoprenoid Synthesis. Annual Review of Plant Biology **64**, 665–700.

Wada M. 2013. Chloroplast movement. Plant Science **210**, 177–182.

Van Der Weele CM, Spollen WG, Sharp RE, Baskin TI. 2000. Growth of *Arabidopsis thaliana* seedlings under water deficit studied by control of water potential in nutrient-agar media. Journal of Experimental Botany **51**, 1555–1562.

Weigel D, Jürgens G. 2002. Stem cells that make stems. Nature **415**, 751–754.

Wilson PB, Estavillo GM, Field KJ, Pornsiriwong W, Carroll AJ, Howell KA, Woo NS, Lake JA, Smith SM, Millar AH, Von Caemmerer S, Pogson BJ. 2009. The nucleotidase/phosphatase SAL1 is a negative regulator of drought tolerance in Arabidopsis. Plant Journal **58**, 299–317.

Xiao Y, Savchenko T, Baidoo EEK, Chehab WE, Hayden DM, Tolstikov V, Corwin JA, Kliebenstein DJ, Keasling JD, Dehesh K. 2012. Retrograde signaling by the plastidial metabolite MEcPP regulates expression of nuclear stress-response genes. Cell **149**, 1525–1535.

Xiao Y, Wang J, Dehesh K. 2013. Review of stress specific organelles-to-nucleus metabolic signal molecules in plants. Plant Science **212**, 102–107.

Xiong JY, Lai CX, Qu Z, Yang XY, Qin XH, Liu GQ. 2009. Recruitment of AtWHY1 and AtWHY3 by a distal element upstream of the kinesin gene *AtKP1* to mediate transcriptional repression. Plant Molecular Biology **71**, 437–449.

Xiong L, Lee H, Huang R, Zhu JK. 2004. A single amino acid substitution in the *Arabidopsis* FIERY1/HOS2 protein confers cold signaling specificity and lithium tolerance. Plant Journal **40**, 536–545.

Xiong L, Lee BH, Ishitani M, Lee H, Zhang C, Zhu J-K. 2001. *FIERY1* encoding an inositol polyphosphate 1-phosphatase is negative regulator of abscisic acid and stress signaling in *Arabidopsis*. Genes & Development **15**, 1971–1984.

Xu W, Jia L, Shi W, Liang J, Zhou F, Li Q, Zhang J. 2013. Abscisic acid accumulation modulates auxin transport in the root tip to enhance proton secretion for maintaining root growth under moderate water stress. New Phytologist **197**, 139–150.

Yokawa K, Kagenishi T, Kawano T, Mancuso S, Baluska F. 2011. Illumination of Arabidopsis roots induces immediate burst of ROS production. Plant Signaling & Behavior **6**, 1460-1464.

Yun KY, Park MR, Mohanty B, Herath V, Xu F, Mauleon R, Wijaya E, Bajic VB, Bruskiewich R, De Los Reyes BG. 2010. Transcriptional regulatory network triggered by oxidative signals configures the early response mechanisms of japonica rice to chilling stress. BMC Plant Biology **10**, 1–29.

Zarkovic J, Anderson SL, Rhoads DM. 2005. A reporter gene system used to study developmental expression of alternative oxidase and isolate mitochondrial retrograde regulation mutants in Arabidopsis. Plant Molecular Biology **57**, 871–888.

Zhang Z-W, Yuan S, Feng H, Xu F, Cheng J, Shang J, Zhang D-W, Lin HH. 2011. Transient accumulation of Mg-protoporphyrin IX regulates expression of PhANGs - New evidence for the signaling role of tetrapyrroles in mature *Arabidopsis* plants. Journal of Plant Physiology **168**, 714–721.

Zhao C, Yang Y, Chan KX, Marchant DB, Franks PJ, Randall D, Tee EE, Chen G, Ramesh S, Phua SY, Zhang B, Hills A, Dai F, Xue D, Gilliham M, Tyerman S, Nevo E, Wu F, Zhang G, Wong GK-S, Leebans-Mack JH, Melkonian M, Blatt MR, Soltis PS, Soltis DE, Pogson BJ, Chen Z-H. 2019. Evolution of chloroplast retrograde signaling facilitaties green plant adaptation to land. Proceedings of the National Academy of Sciences USA **116**, 5015-5020.

Zhou L, Hou H, Yang T, Lian Y, Sun Y, Bian Z, Wang C. 2018. Exogenous hydrogen peroxide inhibits primary root gravitropism by regulating auxin distribution during Arabidopsis seed germination. Plant Physiology and Biochemistry **128**, 126–133.

Figure 2.1 LOF1-mCherry-GFP localization following estradiol induction. Seeds were sown on MS plates (1% agarose) and grown vertically for four days. Seedlings were removed from plates, floated in MS, and exposed to 24-hours of light or 24-hours of dark (plates covered in foil). MS solutions also contained 80 μM β-estradiol for induction of transgene expression. A) LOF1-mCherry-GFP with 24-hours of standard light treatment. B) LOF1-mCherry-GFP with 24-hours of dark treatment. C) non-transgenic sibling of LOF1-mCherry-GFP transgenic seedling with 24-hours of dark treatment. Top panels show root elongation zone. Bottom panel shows root meristematic zone. Left column shows fluorescence from the PI stain. Middle column shows fluorescence from GFP. Right column shows an overlay of PI and GFP fluorescence images. All seedlings were imaged in the T2 generation. All scale bars are 50 μm in length.

A

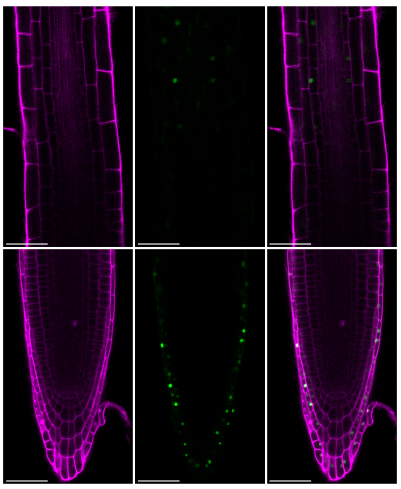

B

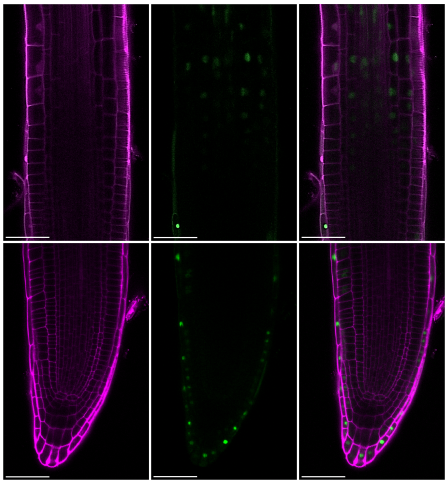

C

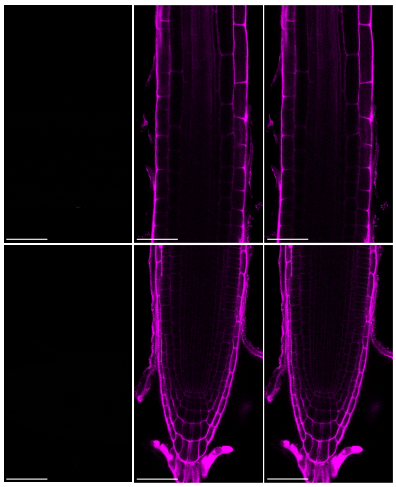

Figure 2.2 GFP show no specific subcellular localization in 24-hours dark, 24-hours high light, or 24-hours standard light. Seeds were sown on MS plates (1% agarose) and grown vertically for four days. Inducible GFP transgenic seedlings were removed from plates, floated in MS, and exposed to the following conditions: A) 24-hours of dark, B) 24-hours of high light, and C) 24-hours of standard light. MS solutions also contained 80 μM β-estradiol for induction of transgene expression. Top panels show root elongation zone. Bottom panel shows root meristematic zone. Left column shows fluorescence from the PI stain. Middle column shows fluorescence from GFP. Right column shows an overlay of PI and GFP fluorescence images. All seedlings were imaged in the T2 generation. All scale bars are 50 μm in length.

A

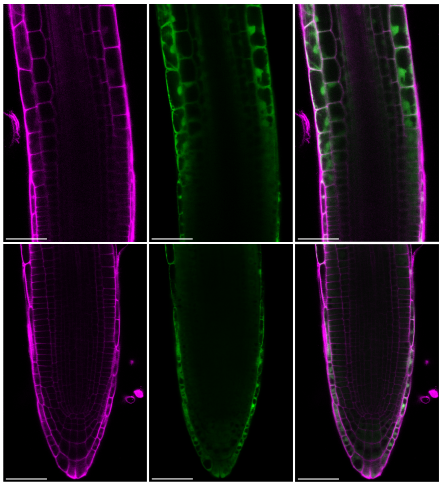

B

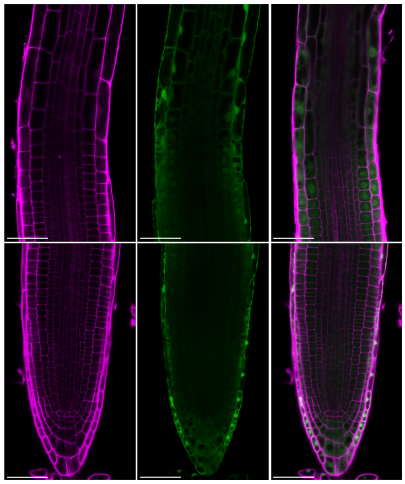

C

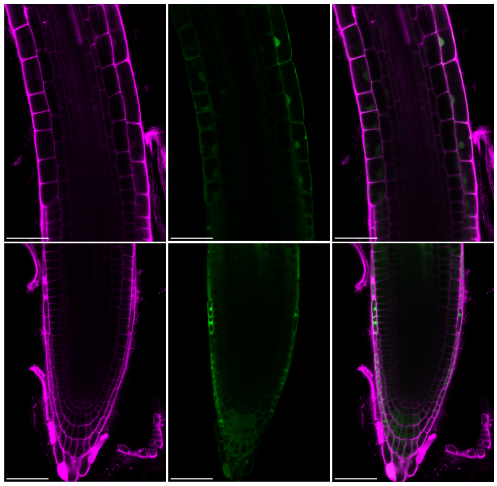

Figure 2.3 LOF1-mCherry-GFP does not change subcellular localization in the root in response to high-light treatment. LOF1-mCherry-GFP transgenic seeds were sown on MS plates (1% agarose) and grown vertically for four days. Seedlings were removed from plates, floated in MS, and exposed to the following conditions: A) 1-hour, B) 2-hours, C) 4-hours of high light-treatment. MS solutions also contained 80μM β-estradiol for induction of transgene expression. Roots were imaged after the 24-hour incubation period. Top panels show root elongation zone. Bottom panel shows root meristematic zone. Left column shows fluorescence from the PI stain. Middle column shows fluorescence from GFP. Right column shows an overlay of PI and GFP fluorescence images. All seedlings were imaged in the T2 generation. All scale bars are 50 μm in length.

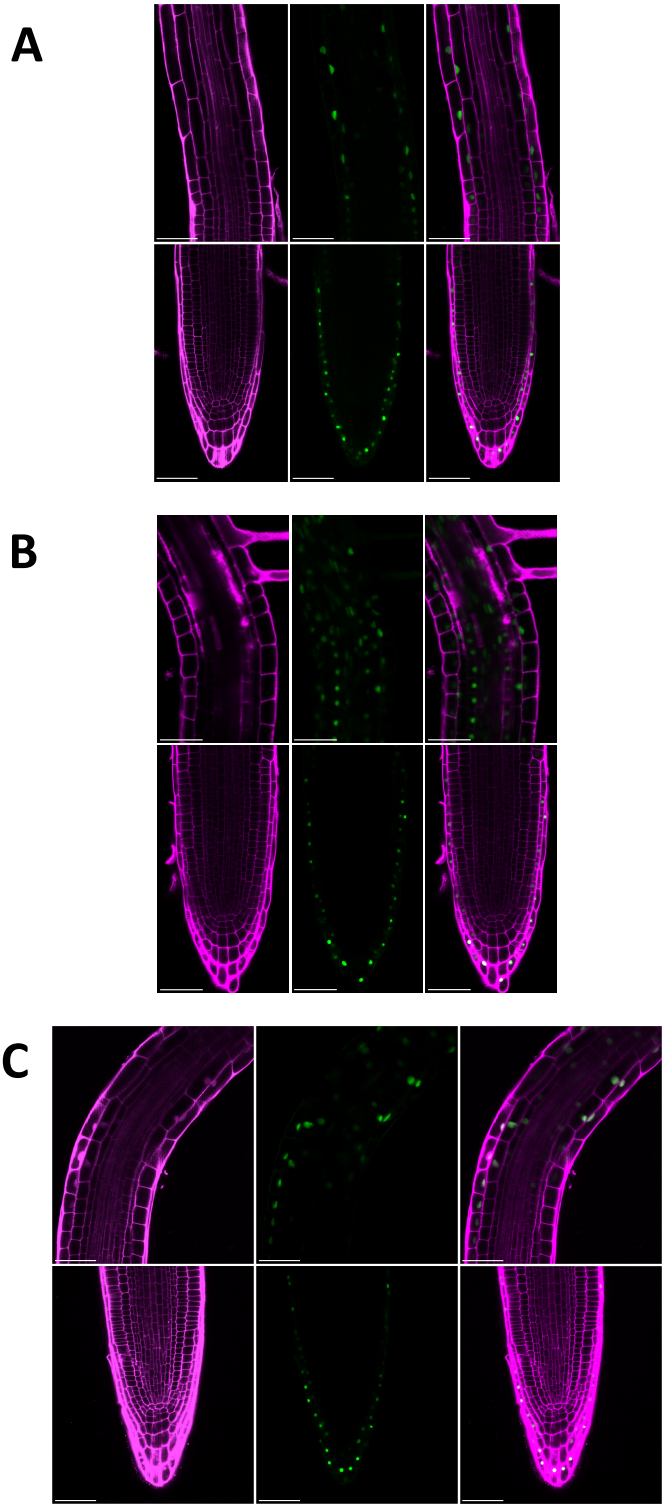
A
B
C

Figure 2.4 LOF1-mCherry-GFP does not change subcellular localization in the root in response to prolonged high-light treatment. LOF1-mCherry-GFP transgenic seeds were sown on MS plates (1% agarose) and grown vertically for four days. Seedlings were removed from plates, floated in MS, and exposed to the following conditions: A) 6-hours, B) 12-hours, and C) 24-hours of high-light treatment. MS solutions also contained 80 μM β-estradiol for induction of transgene expression. Roots were imaged after the 24-hour incubation period. Top panels show roots elongation zone. Bottom panel shows root meristematic zone. Left column shows fluorescence from the PI stain. Middle column shows fluorescence from GFP. Right column shows an overlay of PI and GFP fluorescence images. All seedlings were imaged in the T2 generation. All scale bars are 50 μm in length.

A

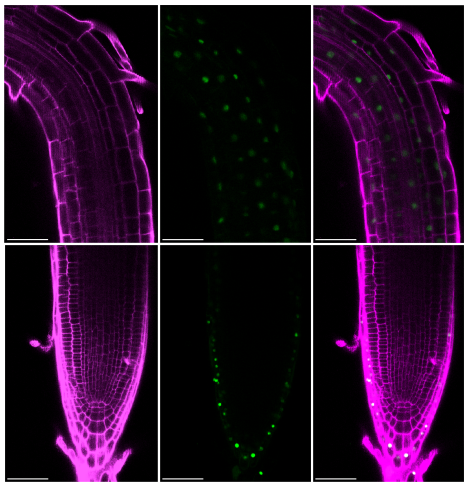

B

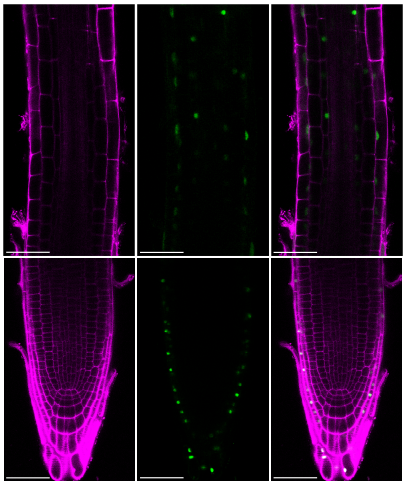

C

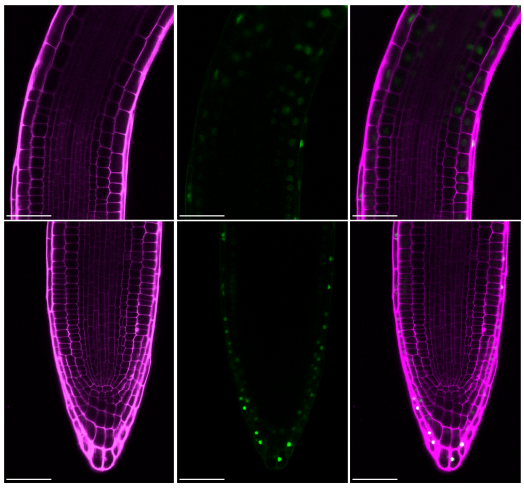

Figure 2.5 LOF1-mCherry-GFP does not change subcellular localization in the root in the presence of reactive oxygen species (ROS). LOF1-mCherry-GFP transgenic seedlings were sown on MS plates (1% agarose) and grown vertically for four days. Seedlings were removed from plates and floated in solutions of MS containing the following concentrations of hydrogen peroxide for a period of 24-hours: A) 100 μM, B) 500 μM, or C) 1000 μM. Solutions also contained 80 μM β-estradiol for induction of transgene expression. Top panels show roots elongation zone. Bottom panel shows root meristematic zone. Left column shows fluorescence from the PI stain. Middle column shows fluorescence from GFP. Right column shows an overlay of PI and GFP fluorescence images. All seedlings were imaged in the T2 generation. All scale bars are 50 μm in length.

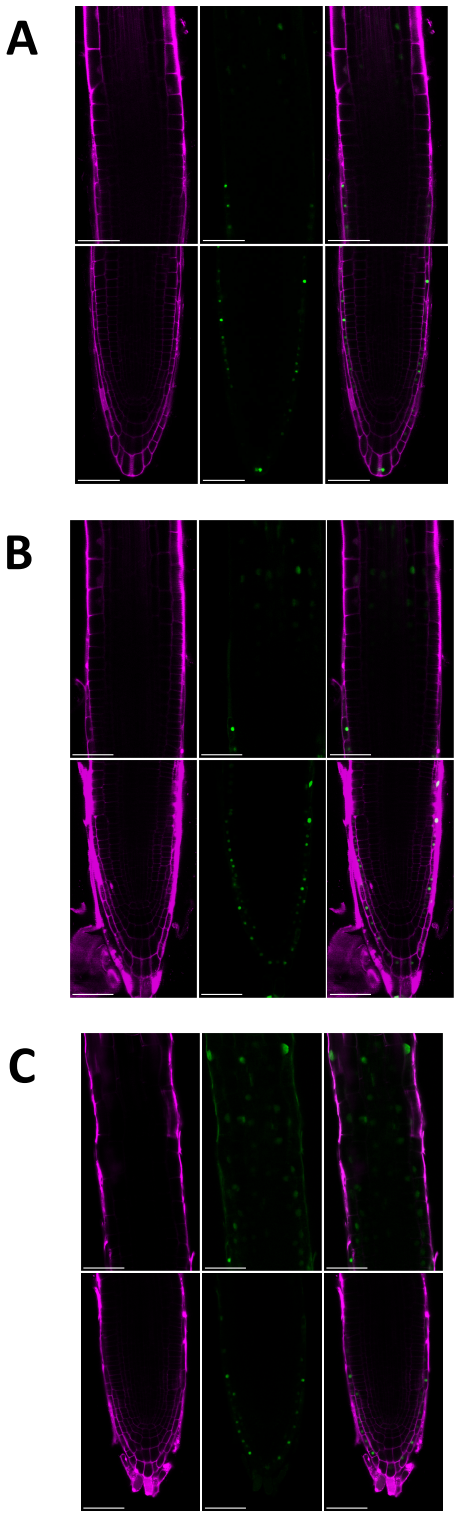
A
B
C

Figure 2.6 Semi-quantitative RT-PCR of *RD19* in response to water deficit. Semi-quantitative RT-PCR was performed on tissue collected from Col-0 10-day old seedlings. Water deficit was imposed by floating in a solution of 25 % PEG 6000 (dissolved in MS), 30% PEG 6000 (dissolved in MS), or a mock solution of MS for a period of 24 hours. Untreated 10-day old seedlings grown on plates were used as unstressed controls. *ACT2* RT-PCR was amplified for 22 cycles. *RD19* RT-PCR was amplified for 22 cycles.

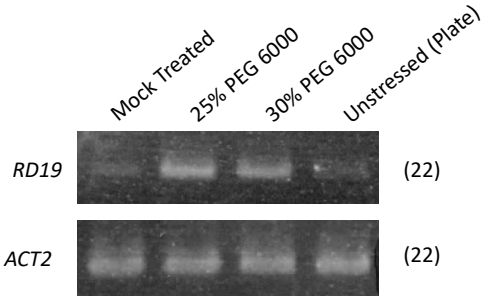
Mock Treated
25% PEG 6000
30% PEG 6000
Unstressed (Plate)
RD19
(22)
ACT2
(22)

Figure 2.7 LOF1-mCherry-GFP does not change subcellular localization in the root under water deficit. LOF1-mCherry-GFP transgenic seedlings were sown on MS plates (1% agarose) and grown vertically for four days. Seedlings were removed from plates and floated in a solution of 25 % PEG 6000 (dissolved in MS) for a period of 24 hours to impose water-deficit stress. 25% PEG MS solution also contained 80 μM β-estradiol for induction of transgene expression. Top panels show roots elongation zone. Bottom panel shows root meristematic zone. Left column shows fluorescence from the PI stain. Middle column shows fluorescence from GFP. Right column shows an overlay of PI and GFP fluorescence images. All seedlings were imaged in the T2 generation. All scale bars are 50 μm in length.

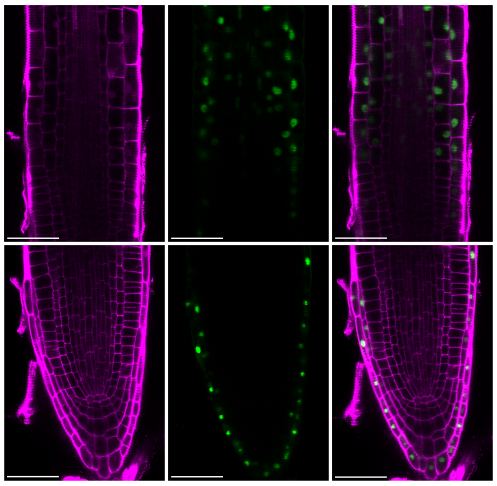

Table 2.1 List of oligonucleotide sequences

Primer	Sequence (5' --> 3')	Tm	Use
ACT2-C	ACTCACCACCACGAACCAG	63.8	RT-PCR of *ACT2*
ACT2-N	AAAATGGCCGATGGTGAGG	66.9	RT-PCR of *ACT2*
RD19AF_01	AAGTTCGGGAAGGTCTACGC	64.7	RT-PCR of *RD19*
RD19AR_01	ACAGAGGCAACGATCTTGGA	64.2	RT-PCR of *RD19*
GFP_R	TCATCCATGCCATGTGTAATC	52.8	Genotyping of inducible LOF1-GFP, LOF1-GFP-mCherry, and GFP expressing transgenic plants
MYB117_seq	CCTAACCCTAACCCTAATTACC	60.1	Genotyping of inducible LOF1-GFP and LOF1-GFP-mCherry expressing transgenic plants
hyg_R	AGTTTAGCGAGAGCCTGACCTAT	57.4	Genotyping of inducible GFP expressing transgenic plants
GFPgate_F	CACCATGAGTAAAGGAGAAGAAC	54.9	Cloning of *eGFP* from paBindGFP
GFPgate_R	CTATTTGTATAGTTCATCCATGCCATG	54.0	Cloning of *eGFP* from paBindGFP

Chapter 3

A Dominant PHABULOSA (PHB) Truncation Suppresses *lof1-1*

Abstract

Lateral organs form on the periphery of the shoot meristem. Separation of the developing lateral organs from the meristem is essential for plant development. The boundary region, a domain of small cells that divide infrequently, functions in separating the meristem from developing organs. *Arabidopsis LATERAL ORGAN FUSION 1* (*LOF1*) encodes a MYB transcription factor that is expressed in organ boundaries in shoots. *LOF1* is expressed in the paraclade junction, where the cauline leaf, axillary branch, and primary stem meet. The *lof1-1* mutant does not form accessory buds, which serve as reserve meristems that grow out to form a new branch if the axillary branch is damaged. *lof1-1* plants also exhibit fusion between the axillary branch and cauline leaf. A screen was performed to identify mutants that suppress the *lof1-1* phenotype, allowing for the formation of accessory buds. *lof1-1 suppressor* (*lfs-1D*), is characterized by the formation of multiple accessory buds per paraclade junction and genetic dominance. A mutation in *PHABULOSA* (*PHB*) was found in *lfs-1D* plants. *PHB* encodes an HD-Zip III transcription factor involved in meristem specification and organ polarity. A mutant version of *PHB*, *mPHB*, containing the *lfs-1D* mutation produced the *lfs-1D* phenotype when introduced into Col-0 plants. Plants expressing *mPHB* plants also occasionally formed fused leaves. Organ fusion phenotypes arise as a result of boundary defects. Thus, the fused leaves could indicate the involvement of *PHB* in the boundary region for organ separation. The *phb-13* loss-of-function mutant has an increased number of accessory

buds, indicating that *PHB* is involved in repressing accessory bud formation. Plants overexpressing *LOF1* sometimes had upwards curling leaves. Because upwards leaf curling is a polarity defect, this phenotype could mean that *LOF1* represses *PHB* and/or other *HD-Zip IIIs*. *lof1-1* single mutants have fewer paraclade junctions, indicating that *LOF1* may be involved in formation of the paraclade junction itself. *LOF1*, *PHB*, and other *HD-Zip III* genes play a role in controlling accessory bud formation and may also help specify overall plant architecture.

Introduction

In plants, all above ground organs, such as leaves, are produced from a structure at the tip of the shoot called the shoot apical meristem (SAM). The SAM must maintain a population of stem cells while continuing to form new lateral organs (Weigel and Jürgens, 2002). The SAM is dome-shaped with a population of stem cells at the apex, in the central zone. Progeny of the stem cells are displaced outwards to the peripheral zone on the sides of the dome and downwards to the rib zone underneath the stem cells (Evans and Barton, 2002; Soyars *et al.*, 2016). The SAM and developing lateral organs are separated by the boundary, a region of small cells that divide infrequently compared with surrounding regions (Hussey, 1971; Breuil-Broyer *et al.*, 2004).

The boundary is important to development of lateral organs and plant architecture. One function of the boundary region is to physically separate the meristem from developing organs. When the boundary does not form properly, organs become fused to one another and to the SAM (Aida *et al.*, 1997; Lee *et al.*, 2009; Bell *et al.*, 2012; Colling

et al., 2015). Decurrent strands, or strands of tissue from one organ that remain attached to another organ, are also a sign of boundary defects (Emery *et al.*, 2003; Lee *et al.*, 2009; Colling *et al.*, 2015).

The *CUP-SHAPED COTYLEDON* (*CUC*) genes encode NAC [NO APICAL MERISTEM, ATAF, CUC] domain transcription factors that are boundary expressed. There are three *CUC* genes in *Arabidopsis* (Aida *et al.*, 1997; Takada *et al.*, 2001). Single *cuc* mutants do not have strong phenotypes, but *cuc* double mutants have fused cotyledons that are cup shaped and do not have post-embryonic shoot meristem activity (Aida *et al.*, 1999; Hibara *et al.*, 2006). This suggests that *CUC* genes function in organ separation and meristem maintenance.

LATERAL ORGAN FUSION1 (*LOF1*) is a boundary-expressed R2R3 MYB transcription factor that was identified via an enhancer-trap screen (Lee *et al.,* 2009). In vegetative plants, *LOF1* is expressed at the base of rosette leaves. After flowering, *LOF1* is expressed in the base of the floral organs, junctions between stems and petioles, junctions between the primary and axillary stems, axillary stems and cauline leaves, and inflorescence meristems and flower primordia. *lof1* mutants have fusions between the axillary branch and cauline leaf. Mutants also lack accessory buds between the axillary branch and cauline leaf in the paraclade junction. Therefore, *LOF1* functions in organ separation and accessory bud formation (Lee *et al.*, 2009). *LOF1* is closely related to another MYB transcription factor, *LATERAL ORGAN FUSION2* (*LOF2*), that has a partially overlapping expression pattern and function. *lof2* single mutants have no abnormal phenotypes. *lof1 lof2* double mutants display radialized vasculature in addition

to further organ separation defects (Lee *et al.,* 2009), which may indicate a connection to leaf polarity.

Genetic interactions between *LOF1* and other genes have been described. *lof1-1* was found to enhance a weak allele of *SHOOT MERISTEMLESS* (*STM*), which is involved in SAM maintenance (Barton and Poethig, 1993; Kanrar *et al.*, 2006; Lee *et al.*, 2009). This reveals that *LOF1* is involved in SAM maintenance as well as accessory bud formation. When *cuc* mutants are combined with the *lof1-1* mutation, fusion phenotypes are enhanced in *lof1-1 cuc* compared to the *lof1-1* mutant alone – resulting in additional fusions (Lee *et al.*, 2009). This indicates that *LOF1* functions with *CUC* genes in boundary formation.

The long and flat structure of a leaf blade is complex to form. Additionally, the top of the leaf, or adaxial side, must be different from the bottom of the leaf, or abaxial side (Moon and Hake, 2011). The adaxial side has chloroplasts arranged for optimum capture of light, whereas the abaxial side contains a high density of stomata for gas exchange and transpiration. The structure is important for leaf function. For example, having too many stomata on the adaxial side of the leaf could result in too much water loss for the plant (Husbands *et al.*, 2009). Physically separating the developing primordia from the meristem using a surgical incision results in loss of adaxial-abaxial polarity (Sussex, 1951; 1954), suggesting a signal from the meristem is required for adaxial-abaxial polarity. Leaves that have lost adaxial-abaxial polarity appear radially symmetric and no blade tissue can be discerned [reviewed in (Bowman *et al.*, 2002)].

One family of MYB transcription factors, known as the [ASYMMETRIC LEAVES1 (AS1); ROUGH SHEATH2 (RS2); PHAN] ARP family, are involved in leaf primordia development (Schneeberger *et al.*, 1998; Timmermans *et al.*, 1999; Tsiantis *et al.*, 1999). In *Antirrhinum majus* (snapdragon), loss-of-function mutations in *PHANTASTICA* (*PHAN*) led to abaxialized radial or partially radial leaves, among other phenotypes. The adaxial side of *phan* mutant leaves has patches of adaxial and abaxial tissue and lamina-like outgrowths at the adaxial and abaxial boundaries (Waites and Hudson, 1995; Waites *et al.*, 1998). *AS1* is the *PHAN* ortholog in *Arabidopsis*, and *as1* mutants produce abaxialized phenotypes at a low frequency (Xu *et al.*, 2003). *RS2* is the *PHAN* ortholog in maize, and *rs2* mutants produce semi-bladeless leaves (Schneeberger *et al.*, 1998), although adaxial-abaxial polarity seems to be maintained (Tsiantis *et al.*, 1999). Based on these discoveries, ARP genes are considered determinants of both adaxial-abaxial polarity and proximal-distal axes.

In *Arabidopsis*, a group of homeodomain leucine zipper (HD-Zip) class III proteins were found to be adaxial determinants (Talbert *et al.*, 1995; McConnell and Barton, 1998; McConnell *et al.*, 2001; Otsuga *et al.*, 2001; Emery *et al.*, 2003; Green *et al.*, 2005). HD-Zip transcription factors have been classified into four main groups based on gene structure and unique protein domains. All proteins have a homeodomain involved in DNA binding as well as a leucine zipper (Zip) domain involved in homodimer and heterodimer formation (Ariel *et al.*, 2007). Although all HD-Zip proteins have a conserved homeodomain, they do not all bind DNA of the same sequence. HD-Zip class III proteins are comprised of five members – PHABULOSA (PHB), PHAVOLUTA

(PHV), REVOLUTA (REV), CORONA (CNA), and ARABIDOPSIS THALIANA HOMEOBOX GENE 8 (ATHB8). These proteins share several domains in common in addition to the HD and Zip domains. One of these domains - the START (steroidogenic acute regulatory protein-related lipid transfer) domain - is thought to be a lipid-binding domain, based on its function in animals. However, the lipid-binding function has not been confirmed in plants (Schrick *et al.*, 2004). HD-Zip class III proteins have many roles in plant development. Organ polarity, embryo patterning, vascular development, and meristem formation and maintenance are the main developmental functions of HD-Zip class III proteins (McConnell and Barton, 1998; McConnell *et al.*, 2001; Emery *et al.*, 2003; Prigge *et al.*, 2005).

ATHB8 is mainly expressed in the root vasculature and mutants appear phenotypically wild-type (Baima *et al.*, 2001). *ATHB8* is positively regulated by auxin (Baima *et al.*, 1995), and plants overexpressing *ATHB8* overproduced xylem. It has been proposed that *ATHB8* participates in a positive feedback loop with auxin for differentiation of xylem cells in the root (Baima *et al.*, 2001).

PHB and *PHV* were first discovered as dominant, gain-of-function mutants, which developed radial leaves with only adaxial identity (McConnell and Barton, 1998; McConnell *et al.*, 2001). These mutations were later revealed to disrupt the binding site for *miRNA 165* and *miRNA 166* – miRNAs that regulate *HD-Zip class III* mRNAs. *miRNA 165/166* only accumulates in the abaxial domain (Yao *et al.*, 2009). Thus, *HD-Zip class III* transcripts only accumulate adaxially even though the genes are expressed throughout the developing primordia. *HD-Zip class III* mutants, such as *phb-1D*, contain

mutations in the *miRNA 165/166* binding domain, resulting in loss of regulation by *miRNA 165/166* (McConnell and Barton, 1998; Rhoades *et al.*, 2002; Emery *et al.*, 2003; Tang *et al.*, 2003). *phb* and *phv* loss-of-function single mutants do not have any reported abnormal phenotypes, which is thought to be a result of functional redundancy between *HD-Zip III* genes (Emery *et al.*, 2003; Prigge *et al.*, 2005). *35S:PHB* plants have been reported to have no abnormal phenotypes as well (McConnell and Barton, 1998; McConnell *et al.*, 2001; Mallory *et al.*, 2004), which is thought to be the result of post-transcriptional regulation by *miRNA165/166*.

The *rev* loss-of-function mutant has abnormally shaped leaves that curl downwards and fewer paraclade junctions (Talbert *et al.*, 1995). *rev* mutants also have reduction in rosette and cauline leaf axillary buds (Otsuga *et al.*, 2001). A dominant, gain-of-function mutant (*rev-10d*) displays radialized vasculature - with xylem surrounding phloem - and has decurrent strands between the primary stems and cauline leaves (Emery *et al.*, 2003). REV upregulates *SHOOTMERISTEMLESS* (*STM*), a meristem identity gene, directly to establish axillary meristems in leaf axils (Shi *et al.*, 2016). This requires the presence of meristematic cells in the leaf axil. However, if that population differentiates, it is irreversible, and axillary meristems cannot be formed (Shi *et al.*, 2016). Thus, *REV* functions in paraclade junction formation, axillary bud formation, and leaf polarity.

The HD-Zip III transcription factor encoding *CORONA* (*CNA*) was isolated as an enhancer of *clv1-1*, a *CLAVATA1* (*CLV1*) mutant. *CLV1* is involved in meristem maintenance. The *cna-1 clv1-1* double mutant (L*er* background) exhibited enlarged

meristem size, loss of organ formation, formation of organs in the center of the meristem, and the ring-like meristem structure for which *CNA* is named (Green *et al.*, 2005). The *cna-1* single mutant had larger meristems than controls, but this diminished over time such that 24-day old plants appeared phenotypically wild-type (Green *et al.*, 2005). The *cna-2* allele contains a T-DNA insertion in the second exon of *CNA* and is in the Columbia-0 genetic background (Prigge *et al.*, 2005). This mutant also appears wild-type, and the *cna-2 clv* double mutant was phenotypically similar to *cna-1 clv*, although somewhat less severe (Green *et al.*, 2005).

Only *PHB*, *PHV*, and *REV* are implicated directly in adaxial-abaxial leaf polarity. *PHB* and *PHV* are implicated because of their dominant, gain-of-function mutations that cause adaxialized, radial leaves (McConnell and Barton, 1998; McConnell *et al.*, 2001). *REV's* involvement was less obvious, as dominant *rev* mutants do not produce radial leaves (Emery *et al.*, 2003). However, *rev phv* double loss-of-function mutant leaves have ectopic leaf blades emerging the adaxial tissue, which are surrounded by patches of abaxial tissue. Thus, creating a mirror-image pattern of leaf polarity (Prigge *et al.*, 2005). This *rev phv* phenotype also implicates *REV* in adaxial-abaxial leaf polarity.

The *KANADI* (*KAN*) genes are abaxial determinants, and there are four *KAN* genes in *Arabidopsis*. The *KAN* genes are expressed abaxially and encode GARP-domain transcription factors (Eshed *et al.*, 1999; Izhaki and Bowman, 2007). Single *kan* mutants do not have an abnormal phenotype, but double and triple mutants display different degrees of leaf radialization. In *kan* triple mutants, leaves are adaxialized and radial with *HD-Zip III* gene expression throughout the leaves (Eshed *et al.*, 1999, 2004). Conversely,

ectopically overexpressing *KAN* genes throughout primordia, leads to loss of *HD-Zip III* expression (Kerstetter *et al.*, 2001). This means that *KAN* and *HD-ZIP III* genes act in mutual agonism to one another. Additionally, *AS2* and *KAN* genes have been found to have a mutually antagonistic relationship (Lin *et al.*, 2003; Xu *et al.*, 2003). Thus, *KANADI*s act in mutual repressive manner with multiple adaxial determinants.

AUXIN RESPONSE FACTOR3 (*ARF3*) and *AUXIN RESPONSE FACTOR4* (*ARF4*) are also abaxial identity determinants. Single loss-of-function mutants of *arf3* or *arf4* do not result in leaf polarity defects. However, *arf3 arf4* double mutants have adaxialized leaves (Pekker *et al.*, 2005). *ARF3* and *ARF4* are expressed throughout the developing primordia, but *ARF3* and *ARF4* transcripts only accumulate abaxially. This is because *ARF3* and *ARF4* are post-transcriptionally regulated by a trans-acting small-interfering RNA (tasiRNA), which limits *ARF3* and *ARF4* accumulation adaxially (Allen *et al.*, 2005; Fahlgren *et al.*, 2006; Hunter *et al.*, 2006). This *tasiRNA-ARF* (*tasi-ARF*) gradient begins at the adaxial epidermis and opposes the *miRNA 165/166* gradient that starts at the abaxial epidermis. These two small RNA gradients are important for leaf development as they act to buffer against fluctuations in target gene expression (Skopelitis *et al.*, 2012, 2017).

YABBY (*YAB*) genes encode zinc-finger and helix-loop-helix domain containing proteins that function in leaf blade outgrowth. There are six *YABBY* genes in *Arabidopsis* (Siegfried *et al.*, 1999; Villanueva *et al.*, 1999), and four of the six *YABBY* genes are expressed abaxially in lateral organs (Sawa *et al.*, 2002). Single loss-of-function *yab* mutants have no abnormal leaf phenotypes. Quadruple *yab* mutants display a variety of

leaf blade expansion phenotypes. A later analysis revealed that these mutants are not, in fact, abaxial determinants as previously thought based on expression pattern and phenotype (Siegfried *et al.*, 1999). Quadruple *yab* mutants establish adaxial-abaxial polarity but it is not maintained (Sarojam *et al.*, 2010), indicating *YAB* genes function is in leaf blade expansion.

The proposition that lateral organs provide feedback to stem cells has existed for some time (Sussex, 1952). Mutations in more than one *yab* gene leads to an increase in SAM size even though *YAB* genes are not expressed in the meristem (Goldshmidt *et al.*, 2008). Thus, *YAB* genes could be involved in feedback regulation that impacts SAM size by an unknown mobile signal. Modeling experiments revealed that a YAB-derived signal could be transported to the boundary, where another signal is then transported to the meristem (Shi *et al.*, 2018). However, these results have not yet been verified by biological applications.

HD-Zip III genes have other known functions in addition to their involvement in adaxial-abaxial leaf polarity. *REV*, *PHB*, *PHV*, and *CNA* function together in embryo development. While *phb phv* mutants did not have any embryo defects, *rev phb* had embryos lacked SAMs, and occasionally, cotyledons were absent or fused. At low frequency, *rev phv* showed the same phenotypes as *rev phb* (Prigge *et al.*, 2005). The addition of mutations in *cna* or *phv* enhanced the *rev phb* double mutant phenotype, such that bilateral symmetry in the apical portion of the embryo was lost, converting it into a radially symmetric structure. Thus, *rev phb phv* mutants cannot often be studied due to seedling lethality, and some combinations of mutants, such as *rev phb*, are difficult to

study due to meristem termination (Prigge *et al.*, 2005). Thus, *REV*, *PHB*, *PHV*, and *CNA* regulate patterning the apical embryo and bilateral symmetry. Interestingly, *phb phv cna* triple mutants do not have the same defects in embryo development or SAM formation. However, plants had extra cotyledons, enlarged SAMs, meristem fasciation, and flowers with extra organs (Prigge *et al.*, 2005).

PHB, *PHV*, and *CNA* function independently from *REV* and *ATHB8* in meristem regulation. *phb phv cna* mature plants have an enlarged meristem, while *rev*/+ *phb phv cna* plants surprisingly have a meristem that is more wild-type in size (Prigge *et al.*, 2005). This indicates that *REV* likely does not function with *PHB*, *PHV*, and *CNA* in meristem regulation post-embryonically. This also shows *REV*, *CNA*, *PHB*, and *PHV* also sometimes repress each other's meristematic phenotypes post-embryonically or act antagonistically (Prigge *et al.*, 2005).

It has been suggested that *CNA* and *ATHB8* can antagonize *REV* function in axillary meristem formation. *rev cna* and *rev athb8* double mutants appeared like *rev* single mutants, suggesting that *REV* does not share function with *CNA* and *ATHB8* in axillary meristem formation. However, the *rev cna athb8* triple mutant produced more lateral shoot meristems and flowers than *rev* single mutants (Prigge *et al.*, 2005). This is consistent with the idea that some *HD-Zip III* genes function antagonistically. In summary, *REV*, *PHB*, *PHV*, and *CNA* function in embryo development and formation of the SAM in the embryo with *REV* having a critical role in shoot meristem initiation. *PHB*, *PHV*, and *CNA* play redundant, yet antagonistic roles in limiting meristem development (Emery *et al.*, 2003; Prigge *et al.*, 2005).

PHB is not only involved in development in the shoot but also play roles in root growth processes. In the root apical meristem (RAM), the quiescent center (QC) maintains the stem cell population (Dolan *et al.*, 1993). There are two main stem cell populations named for their position relative to the QC. The cells shootward of the QC are called the proximal stem cells and divide for root growth. The cells rootward of the QC are called the distal stem cells and divide to form the columella root cap [reviewed in (Bennett and Scheres, 2010)]. SHORTROOT (SHR) and SCARECROW (SCR) are two GRAS domain transcription factors that work together to maintain the stem cell population and root growth. In the absence of SHR or SCR, the QC in not maintained and root growth terminates (Di Laurenzio *et al.*, 1996; Helariutta *et al.*, 2000). *SHR* is transcribed in the stele and moves one cell layer over to the endodermis, cortex/endodermal initial (CEI), and QC. SHR then transcriptionally activates *SCR* and regulates CEI asymmetric cell division in order to maintain QC identity (Helariutta *et al.*, 2000; Cui *et al.*, 2007). SCR in involved in maintaining the QC through cell-autonomous activity (Sabatini *et al.*, 2003). SHR and SCR regulate *PHB* and other *HD-Zip III*s in the root by transcriptionally regulating *miRNA 165/166* genes, which is thought to restrict *PHB* transcript accumulation to the stele in the root meristem (Carlsbecker *et al.*, 2010).

Cytokinin (CK) is a plant hormone that regulates cell division and also promotes growth and development (Schaller *et al.*, 2014). CK promotes cell division of the QC, which is only rarely mitotically active (Zhang *et al.*, 2013). PHB is involved in a feedback loop with CK to regulate root length. PHB directly activates *ISOPENTYL TRANFERASE7* (*IPT7*), which catalyzes the rate-limiting step in CK biosynthesis, to

promote cell differentiation (Dello Ioio *et al.*, 2012). CK then represses both *PHB* and *miR165/166* to complete the feedback loop (Dello Ioio *et al.*, 2012). In the absence of CK, stem cell proliferation is inhibited, which causes growth defects. Under high CK, stem cell differentiation is promoted, which slows down root growth (Tian *et al.*, 2002). Therefore, a very specific amount of CK is needed for correct root growth.

HD-Zip III proteins work in a feedback loop with LITTLE ZIPPER (ZPR) proteins in maintenance of leaf polarity. ZPR proteins are small, leucine zipper proteins. ZPRs are encoded by four genes in the *Arabidopsis* genome – *ZPR1*, *ZPR2*, *ZPR3*, and *ZPR4* and were discovered based the amino acid sequence similarity of their leucine zipper domains to those of REV, PHB, and PHV (Wenkel *et al.*, 2007). *ZPR* genes are expressed in the shoot meristem and the adaxial epidermis of leaves (Wenkel *et al.*, 2007; Kim *et al.*, 2008; Weits *et al.*, 2019). All four *ZPR* genes were upregulated when a dominant *REV* mutant containing a disruption in the *miRNA 165/166* binding site was expressed (Wenkel *et al.*, 2007). Thus, REV promotes transcriptional activity of *ZPR*s. A co-immunoprecipitation experiment showed that REV and ZPR3 interact *in vitro*. Additionally, it was found that ZPR3 could prevent REV and PHB from binding to DNA by forming an inactive heterodimer (Wenkel *et al.*, 2007; Kim *et al.*, 2008). HD-Zip proteins typically bind DNA as homodimers (Sessa *et al.*, 1998). This suggests that ZPR proteins function to limit HD-Zip III DNA-binding activity. Furthermore, plants overexpressing *ZPR1* or *ZPR3* appear phenotypically similar to mutants with reduced HD-Zip III function (Wenkel *et al.*, 2007). These data suggest a negative feedback loop

in which HD-Zip III proteins transcriptionally activate *ZPR*s, which in turn heterodimerize with HD-Zip IIIs to limit their DNA-binding activity.

Recently, a hypoxic stem cell niche located in the center of the SAM that is required for production of new leaves was discovered. *ZPR2* is active in the organizing center of the meristem, similar in location to the hypoxic niche, which appears to inhibit proteolysis of ZPR2 (Weits *et al.*, 2019). ZPR2 inhibits DNA-binding activities of REV, PHB, and ATHB8 (Weits *et al.*, 2019), similar to what was previously reported for ZPR3 (Wenkel *et al.*, 2007; Kim *et al.*, 2008). Therefore, ZPR2 function requires hypoxic meristem conditions in order to inhibit HD-Zip III DNA-binding activity.

This study aims to better understand *LOF1* function on a molecular level by identifying a genetic suppressor of the *lof1-1* mutant. In this Chapter, we isolate a dominant mutation in *PHB* that increases accessory bud number and suppresses the *lof1-1* mutant phenotype. We found *LOF1* promotes accessory bud formation, while *PHB* and other *HD-Zip III* genes repress accessory bud formation. Plants that overexpress *LOF1* have upward curling leaves, a leaf polarity phenotype, and plants carrying a transgene with a dominant *PHB* mutation sometimes produce fused leaves. Organ fusions indicate boundary defects. This study reveals a complex relationship between *LOF1* and *HD-Zip III* genes in accessory bud formation and specification of overall plant architecture.

Results

LOF1 is Required for Accessory Bud Formation

Vegetative growth of *Arabidopsis* begins with production of rosette leaves that form axillary buds within the leaf axils. There is very little internode elongation during this time. Following the transition to reproductive development, plants bolt, forming a single primary inflorescence with significant internode elongation. Axillary branches (also called paraclades) are produced along the primary inflorescence, subtended by cauline leaves [reviewed in (Teichmann and Muhr, 2015)]. The area where the primary inflorescence, cauline leaf, and axillary branch meet is called the paraclade junction (Figure 3.1 A; 3.2 A-C). Wild-type plants typically produce two to three paraclade junctions per plant (Figure 3.3). The accessory bud, a reserve meristem that grows out into a new branch if the axillary branch is damaged, forms between the cauline leaf and axillary branch at their base (Figure 3.2 A-C).

Wild-type (Col-0) plants typically produce zero to one accessory bud per paraclade junction (Figure 3.2 A-C; 3.3). At low frequency (≤ 3%), Col-0 plants produce more than one accessory bud (Figure 3.4; Table 3.1). The *lof1-1* single mutant has been previously reported to lack accessory buds (Lee *et al.*, 2009). However, we now know that under certain environmental conditions *lof1-1* mutants can infrequently produce accessory buds (data not shown). *lof1-1* mutants rarely produced an accessory bud (≤ 3%); this was observed only once in these experiments (Figure 3.4; Table 3.1). Multiple accessory buds per paraclade junction were never observed in the *lof1-1* single mutant during these experiments. The *lof1-1* mutant has also been reported to contain a fusion

between the axillary branch and cauline leaf in the paraclade junctions [(Lee *et al.*, 2009); Figure 3.2 D]. The *lof1-1* fusion itself is also environmentally variable and can be difficult to distinguish when small and very obvious when large. The most commonly observed size of the *lof1-1* fusion can be viewed in Figure 3.2 D. However, the *lof1-1* mutant fusion is much more severe under short-day conditions (Lee *et al.*, 2009).

Although the general body plan of *Arabidopsis* is genetically determined, branching patterns and plant architecture can be adjusted in response to environmental conditions (Janssen *et al.*, 2014). Branches from cauline-leaf paraclades can form secondary branches from second order paraclades. Additionally, axillary buds in rosette leaf axils can grow out to into branches: rosette-leaf paraclade branches, specifically. These rosette-leaf axil branches are also capable of secondary branching from second order paraclades [Figure 3.1 B; (Weberling, 1989; Hempel and Feldman, 1994; Talbert *et al.*, 1995)**]**. Under standard conditions, it is typical for secondary rosette-leaf axil branches and secondary cauline-leaf axil branches to occur although numbers of branches are variable (data not shown).

Isolation of a Genetic Suppressor of *lof1-1*

To help decipher *LOF1*'s role in organ separation and meristem maintenance, an ethyl methane sulfonate (EMS) mutagenesis was conducted in the *lof1-1* mutant (Columbia-0/Col-0 background) to identify mutations that suppressed the *lof1* phenotype, allowing accessory buds to form. The plants were not screened for suppression of the *lof1-1* fusion phenotype, as it is environmentally sensitive and variable. *lof1 suppressor*

(*lfs-1D*) *lof1-1*, which produced accessory buds, was identified in the M2 population. *lfs-1D lof1-1* plants exhibited supernumerary accessory buds (Figure 3.2 F). Further, accessory buds grew out into additional branches in the double mutant (Figure 3.2 H); this does not usually occur in wild-type plants unless the axillary branch is damaged or the inflorescence tip of the plant is removed. Some *lfs-1D lof1-1* mutants also displayed a change in position of the accessory bud. In these cases, the accessory bud was displaced, or offset, from the center of the axil to the edge, near the cauline leaf margin (Figure 3.2 E).

After selecting for the phenotype in the second generation after EMS (M2) and confirming this phenotype was stable in the third generation after EMS (M3), the M3 *lfs-1D lof1-1* plants were crossed to the ecotype Landsberg *erecta* (L*er*). Resulting F1 plants were selfed and the subsequent F2 population was used to map the location of the l*fs-1D* mutation. The *lfs-1D* mutation was found to be genetically dominant, appearing in approximately 72.2% of the F2 plants (data not shown). Using the F2 mapping population, the *lof1-1* suppressor mutation was mapped to a large ~7.1 Mbp region on chromosome 2 (Table 3.2).

To remove unlinked EMS mutations that might cause other phenotypes, *lfs-1D* M3 plants were backcrossed to Col-0 four times. After each cross, a plant showing the *lfs-1D* phenotype was used as a parent in the subsequent backcross. After four backcrosses to Columbia, plants still contained accessory buds with positional changes, accessory buds that grew out without damage to the axillary branch, and multiple accessory buds (Figure 3.5). The *lof1-1* mutation was segregated out after the second

backcross by genotyping for *LOF1*, allowing the *lfs-1D* phenotype to be analyzed in the absence of the *lof1-1* mutation.

A Mutation in *PHABULOSA* (*PHB*) is Responsible for the *lfs-1D* Phenotype

Because our mapping data could not be further resolved by increasing the total number of plants genotyped (>600 used), we examined the mapping intervals for candidate causal genes. In this region, we identified *PHABULOSA* (*PHB*), which encodes an HD-Zip III transcription factor that is an adaxial identity determinant. A previously identified dominant mutant of *PHB*, *phb-1D*, displays ectopic meristems around the first emerging true leaves (McConnell and Barton, 1998; McConnell *et al.*, 2001), indicating supernumerary accessory buds can be caused by adaxialization of the cauline leaf. This phenotype was similar to that seen in *lfs-1D lof1-1* plants.

Sequencing of *PHB* cDNA from the M3 *lfs-1D lof1-1* plants using overlapping primer pairs (Table 3.3) revealed a mutation of interest, a C to T substitution, which caused a stop codon at position 382 of the protein (*phb382**) (Figure 3.6). This mutation is within the START domain, which is thought to be involved in protein-protein interactions and/or be a sterol-binding site. The causal mutation for *phb-1D* is also located within the START domain although not within the same region as the mutation found in *lfs-1D lof1-1* plants (Figure 3.6). Unlike *lfs-1D*, *phb-1D* and all other dominant *phb* mutations to date have been located in the *miRNA 165/166* binding site of *PHB* (Figure 3.6). Sequencing data showed that the mutation was not present in the parental

plants, indicating that the mutation arose during mutagenesis; and therefore, this mutation could be the cause of the *lfs-1D* phenotype (data not shown).

To determine if the mutation in *PHB* was the cause of the *lfs-1D* phenotype, site-directed mutagenesis was used to introduce the *PHB* mutation found in *lfs-1D lof1-1* plants (a single C to T base pair change). The resulting *mPHB* was fused with the coding region for GFP and driven by the *PHB* native promoter (*pPHB:GFP:mPHB*). This expression vector was transformed into *Arabidopsis* Col-0 and *lof1-1* genetic backgrounds. As a control for *PHB* locus number, the WT *PHB* cDNA sequence (*pPHB:GFP:PHB*) was also transformed into *Arabidopsis* Col-0 and *lof1-1* mutants. For simplicity, these expression vectors will be referred to as *pPHB:mPHB* and *pPHB:PHB*. Because *PHB* overexpressing plants were reported to appear wild-type (McConnell *et al.,* 2001; Mallory *et al.,* 2004), we did not expect *pPHB:PHB* plants to have any abnormal phenotypes. Since the *lfs-1D* mutation is dominant, plants transformed with *mPHB* were expected to show a *lfs-1D*-like phenotype in the T1 generation if *PHB* contains the causal mutation. Surprisingly, both Col-0 and *lof1-1* plants that contained *pPHB:mPHB* or *pPHB:PHB* displayed a range of phenotypes, including multiple accessory buds, offset accessory buds, and accessory buds that grew out without damage to the axillary branch (Figure 3.7; 3.8; Table 3.4; 3.5). Additionally, the *pPHB:PHB* and *pPHB:mPHB* transgenes were genetically dominant as the *lfs-1D*-like phenotype occurred in the first generation of transformants (Table 3.5; 3.6).

To determine if *PHB* transgene expression levels could be a factor in the observed phenotypes, transcript levels of the *pPHB:PHB* transgene and the endogenous *PHB* gene

were determined using RT-PCR. T2 generation plants that were segregating for one or two *pPHB:PHB* loci were used (Figure 3.9). *PHB* transcript levels were also assessed in T2 *pPHB:PHB lof1-1* plants (Figure 3.10). T2 lines that displayed intermediate phenotypes and *pPHB:PHB* transcript levels were used in subsequent studies. Populations that were very severe or mild were not further used. *pPHB:PHB* plants that had mild phenotypes appeared similar in phenotype to their Col-0 wild-type or *lof1-1* mutant backgrounds. Additionally, *pPHB:PHB* plants that were very severe were too small to characterize, did not produce paraclade junctions, showed meristem termination, and/or had severe fusions (discussed later). T2 lines where endogenous *PHB* was silenced or transgene expression was very high were not used in further experiments. T2 lines with higher transcript levels of *pPHB:PHB* tended to have more severe phenotypes than T2 lines with lower transcript levels of *pPHB:PHB* (data not shown).

We also assessed the transcript levels of related *HD-Zip III* genes, *PHV* and *CNA*, in T2 lines to ensure that presence of the *pPHB:PHB* transgene did not lead to altered transcript levels of other *HD-Zip III* genes (data not shown). The *pPHB:PHB* transgene did not greatly alter transcript levels of *PHV* or *CNA* in any T2 line (data not shown).

lof1-1 phb-13 Double Mutants are Phenotypically Similar to *lof1-1* Single Mutants

Because a mutation in *PHB* that results in a stop codon led to suppression of the *lof1-1* mutant phenotype, we addressed genetic interactions by crossing *lof1-1* to *phb-13*. *phb-13* has been previously reported as a null allele (Prigge *et al.*, 2005). *phb* single mutants have no reported abnormal phenotypes (Emery *et al.*, 2003; Prigge *et al.*, 2005),

which is thought to the result of functional redundancy with other *HD-Zip III* genes. To confirm the *phb-13* single mutant as a null allele, *PHB* transcript levels were determined in pools of *phb-13* and Col-0 rosette leaves using RT-PCR. While we did observe lower levels *PHB* transcript in *phb-13* rosette leaves compared to Col-0 control rosette leaves from two-week old plants, some transcript was detectable, suggesting *phb-13* is not a null allele (Figure 3.11 A). However, *PHB* transcript levels were substantially less in *phb-13* mutant leaves.

When mature Col-0, *lof1-1*, *phb-13*, and *lof1-1 phb-13* mutant plants were compared, *lof1-1 phb-13* double mutants most resembled *lof1-1* single mutants, having fusion between the cauline leaf and axillary branch and lacking the formation of accessory buds (Figure 3.12). *phb-13* single mutants most resembled Col-0 plants, as there was no fusion between the cauline leaf and axillary branch and accessory buds were present in the paraclade junctions (Figure 3.12). Therefore, *lof1-1 phb-13* double mutants appear phenotypically similar to *lof1-1* single mutants.

LOF1 and *PHB* Do Not Regulate One Another at the Transcriptional Level

To examine *LOF1* impacts on *PHB* transcript levels, tissue was collected from the paraclade junctions of wild-type (WT), *lof1-1*, *phb-13*, and *lof1-1 phb-13* and examined by RT-PCR. Transcript levels of *PHB* appeared higher in Col-0 and *lof1-1* compared to *phb-13* and *lof1-1 phb-13* (Figure 3.11 B). This suggests that lower levels of *LOF1* transcript in the paraclade junction does not alter transcript levels of *PHB* in the paraclade

junction. These data also show that *PHB* is likely expressed in the paraclade junction in wild-type plants.

To determine the impact of *PHB* on *LOF1* transcript levels, the same paraclade junction cDNA from WT, *lof1-1*, *phb-13*, and *lof1-1 phb-13* as used previously was further examined by RT-PCR (Figure 3.11 B). Transcript levels of *LOF1* appeared higher in WT and *phb-13* compared to *lof1-1* and *lof1-1 phb-13* (Figure 3.11 C). *lof1-1* and *lof1-1 phb-13* did not have detectable levels of transcript accumulation (Figure 3.11 C), which is consistent with previously published results (Lee *et al.*, 2009). This suggests that lower transcript levels of *PHB* in *phb-13* in the paraclade junction does not alter transcript levels of *LOF1*. Thus, any regulation that occurs between *PHB* and *LOF1* likely does not occur at the transcriptional level.

PHB Locus Number Does Not Impact the *lfs-1D* Phenotype

Because the *pPHB:PHB* transgene was segregating in the T2 generation, the T2 *pPHB:PHB* plants in the Col-0 and *lof1-1* genetic backgrounds examined thus far contained copies of the *PHB* transgene as well as two functional copies of the endogenous *PHB* gene. T1 plants were assessed for the number of *PHB* transgene loci but not for *PHB* transgene copy number. The low efficiency of the *pPHB:PHB* and *pPHB:mPHB* transformations made it unlikely that multiple copies of the transgene at one locus would result from the transformation or that there would be multiple loci. Thus, T2 *pPHB:PHB* transgenic plants contained three or more copies of *PHB* in at least two different loci, while the *lfs-1D lof1-1* plants were homozygous for the *phb382** allele and

did not contain a wild-type *PHB* gene. Plants with the *pPHB:mPHB* or *pPHB:PHB* transgene in the *phb-13* and *lof1-1 phb-13* genetic backgrounds were therefore more genetically similar to the *lfs-1D lof1-1* plants.

To determine if *PHB* loci number plays a role in the observed phenotypes, *pPHB:PHB* was assessed in *phb-13* and *lof1-1 phb-13* mutant backgrounds and observed in the T1 generation. However, both *pPHB:mPHB* and *pPHB:PHB* in *phb-13* and *lof1-1 phb-13* mutant backgrounds led to all of the phenotypes observed in the Col-0 and *lof1-1* mutant genetic backgrounds (Table 3.5; 3.6). This suggests that the *lfs-1D* phenotypes in *pPHB:PHB* and *pPHB:mPHB* plants in the Col-0 and *lof1-1* genetic backgrounds are not due to *PHB* locus number variation.

pPHB:PHB **and** ***pPHB:mPHB*** **Plants Have Developmental Defects in Addition to Accessory Bud Defects**

pPHB:PHB or *pPHB:mPHB* plants also displayed a variety of other developmental defects in addition to the accessory bud phenotypes that were not observed in *lfs-1D lof1-1* or *lfs-1D*. *pPHB:PHB* and *pPHB:mPHB* plants occasionally produced radial leaves (Figure 3.13 A-H; 3.14). This phenotype affected both rosette (Figure 3.13 A-H) and cauline leaves (Figure 3.14) of mature plants. Radial rosette leaves were difficult to quantify as their small size often lead to them being hidden under other, larger rosette leaves. Additionally, leaves were produced that appeared to result from fusion of two or more rosette leaves at a low frequency (Figure 3.13 I-O). It is possible that these fused leaves are actually outgrowths of adaxial tissue, as is thought to be the

case in some *kanadi* double mutants (Bowman, 2000; Bowman *et al.*, 2002) and in *rev-10d* (Emery *et al.*, 2003). However, they will continue to be called "fused leaves" in this text for purposes of simplicity. The frequency at which both radial and fused leaves were produced could not be predicted in mature plants, and their appearance did not appear to be associated with a specific leaf number. The appearance of radial of fused leaves was persistent throughout development (Table 3.5; 3.6; 3.7).

Through our observations, it appeared that the first two true leaves were more likely to be impacted by the presence of the *pPHB:PHB* or *pPHB:mPHB* transgenes in seedlings. Therefore, leaf defects in the first pair of true leaves were quantified in 10-day-old T2 seedlings in *pPHB:PHB* Col-0 and *pPHB:PHB lof1-1* grown on plates.

pPHB:PHB seedlings in the Col-0 or *lof1-1* genetic backgrounds displayed a variety true leaf defects and other phenotypes (Table 3.7). True leaves were found to be fused in a "cup-like" shape (Figure 3.15 B and C) or in the "back-to-back" shape (Figure 3.15 D and E) at a low rate. The "back-to-back" shaped, or mirror-image, leaves appeared similar to the fused leaves observed in mature plants. Leaves displayed varying degrees of radialization that were apparent on one or both first true leaves (Figure 3.15 F-I). The distal end of the leaf blade was more likely to be radialized compared to the proximal end of the leaf blade. Sometimes, seedlings produced only a single true leaf (Figure 3.15 J), and seedlings additionally had cotyledon and overall plant defects. Cotyledons were sometimes fused (Figure 3.16 A and B), or there were three cotyledons (Figure 3.16 F). Some seedlings were also much smaller than average (Figure 3.16 C), which is a phenotype that persisted until plants were mature (data not shown). Finally, some

seedlings exhibited meristem termination, either in a pin-shaped structure (Figure 3.16 D) or with no observable pin-shaped structure (Figure 3.16 E). Seedlings with meristem termination (either in a pin or with no pin) were occasionally able to recover and survive until maturity but often had poor fertility (data not shown).

Overall, 0.8% of *lof1-1* control seedlings displayed these defects, while 42.9% of *pPHB:PHB* Col-0 and 63.3% of *pPHB:PHB lof1-1* plants seedlings had these defects. *pPHB:PHB lof1-1* seedlings were more likely to have meristem termination defects compared to *pPHB:PHB* Col-0 seedlings and also displayed more severe levels of leaf radialization (Table 3.7). Therefore, the *pPHB:PHB* seedling phenotypes are more severe in the *lof1-1* background than the Col-0 genetic background. The fused leaf phenotype appeared not only in the *pPHB:PHB lof1-1* seedlings (and adult plants) but also in *pPHB:PHB* Col-0 and fusions. Since organ fusions can indicate defects in the boundary (Aida *et al.*, 1997; Lee *et al.*, 2009; Bell *et al.*, 2012; Colling *et al.*, 2015), these data suggest that *PHB* may be involved in specification of the boundary or have role in the boundary region.

pPHB:PHB or *pPHB:mPHB* plants also displayed defects in phyllotaxy (Figure 3.17 A-C) and silique shape (Figure 3.17 D-F). The frequency of this phenotype could not be accurately determined as wild-type plants sometimes displayed defects in phyllotaxy due to the environmental conditions during some of the experiments.

pPHB:PHB or *pPHB:mPHB* plants also sometimes showed meristem fasciation that was visible by eye (Figure 3.18). To confirm meristem fasciation and rule out stem fusion as the potential cause of this phenotype, flowers and floral buds around the

inflorescence meristem of mature plants containing *pPHB:PHB* in the Col-0 and *lof1-1* backgrounds were removed by dissection to observe meristem shape (data not shown). This validated that the meristem was enlarged and distorted, and the phenotype was not the result of organ fusions.

Decurrent strands are strands of leaf tissue that remain attached to a stem and are continuous with subtending leaves (Wardlaw, 1946). Decurrent strands are thought to occur because organs have not completely separated or have not separated properly, which could be due to boundary region defects (Lee *et al.*, 2009; Colling *et al.*, 2015). *pPHB:PHB* or *pPHB:mPHB* transgenic plants had decurrent strands on the first or second order paraclades between the stem and subtending leaf. These occurred in both cauline-leaf axil paraclades and rosette-leaf axil paraclades (Figure 3.19 A-C). The paraclade junctions of *pPHB:PHB* or *pPHB:mPHB* transgenic plants also sometimes contained more than one cauline leaf (Figure 3.19 D-F). The cauline leaves would either appear side by side (Figure 3.19 E) or with the second cauline leaf deflecting upwards at an angle (Figure 3.19 F). These were not simply cases where internode elongation was defective, as there were paraclade junctions where only one axillary branch and one accessory bud formed, and two cauline leaves were present (Figure 3.19 F).

The phenotypes in *pPHB:PHB* or *pPHB:mPHB* plants that were not related to the accessory bud were absent in the *lfs-1D lof1-1* plants and in *lfs-1D* following backcross to Col-0. Many of these phenotypes were present in both *pPHB:PHB* and *pPHB:mPHB* transgenic plants of the following genetic backgrounds – Col-0, *lof1-1*, *phb-13*, and *lof1-1 phb-13* (Table 3.1; 3.4; 3.5; 3.6). This indicates that the multitude of developmental

defects in *pPHB:PHB* and *pPHB:mPHB* plants were not associated with the number of *PHB* loci. Possible explanations will be discussed later.

pPHB:PHB lof1-1 and *pPHB:mPHB lof1-1 phb-13* Plants Have a Unique Phenotype in the Paraclade Junction

While observing the developmental defects of *pPHB:PHB* and *pPHB:mPHB* plants in different genetic backgrounds, we discovered a phenotype unique to genetic backgrounds containing *lof1-1*. Some transformants contained a decurrent strand connecting a first order paraclade junction to a second order paraclade junction (Figure 3.20). Often, the first paraclade junction contained a decurrent strand between the primary stem and cauline leaf. The decurrent strand connecting to the second order paraclade junction sometimes ripped due to tension (Figure 3.20 D). These phenotypes were never observed in either *pPHB:PHB* or *pPHB:mPHB* plants in the Col-0 or *phb-13* single mutant backgrounds in either the T1 or T2 generations (Table 3.1; 3.4; 3.5; 3.6; 3.7). The decurrent strand is likely due to some type of organ fusion. However, it is unclear why this phenotype forms only in the *lof1-1* and *lof1-1 phb-13* genetic backgrounds.

pPHB:mPHB Plants Have Higher Frequency of Severe Phenotypes Compared to *pPHB:PHB* Plants

To compare plants with the *pPHB:PHB* transgene to those with the *pPHB:mPHB* transgene in all tested genetic backgrounds (Col-0, *lof1-1*, *phb-13*, and *lof1-1 phb-13*), we

looked for clear differences in our data sets (Table 3.1; 3.4; 3.5; 3.6). Specific unique phenotypes were not present in either *pPHB:PHB* or *pPHB:mPHB*. We therefore examined phenotype frequency. Plants containing the *pPHB:mPHB* version of the transgene had higher frequencies of plants with the radial rosette, radial cauline, and small size phenotypes (Table 3.1; 3.4; 3.5; 3.6). Plants with the *pPHB:mPHB* transgene were more likely to contain a fused leaf than *pPHB:PHB* plants. Therefore, *pPHB:mPHB* plants have severe phenotypes at higher frequency than *pPHB:PHB* plants.

LOF1 Overexpression Phenotypes

To evaluate the effects of *LOF1* overexpression in plants with reduced *PHB* transcript levels, *35S:LOF1* was examined the Col-0, *lof1-1*, *phb-13*, and *lof1-1 phb-13* backgrounds. As previous reported, upward curling leaves were present in some of the plants over-expressing *LOF1* in the Col-0 background, and flowering was early [(Lee *et al.*, 2009; Gomez *et al.*, 2011); Figure 3.21]. It is not clear why the upward leaf curling only occurred in the Col-0 background and not in the *lof1-1*, *phb-13*, and *lof1-1 phb-13* backgrounds (Table 3.8). It is also noteworthy that six out of seven of the *35S:LOF1* Col-0 primary transformants that had upward-curling leaves had no accessory buds (Table 3.8). This could be a result of poor *35S* promoter expression in meristems (Benfey and Chua, 1990; Kosugi *et al.*, 1991; Sunilkumar *et al.*, 2002) or transgene silencing. Only first generation transformants (T1) were examined, due to silencing of the *35S:LOF1* transgene in subsequent generations. Although attempted many times, a second generation *35S:LOF1* line that expressed *35S:LOF1* could not be obtained.

In *35S:LOF1*, 21.6% of *lof1-1* and 35% of *lof1-1 phb-13* plants had one centrally located accessory bud (Table 3.8), suggesting that *LOF1* was not silenced in these plants. This also confirms that *35S:LOF1* transgene complements the *lof1-1* mutant phenotype in the *lof1-1 phb-13* background, which was previously documented (Lee *et al.*, 2009). The *35S:LOF1* transgene in Col-0, *lof1-1*, *phb-13*, and *lof1-1 phb-13* backgrounds did not appear to lead to formation of multiple accessory buds (Table 3.8). The accessory bud phenotypes of *35S:LOF1* plants appear similar to the genetic background in which they were transformed (Table 3.8; 3.9). The *35S:LOF1* transgene may not cause multiple accessory buds because the transgene is not expressed strongly in the meristem (as mentioned previously) or because additionally factors are necessary.

Interestingly, *35S:LOF1* plants with upward curling leaves also had floral defects (Figure 3.22). When flowers from *35S:LOF1* plants were dissected under a stereo microscope, it was evident that both sepals and petals were reduced compared to wild-type control plants (Figure 3.22). Although plants with these floral defects were sterile, stamen and carpels appeared developmentally normal and developmental timing seemed unperturbed. The cause of infertility could not be determined through dissection of the carpels or stamens. However, *LOF1* overexpression was previously reported to cause ectopic ovule-like structures on sepals and wrinkled fruits (Gomez *et al.*, 2011). However, we did not observe these structures during this study.

A Specific Floral Phenotype in *lof1-1* Single Mutants and *phb-13 lof1-1* Double Mutants

To observe flowers in the context of *lof1* loss-of-function, flowers six to ten on the primary inflorescence were dissected and analyzed in *lof1-1*, *phb-13*, *lof1-1 phb-13* and WT plants. Sepal fusion was present in ~8-11% of all genotypes tested, suggesting a background effect (Table 3.10). We also observed *phb-13* and *lof1-1 phb-13* mutants were prone to developing one or more extra stamen per flower (Table 3.10).

A stamen-petal structure that represents a petaloid anther, stamenoid petal, or fusion between stamen and petal was observed in *lof1-1* and *lof1-1 phb-13* mutants at a rate of 2.9% and 6.3%, respectively (Figure 3.23; Table 3.10). This structure was never observed in Col-0 wild-type controls or *phb-13* single mutants (Table 3.10). This means that the rate of occurrence of this structure was enhanced in *lof1-1 phb-13* double mutants. Due to the low frequency of these phenotypes, it could not be determined if this stamen-petal structure is a fusion between a stamen and petal, a stamenoid petal, or a petaloid stamen.

phb-13 phv-11 cna-2 er-2 Mutants Have Multiple Floral Defects

Because HD-Zip III transcription factors have primarily been studied in the *er-2* single mutant background (Prigge *et al.*, 2005; Kelley *et al.*, 2009; Lee and Clark, 2015; Yamada *et al.*, 2016), we decided to look for floral phenotypes in *er-2* and *phb-13 er-2* mutants. Because *PHV* is the *HD-Zip III* with the closest phylogenetic relationship to *PHB* (McConnell and Barton, 1998; McConnell *et al.*, 2001; Prigge *et al.*, 2005)**,** *phv-11*

er-2 mutants were also included. Additionally, abnormal floral phenotypes have not been reported among *phb-13 er-2* and *phv-11 er-2* mutants as it has been assumed that *phb* and *phv* single mutants will not have any abnormal phenotypes (Emery *et al.*, 2003; Mallory *et al.*, 2004; Prigge *et al.*, 2005). Flowers were analyzed for floral organ fusions, floral organ shape, and undeveloped floral organs in addition to floral organ number.

The percentage of wild-type appearing flowers in *er-2*, *phb-13 er-2*, and *phv-11 er-2* was 82.2%, 84.4%, and 88%, respectively (Table 3.11). Thus, the phenotypes of *phb-13 er-2* and *phv-11 er-2* flowers did not seem different from the control *er-2* single mutant. The proportion of plants with defects in stamen number among *er-2*, *phb-13 er-2*, and *phv-11 er-2* was 12.8%, 11.7%, and 9.1% (Table 3.11), respectively. These phenotypes could be specific to the *er-2* genetic background or be environmental.

As previously discussed, *HD-Zip III* genes are thought to be redundant in some functions (Prigge *et al.*, 2005)**.** In order to examine floral phenotype in plants that had lost function of more than one *HD-Zip III* gene, a triple *HD-Zip III* loss-of-function mutant was examined in the *er-2* background - *phb-13 phv-11 cna-2 er-2.* This specific mutant was chosen because defects in floral organ number and in ovules have already been documented in *phb-13 phv-11 cna-2 er-2* (Kelley *et al.*, 2009; Lee and Clark, 2015; Yamada *et al.*, 2016). *phb-13 phv-11 cna-2 er-2* mutants were examined for phenotypes in the same way as *er-2*, *phb-13 er-2*, and *phv-11 er-2* mutants. Defects in floral organ number will not discussed, and carpels were not dissected to view ovules as these phenotypes have been previously reported (Kelley *et al.*, 2009; Lee and Clark, 2015; Yamada *et al.*, 2016).

The percentage of flowers that appeared phenotypically wild-type in *phb-13 phv-11 cna-2 er-2* was only 19.4% (Table 3.11), indicating *that phb-13 phv-11 cna-2 er-2* flowers are different from *er-2*, *phb-13 er-2*, and *phv-11 er-2* mutant flowers. Sepal defects were observed in *phb-13 phv-11 cna-2 er-2;* 18.3% of these flowers contained a sepal fusion (Figure 3.24 G), while only 2.8% of *er-2* single mutant contained sepal fusions with the majority of *er-2*, *phb-13 er-2*, and *phv-11 er-2* flowers having well separated sepals (Figure 3.24 F; Table 3.11). Of the 180 *phb-13 phv-11 cna-2 er-2* flowers examined, 6.7% of flowers contained at least one trumpet-shaped petal (Figure 3.24 B) and/or radial petal (Figure 3.24 E). Additionally, "forked" and "lobed" petals (Figure 3.24 C and D) were seen in 12.2% of *phb-13 phv-11 cna-2 er-2* flowers. It is unclear if these occur due to fusions between two petals or the central distal part of one petal failing to develop. It is possible that both these scenarios occur simultaneously. Petal defects of any kind were only observed in 0 to 1.1% of *er-2*, *phb-13*, and *phv-11 er-2* genotypes (Table 3.11). *phb-13 phv-11 cna-2 er-2* flowers also contained a structure that could be a petaloid anther, stamenoid petal, or fusion between stamen and petal (3.9%). This was quite similar to the structure seen in *lof1-1* single and *lof1-1 phb-13* double mutants (Figure 3.23 A and B) and was not seen at all in *er-2*, *phb-13 er-2*, and *phv-11 er-2* genotypes (Table 3.11).

Stamen fusions (stamen to another stamen) were seen in 12.8% of flowers of *phb-13 phv-11 cna-2 er-2* (Figure 3.24 I), while these were present in 0.6% or less in flowers of other tested genotypes (Table 3.11). Undeveloped stamens were seen in 30.6% of *phb-13 phv-11 cna-2 er-2* flowers. Either the anther was undeveloped, the filament was

undeveloped (Figure 3.24 J), or the entire stamen was undeveloped (3.24 K). Stamen developmental abnormalities of any type occurred in 1.1% or less of flowers of other tested genotypes (Table 3.11). In conclusion, *phb-13 phv-11 cna-2 er-2* flowers contain floral organ fusions, floral organ polarity defects, and floral organ developmental abnormalities that were rarely observed in *er-2*, *phb-13 er-2*, and *phv-11 er-2* flowers. The organ fusion phenotypes suggest *HD-Zip III* genes could be involved in separation of floral organs and implicate *HD-Zip III* genes as having a role in the boundary.

pPHB:PHB Col-0 and *pPHB:PHB lof1-1* Plants Have Defects in Petal Polarity Among Other Floral Defects

To determine the impact of *pPHB:PHB* on floral development, flowers six to ten on the primary inflorescence were dissected and phenotypes examined. Two *pPHB:PHB* lines were examined in the Col-0 wild-type and *lof1-1* genetic background together with controls. Two *pPHB:PHB* transgenic lines of differing severity were selected; line #1 was more severe than line #2 in terms of mature plant phenotypes and higher levels of *pPHB:PHB* transgene expression.

The most prominent floral phenotype in *pPHB:PHB* Col-0 and *pPHB:PHB lof1-1* flowers were trumpet-shaped and radial petals (Figure 3.25 C and D; Table 3.12). Occasionally, forked or fused petals were observed in *pPHB:PHB* Col-0 (Figure 3.25 E; Table 3.12). Petal number per flower was additionally affected in *pPHB:PHB* Col-0 and *pPHB:PHB lof1-1* (Figure 3.25 H; Table 3.8). Defects both in petal polarity and number were not observed in Col-0 or *lof1-1* single mutant flowers (Table 3.12). Therefore,

pPHB:PHB Col-0 and *pPHB:PHB lof1-1* flowers have defects in petal number and polarity.

pPHB:PHB Col-0 and *pPHB:PHB lof1-1* flowers exhibited stamen abnormalities as well. Stamen fusion (Figure 3.25 J) occurred in 2.2% and 2.8% of *pPHB:PHB* Col-0 flowers and 5.6% and 1.1% of *pPHB:PHB lof1-1* flowers. Stamen fusion was not observed in the 180 Col-0 flowers and was present in 0.6% of *lof1-1* flowers. Undeveloped stamens (Figure 3.25 I) and changes in stamen number were more common in *pPHB:PHB* Col-0 and *pPHB:PHB lof1-1* than control plants (Table 3.12). Thus, Col-0 or *lof1-1* expressing *pPHB:PHB* were more likely to have floral defects in stamen number, fusion, or to have undeveloped stamen compared to control flowers.

Defects in carpel number (not shown) and carpel shape in *pPHB:PHB* Col-0 and *pPHB:PHB lof1-1* occurred in a low percentage of flowers (Figure 3.25 G; Table 3.12) and displaced ovules were also observed. In the flowers of one *pPHB:PHB lof1-1* plant, ovules were located in the center of the stigma (Figure 3.25 F). No carpel phenotypes were observed in any Col-0 or *lof1-1* single mutant controls flowers. The reason for the carpel shape defect was not investigated, as very few flowers displayed these defects (0.6-1.7%). In summary, *pPHB:PHB* flowers in the Col-0 and *lof1-1* mutant backgrounds had altered floral organ numbers, petal polarity defects, carpel shape, undeveloped stamens, and floral organ fusions when compared to Col-0 and *lof1-1* control flowers. These are similar to floral phenotypes observed in *phb-13 phv-11 cna-2 er-2* mutants.

LOF1 Functions in Paraclade Junction Formation and *PHB* Represses Accessory Bud Formation

To examine genetic interaction between *LOF1* and *PHB*, WT, *lof1-1*, *phb-13*, and *lof1-1 phb-13* were analyzed for plant architecture traits. The number and position of branches and secondary branches, accessory buds, and cauline leaves were recorded. The number of cauline-leaf axil branches and cauline-leaf paraclade junctions per plant are both included in this analysis because occasionally cauline-leaf axil branches failed to grow out. Therefore, the average number of cauline-leaf axil branches is not always equivalent to the average number of paraclade junctions.

The *lof1-1* and *lof1-1 phb-13* plants did not form accessory buds in paraclade junctions (Figure 3.3; Table 3.9). WT plants produced zero or one accessory bud per paraclade junction (Figure 3.3; Table 3.9). The majority of *phb-13* plants formed paraclade junctions with zero to one accessory buds, and 11.1% produced multiple accessory buds per paraclade junction (Figure 3.3; 3.26 B; Table 3.9). *phb-13* had a higher average number of accessory buds per plant than WT controls (Figure 3.26 A). *phb-13* plants also formed fewer rosette-leaf axil branches per plant on average (Figure 3.27 A). This implies that *PHB* functions to repress accessory buds and may promote formation of rosette-leaf branches.

lof1-1 plants formed fewer cauline-leaf branches and paraclade junctions per plant compared to WT controls, which had not been reported previously. Surprisingly, *lof1-1 phb-13* plants did not significantly differ in number of cauline-leaf axil branches per plant from the WT control (Figure 3.27 B and C). *lof1-1* single mutants also had significantly

fewer secondary cauline-leaf branches, consistent with the fact that *lof1-1* produced fewer cauline-leaf branches overall (Figure 3.27 A, B, and D). This indicates that *LOF1* may be involved in paraclade junction formation. The *lof1-1 phb-13* double mutant did not have fewer paraclade junctions than WT controls like *lof1-1* even though *lof1-1 phb-13* phenotypically resembles *lof1-1* (Figure 3.3; 3.12; 3.27 B). This indicates *PHB* may also have a role in regulation of paraclade junction formation. This suggests *PHB* and *LOF1* function together to control both accessory bud and paraclade junction formation.

PHB **Functions to Repress Accessory Bud Formation with a Subset of** ***HD-Zip III*** **Genes**

To investigate the contribution of other *HD-Zip III* genes on plant architecture, we examined plant architecture traits of *er-2*, *phb-13 er-2*, *phv-11 er-2*, and *phb-13 phv-11 cna-2 er-2* mutants. *phb-13 phv-11 cna-2 er-2* was chosen because *CNA* and *ATHB8* are in a different phylogenetic clade within the *HD-Zip III* genes (Byrne, 2006), and phenotypes have been reported for the quadruple mutant: *phb-13 phv-11 cna-2 er-2* (Prigge *et al.*, 2005; Lee and Clark, 2015). *rev* mutants were not included, as abnormal branching phenotypes have already been reported (Talbert *et al.*, 1995; Otsuga *et al.*, 2001). Additionally, *ATHB8* is primarily expressed in the root (Baima *et al.,* 2001), and we examined shoot architecture traits. *LOF1* is not thought to be expressed in the root (Lee *et al.,* 2009).

er-2 and *phv-11 er-2* plants had zero to one accessory bud per paraclade junction with averages of 0.12 and 0.11, respectively. *phb-13 er-2* plants had zero to two

accessory buds per paraclade junction with an average of 0.34. *phb-13 phv-11 cna-2 er-2* plants had zero to three accessory buds per paraclade junction with an average of 1.89 (Figure 3.28). Additionally, all *phb-13 phv-11 cna-2 er-2* plants had at least one paraclade junction with multiple accessory buds (Figure 3.28; 3.29 B; Table 3.13). *phb-13 phv-11 cna -2 er-2* plants had more accessory buds per plant on average than the other genotypes examined (Figure 3.29 A). *phb-13 er-2* also had more accessory buds per plant than the *er-2* and *phv-11 er-2* genotypes (Figure 3.29 A). Thus, *PHB* functions in accessory bud repression with other *HD-Zip III* genes, as *phb-13 phv-11 cna-2 er-2* had more accessory buds per plant than *phb-13 er-2*. Since there was no difference in accessory bud number between *phv-11 er-2* and *er-2*, *PHV* may not function in accessory bud repression. Alternatively, *PHV* may only function in accessory bud repression in the event of loss-of-function of *PHB* or another *HD-Zip III* gene. *PHB* must function with either *PHV* or *CNA,* or *PHV* and *CNA* in accessory bud repression due to *phb-13 phv-11 cna-2 er-2* phenotype.

phb-13 phv-11 cna-2 er-2 plants also had differences in other aspects of plant architecture. *phb-13 phv-11 cna-2 er-2* plants had fewer rosette-leaf branches per plant (Figure 3.30 A), but more cauline-leaf branches and paraclade junctions per plant (Figure 3.30 B and C). *phb-13 phv-11 cna-2 er-2* plants had fewer branches from second order rosette-leaf paraclades than other tested genotypes, but this is likely due to increase in rosette-leaf axil branch number (Figure 3.30 A and D). This may reflect a change in overall plant architecture of *phb-13 phv-11 cna-2 er-2* plants, such that there are more

cauline-leaf axil paraclades and branches but fewer rosette-leaf axil paraclades and branches.

Because 100% of *phb-13 phv-11 cna-2 er-2* plants displayed meristem fasciation and contained at least one paraclade junction with multiple accessory buds (Table 3.13), this indicates that loss-of-function of *HD-Zip III*s leads to increased meristem size. While the meristem fasciation in *phb-13 phv-11 cna-2 er-2* inflorescence meristems was being assessed (Figure 3.31 J and L), it was observed that the meristem in *phb-13 phv-11 cna-2 er-2* terminated in a fused carpel-like structure (Figure 3.31 M). The fused carpel-like structure (Figure 3.31 K) was similar to the ring-like structure described for *cna clv* double mutants (Green *et al.*, 2005). Because *cna* single mutants were reported to have changes in meristem size at different points in development (Green *et al.*, 2005), we examined *cna-1* (L*er*) and *cna-2 er-2* for developmental defects in meristem termination. Meristem fasciation, the fused carpel-like structure, or the ring-like meristem structure were not observed in *cna-1* (L*er*), *cna-2 er-2*, or *er-2* control meristems (Figure 3.31). Additionally, accessory meristems of *cna-1* (L*er*) and *cna-2 er-2* were not visually different from *er-2*, *phb-13 er-2*, and *phv-11 er-2* (Figure 3.32). When *cna-1* (L*er*) and *cna-2 er-2* were examined for accessory bud phenotypes, *cna-1* (L*er*) plants did not produce any paraclade junctions with multiple accessory buds. However, one *cna-2 er-2* plant produced a paraclade junction with two accessory buds (Table 3.14). Both *cna-2 er-2* and *cna-1* (L*er*) produced more accessory buds than the *er-2* single mutant (data not shown), indicating that *CNA* could have a role in repression of accessory bud formation.

The significantly higher average number of accessory buds per plant in *phb-13* and *phb-13 er-2* compared to Col-0 and *er-2* highlights that *phb-13* mutants consistently produce more accessory buds. Therefore, *PHB* likely functions to repress accessory bud formation, while *PHV* may not. Because *phv* mutants have not be described in a wild-type *ER* background, *phv-11 er-2* was crossed to Col-0, and plants were analyzed in the F3 generation. *phv-11* (*ER*) single mutants did not appear to differ from WT control plants. *phv-11* single mutants and WT plants both produced paraclade junctions with zero or one accessory bud and rarely produced paraclade junctions with multiple accessory buds (Table 3.15). There were multiple cauline leaves observed in the *ER* background (Table 3.15). None of the *phv-11* plants had meristem fasciation and accessory buds appeared similar to WT (Table 3.15; Figure 3.31 C, D, G, and H; Figure 3.32 G and H). These results indicate that *phv-11* and *phv-11 er-2* are both similar in phenotype to Col-0 and *er-2*, respectively.

lof1-1 er-2 Has a Phenotype Similar to the *lof1-1* Single Mutant

Because the *lof1-1* mutant has not been studied in the *er-2* background, backcrosses were performed to introduce *lof1-1* into the *er-2* background. F4 populations from the cross were analyzed. Nearly all plants produced paraclade junctions without accessory buds; therefore, *lof1-1 er-2* phenotype is not different from *lof1-1* (Table 3.16). *lof1-1 er-2* also had fusions between the axillary branches and cauline leaves like *lof1-1* (*ER*). Therefore, the *lof1-1* mutant can be validly studied in the Col-0 or *er-2*

backgrounds, and *ER* does not contribute to the *LOF1* pathway for accessory bud formation or organ separation.

Accessory Bud Phenotypes in *pPHB:PHB* Plants

To examine the impact of *pPHB:PHB* on plant architecture, Col-0 and *lof1-1* plants expressing *pPHB:PHB* were evaluated at maturity for plant architecture characteristics. In Col-0 and *lof1-1* backgrounds, the first *pPHB:PHB* lines had more severe phenotypes than the second *pPHB:PHB* lines. Consistent with previous results that *LOF1* is involved in paraclade junction formation (Figure 3.27 C), *lof1-1* single mutants plants had significantly fewer first order paraclade junctions and cauline-leaf paraclade branches per plant than Col-0 (Figure 3.4; 3.33 A; 3.34 A). This defect was rescued by the addition of the *pPHB:PHB* transgene, as the average number of paraclade junctions per plant was the same in *pPHB:PHB* Col-0 and *pPHB:PHB lof1-1* lines (Figure 3.4; 3.33 A). Therefore, the *pPHB:PHB* transgene can suppress the reduced number of paraclade junctions in the *lof1-1* mutant.

Col-0 contained paraclade junctions with zero and one accessory buds and occasionally produced a paraclade junction with multiple accessory buds (Table 3.1; 3.4; 3.33 C). *pPHB:PHB* Col-0 #2 appeared the same as Col-0 in terms of average number of accessory buds per plant, but *pPHB:PHB* Col-0 #1 had more accessory buds per plant (Figure 3.33 B). Both *pPHB:PHB* lines in the *lof1-1* background had an increase in accessory buds per plant compared to the *lof1-1* single mutant alone (Figure 3.33 B). Thus, plants with the *pPHB:PHB* transgene have higher number of accessory buds per

plant than Col-0 and are more likely to have first order paraclade junctions that contain multiple accessory buds.

pPHB:PHB transgenic plants in the Col-0 and *lof1-1* genetic backgrounds also have the potential to form more paraclade junctions on the primary inflorescence than Col-0 or *lof1-1* plants. Col-0 formed a maximum of four paraclade junctions; *lof1-1* mutants produced a maximum of three. *pPHB:PHB* Col-0 produced up to six, and *pPHB:PHB lof1-1* produced up to seven paraclade junctions per plant (Figure 3.4). This indicates that the *pPHB:PHB* transgene allows for the potential to form more first order paraclade junctions. In summation, plants that contain the *pPHB:PHB* transgene form more accessory buds per plant, have more occurrences of multiple accessory buds per paraclade junction, and have the potential to form more first order paraclade junctions in the Col-0 and *lof1-1* backgrounds than control plants.

GFP-PHB is Not Mislocalized in the Root Meristematic Zone in *pPHB:GFP-PHB* Col-0 or *pPHB:GFP-PHB lof1-1* Plants

35S:PHB plants were previously reported to have a wild-type phenotype (McConnell *et al.*, 2001). Therefore, *pPHB:PHB* was not expected to cause abnormal phenotypes. It is possible that PHB mislocalization could cause the developmental defects we observed in *pPHB:PHB* plants, although this transgene was constructed using the previously described *PHB* promoter sequence, which was shown to be sufficient for PHB function (Carlsbecker *et al.*, 2010; Dello Ioio *et al.*, 2012). We examined PHB localization utilizing the N-terminal GFP tag on the PHB protein in the root meristem of

pPHB:PHB expressing Col-0 plants. Previous reports indicate GFP-PHB should localize above the quiescent center in the developing stele cell nuclei with the GFP-PHB signal diminishing as cells enter the elongation zone (Carlsbecker *et al.*, 2010; Dello Ioio *et al.*, 2012). We observed this same pattern of GFP-PHB localization in *pPHB:PHB* Col-0 roots (Figure 3.35). Additionally, GFP-PHB localization was the same in the *lof1-1* single mutant (Figure 3.35). GFP-PHB localization was not examined in the shoot. Therefore, these data indicate that our GFP-PHB reporter is not mislocalized in the root meristem of Col-0 or *lof1-1*. Thus, PHB mislocalization cannot explain the phenotypes we observe in *pPHB:PHB* expressing plants.

Discussion

Accessory Bud Formation is Environmentally Sensitive

Based on the observation that the majority of paraclade junctions in Col-0 and *er-2* single mutants do not form accessory buds (Figure 3.3, 3.4; 3.28), it can be hypothesized that the pathway for forming accessory buds is typically in the "off" position. This pathway may become active due to environmental conditions, such as changes in humidity or light intensity. This response may have evolved such that the cost of producing more accessory buds and thus, branches, is balanced by the improvement in fitness that extra branches provide in certain contexts. Although there are some reports showing one accessory bud formed per paraclade junction in wild-type plants (Raman *et al.*, 2008; Yang *et al.*, 2012; Wang *et al.*, 2014; Shi *et al.*, 2016), other groups found that most paraclade junctions formed no accessory buds (Stirnberg *et al.*, 2002). Overall, the

number of paraclade junctions and accessory buds formed differs greatly, and their formation appears to be highly environmentally sensitive.

A Mutation in PHB Suppresses the lof1-1 Mutant Phenotype

LOF1 is a MYB transcription factor that functions in organ separation and meristem maintenance. *LOF1* is specifically expressed in boundary regions, or areas where organs meet. *lof1-1* mutants have fusion in the paraclade junction between the axillary branch and cauline leaf and fail to produce accessory buds (Lee *et al.*, 2009). In order to find out more about *LOF1* function, we undertook a mutant screen to identify a genetic suppressor of *lof1-1*. The *lof1 suppressor* (*lfs-1D*) mutation identified was genetically dominant and caused formation of multiple accessory buds per paraclade junction and accessory buds that were offset from the center. Also, accessory buds grew out without damage to the axillary branch (Figure 3.2). *lfs-1D* was mapped to the bottom of chromosome 2 (Table 3.2).

Because *PHB* was located within the mapping interval and already had a published dominant mutant (*phb-1D*) that displayed multiple buds above the true leaves (McConnell and Barton, 1998), we explored *PHB* as a candidate suppressor of *lof1-1*. this option. *lfs-1D lof1-1* plants had a single base pair substitution that created a translational stop codon after amino acid 381 within the *PHB* coding sequence (Figure 3.6). To determine if this was the *lfs-1D* causal mutation, a version of *PHB* that contained this mutation driven by the native *PHB* promoter (*pPHB:mPHB*) was introduced into Col-0 and *lof1-1*. The wild-type version of *PHB* (*pPHB:PHB*) was also transformed into the same genotypes. Surprisingly, both the *pPHB:mPHB* and *pPHB:PHB* transgenes were

genetically dominant and caused *lfs-1D*-like accessory bud phenotypes (Figure 3.7; 3.8). Both transgenes also caused numerous other developmental defects, including occasional radial leaves, meristem fasciation, small plants, and others (Figures 3.13 – 3.19). These other developmental defects were not present in *lfs-1D* or *lfs-1D lof1-1* plants.

lfs-1D lof1-1 Plant May Contain a Second Mutation

When mapping the *lfs-1D* mutation, its' location could not be resolved and it appeared to map to two locations on chromosome 2 – one between CIW3 and NGA361 and one between NGA361 and F18O19 (Table 3.2). *PHB* is located between NGA361 and F18O19, thus it is possible that a mutation located in another gene between CIW3 and NGA361 may partially suppress *mPHB*, resulting in a less severe phenotypes. This modifier can explain how the radial leaves, meristem fasciation, and other severe defects observed in *mPHB* plants are rarely present in the *lfs-1D lof1-1* plants. In our EMS mutant population, *mPHB* plants without a modifying mutation between CIW3 and NGA361 may have been selected out of the population because these defects may have been interpreted as arising from additional unrelated mutations caused by the mutagenesis. At approximately 7.1 Mbp in size (Table 3.2), the mapping region was too large for a complete search of other potential candidate genes.

PHB Involvement in the Boundary Region

Organ fusion phenotypes are often seen when the boundary region fails to form correctly or boundary identity is not maintained (Lee *et al.*, 2009; Bell *et al.*, 2012; Colling *et al.*, 2015). The fact that *pPHB:PHB* and *pPHB:mPHB* plants had leaf fusion phenotypes (Figure 3.13; 3.15; 3.16), floral organ fusion phenotypes (Figure 3.25), and

decurrent strands (Figure 3.19) reveals a potential novel role for *HD-Zip IIIs* in boundary formation or maintenance.

LOF1 Overexpression Does Not Cause Multiple Accessory Buds But Does Cause Leaf Polarity Defects

Because previously published work showed *LOF1* overexpressing plants had a phenotype of upward-curling leaves (Lee *et al.*, 2009; Gomez *et al.*, 2011), which could reflect an adaxial-abaxial leaf polarity defect, we re-examined the *35S:LOF1* phenotypes. The upward-curling leaf phenotype (Figure 3.21) occurred in the Col-0 background at a low rate (8% of T1s). This phenotype was not observed in *35S:LOF1* plants in the *lof1-1*, *phb-13*, and *lof1-1 phb-13* genetic backgrounds (Table 3.8). It is possible that endogenous copies of both *LOF1* and *PHB* are needed for the upward curling leaves phenotype. However, this is not consistent with the *LOF1* expression pattern, which is confined to the leaf base. The data are more consistent with LOF1 repressing PHB, and possibly other HD-Zip III transcription factors, in the leaf blade in *LOF1* overexpressing plants. The leaves curl upwards because HD-Zip IIIs, adaxial factors, are repressed. In this scenario, LOF1 in wild-type plants functions to repress PHB in the paraclade junction for accessory bud formation, and leaf polarity is not perturbed.

It was previously reported that overexpressing *LOF1* (*35S:LOF1*) rescues the *lof1-1* mutant accessory bud defect (Lee *et al.*, 2009)**.** Our results also found that multiple accessory buds per paraclade junction appear at a low frequency in many genetic backgrounds (Table 3.1; 3.9; 3.14; 3.16). Therefore, the accessory bud-specific phenotypes of the *T1 35S:LOF1* population in the *lof1-1* genetic background did not

seem out of the ordinary with 23.6% of plants having at least one paraclade junction with one accessory bud and 2% of plants having at least one paraclade junction with multiple accessory buds (Table 3.8). So why doesn't overexpression of *LOF1* lead to multiple accessory buds per paraclade junction more often? There are two primary explanations. First, additional factors may be necessary for accessory bud formation and second, the *35S* promoter does not promote expression well enough in the meristem to cause multiple accessory buds to form. It was previously reported that when *35S:GUS* was transformed into tobacco plants, GUS staining was not seen in the shoot meristem (Kosugi *et al.*, 1991). It was also reported that different *35S* enhancer *cis*-elements could sometimes lead to expression in the meristem, but it was more common for expression to be weak or not visible in the shoot meristem (Benfey and Chua, 1990). When the *35S* promoter was fused to *GFP* and transformed into cotton seedlings, GFP florescence in the shoot meristem could only be visualized when the meristem was dissected from surrounding tissue (Sunilkumar *et al.*, 2002). Together, these data imply that the *35S* promoter drives expression weakly in the shoot meristem. Repeating the *LOF1* overexpression experiments using meristem-specific promoters, such as *pSTM*, or boundary-specific promoters could reveal whether or not poor expression of *35S* in the meristem is the reason for these results.

LOF1 and HD-Zip III Genes Function in Floral Development

The floral defects observed in *35S:LOF1* (reduced sepals and petals and infertility; Figure 3.22) indicate a role for *LOF1* in some aspect of floral development. One study implicated *LOF1* in aspects of floral development (Gomez *et al.*, 2011). In

addition, floral defects were observed in a low percentage of *lof1-1* and *lof1-1 phb-13* plants (Figure 3.23; Table 3.10). The structure associated with these mutations could be a stamen and petal fused together, a petaloid stamen, or a stamenoid petal. Although the *lof1-1* mutant has undetectable levels of *LOF1* transcript in the paraclade junction, low levels were still detected in inflorescence apices, suggesting some *LOF1* function remains (Lee *et al.*, 2009). Because floral phenotypes occur at low frequencies, it was difficult to study. A null *lof1* mutant allele that abolishes *LOF1* expression in/near floral organs would be useful. An option for obtaining a *lof1* null allele would be use clustered regularly interspaced short palindromic repeats (CRISPR) technology to delete a section of the *LOF1* genomic area or create a mutation that results in a frameshift [reviewed in (Puchta, 2017)]. These kinds of mutations would likely lead to a null *lof1* allele with undetectable levels of *LOF1* transcript at the base of floral organs and in other areas of the plant besides only the paraclade junction.

When observing flowers from *phb-13 phv-11 cna-2 er-2* mutant and *pPHB:PHB* plants, we noticed that both genotypes exhibited fusions in floral organs and some organs remained undeveloped (Figure 3.24; 3.25). Another notable phenotype was that *phb-13 phv-11 cna-2 er-2* mutant and *pPHB:PHB* transgenic flowers sometimes produced petals with defects in adaxial-abaxial polarity (Table 3.11; 12; Figure 3.24; 3.25). Sepals and petals have a flattened shape, similar to leaves, which is not shared with other floral organs. Sepals were sometimes thinner (Figure 3.24 G) but were never completely radialized like petals (Figure 3.24 E). Why then was petal polarity impacted more than sepal polarity in these genotypes?

SEUSS (*SEU*) and *LEUNIG* (*LEU*), which encode two transcriptional regulators, were discovered to be required for expression of *PHB* in the petal in order to set up adaxial-abaxial polarity (Franks *et al.*, 2006). However, this does not completely explain the phenotype as *seu leu* double mutants had overall narrower floral organs (Franks *et al.*, 2006) and no completely radialized petals or sepals.

AINTEGUMENTA (*ANT*) encodes an AP2-like transcription factor that regulates organ growth and cell proliferation during development (Elliott *et al.*, 1996; Klucher *et al.*, 1996; Nole-Wilson *et al.*, 2005; Kim *et al.*, 2006*b*). The *ant-1* mutant in the Ws background has petals with adaxial-abaxial polarity defects, including those that are completely radialized, but sepals that still appear flat (Azhakanandam *et al.*, 2008). *seu ant* double mutants have reduced *PHB* transcript accumulation (Azhakanandam *et al.*, 2008), suggesting that *ANT* (along with *SEU* and *LEU*) upregulates *PHB*, which establishes adaxial-abaxial polarity in petals. *PHB* mRNA is found in the adaxial domain of both petals and sepals (Nole-Wilson and Krizek, 2006). This indicates *PHB* is involved in promoting adaxial-abaxial polarity in sepals and petals, but does not help explain why only petals are impacted by *pPHB:PHB* or *ant-1* (Ws). Overall, prior studies have focused on adaxial-abaxial polarity in petals rather than sepals.

Induction of *AINTEGUMENTA-LIKE6* (*AIL6*) overexpression led to a petal/stamen-like phenotype similar to that seen in *lof1-1* and *lof1-1 phb-13* mutants [(Han and Krizek, 2016); Figure 3.21]. *ANT* upregulates *PHB*, but it is currently unknown if *AIL6* can perform the same function; furthermore, it is unclear how or if this relates to the petal/stamen structure observed in *lof1-1* and *lof1-1 phb-13*. However, it

appears that alteration of genes involved in adaxial-abaxial polarity can lead to a similar phenotype.

LOF1 and PHB Function Together in Regulation of Accessory Bud and Paraclade Formation

lof1-1 mutants consistently produced fewer accessory buds than control plants and also had fewer average paraclade junctions per plant (Figure 3.26 A; 3.27 C; 3.33 A and B), suggesting *LOF1* plays a role in paraclade junction formation. *PHB* may be involved in repressing accessory bud formation as *phb-13* plants consistently produced higher average number of accessory buds per plant and more occurrences of multiple accessory buds per paraclade junction than control plants in both the Col-0 and *er-2* backgrounds (Figure 3.26; 3.29). This is correlated with the role of *PHB* in adaxial specification as accessory buds form only the adaxial side of the cauline leaf, near the base of the axillary branch, and do not form on the abaxial side of the leaf. The expression patterns of *PHB* and *LOF1* overlap and co-occur at the site of accessory bud formation (McConnell *et al.*, 2001; Lee *et al.*, 2009), providing further evidence that *PHB* and *LOF1* could function together in accessory bud formation.

If *PHB* functioned alone to repress accessory bud formation, then *lof1-1 phb-13* mutants should have accessory buds. However, we observed that *lof1-1 phb-13* double mutants phenotypically resemble *lof1-1* single mutants (Figure 3.12). This indicates that in the event of loss-of-function of both *LOF1* and *PHB*, other HD-Zip III proteins could be able to repress accessory bud formation.

When evaluating the F4 populations of WT, *lof1-1*, *phb-13*, and *lof1-1 phb-13*, we were surprised to find that the *phb-13* mutant may not be a null allele (Figure 3.11). *phb-13* was previously published as a null allele (Prigge *et al.*, 2005). However, it is possible that the primers we used in our experiments to test for the presence of *PHB* transcript could explain these differing results, as we did not use the same primer sequences as were previously published [Table 3.3; (Prigge *et al.*, 2005)].

A Subset of HD-Zip III's Function in Accessory Bud Repression

Our results additionally suggest that *CNA* and/or *PHV* are involved in repressing accessory bud formation since *phb-13 phv-11 cna-2 er-2* plants produced a higher average number of accessory buds per plant and occurrences of multiple accessory bud per paraclade junction than other genotypes (Figure 3.28; 3.29). We also determined that more *cna-2 er-2* plants had multiple accessory buds per paraclade junction than *er-2* controls (Table 3.14). Since *phv-11 er-2* produced zero to one accessory bud per paraclade junction and did not have more accessory buds than *er-2* (Figure 3.38; 3.29), it is possible that *PHV* does not function to repress accessory bud formation like *PHB* does. Alternatively, *PHV* may function in repression of accessory bud formation only when the function of *PHB* and/or *CNA* is lost. In order to test this, accessory bud formation in *phv-11 phb-13 er-2* would need to be compared to *phb-13 er-2* and *phv-11 er-2*. Comparing *phv-11 cna-2 er-2* and *phb-13 cna-2 er-2* would also give us more of a clear idea of the role of *CNA* in accessory bud formation.

REV upregulates *STM* in leaf axil meristematic cells for accessory bud formation (Shi *et al.*, 2016). Also, *rev* mutants are known to produce fewer paraclade junctions and

accessory buds (Talbert *et al.*, 1995; Otsuga *et al.*, 2001). The fact that *REV* may function to promote accessory bud formation and *PHB* appears to repress accessory bud formation is not surprising as *HD-Zip III*s have previously been shown to sometimes play antagonistic roles in development (Prigge *et al.*, 2005). Whether *REV* and *STM* are involved in the same or separate pathways as *LOF1* and *PHB* for accessory bud formation remains an unanswered question. It is important to note that the *lof1-1* mutant has previously been reported to lack *STM* promoter activity in the paraclade junction (Lee *et al.*, 2009), but this does not necessarily mean that *LOF1* regulates *STM*.

pPHB:PHB Impacts Plant Architecture

The *pPHB:PHB* transgene leads to alterations in plant architecture. *pPHB:PHB* plants produce fewer branches from second order cauline-leaf axils and more accessory buds than Col-0 and *lof1-1* controls (Figure 3.33 B; 3.34 C). *pPHB:PHB* plants are also more likely to have multiple accessory buds per paraclade junction and have the potential to develop more paraclade junctions per plant (Figure 3.4; 3.33 C). These data suggest that plant architecture is highly sensitive to *PHB* levels.

Regulation and Localization of mPHB mRNA and Protein

Since the *mPHB* mutation results in a truncated protein near the end of the START domain, after the *miRNA 165/166*-binding site, the *mPHB* mRNA should be post-transcriptionally regulated by *miRNA 165/166* in a similar way to the wild-type *PHB* mRNA. It is therefore unclear why *pPHB:mPHB* and *pPHB:PHB* constructs cause an abnormal phenotype. *35S:PHB* plants appear similar to control plants, putatively because *PHB* mRNA is post-transcriptionally regulated by *miRNA 165/166*. However, authors

reported one to two radialized leaves per plant (McConnell and Barton, 1998; McConnell *et al.*, 2001; Mallory *et al.*, 2004)**,** demonstrating that *35S:PHB* plants exhibit occasional leaf polarity phenotypes. However, this phenotype is less severe than observed in *phb-1D* mutants (McConnell *et al.*, 2001). The low frequency of radial leaves in *35S:PHB* plants may be due to incomplete regulation of *PHB* transcripts by the *miRNA 165/166* system. Careful examination of *35S:PHB* transgenic plants, specifically for phenotypes such as radial leaves, fused leaves, meristem fasciation, and multiple accessory buds per paraclade junction, is needed.

Expression of either *pPHB:PHB* or *pPHB:mPHB* caused *lfs-1D*-like accessory bud phenotypes, suggesting that plants could be sensitive to *PHB* transcript levels. Alternatively, the *PHB* promoter (*pPHB*) used here may be missing regulatory elements essential for correct expression level or pattern. We verified that our PHB reporters were not mislocalized in the root meristem (Figure 3.35). However, it is possible that a missing regulatory element in the promoter causes misexpression or overexpression only in the shoot without impacting root tissues. To rule out misexpression and/or mislocalization of PHB, GFP-PHB would need to be observed in shoot tissue (shoot meristem and developing organs), which is more technically challenging.

It is of substantial interest that the *mPHB* mutation causes a premature translational stop codon and results in a more severe phenotype than plants transformed with wild-type *PHB*. *mPHB* is predicted to form a truncated PHB protein with intact homeodomain and leucine zipper domains. In theory, this truncated protein could bind DNA and form homodimers with other PHB proteins and heterodimers with other HD-

Zip IIIs (and ZPRs) since the homeodomain and leucine zipper domains are predicted to be intact (Figure 3.6). HD-Zip III protein heterodimerization with ZPR proteins prevents the HD-Zip III protein from binding DNA (Wenkel *et al.*, 2007; Kim *et al.*, 2008). Since the mPHB protein can likely still dimerize with PHB, this may explain how mPHB could act as a dominant negative mutation.

The noticeable phenotypic similarity between *pPHB:PHB* plants and *phb-13 phv-11 cna-2 er-2* plants provides further evidence that *pPHB:mPHB* and *pPHB:PHB* act in a dominant negative manner. Both genotypes have multiple accessory buds per paraclade junction and more accessory buds per plant, meristem fasciation, and the potential to produce more paraclade junctions (Figure 3.4; 3.18; 3.28; 3.29; 3.31). Additionally, both genotypes have floral organs that are fused, have developmental defects, and petals with defects in polarity (Figure 3.24; 3.25).

PHB, LOF1, and Other HD-Zip Proteins Could Act in Complexes

If higher *PHB* levels causes fewer accessory buds, due to higher accessory bud repression, then the *lof1-1 phb-13* double mutant should have accessory buds. However, this is not what was observed (Figure 3.3; 3.12). In the event that levels of both *LOF1* and *PHB* are low, other *HD-Zip III* genes may be able to act in a functionally redundant manner to *PHB* in accessory bud repression. A *miRNA 165/166*-resistant version of *PHB* contained multiple buds around leaves and radialized leaves (McConnell and Barton, 1998; McConnell *et al.*, 2001), suggesting that adaxialization of leaves causes multiple buds. The *phb-13* mutant also had cases of multiple accessory buds per paraclade junction (Figure 3.2; 3.29 B). Therefore, the *PHB* overexpression phenotype is similar to

the *phb* loss-of-function phenotype. This has been documented to occur when proteins act in complexes, and the stoichiometry of proteins in the complex is altered [reviewed in (Prelich, 2012)]. One well studied example of this phenomena is the SUPPRESSOR OF TY (SPT) transcription factors in yeast (Clark-Adams and Winston, 1987; Clark-Adams *et al.*, 1988). Some evidence for this theory is that HD-Zip III proteins have previously been reported to homodimerize with one another (Sessa *et al.*, 1998; Magnani and Barton, 2011). It has also been documented that HD-Zip III proteins heterodimerize with HD-Zip II (Merelo *et al.*, 2016) and with other proteins (Wenkel *et al.*, 2007; Kim *et al.*, 2008). PHB and REV have been documented to interact with HAT3 and ATHB4, two closely related HD-Zip II proteins. It was additionally shown that HAT3-PHB and ATHB4-PHB bound DNA (Merelo *et al.*, 2016). Because LOF1 also interacts with ATHB4 (Chapter 1), this could indicate that LOF1, ATHB4, ZPRs, PHB, and/or other HD-Zip III proteins act in complexes with one another.

An experiment to test this hypothesis would be to determine if LOF1 and PHB interact directly at the protein level. RT-PCR experiments indicated that in *lof1-1* mutants there was no visible alteration in *PHB* transcript levels (Figure 3.11 B) and in *phb-13* mutants there is no visible alteration in *LOF1* transcript levels (Figure 3.11 C). These data suggest that regulation between LOF1 and PHB could occur on the protein level or be indirect. It should be noted that PHB was not recovered as a protein interactor of LOF1 in Chapter 1. However, because the *PHB* cDNA is quite large compared to other cDNAs in *Arabidopsis*, *PHB* clones may have been be underrepresented in the yeast two-hybrid library (Kempin *et al.,* 1995; Wortman *et al.*, 2003). Other *HD-Zip III* cDNA

clones are also of large size and would also be predicted to be underrepresented in libraries constructed using this method.

Conclusion

Our data support a model where *LOF1* promotes accessory bud formation in the paraclade junction (and paraclade junction formation as a whole) in response to environmental input through *PHB* and potentially other *HD-Zip III* genes. This is evidenced by the fact that *lof1-1* mutants develop significantly fewer accessory buds and paraclade junctions per plant compared to wild-type controls. Our data showed that *phb-13* single mutants consistently formed more accessory buds than control plants, indicating *PHB* represses accessory bud formation in the paraclade junction. However, *LOF1* and *PHB* do not appear to regulate one another at the transcriptional level, as in paraclade junctions *PHB* transcript levels are not reduced in *lof1-1* and *LOF1* transcript levels are not reduced in *phb-13*. If *LOF1* antagonizes *PHB*, then increased *PHB* activity in *lof1* could be responsible for the loss of accessory buds. Additionally, we know that *LOF2* does not function redundantly with *LOF1* in its role to repress *PHB* because *lof2* single mutants produce accessory buds regularly. Furthermore, in *35S:LOF1* plants where *LOF1* is ectopically overexpressed, there is a leaf polarity phenotype and occasionally leaves curl upwards. This phenotype is consistent with a reduction in adaxial identity and/or abaxial identity determinants being activated. Therefore, *LOF1* represses *PHB* in the paraclade junction in order to allow formation of accessory buds.

phb-13 lof1-1 double mutants are phenotypically indistinguishable from *lof1-1* single mutants, as they lack accessory buds and have fusion between the cauline leaf and axillary branch. The *phb-13 lof1-1* double mutant phenotype suggests that in *LOF1* and *PHB* loss-of-function plants other *HD-Zip III* gene may be able to act in accessory bud repression. This may indicate accessory bud formation is tightly controlled by *PHB*, other *HD-Zip III*s, *LOF1*, and environmental conditions. The loss of accessory buds in *lof1-1* can be overcome by a dominant negative or misexpressed version of *PHB* (*pPHB:PHB*, *lfs-1D*/ endogenous *mPHB*, or *pPHB:mPHB*). Because PHB, REV, and LOF1 are known to interact with ATHB4 on the protein level (Chapter 1; Merelo *et al.*, 2016), this indicates that PHB, LOF1, and/or other HD-Zip proteins may act in complexes to regulate gene expression in response to environmental conditions to control paraclade junction and accessory bud formation. An intricate relationship can be visualized between LOF1, ATHB4, PHB, and other HD-Zip III transcription factors in the regulation of SAM maintenance, leaf polarity, formation of paraclade junctions, and formation of axillary and accessory buds (Figure 3.36). Further experiments are necessary to determine how these proteins work together to regulate multiple aspects of plant development.

Materials and Methods

Plant Materials and Growth Conditions

Columbia (Col-0) was used as the wild-type control in all experiments except when otherwise indicated.

Soil Method: Seeds were treated at -80ºC overnight. They were then sterilized with 95% ethanol and allowed to dry before being sown on Sunshine LC1 mix with Osmocote 14-14-14 (150g/bag) and Marathon (225g/bag) added to soil. Plants were grown at 18-23ºC in 16-hour light/8-hour dark cycles.

Plate Method: Seeds were sterilized with 95% ethanol for 5 minutes, treated with 20% bleach/0.01% Tween 20 for 5 minutes, and rinsed five times with sterile water. Seeds were then sown on Murashige and Skoog (MS) media (pH 5.7) (Murashige and Skoog, 1962) with added 1% sucrose. They were stratified at 4ºC in the dark for 48 hours before being transferred to a growth chamber with 120 μM/m^2s white light with a 16-hour light/ 8-hour dark cycle at a constant temperature of 22ºC.

The *lof1-1* mutant (SALK_025235) was as previously described (Lee *et al.*, 2009). *lof1-1* plants contain a T-DNA insertion 71 base pairs before the translational start site, and have no detectable levels of *LOF1* transcript accumulation in the paraclade junctions (Lee *et al.*, 2009). *phb-13* (SALK_021684), *phv-11 er-2* (CS6966), and *cna-2 er-2* (CS6968) were previously described (Prigge *et al.*, 2005). *cna-1* (L*er*) was as previously described (Green *et al.*, 2005). *er-2* (Columbia) was as previously described (Lease *et al.*, 2001). The *35S:LOF1* construct (pCAMBIA 3300 backbone) has been described (Lee *et al.*, 2009). All alleles used are in the Col-0 genetic background unless stated otherwise. *PHB* gene diagram exon-intron structure (Figure 3.6) was created using the following website: http://wormweb.org/exonintron. All plant images were captured on a Leica MZ12 stereoscope (UCR).

Ethyl Methane Sulfonate (EMS) Mutagenesis Screen

lof1-1 seeds in the Col-0 genetic background were incubated in 0.2% EMS (v/v) for 15 hours in a tube rotator. Seeds were rinsed eight times with distilled water. The last rinse was kept in the tube for greater than one hour in order for EMS to diffuse out (Kim *et al.*, 2006*a*). M1 plants were grown, and M2 seeds collected from individual M1 plants. Approximately 800 M2 families were screened to identify plants that produced accessory buds. The *lfs-1D* mutant phenotype of multiple accessory buds per paraclade junction, offset accessory bud, and accessory buds that grow out was identified in the M2 generation and stabilized in the M3 generation.

Mapping of the lfs-1D Mutation

lfs-1D lof1-1 suppressor plants (Col-0) were crossed to the Landsberg *erecta* (L*er*) accession. The F2 plants resulting from this cross were used for genetic mapping. For course mapping, at least one genetic marker on each chromosomal arm was chosen for all five chromosomes in the *Arabidopsis* genome. The genetic markers used on each chromosome were as follows: NGA63 and NGA280 (chromosome 1); CIW2, CIW3, and NGA168 (chromosome 2); NGA172, NGA162, CIW4, and NGA6 (chromosome 3); CIW5, CIW6, and NGA1107 (chromosome 4); and CIW9 and CIW10 (chromosome 5).

Because NGA168 was the only marker that showed a recombination frequency of less than 0.4, additional markers in this region were assessed.

For mapping on chromosome 2, markers between CIW3 and the bottom of chromosome two were analyzed (NGA1126, NGA361, and F18O19). All plants were first genotyped for *LOF1* and *lof1-1*. Because the *lfs-1D* mutation was genetically

dominant, the mapping was performed by first genotyping plants for the *lof1-1* allele. *lof1-1* mutants lacking the *lfs-1D* mutant phenotype were used in mapping, and the recombination frequency was calculated for each genetic marker in association with the L*er* allele. Plants homozygous for *lof1-1* and without the *lfs-1D* mutant phenotype should not contain any copies of the *lfs-1D* mutation (Col-0) and should have two copies of the L*er* allele at the *lfs-1D* locus. The recombination frequencies indicated that there may be two mutations on chromosome 2 – one between CIW3 and NGA361 and one between NGA361 and F18O19 (Table 3.2). Adding additional plants to the F2 mapping population did not improve resolution. Primer pairs used for genetic markers on chromosome 2 are listed in Table 3.3. Primer pairs used for genetic markers on chromosomes 1, 3, 4, and 5 were previously described (Bell and Ecker, 1994; Lukowitz *et al.*, 2000).

Site-Directed Mutagenesis

The pEGAD *pPHB:GFP:PHB* vector used as control transformation for *PHB* copy number and for site-directed mutagenesis was as previously described (Dello Ioio *et al.*, 2012). pEGAD *pPHB:GFP:PHB* is a binary vector that is approximately 17,300 base pairs in size. The 2.8 kb endogenous *PHB* promoter sequence drives expression of an *eGFP* reporter translationally fused to the *PHB* coding sequence followed by the *nos* terminator (Dello Ioio *et al.*, 2012). Two copies of the *35S* promoter are used to drive the *BAR* resistance gene. Site-directed mutagenesis was carried out using a Q5 Site-Directed Mutagenesis Kit (New England Biolabs) according to manufacturer instructions. Primers

for site-directed mutagenesis were designed using NEBaseChanger (New England Biolabs). Primers used in site-directed mutagenesis are listed in Table 3.3.

Plant Transformation

For transformation, binary vectors were transformed into *Agrobacterium tumefaciens* GV3101. Transformation of *Arabidopsis* was performed using the floral dip method (Clough and Bent, 1998).

Mature Plant Phenotyping Experiments

This description applies to data provided in Tables 3.1, 3.4, 3.5, 3.6, 3.7, 3.8, 3.9, 3.13, 3.14, 3.15, and 3.16. The accessory bud categories were designed based on observations of the *lfs-1D* mutant plants, as it was observed in this genotype that one accessory bud typically forms offset from the center in a paraclade junction before the second accessory bud forms. The offset accessory bud acts as a predictor that multiple accessory buds per paraclade junction are possible as being offset may allow for more room for the second accessory bud. However, an offset accessory bud does not guarantee that multiple accessory buds will form in the paraclade junction. Phenotypic categories are as follows:

Accessory Buds (all categories are exclusive unless indicated otherwise):

- No accessory buds –no accessory buds in any paraclade junction on the plant.
- One centrally located accessory bud – the plant contained at least one paraclade junctions with an accessory bud and no accessory buds were offset.
- Offset accessory bud – the plant had paraclade junctions with zero to one accessory bud each and at least one offset accessory bud.

- Multiple accessory buds – the plant had at least one paraclade junctions with two or more accessory buds.
- Accessory bud grew out – at least one accessory bud grew out without damage to the axillary branch on the plant. This category was inclusive of other categories.

Other phenotypes (all categories are inclusive and were recorded if they were present at least once per plant unless indicated otherwise):

- Small – plant was at least 50% smaller than the average size of control plants.
- Decurrent strand – a decurrent strand occurred between a stem and leaf somewhere on the shoot.
- Meristem fasciation – meristem fasciation was evident on viewing the primary inflorescence stem or a branch from the primary inflorescence stem (Figure 3.18).
- Silique shape – a silique on the plant had the shape observed in Figure 3.17 E and F.
- Multiple cauline leaves – plants had at least one paraclade junction with two or more cauline leaves.
- Radial rosette leaf – a radial rosette leaf occurred on the plant (Figure 3.13).
- Radial cauline leaf – a radial cauline leaf occurred on the plant (Figure 3.14).
- Fused leaves – fused rosette leaves occurred on the plant (Figure 3.13 I-O).
- Paraclade connected to second order paraclade by decurrent strand – at least two paraclade junctions on the plant were connected by an obvious decurrent strand (Figure 3.20). This phenotype was recorded separately from the “decurrent strand” phenotype.

Analysis of T1 and T2 pPHB:PHB and pPHB:mPHB Transgenic Populations

T2 populations in each genetic background were screened for insertion locus number by plating on basta and observing segregation ratios. Transgene expression was examined in resistant plants using RT-PCR (Figure 3.9; 3.10). T2 populations with medium-high levels of transgene expression and one transgene locus were used for phenotypic analysis. Twenty-four plants for each T2 line were scored for phenotypes. Some T1 transformants exhibited a small/dwarf phenotype and were developmentally delayed. These transformants were not used in T2 analysis due to size and potential lack of paraclade junctions. Some T1 transformants also had very low fertility. Thus, the progeny of these T1 transformants were not used for T2 phenotypic analysis.

T1 plants were grown on soil and selected for basta resistance. They were additionally genotyped for the *pPHB:PHB* or *pPHB:mPHB* transgene as well as the specific genetic background. The phenotypes of each plant were recorded at two-weeks and seven-weeks after germination.

Seedling Phenotyping Experiments

Cotyledon and meristem (phenotypes observed one or more times per plant were recorded unless stated otherwise; examples of each phenotype can be viewed in Figure 3.16):

- Cotyledons defects - either fused cotyledons or three cotyledons were found on the seedling. This category was inclusive of true leaf phenotypes.
- Meristem termination with a pin-like structure – SAM terminated in a visible pin-like structure. This category was exclusive of true leaf categories.

- Meristem termination with no pin structure - SAM terminated with no visible tissue or organs near the meristem. This category was exclusive of true leaf categories.

True leaf (all categories are exclusive):

- Fused leaf – fused leaves were found on the seedling (Figure 3.15 B-E)
- Examples of each remaining category are given in Figure 3.15 F-J.

Floral Analysis Experiments

Thirty-six plants of each genotype were grown. Flowers six to ten that developed on the primary inflorescence were used in the analysis and dissected under a stereomicroscope. Flower one is the first flower to form on the primary inflorescence. Flowers were analyzed per genotype (n=180) unless a plant died or was damaged. Flowers were analyzed as they developed, not according to a timed schedule. Planting took place in three different groups over the span of three weeks. Plants within the same groups were analyzed together. Group 1 consisted of Col-0, *lof1-1*, *phb-13*, and *phb-13 lof1-1*. Group 2 consisted of *er-2*, *phb-13 er-2*, *phv-11 er-2*, and *phb-13 phv-11 cna-2 er-2*. Group 3 consisted of Col-0, T2 *pPHB:PHB* Col-0 #1, T2 *pPHB:PHB* Col-0 #2, *lof1-1*, T2 *pPHB:PHB lof1-1* #1, and T2 *pPHB:PHB lof1-1* #2.

Floral phenotyping (categories are inclusive unless stated otherwise and were recorded if present once per flower; examples of all phenotypes can be viewed in Figure 3.23; 3.24; 3.25):

- Wild-type (WT) – flower had wild-type numbers of floral organs, no fusions, complete organ identity, and correct developmental timing. This category was exclusive of others.
- Carpel shape – flower had carpels with abnormal shape.
- Abnormal carpel number – flower had greater than or fewer than two carpels.
- Stamen fusion – two or more stamen were fused or a stamen was fused to a petal.
- Undeveloped stamen – a stamen had undeveloped anther, undeveloped filament, or both anther and filament were undeveloped.
- Abnormal stamen number – a flower had a number of stamens that was not six.
- Stamen/petal structure – presence of the stamenoid petal, petaloid stamen, or fusion between stamen and petal as shown in Figure 3.23.
- Petal polarity – a flower had petal with adaxial-abaxial polarity defects. This includes both trumpet and radial petals.
- Radial petal – a flower had petal that was completely radialized.
- Trumpet petal – a flower had petal with trumpet shape.
- Forked/fused/lobed petal – a flower had a petal that was either forked, fused, or lobed.
- Abnormal petal number – a flower had number of petals that was not four.
- Sepal fusion – two or more sepals were fused at the base of a flower.
- Abnormal sepal number – a flower had sepal number that was not four.
- Other – category encompasses all other phenotypes observed, excluding those listed in the table.

Transcript Analysis

Total RNA was extracted from whole 10-day-old seedlings, rosette leaves, or paraclade junctions by TRIZOL® reagent (Invitrogen) and precipitated by 100% isopropanol. Pellets were washed with 75% ethanol. RNA (2 μg) was used for cDNA synthesis using SuperScript IV Reverse Transcriptase (Thermo Fisher Scientific) according to manufacturer's protocol. *ACTIN2* (*ACT2*) primers were used to equalize cDNA for RT-PCR (Table 3.3) using 21 or 22 cycles of amplification. *PHB* transgene and *PHB* wild-type primers used in RT-PCR are listed in Table 3.3.

Plant Architecture Experiments

Thirty-six plants of each genotype were grown. Planting took place in three different groups over the span of three weeks. Plants within the same groups were analyzed together. The groups were the same as used in the floral analysis experiments.

Plant architecture was analyzed when plants were seven-weeks old. All plants in the same group were analyzed in the same day. First, plants were analyzed for presence or absence of mature plant phenotypes observed in *pPHB:PHB* and *pPHB:mPHB* transgenic plants (Figure 3.5, 3.7, 3.8, 3.13, 3.14, 3.17, 3.18, 3.19, and 3.20). Data were recorded for a number of plant architecture parameters, including number of cauline-leaf axil branches, number of first order cauline-leaf paraclade junctions, and number of rosette-leaf axil branches. The number of accessory buds and the location of the paraclade junction where each was found was recorded. The number and placement of secondary cauline-leaf axil branches as well the number of rosette-leaf branches with

secondary branches was recorded. Finally, the number of cauline leaves and the paraclade junction where each was located was documented.

Confocal Microscopy

Roots were stained with 10 μM propidium iodide (PI) dissolved in distilled water for 30-60 seconds. Roots were then visualized using laser scanning confocal microscopy with a Leica SP8 upright microscope (Van Norman lab, UCR). Root meristematic and elongation zones were viewed in the median longitudinal plane using LAS X software (Leica). Fluorescent signals were captured according to the following: GFP (excitation 488 nm, emission 492-530 nm) and PI (excitation 536 nm, emission 585-660 nm) [adapted from (Campos *et al.*, 2019)].

References

Aida M, Ishida T, Fukaki H, Fujisawa H, Tasaka M. 1997. Genes involved in organ separation in *Arabidopsis*: An analysis of the *cup-shaped cotyledon* mutant. Plant Cell **9**, 841–857.

Aida M, Ishida T, Tasaka M. 1999. Shoot apical meristem and cotyledon formation during Arabidopsis embryogenesis: Interaction among the *CUP-SHAPED COTYLEDON* and *SHOOT MERISTEMLESS* genes. Development **126**, 1563–1570.

Allen E, Xie Z, Gustafson AM, Carrington JC. 2005. microRNA-directed phasing during trans-acting siRNA biogenesis in plants. Cell **121**, 207–221.

Ariel FD, Manavella PA, Dezar CA, Chan RL. 2007. The true story of the HD-Zip family. Trends in Plant Science **12**, 419–426.

Azhakanandam S, Nole-Wilson S, Bao F, Franks RG. 2008. *SEUSS* and *AINTEGUMENTA* mediate patterning and ovule initiation during gynoecium medial domain development. Plant Physiology **146**, 1165–1181.

Baima S, Nobili F, Sessa G, Lucchetti S, Ruberti I, Morelli G. 1995. The expression of the *Athb-8* homeobox gene is restricted to provascular cells in *Arabidopsis thaliana*. Development **121**, 4171–4182.

Baima S, Possenti M, Matteucci A, Wisman E, Altamura MM, Ruberti I, Morelli G. 2001. The Arabidopsis ATHB-8 HD-Zip protein acts as a differentiation-promoting transcription factor of the vascular meristems. Plant Physiology **126**, 643–655.

Barton MK, Poethig RS. 1993. Formation of the shoot apical meristem in *Arabidopsis* thaliana: An analysis of development in the wild type and in the *shoot meristemless* mutant. Development **119**, 823–831.

Bell CJ, Ecker JR. 1994. Assignment of 30 microsatellite loci to the linkage map of *Arabidopsis*. Genomics **19**, 137–144.

Bell EM, Lin W, Husbands AY, Yu L, Jaganatha V, Jablonska B, Mangeon A, Neff MM, Girke T, Springer PS. 2012. *Arabidopsis* lateral organ boundaries negatively regulates brassinosteroid accumulation to limit growth in organ boundaries. Proceedings of the National Academy of Sciences USA **109**, 21146–21151.

Benfey PN, Chua N. 1990. CaMV 35S enhancer subdomains. EMBO Journal **9**, 1685–1696.

Bennett T, Scheres B. 2010. Chapter three - root development - two meristems for the price of one? Current Topics in Developmental Biology **91**, 67–102.

Bowman JL. 2000. The YABBY gene family and abaxial cell fate. Current Opinion in Plant Biology **3**, 17–22.

Bowman JL, Eshed Y, Baum SF. 2002. Establishment of polarity in angiosperm lateral organs. Trends in Genetics **18**, 134–141.

Breuil-Broyer S, Morel P, De Almeida-Engler J, Coustham V, Negrutiu I, Trehin C. 2004. High-resolution boundary analysis during *Arabidopsis thaliana* flower development. Plant Journal **38**, 182–192.

Byrne ME. 2006. Shoot meristem function and leaf polarity: The role of class III HD-ZIP genes. PLoS Genetics **2**, 785–790.

Campos R, Goff J, Rodriguez-Furlan C, Van Norman JM. 2019. The Arabidopsis receptor kinase IRK is polarized and represses specific cell divisions in roots. Developmental Cell **52**, 1–13.

Carlsbecker A, Lee J-Y, Roberts CJ, Dettmer J, Lehesranta S, Zhou J, Lindgren O, Moreno-Risueno MA, Vatén A, Thitamadee S, Campilho A, Sebastian J, Bowman JL, Helariutta Y, Benfey PN. 2010. Cell signalling by microRNA165/6 directs gene dose-dependent root cell fate. Nature **465**, 316–321.

Clark-Adams CD, Norris D, Osley MA, Fassler JS, Winston F. 1988. Changes in histone gene dosage alter transcription in yeast. Genes & Development **2**, 150–159.

Clark-Adams CD, Winston F. 1987. The *SPT6* gene is essential for growth and is required for delta-mediated transcription in *Saccharomyces cerevisiae*. Molecular and Cellular Biology **7**, 679–686.

Clough SJ, Bent AF. 1998. Floral dip: A simplified method for *Agrobacterium*-mediated transformation of *Arabidopsis thaliana*. The Plant Journal **16**, 735–743.

Colling J, Tohge T, De Clercq R, Brunoud G, Vernoux T, Fernie AR, Makunga NP, Goossens A, Pauwels L. 2015. Overexpression of the *Arabidopsis thaliana* signalling peptide TAXIMIN1 affects lateral organ development. Journal of Experimental Botany **66**, 5337–5349.

Cui H, Levesque MP, Vernoux T, Jung JW, Paquette AJ, Gallagher KL, Wang JY, Blilou I, Scheres B, Benfey PN. 2007. An evolutionarily conserved mechanism delimiting SHR movement defines a single layer of endodermis in plants. Science **316**, 421–425.

Dolan L, Janmaat K, Willemsen V, Linstead P, Poethig S, Roberts K, Scheres B. 1993. Cellular organisation of the *Arabidopsis thaliana* root. Development **119**, 71–84.

Elliott RC, Betzner AS, Huttner E, Oakes MP, Tucker WQJ, Gerentes D, Perez P, Smyth DR. 1996. *AINTEGUMENTA*, an *APETALA2*-like gene of Arabidopsis with pleiotropic roles in ovule development and floral organ growth. Plant Cell **8**, 155–168.

Emery JF, Floyd SK, Alvarez J, Eshed Y, Hawker NP, Izhaki A, Baum SF, Bowman JL. 2003. Radial patterning of *Arabidopsis* shoots by class III HD-ZIP and KANADI genes. Current Biology **13**, 1768–1774.

Eshed Y, Baum SF, Bowman JL. 1999. Distinct mechanisms promote polarity establishment in carpels of *Arabidopsis*. Cell **99**, 199–209.

Eshed Y, Izhaki A, Baum SF, Floyd SK, Bowman JL. 2004. Asymmetric leaf development and blade expansion in *Arabidopsis* are mediated by KANADI and YABBY activities. Development **131**, 2997–3006.

Evans MMS, Barton MK. 2002. Genetics of angiosperm shoot apical meristem development. Annual Review of Plant Physiology and Plant Molecular Biology **48**, 673–701.

Fahlgren N, Montgomery TA, Howell MD, Allen E, Dvorak SK, Alexander AL, Carrington JC. 2006. Regulation of *AUXIN RESPONSE FACTOR3* by *TAS3* ta-siRNA affects developmental timing and patterning in *Arabidopsis*. Current Biology **16**, 939–944.

Franks RG, Liu Z, Fischer RL. 2006. *SEUSS* and *LEUNIG* regulate cell proliferation, vascular development and organ polarity in *Arabidopsis* petals. Planta **224**, 801–811.

Goldshmidt A, Alvarez JP, Bowman JL, Eshed Y. 2008. Signals derived from *YABBY* gene activities in organ primordia regulate growth and partitioning of *Arabidopsis* shoot apical meristems. Plant Cell **20**, 1217–1230.

Gomez MD, Urbez C, Perez-Amador MA, Carbonell J. 2011. Characterization of *constricted fruit* (*ctf*) mutant uncovers a role for *AtMYB117*/*LOF1* in ovule and fruit development in *Arabidopsis thaliana*. PLoS ONE **6**, 1–10.

Green KA, Prigge MJ, Katzman RB, Clark SE. 2005. *CORONA*, a member of the class III homeodomain leucine zipper gene family in Arabidopsis, regulates stem cell specification and organogenesis. Plant Cell **17**, 691–704.

Han H, Krizek BA. 2016. *AINTEGUMENTA-LIKE6* can functionally replace *AINTEGUMENTA* but alters *Arabidopsis* flower development when misexpressed at high levels. Plant Molecular Biology **92**, 597–612.

Helariutta Y, Fukaki H, Wysocka-Diller J, Nakajima K, Jung J, Sena G, Hauser MT, Benfey PN. 2000. The *SHORT-ROOT* gene controls radial patterning of the *Arabidopsis* root through radial signaling. Cell **101**, 555–567.

Hempel FD, Feldman LJ. 1994. Bi-directional inflorescence development in *Arabidopsis thaliana*: Acropetal initiation of flowers and basipetal initiation of paraclades. Planta **192**, 276–286.

Hibara K, Karim MR, Takada S, Taoka K, Furutani M, Aida M, Tasaka M. 2006. *Arabidopsis CUP-SHAPED COTYLEDON3* regulates postembryonic shoot meristem and organ boundary formation. Plant Cell **18**, 2946–2957.

Hunter C, Willmann MR, Wu G, Yoshikawa M, De la Luz Gutierrez-Nava M, Poethig SR. 2006. Trans-acting siRNA-mediated repression of ETTIN and ARF4 regulates heteroblasty in *Arabidopsis*. Development **133**, 2973–2981.

Husbands AY, Chitwood DH, Plavskin Y, Timmermans MCP. 2009. Signals and prepatterns: New insights into organ polarity in plants. Genes & Development **23**, 1986–1997.

Hussey G. 1971. Cell division and expansion and resultant tissue tensions in the shoot apex during the formation of a leaf primordium in the tomato. Journal of Experimental Botany **22**, 702–714.

Ioio RD, Galinha C, Fletcher AG, Grigg SP, Molnar A, Willemsen V, Scheres B, Sabatini S, Baulcombe D, Maini PK, Tsiantis M. 2012. A PHABULOSA/cytokinin feedback loop controls root growth in *Arabidopsis*. Current Biology **22**, 1699–1704.

Izhaki A, Bowman JL. 2007. KANADI and class III HD-Zip gene families regulate embryo patterning and modulate auxin flow during embryogenesis in *Arabidopsis*. Plant Cell **19**, 495–508.

Janssen BJ, Drummond RSM, Snowden KC. 2014. Regulation of axillary shoot development. Current Opinion in Plant Biology **17**, 28–35.

Kanrar S, Onguka O, Smith HMS. 2006. *Arabidopsis* inflorescence architecture requires the activities of KNOX-BELL homeodomain heterodimers. Planta **224**, 1163–1173.

Kelley DR, Skinner DJ, Gasser CS. 2009. Roles of polarity determinants in ovule development. Plant Journal **57**, 1054–1064.

Kempin SA, Savidge B, Yanofsky MF. 1995. Molecular basis of the cauliflower phenotype in Arabidopsis. Science **267**, 522–525.

Kerstetter RA, Bollman K, Taylor RA, Bomblies K, Poethig RS. 2001. *KANADI* regulates organ polarity in *Arabidopsis*. Nature **411**, 706–709.

Kim Y-S, Kim S-G, Lee M, Lee I, Park H-Y, Seo PJ, Jung J-H, Kwon E-J, Suh SW, Paek K-H, Park C-M. 2008. HD-ZIP III activity is modulated by competitive inhibitors via a feedback loop in *Arabidopsis* shoot apical meristem development. Plant Cell **20**, 920–933.

Kim YS, Schumaker KS, Zhu JK. 2006*a*. EMS mutagenesis of *Arabidopsis*. Methods in Molecular Biology. **323**, 101–103.

Kim S, Soltis PS, Wall K, Soltis DE. 2006*b*. Phylogeny and domain evolution in the *APETALA2*-like gene family. Molecular Biology and Evolution **23**, 107–120.

Klucher KM, Chow H, Reiser L, Fischer RL. 1996. The *AINTEGUMENTA* gene of Arabidopsis required for ovule and female gametophyte development is related to the floral homeotic gene *APETALA2*. Plant Cell **8**, 137–153.

Kosugi S, Suzuka I, Ohashi Y, Murakami T, Arai Y. 1991. Upstream sequences of rice proliferating cell nuclear antigen (PCNA) gene mediate expression of PCNA-GUS chimeric gene in meristems of transgenic tobacco plants. Nucleic Acids Research **19**, 1571–1576.

Di Laurenzio L, Wysocka-Diller J, Malamy JE, Pysh L, Helariutta Y, Freshour G, Hahn MG, Feldmann KA, Benfey PN. 1996. The *SCARECROW* gene regulates an asymmetric cell division that is essential for generating the radial organization of the Arabidopsis root. Cell **86**, 423–433.

Lease KA, Lau NY, Schuster RA, Torii KU, Walker JC. 2001. Receptor serine/threonine protein kinases in signalling: Analysis of the erecta receptor-like kinase of *Arabidopsis thaliana*. New Phytologist **151**, 133–143.

Lee C, Clark SE. 2015. A WUSCHEL-independent stem cell specification pathway is repressed by PHB, PHV and CNA in Arabidopsis. PLoS ONE **10**, 1–19.

Lee D-K, Geisler M, Springer PS. 2009. *LATERAL ORGAN FUSION1* and LATERAL *ORGAN FUSION2* function in lateral organ separation and axillary meristem formation in *Arabidopsis*. Development **136**, 2423–2432.

Lin W, Shuai B, Springer PS. 2003. The *Arabidopsis LATERAL ORGAN BOUNDARIES*-domain gene *ASYMMETRIC LEAVES2* functions in the repression of *KNOX* gene expression and in adaxial-abaxial patterning. Plant Cell **15**, 2241–2252.

Liu J, Huang S, Sun M, Liu S, Liu Y, Wang W, Zhang X, Wang H, Hua W. 2012. An improved allele-specific PCR primer design method for SNP marker analysis and its application. Plant Methods **8**, 1-9.

Lukowitz W, Gillmor CS, Scheible WR. 2000. Positional cloning in Arabidopsis. Why it feels good to have a genome initiative working for you. Plant Physiology **123**, 795–805.

Magnani E, Barton MK. 2011. A Per-ARNT-sim-like sensor domain uniquely regulates the activity of the homeodomain leucine zipper transcription factor REVOLUTA in *Arabidopsis*. Plant Cell **23**, 567–582.

Mallory AC, Dugas DV, Bartel DP, Bartel B. 2004. MicroRNA regulation of NAC-domain targets is required for proper formation and separation of adjacent embryonic, vegatative, and floral organs. Current Biology **14**, 1035–1046.

McConnell JR, Barton MK. 1998. Leaf polarity and meristem formation in *Arabidopsis*. Development **125**, 2935–2942.

McConnell JR, Emery J, Eshed Y, Bao N, Bowman J, Barton MK. 2001. Role of *PHABULOSA* and *PHAVOLUTA* in determining radial patterning in shoots. Nature **411**, 709–713.

Merelo P, Ram H, Caggiano MP, Ohno C, Ott F, Straub D, Graeff M, Cho SK, Yang SW, Wenkel S, Heisler MG. 2016. Regulation of *MIR165/166* by class II and class III homeodomain leucine zipper proteins establishes leaf polarity. Proceedings of the National Academy of Sciences USA **113**, 11973–11978.

Moon J, Hake S. 2011. How a leaf gets its shape. Current Opinion in Plant Biology **14**, 24–30.

Murashige T, Skoog F. 1962. A revised medium for rapid growth and bio assays with tobacco tissue cultures. Physiologia Plantarum **15**, 473–497.

Nole-Wilson S, Krizek BA. 2006. AINTEGUMENTA contributes to organ polarity and regulates growth of lateral organs in combination with YABBY genes. Plant Physiology **141**, 977–987.

Nole-Wilson S, Tranby TL, Krizek BA. 2005. *AINTEGUMENTA*-like (*AIL*) genes are expressed in young tissues and may specify meristematic or division-competent states. Plant Molecular Biology **57**, 613–628.

Otsuga D, DeGuzman B, Prigge MJ, Drews GN, Clark SE. 2001. *REVOLUTA* regulates meristem initiation at lateral positions. The Plant Journal **25**, 223–236.

Pekker I, Alvarez JP, Eshed Y. 2005. Auxin response factors mediate *Arabidopsis* organ asymmetry via modulation of KANADI Activity. Plant Cell **17**, 2899–2910.

Prelich G. 2012. Gene overexpression: Uses, mechanisms, and interpretation. Genetics **190**, 841–854.

Prigge MJ, Otsuga D, Alonso JM, Ecker JR, Drews GN, Clark SE. 2005. Class III homeodomain-leucine zipper gene family members have overlapping, antagonistic, and distinct roles in Arabidopsis development. Plant Cell **17**, 61–76.

Puchta H. 2017. Applying CRISPR/Cas9 for genome engineering in plants: The best is yet to come. Current Opinion in Plant Biology **36**, 1–8.

Raman S, Greb T, Peaucelle A, Blein T, Laufs P, Theres K. 2008. Interplay of miR164, *CUP-SHAPED COTYLEDON* genes and *LATERAL SUPPRESSOR* controls axillary meristem formation in *Arabidopsis thaliana*. Plant Journal **55**, 65–76.

Rhoades MW, Reinhart BJ, Lim LP, Burge CB, Bartel B, Bartel DP. 2002. Prediction of plant microRNA targets. Cell **110**, 513–520.

Sabatini S, Heidstra R, Wildwater M, Scheres B. 2003. SCARECROW is involved in positioning the stem cell niche in the *Arabidopsis* root meristem. Genes and Development **17**, 354–358.

Sarojam R, Sappl PG, Goldshmidt A, Efroni I, Floyd SK, Eshed Y, Bowman JL. 2010. Differentiating Arabidopsis shoots from leaves by combined YABBY activities. Plant Cell **22**, 2113–2130.

Sawa S, Ohgishi M, Goda H, Higuchi K, Shimada Y, Yoshida S, Koshiba T. 2002. The *HAT2* gene, a member of the HD-Zip gene family, isolated as an auxin inducible gene by DNA microarray screening, affects auxin response in *Arabidopsis*. Plant Journal **32**, 1011–1022.

Schaller GE, Street IH, Kieber JJ. 2014. Cytokinin and the cell cycle. Current Opinion in Plant Biology **21**, 7–15.

Schneeberger R, Freeling M, Tsiantis M, Langdale JA. 1998. The *rough sheath2* gene negatively regulates homeobox gene expression during maize leaf development. Development **125**, 2857–2865.

Schrick K, Nguyen D, Karlowski WM, Mayer KFX. 2004. START lipid/sterol-binding domains are amplified in plants and are predominantly associated with homeodomain transcription factors. Genome biology **5**, 1–16.

Sessa G, Steindler C, Morelli G, Ruberti I. 1998. The *Arabidopsis Athb-8*, *-9* and *-14* genes are members of a small gene family coding for highly related HD-ZIP proteins. Plant Molecular Biology **38**, 609–622.

Shi B, Guo X, Wang Y, Xiong Y, Wang J, Hayashi K, Lei J. 2018. Feedback from lateral organs controls shoot apical meristem growth by modulating auxin transport article feedback from lateral organs controls shoot apical meristem growth by modulating auxin transport. Developmental Cell **44**, 204–216.

Shi B, Zhang C, Tian C, Wang J, Wang Q, Xu T, Xu Y, Ohno C, Sablowski R, Heisler MG, Theres K, Wang Y, Jiao Y. 2016. Two-step regulation of a meristematic cell population acting in shoot branching in *Arabidopsis*. PLoS Genetics **12**, 1–20.

Siegfried KR, Eshed Y, Baum SF, Otsuga D, Drews GN, Bowman JL. 1999. Members of the *YABBY* gene family specify abaxial cell fate in *Arabidopsis*. Development **126**, 4117–4128.

Skopelitis DS, Benkovics AH, Husbands AY, Timmermans MCP. 2017. Boundary formation through a direct threshold-based readout of mobile small RNA gradients. Developmental Cell **43**, 265-273.

Skopelitis DS, Husbands AY, Timmermans MCP. 2012. Plant small RNAs as morphogens. Current Opinion in Cell Biology **24**, 217–224.

Soyars CL, James SR, Nimchuk ZL. 2016. Ready, aim, shoot: Stem cell regulation of the shoot apical meristem. Current Opinion in Plant Biology **29**, 163–168.

Stirnberg P, Van de Sande K, Leyser HMO. 2002. *MAX1* and *MAX2* control shoot lateral branching in *Arabidopsis*. Development **129**, 1131–1141.

Sunilkumar G, Mohr L, Lopata-Finch E, Emani C, Rathore KS. 2002. Developmental and tissue-specific expression of CaMV 35S promoter in cotton as revealed by GFP. Plant Molecular Biology **50**, 463–479.

Sussex IM. 1951. Experiments on the cause of dorsiventrality in leaves. Nature **167**, 651–652.

Sussex IM. 1952. Regeneration of the potato shoot apex. Nature **170**, 755–757.

Sussex IM. 1954. Experiments on the cause of dorsiventrality in leaves. Nature **174**, 351–352.

Takada S, Hibara K, Ishida T, Tasaka M. 2001. The *CUP-SHAPED COTYLEDON1* gene of *Arabidopsis* regulates shoot apical meristem formation. Development **128**, 1127–1135.

Talbert PB, Adler HT, Parks DW, Comai L. 1995. The *REVOLUTA* gene is necessary for apical meristem development and for limiting cell divisions in the leaves and stems of *Arabidopsis thaliana*. Development **121**, 2723–2735.

Tang G, Reinhart BJ, Bartel DP, Zamore PD. 2003. A biochemical framework for RNA silencing in plants. Genes & Development **17**, 49–63.

Teichmann T, Muhr M. 2015. Shaping plant architecture. Frontiers in Plant Science **6**, 1–18.

Tian Q, Uhlir NJ, Reed JW. 2002. Arabidopsis SHY2/IAA3 inhibits auxin-regulated gene expression. Plant Cell **14**, 301–319.

Timmermans MCP, Hudson A, Becraft PW, Nelson T. 1999. ROUGH SHEATH2: A MYB protein that represses *KNOX* homeobox genes in maize lateral organ primordia. Science **284**, 151–153.

Tsiantis M, Schneeberger R, Golz JF, Freeling M, Langdale JA. 1999. The maize *rough sheath2* gene and leaf development programs in monocot and dicot plants. Science **284**, 154–156.

Villanueva JM, Broadhvest J, Hauser BA, Meister RJ, Schneitz K, Gasser CS. 1999. *INNER NO OUTER* regulates abaxial-adaxial patterning in *Arabidopsis* ovules. Genes & Development **13**, 3160–3169.

Waites R, Hudson A. 1995. *Phantastica*: A gene required for dorsoventrality of leaves in *Antirrhinum majus*. Development **121**, 2143–2154.

Waites R, Selvadurai HRN, Oliver IR, Hudson A. 1998. The *PHANTASTICA* gene encodes a MYB transcription factor involved in growth and dorsoventrality of lateral organs in *Antirrhinum*. Cell **93**, 779–789.

Wang Y, Wang J, Shi B, Yu T, Qi J, Meyerowitz EM, Jiao Y. 2014. The stem cell niche in leaf axils is established by auxin and cytokinin in *Arabidopsis*. Plant Cell **26**, 2055–2067.

Wardlaw W. 1946. Experimental and analytical studies of Pteridophytes: IX. The effect of removing leaf primordia on the development of Angiopteris evecta. Annals of Botany **10**, 223–235.

Weberling F. 1989. Morphology of the inflorescence. Morphology of flowers and inflorescences.201–307.

Weigel D, Jürgens G. 2002. Stem cells that make stems. Nature **415**, 751–754.

Weits DA, Kunkowska AB, Kamps NCW, Portz KMS, Packbier NK, Venza ZN, Gaillochet C, Lohmann JU, Pedersen O, Van Dongen JT, Licausi F. 2019. An apical hypoxic niche sets the pace of shoot meristem activity. Nature **569**, 714–717.

Wenkel S, Emery J, Hou BH, Evans MMS, Barton MK. 2007. A feedback regulatory module formed by LITTLE ZIPPER and HD-ZIPIII genes. Plant Cell **19**, 3379–3390.

Wortman JR, Haas BJ, Hannick LI, Smith RK, Maiti R, Ronning CM, Chan AP, Yu C, Ayele M, Whitelaw CA, White OR, Town CD. 2003. Annotation of the Arabidopsis genome. Plant Physiology **132**, 461–468.

Xu L, Xu Y, Dong A, Sun Y, Pi L, Xu Y, Huang H. 2003. Novel *as1* and *as2* defects in leaf adaxial-abaxial polarity reveal the requirement for *ASYMMETRIC LEAVES1* and *2* and *ERECTA* functions in specifying leaf adaxial identity. Development **130**, 4097–4107.

Yamada T, Sasaki Y, Hashimoto K, Nakajima K, Gasser CS. 2016. *CORONA*, *PHABULOSA* and *PHAVOLUTA* collaborate with *BELL1* to confine *WUSCHEL* expression to the nucellus in *Arabidopsis* ovules. Development **143**, 422–426.

Yang F, Wang Q, Schmitz G, Müller D, Theres K. 2012. The bHLH protein ROX acts in concert with RAX1 and LAS to modulate axillary meristem formation in Arabidopsis. Plant Journal **71**, 61–70.

Yao X, Wang H, Li H, Yuan Z, Li F, Yang L, Huang H. 2009. Two types of *cis*-acting elements control the abaxial epidermis-specific transcription of the *MIR165a* and *MIR166a* genes. FEBS Letters **583**, 3711–3717.

Zhang W, Swarup R, Bennett M, Schaller GE, Kieber JJ. 2013. Cytokinin induces cell division in the quiescent center of the *Arabidopsis* root apical meristem. Current Biology **23**, 1979–1989.

Figure 3.1 Graphic representations of anatomy of mature *Arabidopsis* plants. Some organs have been omitted for simplicity. A) Basic anatomy of mature plant. Gray arrowhead shows primary stem. Purple arrow points to cauline leaf. Red arrowhead indicates axillary branch. Black arrow points to accessory bud. Numbers indicate paraclade junctions – the area where axillary branch, cauline leaf, and primary stem meet. The first paraclade junction formed is labeled "1", the second paraclade junction formed is labeled "2", and the third paraclade junction formed is labeled "3". The area outlined by black dotted lines represents the region shown in Figure 3.2 C, also known as the cauline-leaf paraclade. B) More detailed branching patterns in mature plant. Box with black dotted line outlines second-order cauline-leaf paraclade. Blue arrow indicates branches from the second-order cauline-leaf paraclades. Black arrowhead shows branch from rosette-leaf paraclade. Box with purple dotted line outlines second-order rosette-leaf paraclade. Red arrows indicate branches from second-order rosette-leaf paraclades.

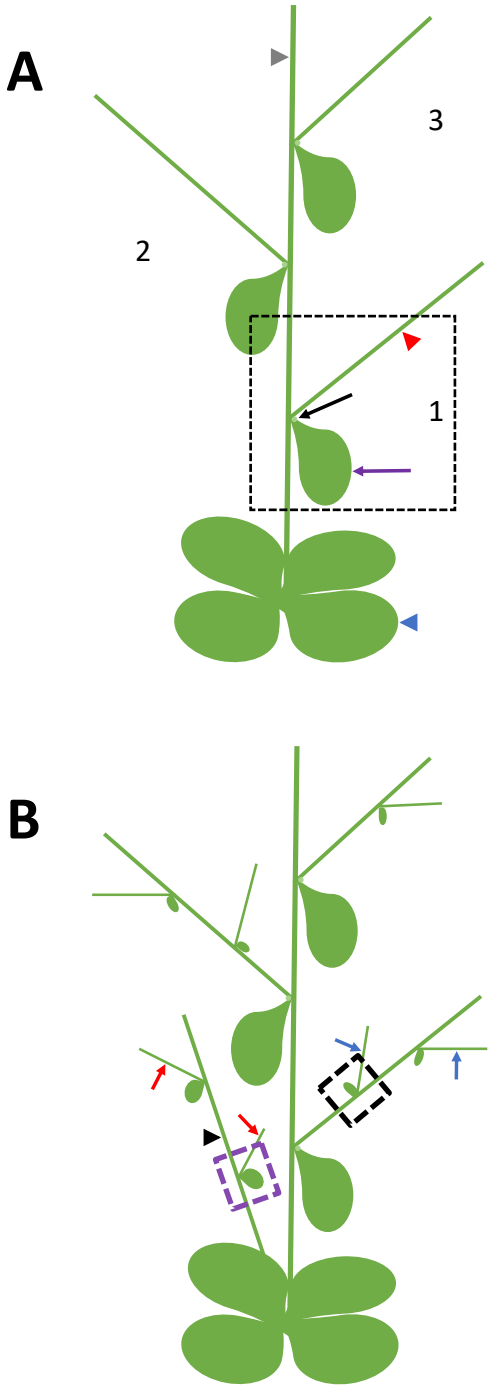
A
3
2
1
B

Figure 3.2 Phenotypes in Col-0, *lof1-1* single mutant, and *lfs-1D lof1-1* double mutant plants. A) Col-0 wild-type paraclade junction viewed from directly between cauline leaf and axillary branch (front). One accessory bud is visible. B) Col-0 wild-type paraclade junction viewed at an angle between cauline leaf and axillary branch. Accessory bud has initiated from directly between cauline leaf and axillary branch. C) Paraclade junction of Col-0 wild-type plant viewed from the side. D) *lof1-1* single mutant paraclade junction viewed from the side. E) *lfs-1D lof1-1* double mutant paraclade junction viewed from front. Accessory bud has initiated from side of junction between primary stem, axillary branch, and cauline leaf – a positional change in accessory bud position. F) *lfs-1D lof1-1* double mutant paraclade junction with multiple accessory buds. G) Col-0 wild-type paraclade junction viewed from the side. Accessory bud has not grown out. H) *lfs-1D lof1-1* double mutant paraclade junction viewed from the side. The accessory bud has grown out without damage to the axillary branch. All plants are six-weeks old at time of imaging. Adjustments to brightness and contrast have been applied throughout entire images. All scale bars are 1 mm in size.

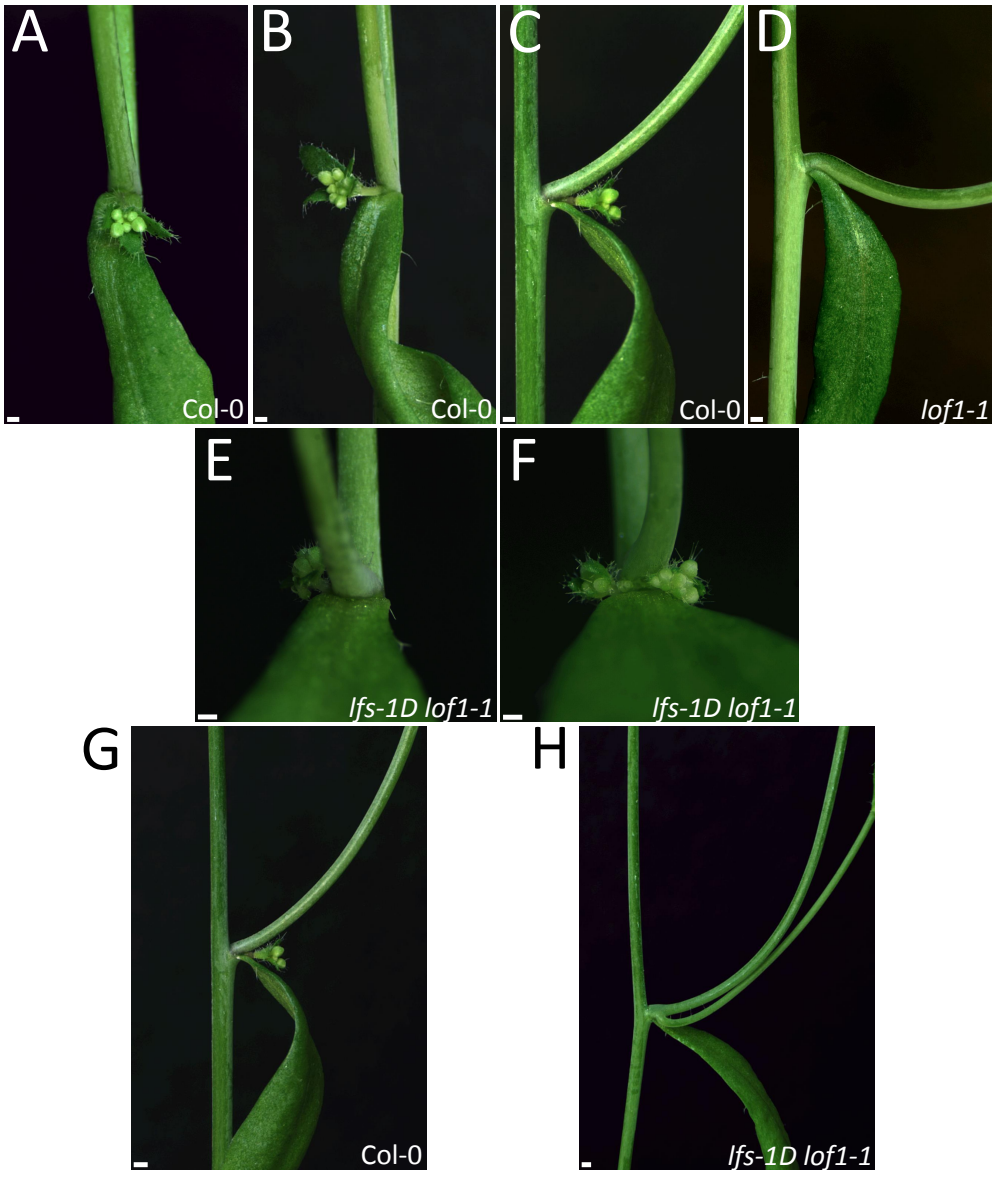
A
Col-0
B
Col-0
C
Col-0
D
lof1-1
E
lfs-1D lof1-1
F
lfs-1D lof1-1
G
Col-0
H
lfs-1D lof1-1

Figure 3.3 Graphic representation of paraclade junctions and accessory buds in WT, *phb-13*, *lof1-1* and *phb-13 lof1-1*. Each column represents an individual plant. Each row represents a paraclade junction on the plant; position is indicated "P1" for the first paraclade junction formed, "P2" for the second paraclade junction formed, and so on. Each box is an individual paraclade junction. The number in each box is the number of accessory buds formed in that paraclade junction. Boxes are color coded for ease of visualization. Yellow indicates zero accessory buds, green indicates one centrally-located accessory bud, blue indicates one offset accessory bud, and red indicates two accessory buds. *lof1-1* single mutants and *phb-13 lof1-1* double mutants did not typically form accessory buds. Wild-type plants formed zero to one accessory bud per paraclade junction with an occasional offset accessory bud. *phb-13* single mutants produce more accessory buds than WT and contained paraclade junctions with multiple accessory buds.


WT
phb-13
lof1-1
phb-13 lof1-1
P5
P4
P3
P2
P1

Figure 3.4 Graphic representation of paraclade junctions and accessory buds in Col-0, *pPHB:PHB* Col-0, *lof1-1*, and *pPHB:PHB lof1-1*. Graphic representation is the same as in Figure 3.3. Yellow indicates zero accessory buds, green indicates one centrally-located accessory bud, blue indicates one offset accessory bud, red indicates two accessory buds, and purple indicates three accessory buds. T2 *pPHB:PHB* transgenic lines were chosen so that line #1 in each genetic background was more severe than line #2 according to phenotypic and transgene expression data. Col-0 plants typically contained zero to one accessory bud per paraclade junction. On rare occasions, multiple accessory buds formed in one of the paraclade junctions. *pPHB:PHB* Col-0 #1 had more accessory buds overall and more cases of multiple accessory buds per paraclade junction compared to Col-0. *pPHB:PHB* Col-0 #2 did not appear different from Col-0. B) *lof1-1* single mutants rarely produced accessory buds in their paraclade junctions. *pPHB:PHB lof1-1* #1 plants regularly produced paraclade junctions with zero to two accessory buds per paraclade junction. Accessory buds were occasionally offset, and sometimes, three accessory buds were formed within the same paraclade junction. *pPHB:PHB lof1-1* #2 plants primarily produced paraclade junctions with no accessory buds. However, it was not uncommon for one offset accessory bud or two accessory buds to form per paraclade junction. *pPHB:PHB lof1-1* #1 and #2 both appeared different from *lof1-1* mutant controls.

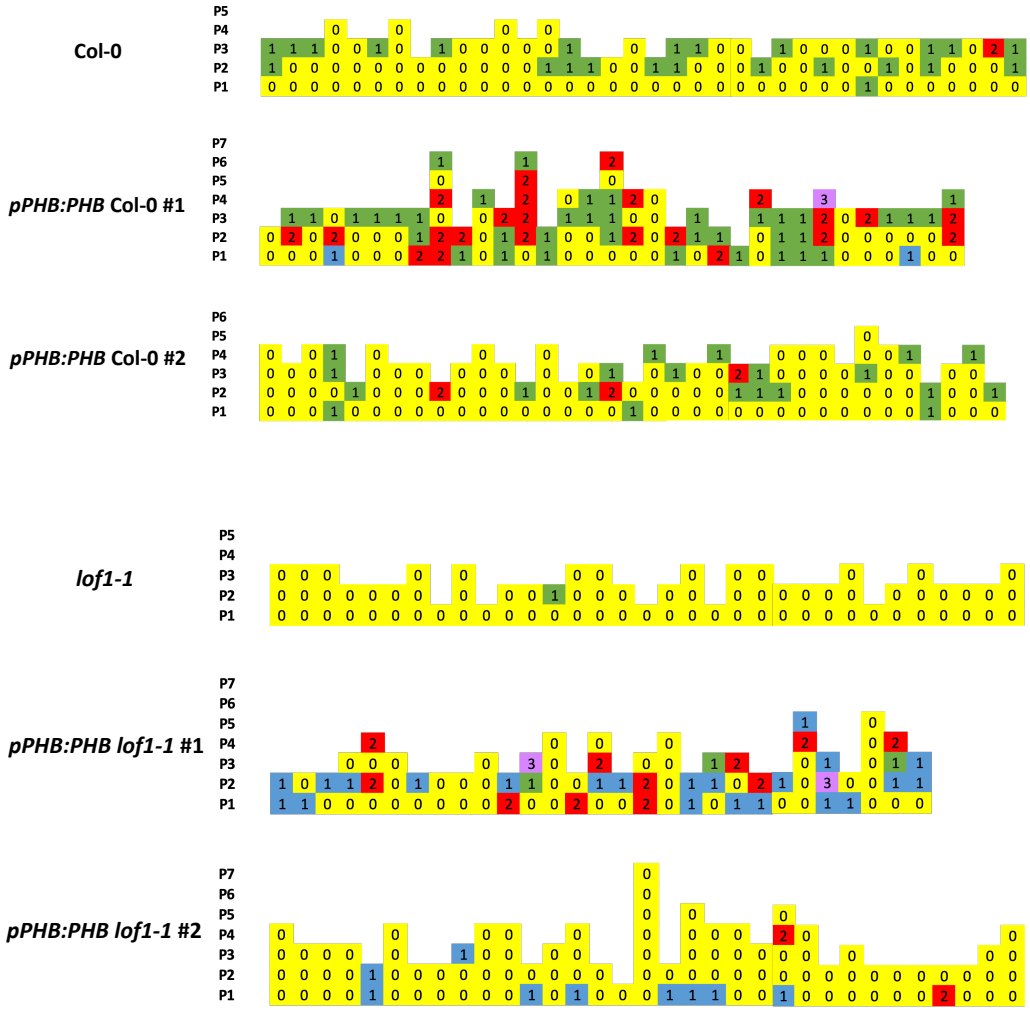
Col-0
pPHB:PHB Col-0 #1
pPHB:PHB Col-0 #2
lof1-1
pPHB:PHB lof1-1 #1
pPHB:PHB lof1-1 #2

Figure 3.5 Phenotypes of the *lfs-1D* single mutant plants. All images show six-week old *lfs-1D* mutant plants. A) Paraclade junction viewed from front. Accessory bud has initiated from side of junction between primary stem, axillary branch, and cauline leaf. B) Paraclade junction viewed from front with two accessory buds. C) Paraclade junction viewed from below directly between cauline leaf and axillary branch. Two accessory buds are present, and one accessory bud has grown out without visible damage to the axillary branch. *lfs-1D lof1-1* double mutants were backcrossed four times to Col-0 before imaging. *lof1-1* was segregated out after the second backcross to Col-0. Adjustments to brightness and contrast have been applied throughout entire images. All scale bars are 1 mm in size.

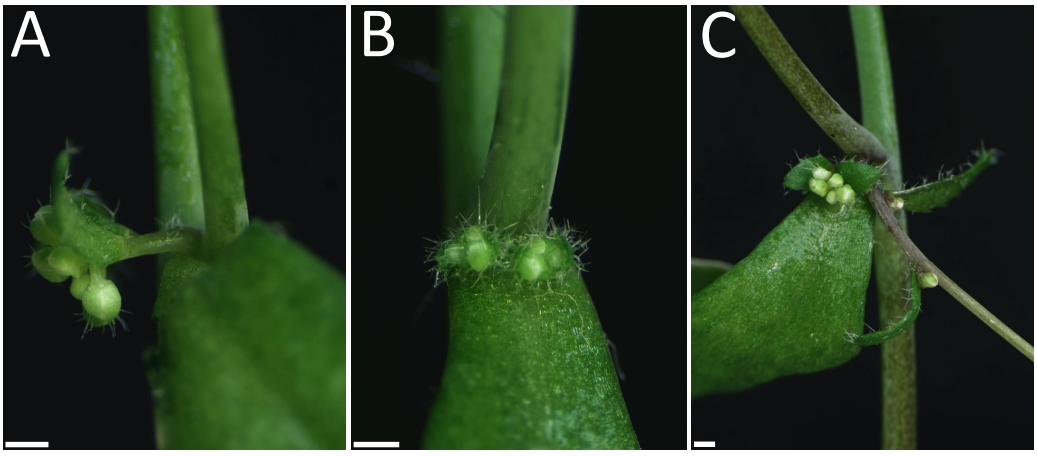

lfs-1D

Figure 3.6 *lfs-1D* mutant plants contain a mutation in *PHABULOSA* (*PHB*). Schematic representation of *PHB* gene structure. The gene is drawn in the 5' to 3' orientation. Filled boxes represent exons; lines represent introns. Open boxes represent the 5' and 3' untranslated regions (UTRs). The green box denotes the homeodomain of the PHB protein. The leucine zipper domain is indicated by the red box. The START domain is symbolized by the orange boxes. The black arrowheads represent the location of the *phb-1D* and *lfs-1D*/*phb382** mutations. The brackets give the location of the *miRNA 165/166* binding site, which spans exons 4 and 5. The blue triangle marks the T-DNA insertion site for *phb-13/*SALK_021684 mutation. The purple arrowheads show the sites of primers used for RT-PCR of the *PHB* endogenous sequence. The length of the scale bar represents 100 base pairs.

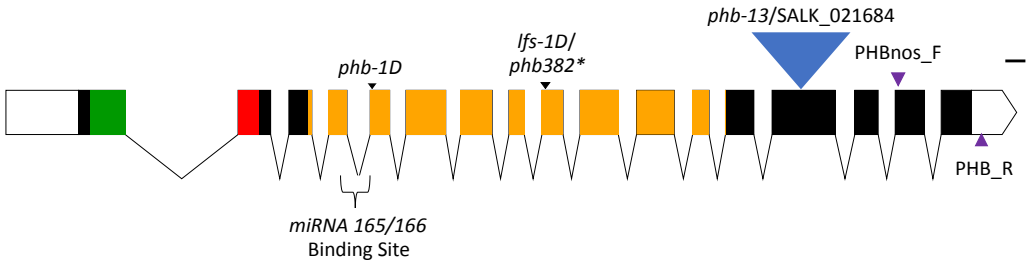
phb-13/SALK_021684
PHBnos_F
lfs-1D/
phb382*
phb-1D
PHB_R
miRNA 165/166
Binding Site

Figure 3.7 Phenotype of *pPHB:mPHB* plants in Col-0 background. A) Col-0 paraclade junction viewed from front. One accessory is visible. B) *pPHB:mPHB* paraclade junction viewed from front. Two accessory buds are visible. C) *pPHB:mPHB* paraclade junction viewed from front. Accessory bud has initiated from side of junction between primary stem, axillary branch, and cauline leaf. The cauline leaf has been excised to facilitate viewing the accessory bud. D) *pPHB:mPHB* paraclade junction viewed from the side. Two accessory buds are visible and one appears to be growing out without damage to the axillary branch. All plants are six-weeks old at time of imaging. All images of *pPHB:mPHB* plants are taken in the T1 generation. Adjustments to brightness and contrast have been applied throughout entire images. Scale bars in A, B, and C are 1 mm in size. Scale bar in D is 2 mm.

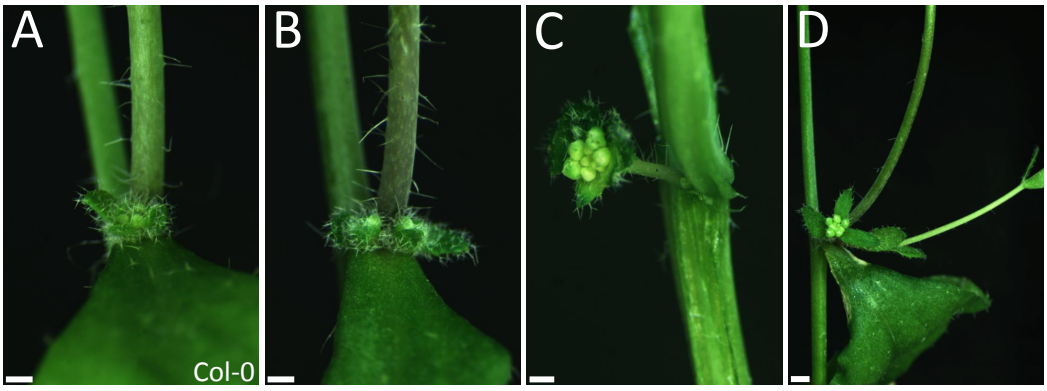
A
B
C
D
Col-0
pPHB:mPHB

Figure 3.8 Phenotype of *pPHB:PHB* plants in Col-0 background. A) Col-0 paraclade junction viewed from front. One accessory is visible. B) *pPHB:PHB* paraclade junction viewed from front. Two accessory buds are visible. C) *pPHB:PHB* paraclade junction viewed front. Accessory bud has initiated from side of junction between primary stem, axillary branch, and cauline leaf. The cauline leaf has been excised to facilitate viewing the accessory bud. D) *pPHB:PHB* paraclade junction viewed from the side. Two accessory buds are visible and both appear to be growing out without damage to the axillary branch. All plants are six-weeks old at time of imaging. Adjustments to brightness and contrast have been applied throughout entire images. All images of *pPHB:PHB* plants are in the T2 generation. Scale bars in A, B, and C are 1 mm in size. Scale bar in D is 2 mm.


A
B
C
D
Col-0
pPHB:PHB

Figure 3.9 *PHB* transgene and wild-type *PHB* transcript levels in T2 *pPHB:PHB* Col-0 and Col-0 controls. Semi-quantitative RT-PCR of *PHB* transgene and *PHB* endogenous transcript levels. Numbers above gel lanes indicate each individual T2 line used. "C" indicates Col-0 control. RNA was isolated from pooled *pPHB:PHB lof1-1* seedlings at 10-days of age, grown on selective media. Controls were grown on non-selective media. T2 lines were chosen based on segregation ratios on selective media (ppt) indicating one transgene locus and T1 phenotype. Primers PHBnosRT_F and PHBnosRT_R were used for the *PHB* transgene. Primers PHBnosRT_F and PHB_R were used for wild-type *PHB*. Sequences of primers used for RT-PCR are listed in Table 3.3. Cycle numbers are indicated to the right of the gel lanes in parentheses.

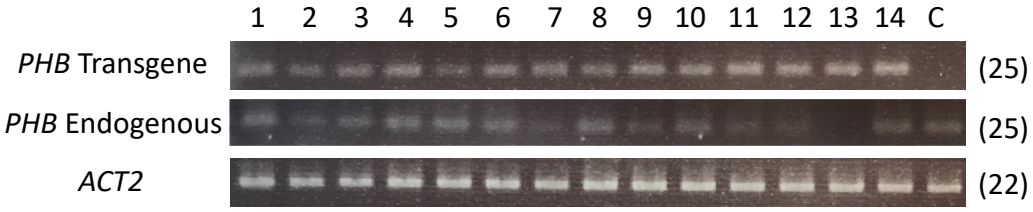
1 2 3 4 5 6 7 8 9 10 11 12 13 14 C
PHB Transgene
(25)
PHB Endogenous
(25)
ACT2
(22)

Figure 3.10 *PHB* transgene and wild-type *PHB* transcript levels in T2 *pPHB:PHB lof1-1* and Col-0 controls. Semi-quantitative RT-PCR of *PHB* transgene and *PHB* endogenous transcript levels. Numbers above gel lanes indicate each individual T2 line used. "C" indicates Col-0 control. RNA was isolated from pooled *pPHB:PHB lof1-1* seedlings at 10-days of age, grown on selective media. Controls were grown on non-selective media. T2 lines were chosen based on segregation ratios on selective media (ppt) indicating one transgene locus and T1 phenotype. Primers PHBnosRT_F and PHBnosRT_R were used for the *PHB* transgene. Primers PHBnosRT_F and PHB_R were used for wild-type *PHB*. Sequences of primers used for RT-PCR are listed in Table 3.3. Cycle numbers are indicated to the right of the gel lanes in parentheses.

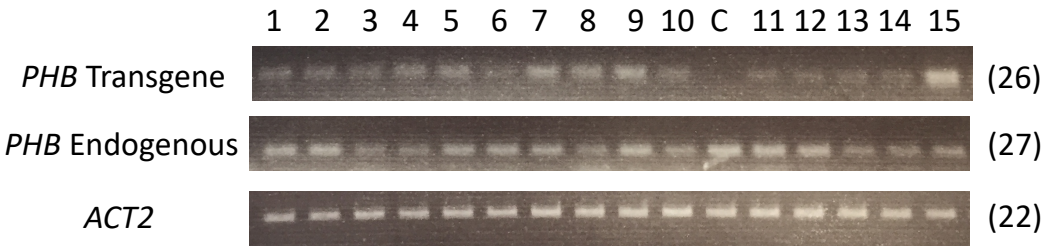
1 2 3 4 5 6 7 8 9 10 C 11 12 13 14 15
PHB Transgene
(26)
PHB Endogenous
(27)
ACT2
(22)

Figure 3.11 *PHB* and *LOF1* transcript levels in WT, *lof1-1*, *phb-13*, and *phb-13 lof1-1* rosette leaves and paraclade junctions. A) Semi-quantitative RT-PCR of endogenous *PHB* transcript levels WT (Col-0) and *phb-13* mutant rosette leaves. RNA was isolated from two-week old plants. Each biological replicate consists of tissue pooled from five rosette leaves. There are two replicates for each genotype. B) Semi-quantitative RT-PCR levels of endogenous *PHB* transcript levels between WT, *lof1-1*, *phb-13*, and *lof1-1 phb-13* paraclade junctions. Each sample contains five pooled paraclade junctions. C) Semi-quantitative RT-PCR of *LOF1* transcript levels between WT, *lof1-1*, *phb-13*, and *lof1-1 phb-13* paraclade junctions. Tissue is the same as in panel B. All samples in panels A, B, and C are from F4 populations derived from the same F1 parent of a cross between *phb-13 er-2* double and *lof1-1* single mutants. Primers PHBnosRT_F and PHB_R were used for wild-type *PHB*. Primers MYB117seq and LOF1RT_R were used for *LOF1*. Sequences of primers used for RT-PCR are listed in Table 3.3. Cycle numbers are indicated to the right of the gel lanes in parentheses.

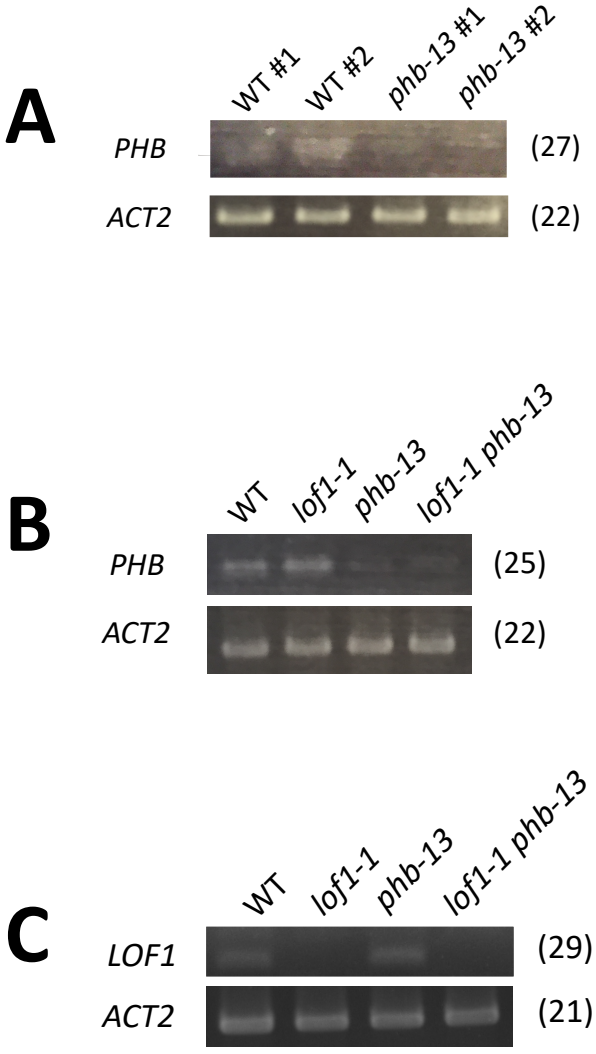
A
WT #1
WT #2
phb-13 #1
phb-13 #2
PHB
(27)
ACT2
(22)
B
WT
lof1-1
phb-13
lof1-1 phb-13
PHB
(25)
ACT2
(22)
C
WT
lof1-1
phb-13
lof1-1 phb-13
LOF1
(29)
ACT2
(21)

Figure 3.12 *phb-13 lof1-1* double mutant phenotype. A) Col-0 paraclade junction viewed from the side. There is one accessory bud and no visible fusion. B) *lof1-1* single mutant paraclade junction viewed from the side. There are no accessory buds and fusion between the axillary branch and cauline leaf. C) *phb-13* paraclade junction viewed from the side. There is one accessory bud and no visible fusion. D) *lof1-1 phb-13* single mutant paraclade junction viewed from the side. There are no accessory buds and fusion between the axillary branch and cauline leaf. All plants are six-weeks old at time of imaging and from F4 populations derived from a cross between *phb-13 er-2* double and *lof1-1* single mutant. Adjustments to brightness and contrast have been applied throughout entire images. All scale bars are 1 mm in size.

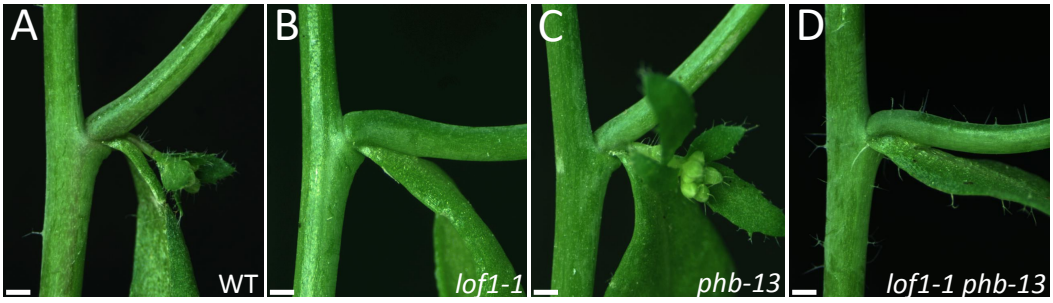
A
WT
B
lof1-1
C
phb-13
D
lof1-1 phb-13

Figure 3.13 *pPHB:PHB* and *pPHB:mPHB* rosette leaves. A) Col-0 rosette leaf adaxial side. B) Col-0 rosette leaf abaxial side. C-D) Radial rosette leaf from *pPHB:PHB* plant. E) Col-0 rosette leaf adaxial side. F) Col-0 rosette leaf abaxial side. G) Radial rosette leaf from *pPHB:mPHB* plant. H) Magnification of panel G. I) Rosette leaf from *pPHB:PHB* plant side that was facing upwards towards the top of the plant. J) Underside of rosette leaf shown in panel I. K) Rosette leaf from *pPHB:mPHB* plant side that was facing upwards towards the top of the plant. L) Underside of rosette leaf shown in panel K. M) Rosette leaf from *pPHB:mPHB* plant side that was facing upwards towards the top of the plant. N) Underside of rosette leaf shown in panel M. O) Magnification of panel M. Panels A and B are controls for panels C, D, I, and J. Panels E and F are controls for panels G, H, and K-O. All plants are four-weeks old at time of imaging. All *pPHB:PHB* and *pPHB:mPHB* plants pictured are in the T1 generation. Adjustments to brightness and contrast have been applied throughout entire images. In panels C-M, scale bars are 1 mm in size. In panels A and B, scale bars are 2 mm.

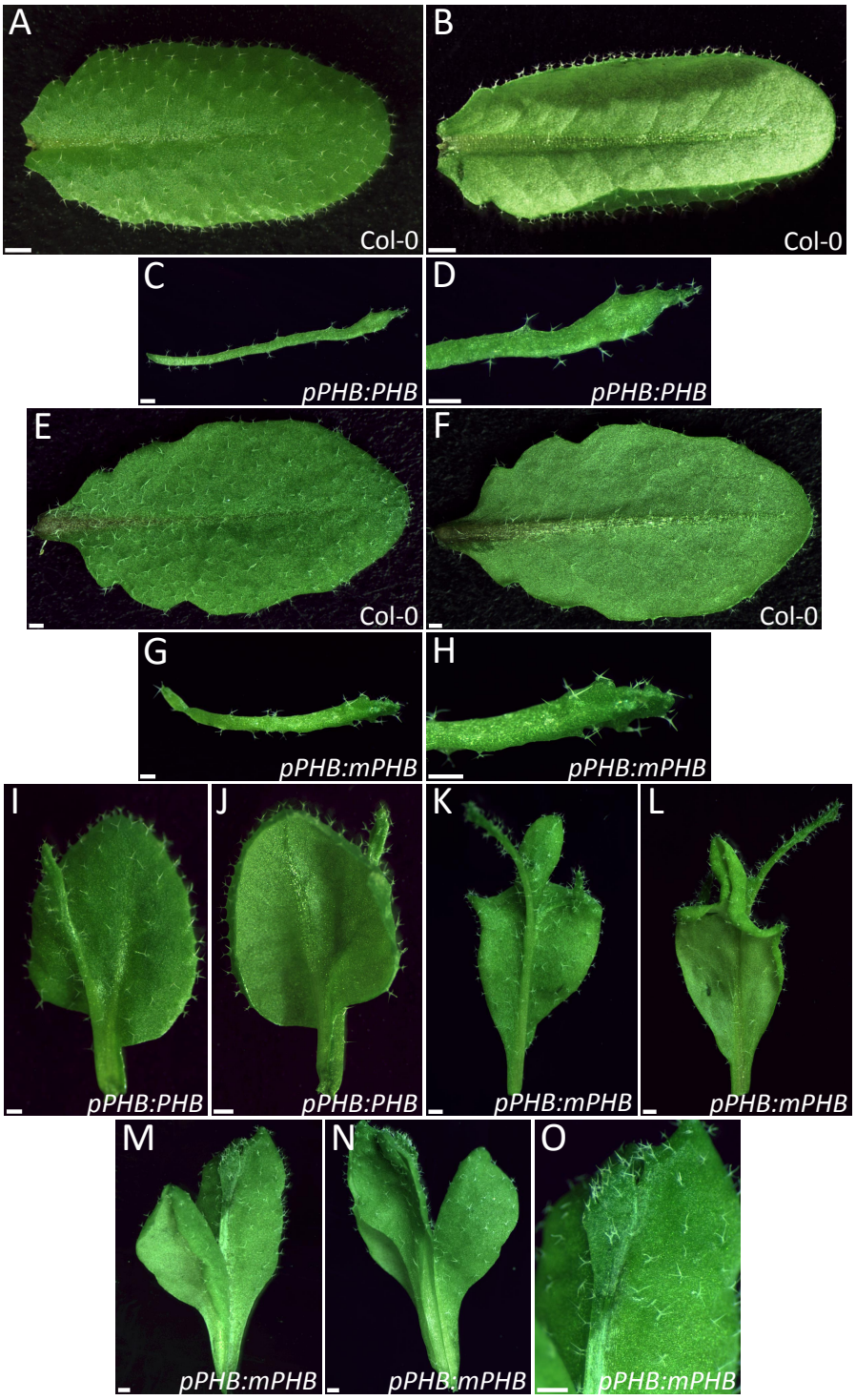
A
Col-0
B
Col-0
C
pPHB:PHB
D
pPHB:PHB
E
Col-0
F
Col-0
G
pPHB:mPHB
H
pPHB:mPHB
I
pPHB:PHB
J
pPHB:PHB
K
pPHB:mPHB
L
pPHB:mPHB
M
pPHB:mPHB
N
pPHB:mPHB
O
pPHB:mPHB

Figure 3.14 *pPHB:PHB* and *pPHB:mPHB* cauline leaves. A) Col-0 cauline leaf view of the adaxial side from above. B) Col-0 cauline leaf view of the abaxial side from above. C) Radial cauline leaf on *pPHB:PHB* plant. D) Radial cauline leaf on *pPHB:mPHB* plant. All plants are six-weeks old at time of imaging. All *pPHB:PHB* and *pPHB:mPHB* plants pictured are in the T1 generation. Adjustments to brightness and contrast have been applied throughout entire images. All scale bars are 1 mm in size.

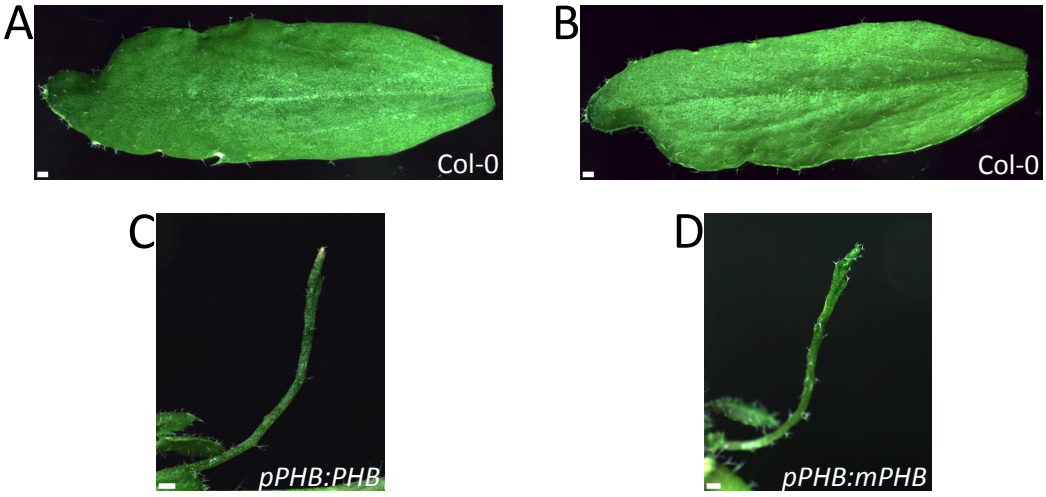
A
Col-0
B
Col-0
C
pPHB:PHB
D
pPHB:mPHB

Figure 3.15 *pPHB:PHB* seedling true leaves. A) Col-0 seedling with two rounded true leaves. B-C) T2 *pPHB:PHB* seedling with true leaves fused in a cup-like shape. D-E) *pPHB:PHB* seedling with fused true leaves. F) *pPHB:PHB* seedling with two radial first true leaves. G) *pPHB:PHB* seedling with two partially radial first true leaves. Distal ends of leaves are more prone to radialization. H) *pPHB:PHB* seedling with one radial and one partially radial true leaf. I) *pPHB:PHB* seedling with one rounded (wild-type appearance) and one partially radial true leaf. J) *pPHB:PHB* seedling with one partially radial true leaf. Seedlings in A-C and F-J are 10-days old at time of imaging. Seedlings in D and E are 16-days old at time of imaging. All *pPHB:PHB* seedlings pictured are in the T2 generation. T2 plants were grown without selection and were segregating for the transgene locus. Adjustments to brightness and contrast have been applied throughout entire images. All scale bars are 1 mm in size.

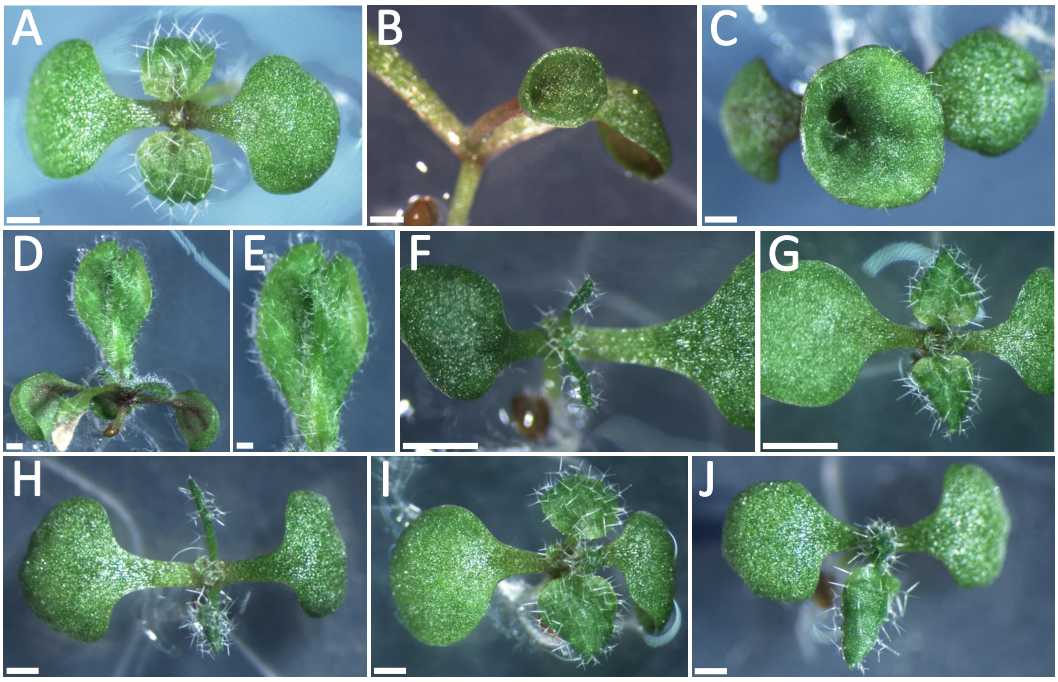

A: Col-0
B-J: *pPHB:PHB*

F**igure 3.16 *pPHB:PHB* seedling meristems and cotyledons.** All images show *pPHB:PHB* seedlings. A and B) fused cotyledons. C) Some *pPHB:PHB* seedlings are small in size (seedling on right), while some are similar in size to Col-0 seedlings (on left). D) Meristem terminated in a visible pin (red arrowhead). E) Meristem terminated without a visible pin. F) Three cotyledons. Seedlings are all 10-days old at time of imaging. All *pPHB:PHB* seedlings pictured are in the T2 generation. T2 plants were grown without selection and were segregating for the transgene locus. Adjustments to brightness and contrast have been applied throughout entire images. Scale bars in A, B, and D-F are 1 mm in size. Scale bar in C is 2 mm in size.

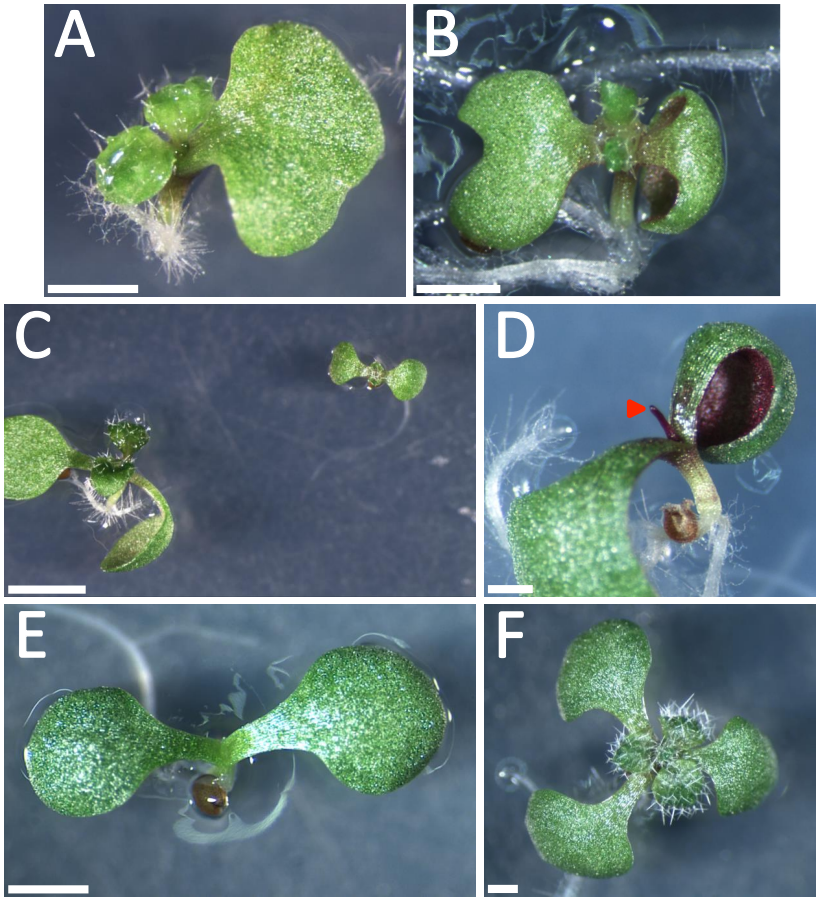

pPHB:mPHB

Figure 3.17 Phyllotaxy and silique shape in *pPHB:PHB* and *pPHB:mPHB*. A) Phyllotaxy of siliques on the primary inflorescence of Col-0 plant above the paraclade junctions. B) Phyllotaxy of siliques on the primary inflorescence of a *pPHB:PHB* plant above the paraclade junctions. C) Phyllotaxy of siliques on the primary inflorescence of *pPHB:mPHB* plant above the paraclade junctions. D) Col-0 silique. E) *pPHB:PHB* silique. F) *pPHB:mPHB* silique. Plants are all six-weeks old at time of imaging. All *pPHB:PHB* and *pPHB:mPHB* plants pictured are in the T1 generation. Adjustments to brightness and contrast have been applied throughout entire images. All scale bars are 1 mm in size.

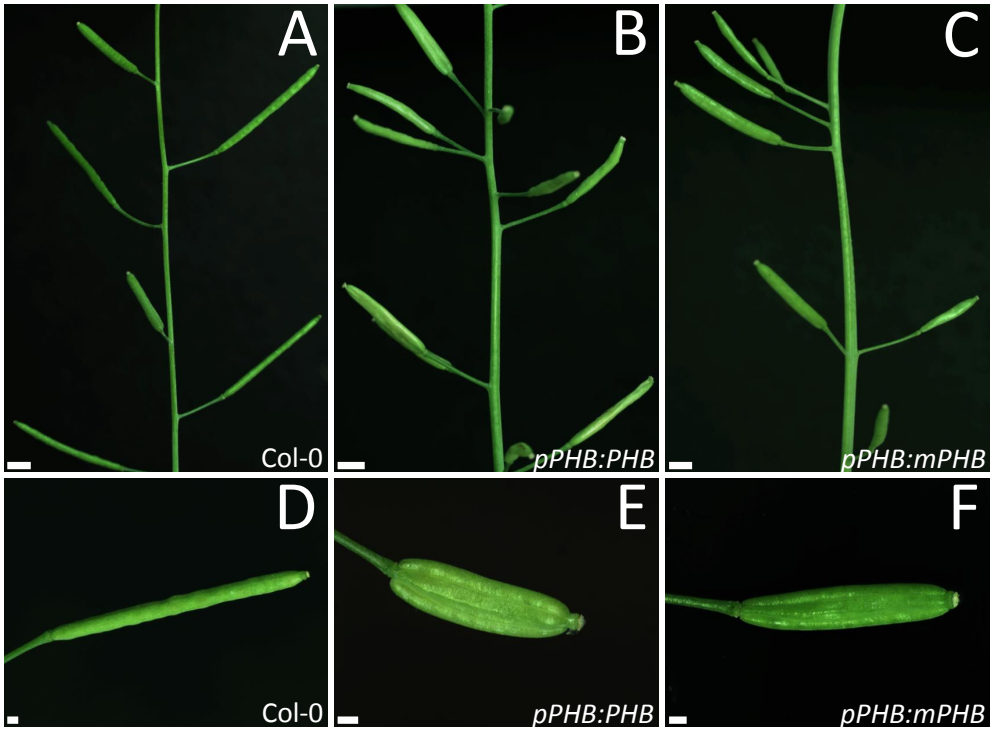
A
Col-0
B
pPHB:PHB
C
pPHB:mPHB
D
Col-0
E
pPHB:PHB
F
pPHB:mPHB

Figure 3.18 Meristems in *pPHB:PHB* and *pPHB:mPHB* plants. A) Col-0 primary inflorescence tip viewed from above. B) *pPHB:PHB* primary inflorescence tip viewed from above. C) *pPHB:mPHB* primary inflorescence tip viewed from above. D) Col-0 primary inflorescence stem above the paraclade junctions. E) *pPHB:PHB* primary inflorescence stem above the paraclade junctions. F) *pPHB:mPHB* primary inflorescence stem above the paraclade junctions. All plants were six-weeks old at time of imaging. All *pPHB:PHB* and *pPHB:mPHB* plants pictured are in the T1 generation. Adjustments to brightness and contrast have been applied throughout entire images. All scale bars are 1 mm in size.

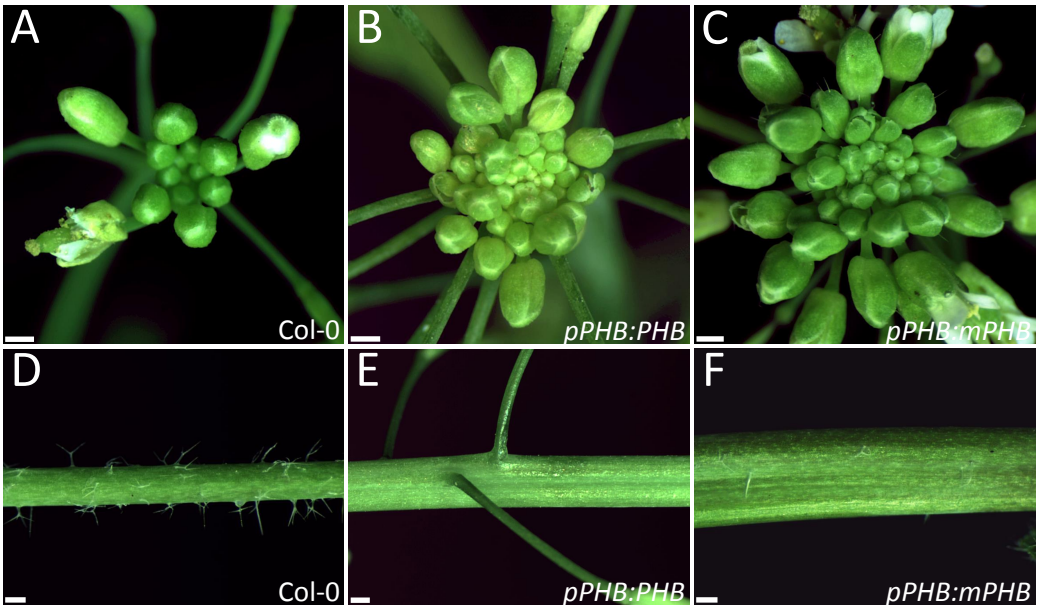
A
Col-0
B
pPHB:PHB
C
pPHB:mPHB
D
Col-0
E
pPHB:PHB
F
pPHB:mPHB

Figure 3.19 Decurrent strands and paraclade junctions in *pPHB:PHB lof1-1* and *pPHB:mPHB lof1-1*. A) Col-0 paraclade junction viewed from the side, showing clear separation between primary stem and cauline leaf. B) *pPHB:PHB lof1-1* paraclade junction with decurrent strand between primary stem and cauline leaf. C) *pPHB:mPHB lof1-1* paraclade junction with decurrent strand between primary stem and cauline leaf. Occasionally, the axillary branch fails not grow out as seen here. D) Col-0 paraclade junction viewed from front with one cauline leaf. E) *pPHB:PHB lof1-1* paraclade junction viewed from front with two cauline leaves. F) *pPHB:mPHB lof1-1* paraclade junction viewed from front with two cauline leaves. White arrows indicate decurrent strands. All plants were six-weeks old at time of imaging. All *pPHB:PHB lof1-1* and *pPHB:mPHB lof1-1* plants pictured are in the T1 generation. Adjustments to brightness and contrast have been applied throughout entire images. All scale bars are 1 mm in size.

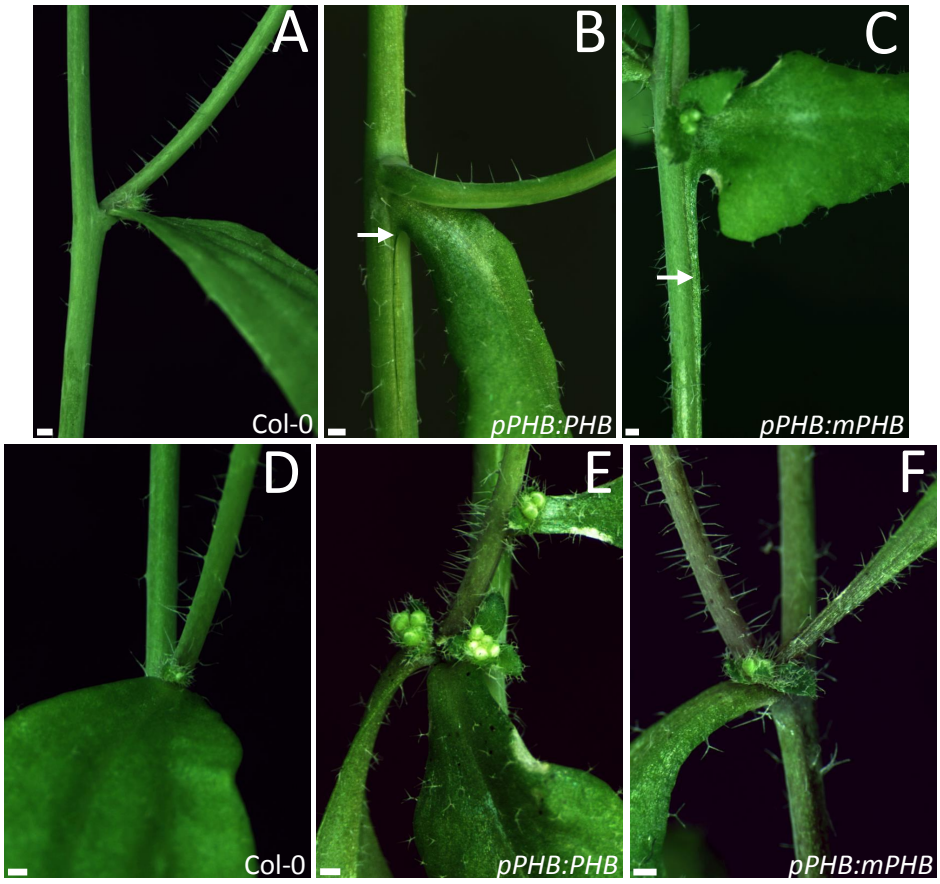
A
Col-0
B
pPHB:PHB
C
pPHB:mPHB
D
Col-0
E
pPHB:PHB
F
pPHB:mPHB

Figure 3.20 Paraclade junctions of *pPHB:PHB* and *pPHB:mPHB* plants in the *lof1-1* and *phb-13 lof1-1* genetic backgrounds. A) Col-0 paraclade junction viewed from the front. B) Col-0 paraclade junction viewed from the side. C) *pPHB:PHB* paraclade junction viewed from the side. Paraclade is connected to second order paraclade by a decurrent strand. D) *pPHB:PHB* paraclade junction viewed from the side. Paraclade junction is connected to second order paraclade by a decurrent strand that has torn due to stress. Another branch has grown out that appears similar to a secondary branch. E) *pPHB:mPHB* paraclade junction viewed from the front. Paraclade is connected to second order paraclade by a decurrent strand. F) *pPHB:mPHB* paraclade junction viewed from the side. White arrows indicate decurrent strands. Red arrowheads indicate tearing of decurrent strands. All plants are six-weeks old at time of imaging. All *pPHB:PHB* and *pPHB:mPHB* plants pictured are in the T1 generation. Adjustments to brightness and contrast have been applied throughout entire images. All scale bars are 1 mm in size.

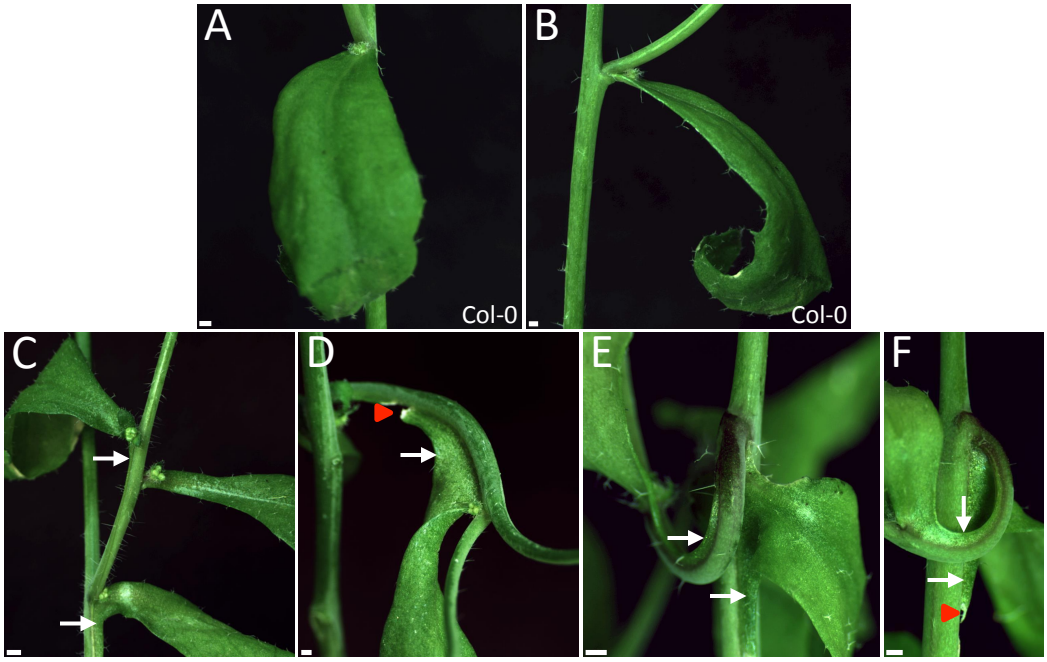
A
Col-0
B
Col-0
C
D
E
F
pPHB:PHB lof1-1
pPHB:mPHB lof1-1

Figure 3.21 Rosette leaves in plants that misexpress *LOF1*. A) Col-0 whole plant. B) *LOF1* overexpressing (T1 *35S:LOF1*) plant. Leaves curl upwards. *LOF1* overexpressing plants are typically smaller and flower earlier than wild-type controls. C) Close-up view of rosette leaf from panel B showing upward leaf curling. All plants were 3.5-weeks old at time of imaging. Adjustments to brightness and contrast have been applied throughout entire images. Scale bars in A and B are 5 mm in length. Scale bar in C is 1 mm in length.


A
Col-0
B
35S:LOF1
C
35S:LOF1

Figure 3.22 Flower phenotypes in plants that overexpress *LOF1*. A) Col-0 control flower viewed from above. B) Col-0 control flower viewed from the side. C) Tip of inflorescence of Col-0 control plant. D) *35S:LOF1* flower viewed from above. E) *35S:LOF1* flower viewed from the side. Reduced sepal is directly under the blue asterisk. Reduced petal directly under the red arrowhead. F) Tip of inflorescence meristem of *35S:LOF1* plant. All flowers are from five-week old plants at time of imaging. All *35S:LOF1* flowers pictured are from T1 generation plants. Adjustments to brightness and contrast have been applied throughout entire images. All scale bars are 1 mm in length.

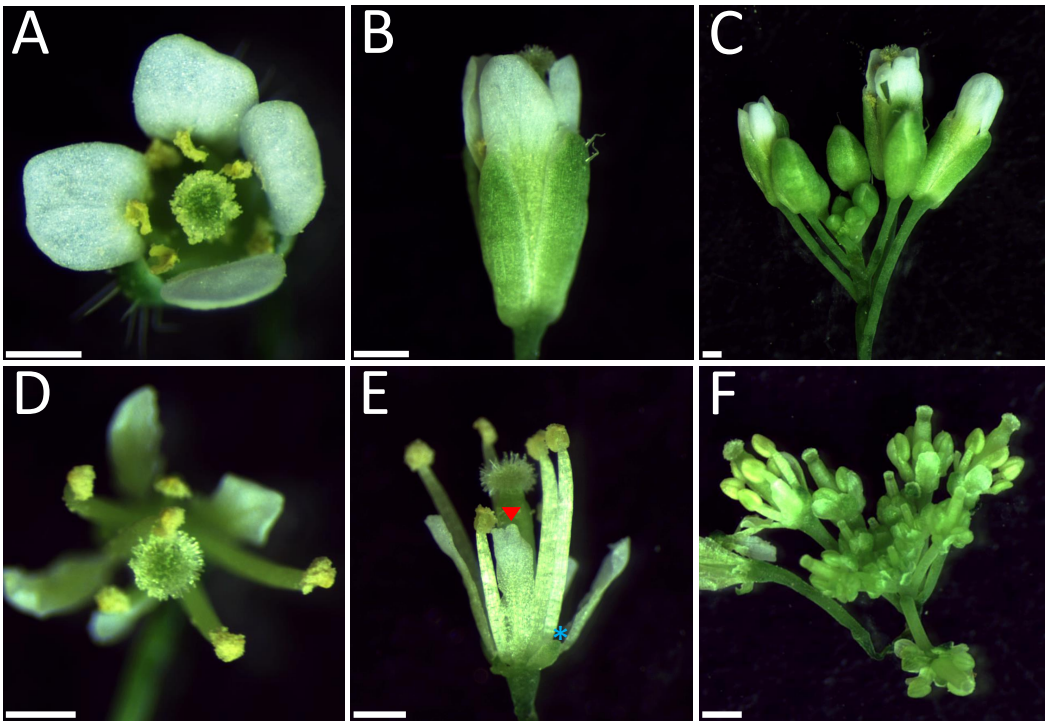

A-C: WT
D-F: *35S:LOF1*

Figure 3.23 Flower phenotypes in *lof1-1* and *lof1-1 phb-13* mutants. A) Col-0 flower with typical petal and stamen shape. Sepals have been removed for ease of viewing. B) *lof1-1 phb-13* petal/stamen organ that appears more stamen-like. C) *lof1-1 phb-13* petal/stamen organ that appears more petal-like. Phenotypes shown in B and C were present in *lof1-1* single mutants but occurred at a higher frequency in *lof1-1 phb-13* double mutant plants. All images were captured when plants were four-weeks old. Flowers are from F4 population derived from a cross between *phb-13 er-2* double and *lof1-1* single mutant plants. Adjustments to brightness and contrast have been applied throughout entire images. All scale bars are 1 mm in length.

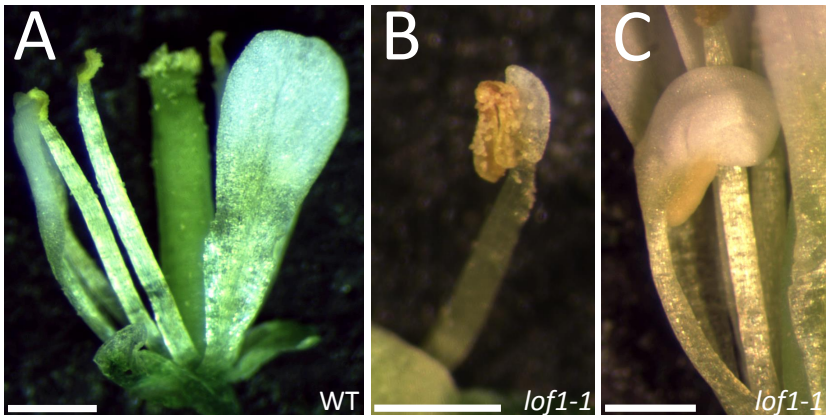
A
WT
B
lof1-1
C
lof1-1

Figure 3.24 Flower phenotypes in *phb-13 phv-11 cna-2 er-2* quadruple mutants. A) *phb-13 phv-11 cna-2 er-2* mutant flower with wild-type petal shape, indicated by a red arrowhead. B) *phb-13 phv-11 cna-2 er-2* petal with trumpet-like shape. C) *phb-13 phv-11 cna-2 er-2* mutant with a forked/fused-like shape, indicated by a blue asterisk. D) *phb-13 phv-11 cna-2 er-2* mutant petal with lobed/fused-like shape. E) *phb-13 phv-11 cna-2 er-2* mutant radial petals. Red arrowhead points to radial petal. F) *er-2* single mutant flower with well separated sepals. G) *phb-13 phv-11 cna-2 er-2* mutant fused sepals as shown by orange square. H) *er-2* single mutant flower with sepals removed showing WT shape and development of stamens. I) *phb-13 phv-11 cna-2 er-2* mutant with fused stamens (red arrow). J) *phb-13 phv-11 cna-2 er-2* mutant flower with stamen with undeveloped anther (red arrow). K) *phb-13 phv-11 cna-2 er-2* mutant flower with undeveloped stamen (red arrow). L) *er-2* single mutant flower with four petals and six stamens. M) *phb-13 phv-11 cna-2 er-2* mutant flower with five petals. N) *phb-13 phv-11 cna-2 er-2* mutant flower with extra stamens. All images were captured when plants were six-weeks old. Adjustments to brightness and contrast have been applied throughout entire images. All scale bars are 1 mm in length.

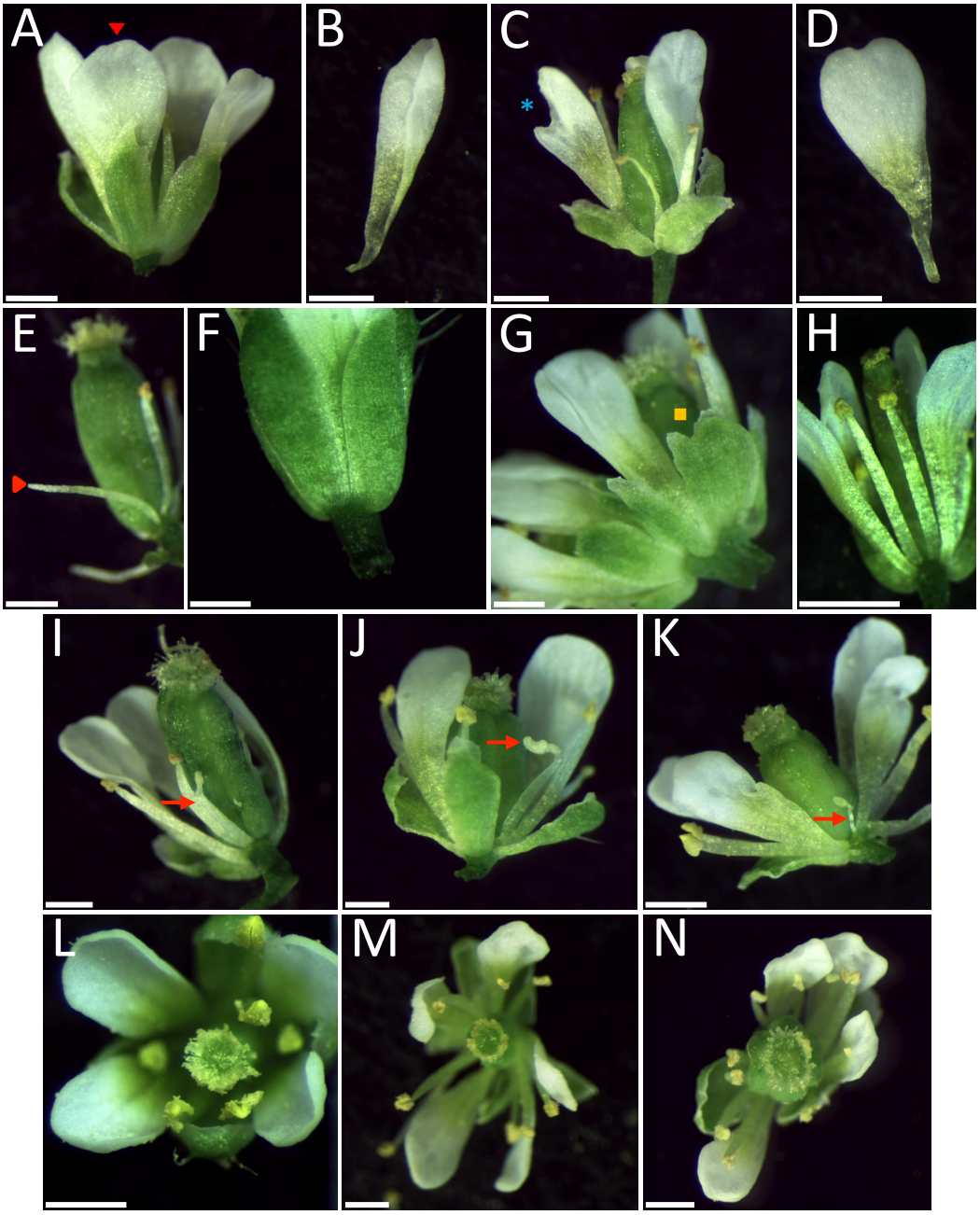

A-E,G, I-K, and M-N: *phb-13 phv-11 cna-2 er-2*
F,H, and L: *er-2*

Figure 3.25 Flower phenotypes in *pPHB:PHB* in Col-0 and *lof1-1* genetic backgrounds. A) Col-0 control flower with four petals and six stamens viewed from above. B) Col-0 control flower viewed from the side showing typical petal shape and stamen development. Sepal has been pushed down for ease for viewing. C) *pPHB:PHB* flower with radial petal (left) and trumpet shaped petal (right). D) Isolated radial (left) and trumpet-shaped (right) petals that were removed from *pPHB:PHB* plant. Radial petal is labeled "R" and trumpet petal is labeled "T" in panels C and D. E and F) *pPHB:PHB* flower with carpel defects. Red arrowhead points to forked petal. White arrow points to ovules on top of carpel. H) *pPHB:PHB* flower with five petals. I) *pPHB:PHB* flower with underdeveloped stamens (blue arrowheads). Some sepals and petals have been removed to facilitate viewing. J) *pPHB:PHB* flower with fused stamens (red arrowhead). K) *pPHB:PHB* flower with seven stamens. All images were captured when plants were six-weeks old. All *pPHB:PHB* plants pictured are in the T2 generation. Adjustments to brightness and contrast have been applied throughout entire images. All scale bars are 1 mm in length.

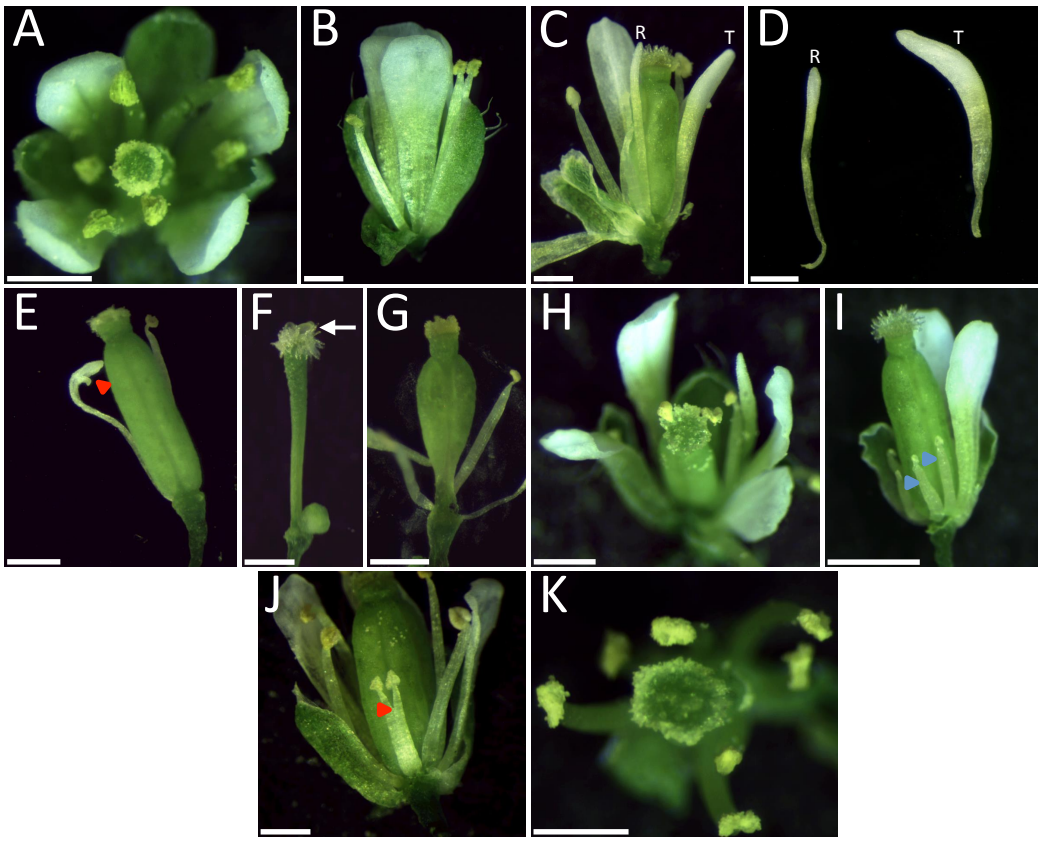

A-B: Col-0
C-K: *pPHB:PHB*

Figure 3.26 Accessory bud phenotypes in WT, *lof1-1*, *phb-13*, and *lof1-1 phb-13*. A) Average number of accessory buds per plant for WT and *phb-13*. *lof1-1* and *lof1-1 phb-13* had no accessory buds on any plants, so these genotypes were excluded from the graph. B) 100% stacked column graph for accessory bud phenotype in each genotype. Plants were seven-weeks old at time data was collected. *= $p < 0.05$. **= $p < 0.01$. Significance measured by student t-test. Bars represent standard error.

A

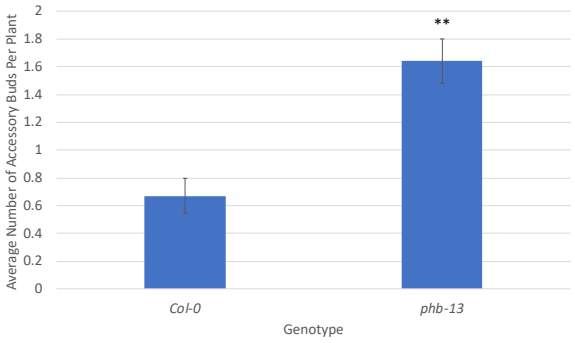
Average Number of Accessory Buds Per Plant
2
1.8
1.6
1.4
1.2
1
0.8
0.6
0.4
0.2
0
**
Col-0
phb-13
Genotype

B

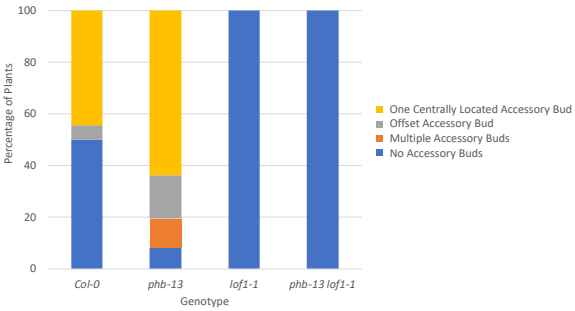
Percentage of Plants
100
80
60
40
20
0
Col-0
phb-13
lof1-1
phb-13 lof1-1
Genotype
One Centrally Located Accessory Bud
Offset Accessory Bud
Multiple Accessory Buds
No Accessory Buds

Figure 3.27 Branching and paraclade junction phenotypes in WT, *lof1-1*, *phb-13*, and *lof1-1 phb-13*. A) Average number of rosette-leaf paraclade branches per plant. B) Average number of cauline-leaf paraclade branches per plant. C) Average number of first order cauline-leaf paraclade junctions per plant. D) Average number of second order cauline-leaf paraclade branches per plant. Plants were seven-weeks old at time data was collected. *= $p < 0.05$. **= $p < 0.01$. Significance measured by student t-test. Bars represent standard error.

A

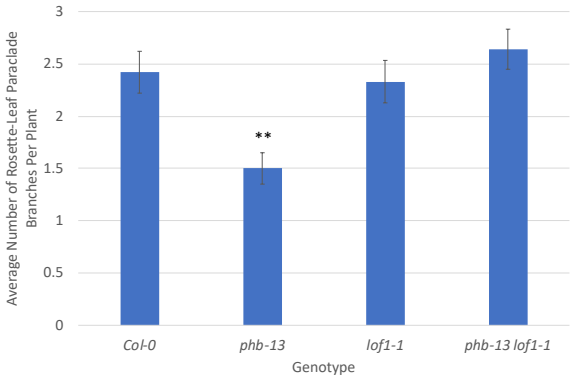
Average Number of Rosette-Leaf Paraclade Branches Per Plant
3
2.5
2
1.5
1
0.5
0
**
Col-0
phb-13
lof1-1
phb-13 lof1-1
Genotype

B

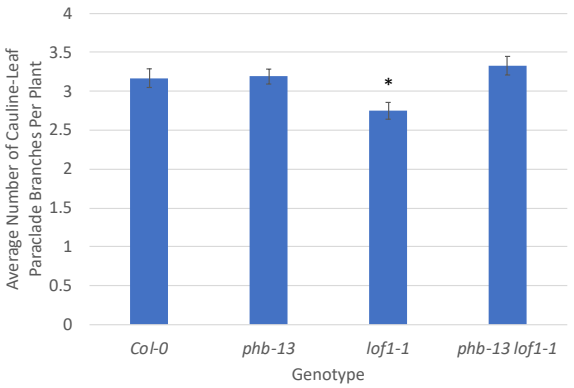
Average Number of Cauline-Leaf Paraclade Branches Per Plant
4
3.5
3
2.5
2
1.5
1
0.5
0
*
Col-0
phb-13
lof1-1
phb-13 lof1-1
Genotype

C

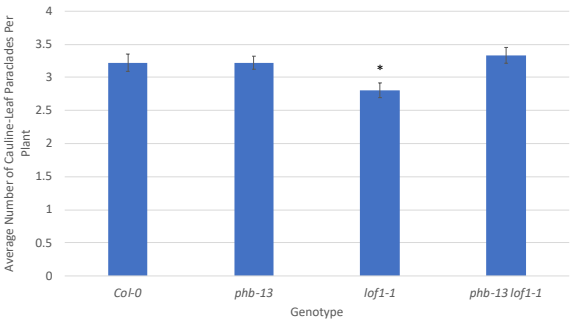
Average Number of Cauline-Leaf Paraclades Per Plant
4
3.5
3
2.5
2
1.5
1
0.5
0
*
Col-0
phb-13
lof1-1
phb-13 lof1-1
Genotype

D

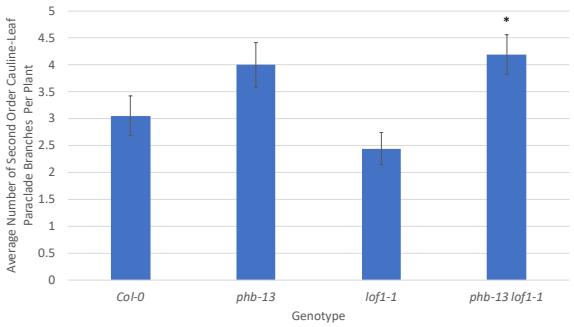
Average Number of Second Order Cauline-Leaf Paraclade Branches Per Plant
5
4.5
4
3.5
3
2.5
2
1.5
1
0.5
0
*
Col-0
phb-13
lof1-1
phb-13 lof1-1
Genotype

Figure 3.28 Graphic representation of paraclade junctions and accessory buds in *er-2*, *phb-13 er-2*, *phv-11 er-2*, and *phb-13 phv-11 cna-2 er-2*. Graphic representation is the same as in Figure 3.3. Yellow indicates zero accessory buds, green indicates one centrally-located accessory bud , blue indicates one offset accessory bud, red indicates two accessory buds, and purple indicates three accessory buds. The *er-2* mutant contained paraclade junctions that formed one centrally located accessory bud or formed no accessory buds. *phb-13 er-2* double mutant formed more accessory buds than the *er-2* mutant and contained multiple accessory buds per paraclade junction. *phv-11 er-2* double mutant appeared similar to the *er-2* single mutant as it contained paraclade junctions that formed one centrally located accessory bud or form no accessory buds. The *phb-13 phv-11 cna-2 er-2* quadruple mutant most often formed two accessory buds per paraclade junction. However, three, one, or zero accessory buds per paraclade junction also occurred. While *er-2*, *phb-13 er-2*, and *phv-11 er-2* plants all formed 2-5 paraclade junctions per plant, *phb-13 phv-11 cna-2 er-2* mutants produced 3-11 paraclade junctions per plant. Fewer *phb-13 phv-11 cna-2 er-2* mutants were phenotypically analyzed compared to other genotypes due to small plant size and severe phenotype.

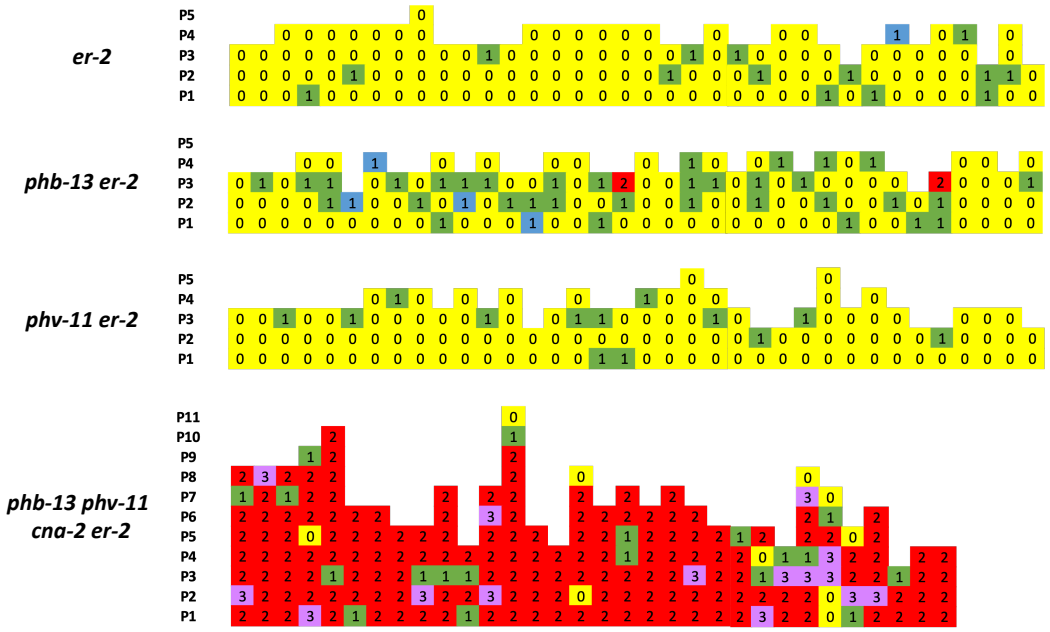
er-2
phb-13 er-2
phv-11 er-2
phb-13 phv-11
cna-2 er-2
P11
P10
P9
P8
P7
P6
P5
P4
P3
P2
P1

Figure 3.29 Accessory bud phenotypes in *er-2*, *phb-13 er-2*, *phv-11 er-2*, and *phb-13 phv-11 cna-2 er-2*. A) Average number of accessory buds per plant. B) 100% stacked column graph for accessory bud phenotype in each genotype. Plants were seven-weeks old at time data was collected. **= $p < 0.01$. Significance measured by student t-test. Bars represent standard error.

A

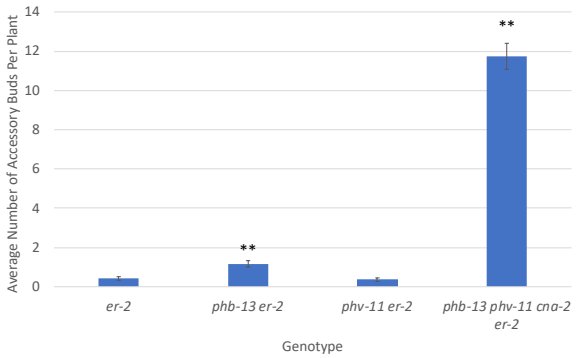
Average Number of Accessory Buds Per Plant
14
12
10
8
6
4
2
0
**
**
er-2
phb-13 er-2
phv-11 er-2
phb-13 phv-11 cna-2 er-2
Genotype

B

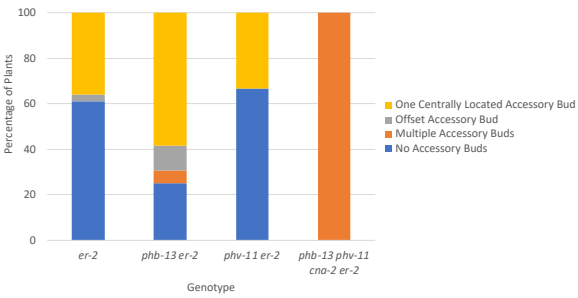
Percentage of Plants
100
80
60
40
20
0
er-2
phb-13 er-2
phv-11 er-2
phb-13 phv-11 cna-2 er-2
Genotype
One Centrally Located Accessory Bud
Offset Accessory Bud
Multiple Accessory Buds
No Accessory Buds

Figure 3.30 Branching and paraclade junction phenotypes in *er-2*, *phb-13 er-2*, *phv-11 er-2*, and *phb-13 phv-11 cna-2 er-2*. A) Average number of rosette-leaf paraclade branches per plant. B) Average number of cauline-leaf paraclade branches per plant. C) Average number of first order cauline-leaf paraclade junctions per plant. D) Average number of rosette-leaf paraclade branches second order branches per plant. Plants were seven-weeks old at time data was collected. *= $p < 0.05$. **= $p < 0.01$. Significance measured by student t-test. Bars represent standard error.

A

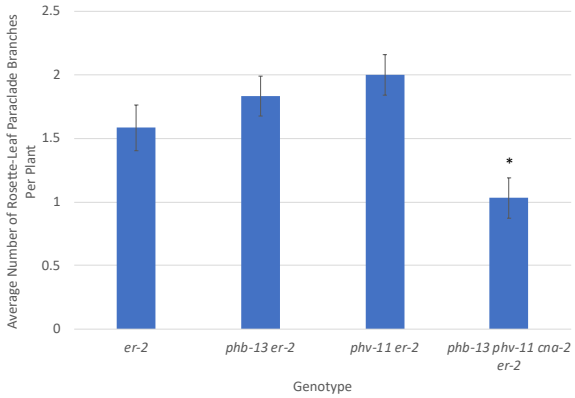
Average Number of Rosette-Leaf Paraclade Branches Per Plant
2.5
2
1.5
1
0.5
0
*
er-2
phb-13 er-2
phv-11 er-2
phb-13 phv-11 cna-2 er-2
Genotype

B

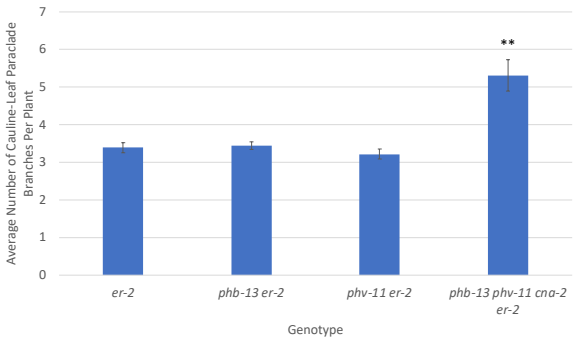
Average Number of Cauline-Leaf Paraclade Branches Per Plant
7
6
5
4
3
2
1
0
**
er-2
phb-13 er-2
phv-11 er-2
phb-13 phv-11 cna-2 er-2
Genotype

C

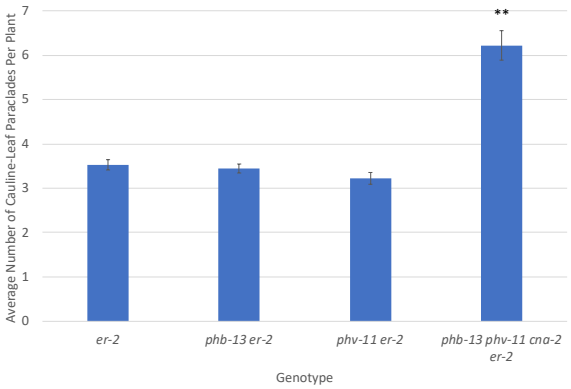
Average Number of Cauline-Leaf Paraclades Per Plant
7
6
5
4
3
2
1
0
**
er-2
phb-13 er-2
phv-11 er-2
phb-13 phv-11 cna-2 er-2
Genotype

D

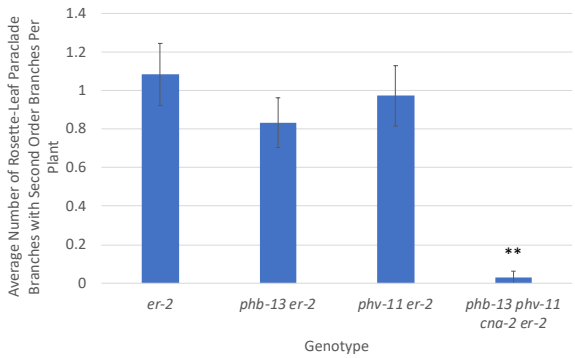
Average Number of Rosette-Leaf Paraclade Branches with Second Order Branches Per Plant
1.4
1.2
1
0.8
0.6
0.4
0.2
0
**
er-2
phb-13 er-2
phv-11 er-2
phb-13 phv-11 cna-2 er-2
Genotype

Figure 3.31 Inflorescence meristems in *er-2*, *phb-13 er-2*, *phv-11 er-2*, *phb-13 phv-11 cna-2 er-2*, *cna er*, and *phv-11*. A) *er-2* single mutant inflorescence tip viewed from above. B) *cna-2 er-2* double mutant inflorescence tip viewed from above. C) Col-0 wild-type inflorescence tip viewed from above. D) *phv-11* mutant inflorescence tip viewed from above. E) *er-2* single mutant inflorescence tip viewed from the side. F) *cna-2 er-2* double mutant inflorescence tip viewed from the side. G) Col-0 wild-type inflorescence tip viewed from the side. H) *phv-11* mutant inflorescence tip viewed from the side. I) *cna-1* (L*er* background) mutant inflorescence tip viewed from the top. J) Close up of meristem fasciation on primary inflorescence stem of *phb-13 phv-11 cna-2 er-2*. K) *phb-13 phv-11 cna-2 er-2* mutant primary inflorescence at termination with visible ring-like structure to meristem. L) *phb-13 phv-11 cna-2 er-2* mutant primary inflorescence viewed from the side. M) *phb-13 phv-11 cna-2 er-2* mutant primary inflorescence at termination in fused carpel-like structure. Fasciation is evident. Images in B, F, I, K, and M were captured when plants were eight-weeks old. Images in A, C-E, G, H, J, and L were captured when plants were six-weeks old. Adjustments to brightness and contrast have been applied throughout entire images. All scale bars are 1 mm in length.

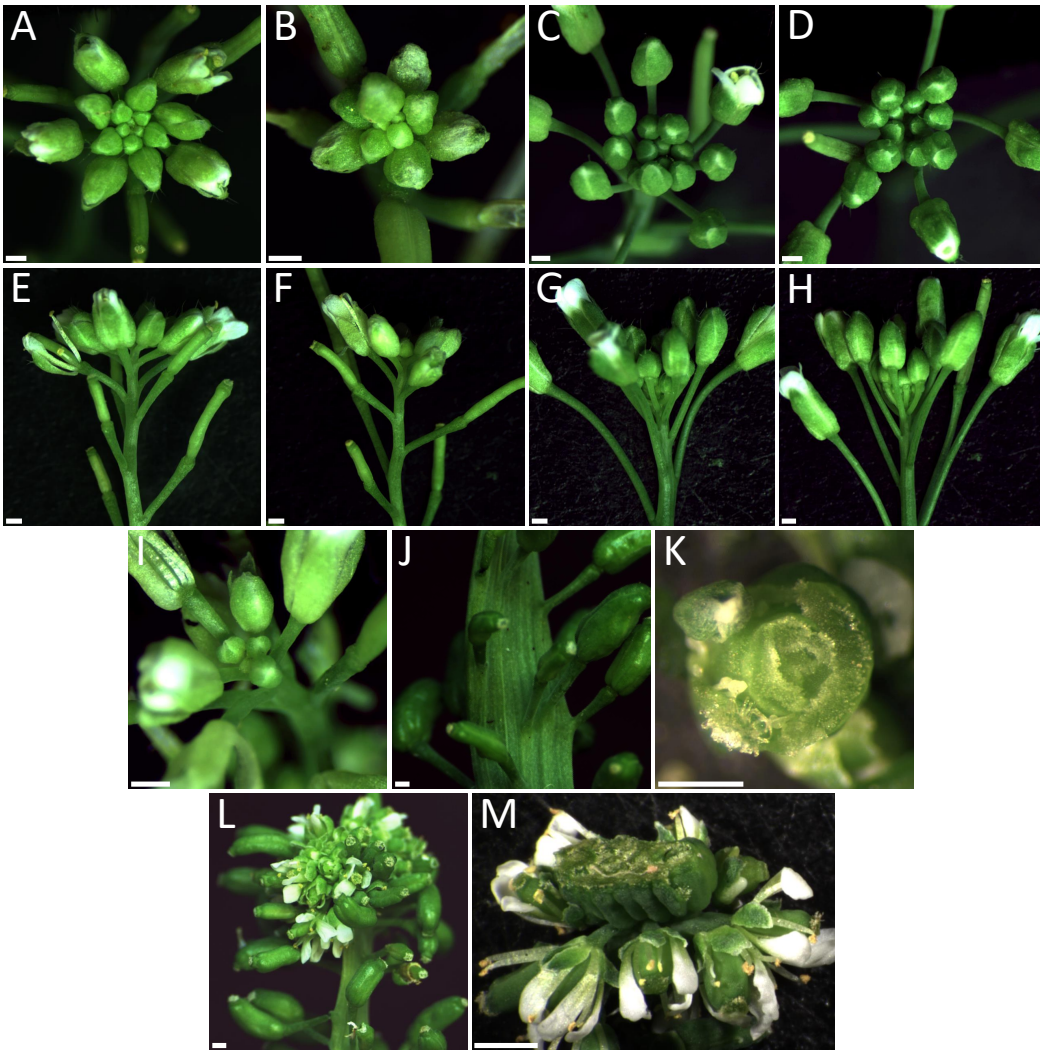

A and E: *er-2*
B and F: *cna-2 er-2*
C and G: Col-0
D and H: *phv-11*
I: *cna-1* (L*er*)
J-M: *phb-13 phv-11 cna-2 er-2*

Figure 3.32 Paraclade junction phenotypes of *er-2*, *phb-13 er-2*, *phv-11 er-2*, *phb-13 phv-11 cna-2 er-2*, *cna er*, and *phv-11*. A) *er-2* single mutant paraclade junction viewed from the front. B) *phb-13 er-2* double mutant paraclade junction viewed from the front. C) *phv-11 er-2* double mutant paraclade junction viewed from the front. D) *phb-13 phv-11 cna-2 er-2* mutant paraclade junction viewed from the front. E) *cna-1* (L*er* background) single mutant paraclade junction viewed from the front. F) *cna-2 er-2* double mutant paraclade junction viewed from the front. G) Col-0 paraclade junction viewed from the front. H) *phv-11* single mutant paraclade junction viewed from the front. All plants are six-weeks old at time of imaging. Adjustments to brightness and contrast have been applied throughout entire images. All scale bars are 1 mm in length.

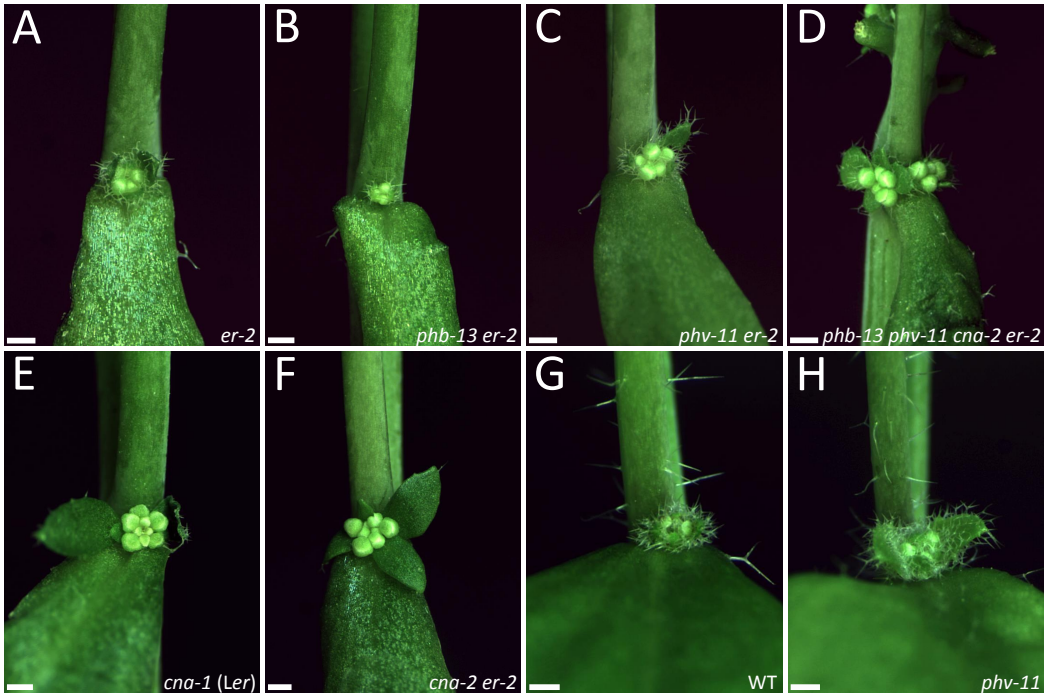
A
er-2
B
phb-13 er-2
C
phv-11 er-2
D
phb-13 phv-11 cna-2 er-2
E
cna-1 (Ler)
F
cna-2 er-2
G
WT
H
phv-11

Figure 3.33 Paraclade junctions and accessory buds in Col-0, *pPHB:PHB* Col-0, *lof1-1*, and *pPHB:PHB lof1-1*. A) Average number of first order cauline-leaf paraclade junctions per plant. B) Average number of accessory buds per plant. C) 100% stacked column graph for accessory bud phenotype in each genotype. Plants were seven-weeks old at time data was collected. **= $p < 0.01$. Significance measured by student t-test. Bars represent standard error.

A

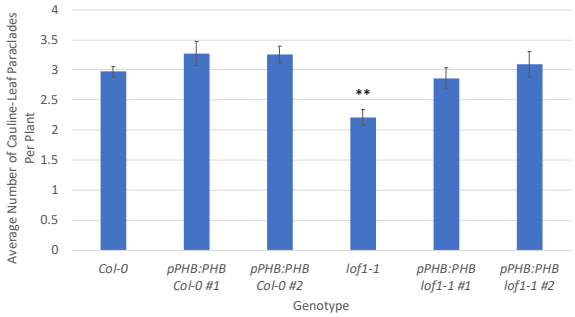
Average Number of Cauline-Leaf Paraclades Per Plant
4
3.5
3
2.5
2
1.5
1
0.5
0
**
Col-0
pPHB:PHB Col-0 #1
pPHB:PHB Col-0 #2
lof1-1
pPHB:PHB lof1-1 #1
pPHB:PHB lof1-1 #2
Genotype

B

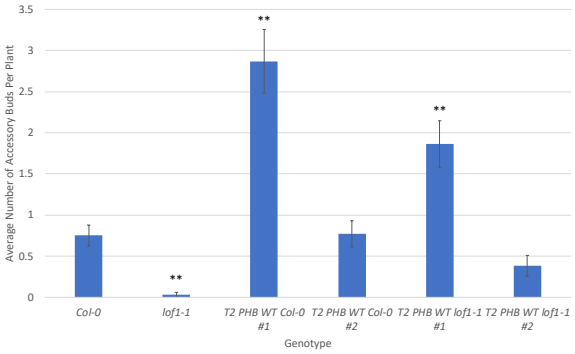
Average Number of Accessory Buds Per Plant
3.5
3
2.5
2
1.5
1
0.5
0
**
**
**
Col-0
lof1-1
T2 PHB WT Col-0 #1
T2 PHB WT Col-0 #2
T2 PHB WT lof1-1 #1
T2 PHB WT lof1-1 #2
Genotype

C

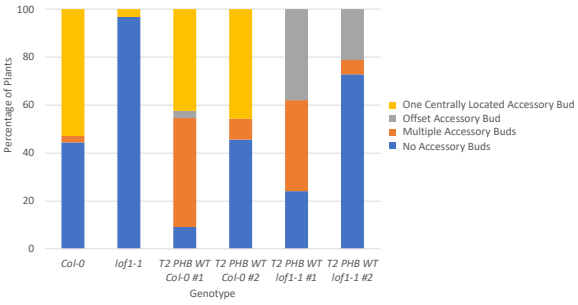
Percentage of Plants
100
80
60
40
20
0
Col-0
lof1-1
T2 PHB WT Col-0 #1
T2 PHB WT Col-0 #2
T2 PHB WT lof1-1 #1
T2 PHB WT lof1-1 #2
Genotype
One Centrally Located Accessory Bud
Offset Accessory Bud
Multiple Accessory Buds
No Accessory Buds

Figure 3.34 Branches in Col-0, *pPHB:PHB* Col-0, *lof1-1*, and *pPHB:PHB lof1-1.* A) Average number of rosette-leaf branches per plant. B) Average number of cauline-leaf paraclade branches per plant. C) Average number of second order cauline-leaf branches per plant. D) Average number of rosette-leaf paraclade branches with second order branches per plant. Plants were seven-weeks old at time data was collected. **= $p < 0.01$. Significance measured by student t-test. Bars represent standard error.

A

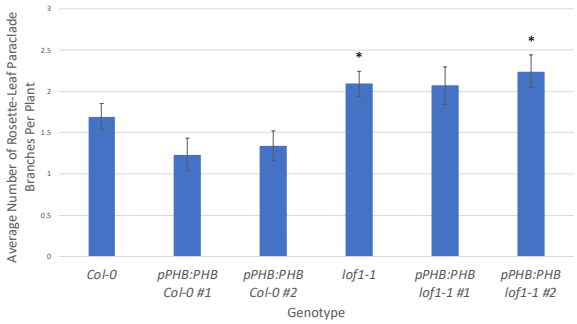
Average Number of Rosette-Leaf Paraclade Branches Per Plant
3
2.5
2
1.5
1
0.5
0
*
*
Col-0
pPHB:PHB Col-0 #1
pPHB:PHB Col-0 #2
lof1-1
pPHB:PHB lof1-1 #1
pPHB:PHB lof1-1 #2
Genotype

B

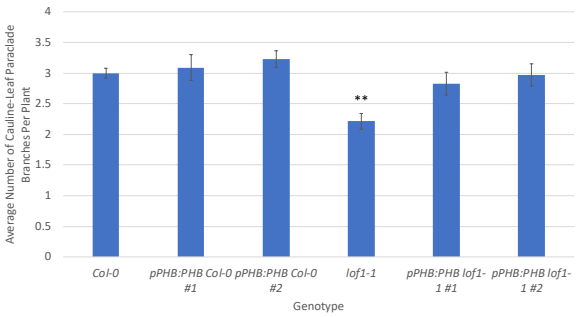
Average Number of Cauline-Leaf Paraclade Branches Per Plant
4
3.5
3
2.5
2
1.5
1
0.5
0
**
Col-0
pPHB:PHB Col-0 #1
pPHB:PHB Col-0 #2
lof1-1
pPHB:PHB lof1-1 #1
pPHB:PHB lof1-1 #2
Genotype

C

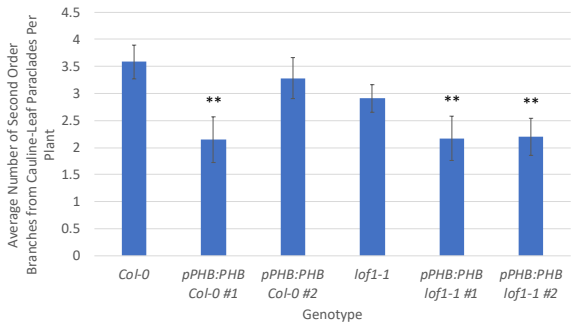
Average Number of Second Order Branches from Cauline-Leaf Paraclades Per Plant
4.5
4
3.5
3
2.5
2
1.5
1
0.5
0
**
**
**
Col-0
pPHB:PHB Col-0 #1
pPHB:PHB Col-0 #2
lof1-1
pPHB:PHB lof1-1 #1
pPHB:PHB lof1-1 #2
Genotype

D

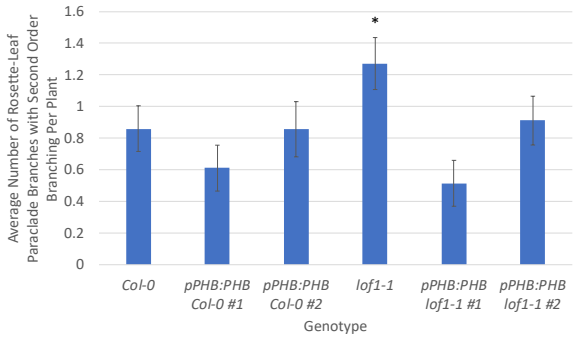
Average Number of Rosette-Leaf Paraclade Branches with Second Order Branching Per Plant
1.6
1.4
1.2
1
0.8
0.6
0.4
0.2
0
*
Col-0
pPHB:PHB Col-0 #1
pPHB:PHB Col-0 #2
lof1-1
pPHB:PHB lof1-1 #1
pPHB:PHB lof1-1 #2
Genotype

Figure 3.35 GFP-PHB localization in *pPHB:GFP-PHB* in Col-0 and *lof1-1* backgrounds in the root meristematic zone. *pPHB:GFP-PHB* is the same transgene as used in *pPHB:PHB* and *pPHB:mPHB*. The *GFP* is not mentioned in other figures and tables for purposes of simplicity. Left column shows fluorescence from the PI stain. Middle column shows fluorescence from GFP. Right column shows an overlay of PI and GFP fluorescence images. Top row: *pPHB:PHB* Col-0. Bottom row: *pPHB:PHB lof1-1*. All images were obtained when seedlings were three days old. All *pPHB:PHB* Col-0 and *pPHB:PHB lof1-1* plants were imaged in the T2 generation. T2 lines were chosen based on phenotypic severity, *PHB* transgene transcript accumulation, and endogenous *PHB* transcript accumulation. Scale bars are 50 μm in length.

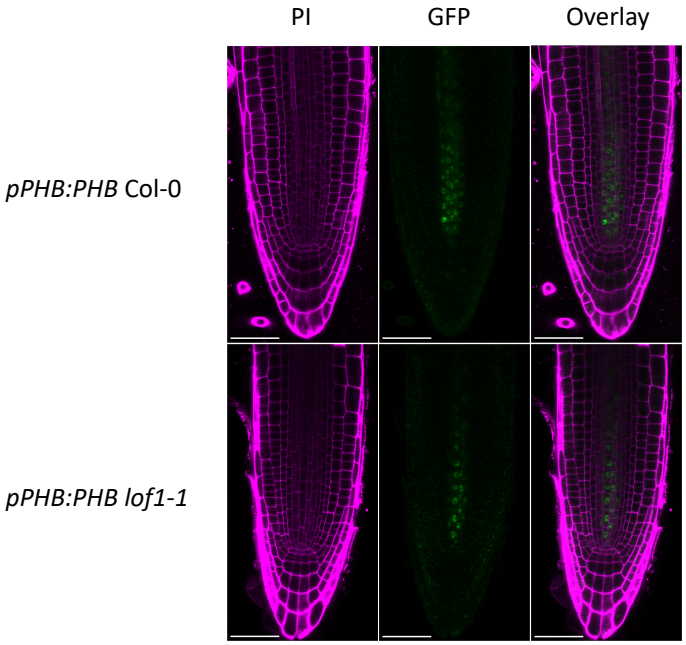
PI
GFP
Overlay
pPHB:PHB Col-0
pPHB:PHB lof1-1

Figure 3.36 LOF1, ATHB4, and HD-Zip class III transcription factors have a complex relationship in the regulation of leaf polarity, SAM maintenance, and plant architecture traits. Known protein interactions are connected by a black line. Promotion of a process is represented by a green arrow. Repression of a process is represented by a red line. Figure is based on results of previous studies conducted by other groups and results from this study.

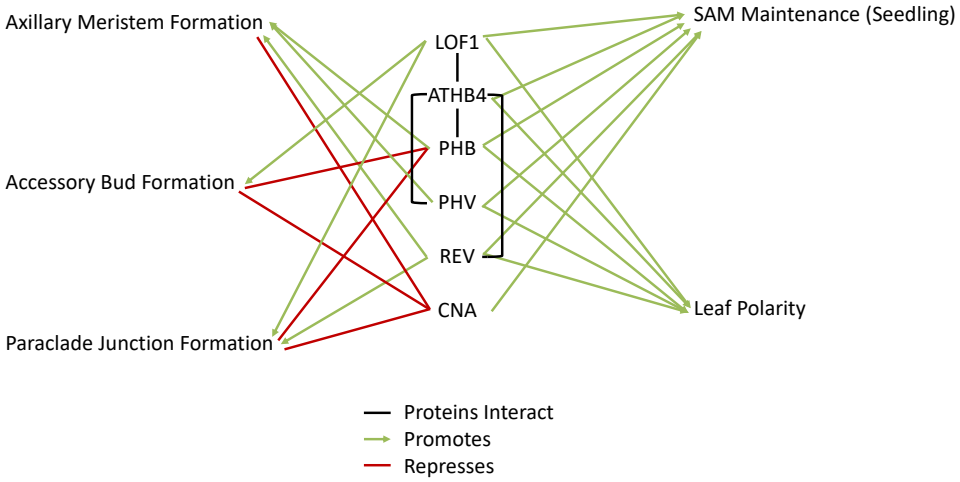
Axillary Meristem Formation
Accessory Bud Formation
Paraclade Junction Formation
LOF1
ATHB4
PHB
PHV
REV
CNA
SAM Maintenance (Seedling)
Leaf Polarity
Proteins Interact
Promotes
Represses

Table 3.1 Mature plant phenotypes of Col-0, *lof1-1*, *pPHB:PHB* Col-0, and *pPHB:PHB lof1-1*. Percentage of plants containing each phenotype is given for each genotype. Percentages are rounded to the nearest 0.1%. Seeds were sown on non-selective media and transplanted to soil at 2-weeks old. Plant phenotypes were determined at seven-weeks of age.

	Col-0	***pPHB:PHB* Col-0 #1**	***pPHB:PHB* Col-0 #2**	***lof1-1***	***pPHB:PHB lof1-1* #1**	***pPHB:PHB lof1-1* #2**
Phyllotaxy	22.2	47.2	71.4	9.1	68.8	58.8
Decurrent Strand	8.3	42.2	2.9	27.3	68.8	70.6
Silique Shape	0	33.3	14.3	0	78.1	61.8
Meristem Fasciation	0	25	0	0	28.1	14.7
Radial Rosette Leaf	0	8.3	0	0	12.5	8.8
Radial Cauline Leaf	0	12.1	0	0	6.9	0
Paraclade Connected to Second Order Paraclade by Decurrent Strand	0	0	0	0	75.9	72.7
Multiple Cauline Leaves	0	0	0	0	0	0
Fused Leaf/Leaves	0	0	0	0	0	0
Small	0	9.1	0	0	9.4	2.9
No Accessory Buds	44.4	9.1	48.6	97	24.1	72.7
One Centrally Located Accessory Bud	52.8	42.4	45.7	0	0	0
Multiple Accessory Buds	2.8	45.5	5.7	0	37.9	6.1
Offset Accessory Bud	0	3	0	3	41.4	21
Accessory Bud Grew Out	2.8	0	0	0	13.8	3
Number of Plants Phenotyped	36	36	35	33	32	34

Approximate Position (Mbp)	Marker Name	Recombination Frequency
1.19	CIW2	0.47
6.4	CIW3	0.57
~11	NGA1126	0.25
13.22	NGA361	0.31
16.29	NGA168	0.27
18.1	F18019	0.35

Table 3.2 The *lof1-1 suppressor* (*lfs-1D*) mutation maps to the bottom of Chromosome 2. Approximate position in megabase pairs (Mbp) of each marker on chromosome 2 is given along with marker name. Recombination frequencies were calculated using an F2 *lfs-1D lof1-1* x L*er* mapping population. The results suggest the *lfs-1D* mutation lies in a ~7.1 Mbp area on the bottom of chromosome 2 between markers NGA361 and F18O19. The data suggests that the *lfs-1D* mutant plants could contain two different mutations since the recombination frequency is lowest at both NGA1126 and NGA168 and higher at surrounding markers (n= 32 plants used for mapping). Primers used for these markers are listed in Table 3.3.

Table 3.16 List of oligonucleotide sequences. Primers designed using the following reference are indicated (Liu *et al.*, 2012).

Name	Sequence	Tm	Use	Source
CIW2a	CCCAAAAGTTAATTATACTGT	48	Mapping of *lof1-1* suppressor mutation	(Bell and Ecker, 1994)
CIW2b	CCGGGTTAATAATAAATGT	49	Mapping of *lof1-1* suppressor mutation	(Bell and Ecker, 1994)
CIW3a	GAAACTCAATGAAATCCACTT	53	Mapping of *lof1-1* suppressor mutation	(Bell and Ecker, 1994)
CIW3b	TGAACTTGTGAGCTTTGA	57	Mapping of *lof1-1* suppressor mutation	(Bell and Ecker, 1994)
NGA1126a	GCACAGTCCAAGTCACAACC	59	Mapping of *lof1-1* suppressor mutation	
NGA1126b	CGCTACGCTTTTCGGTAAAG	60	Mapping of *lof1-1* suppressor mutation	
NGA361-F	ACATATCAATATATTAAAGT	39.9	Mapping of *lof1-1* suppressor mutation	
NGA361-R	AAAGAGATGAGAATTTGGAC	44.5	Mapping of *lof1-1* suppressor mutation	
F18O19-F	TAGTCCTTCATGTTTCCTC	43.1	Mapping of *lof1-1* suppressor mutation	
F18O19-R	CAAGGGAAGAAGATAATTC	42.5	Mapping of *lof1-1* suppressor mutation	
NGA168a	GAGGACATGTATAGGAGCCTCG	60	Mapping of *lof1-1* suppressor mutation	
NGA168b	TGCTCTACTGCACTGCCG	60	Mapping of *lof1-1* suppressor mutation	
PHBgDNA_F3	TGTGATACCTGCTGGAAACG	54.9	Sequencing of *PHB* genomic DNA	
PHB5'seq_R	TTGCTGATGCTGAGGATTTG	53.3	Genotyping for *PHB* transgene in plants and *PHB* genomic DNA sequencing	
eGFPRT_F	TATATCATGGCCGACAAGCA	53.8	Genotyping for *PHB* transgene	
GFPRT_F	TCAAGGAGGACGGAAACATC	54.4	Genotyping for *PHB* transgene	
PHBgDNA_R	TTCTTAAAACCGCAGGTTGG	53.4	Sequencing of *PHB* genomic DNA	
PHBgDNA_F	CGACTTGGTATGCTGCAATG	54.3	Sequencing of *PHB* genomic DNA	
PHBmiddle_R	GCTTGACGTGTGGATCCTTC	56	Sequencing of *PHB* genomic DNA	
PHBmiddle_F	GCGGTGTTGATGAAAATGTG	52.8	Sequencing of *PHB* genomic DNA and *PHB* genotyping	

PHB_R	TTTGGAGCATAGTGGCACCT	56.6	Sequencing of *PHB* genomic DNA, *PHB* genotyping, and *PHB* wild-type RT-PCR	
PHB_F	TCTGGCGTTTTCTGTCTTGA	54.3	Sequencing of *PHB* genomic DNA	
PHBsdm_F2	ACATGAAGATAAATTGCACAAG	49.6	Site-directed mutagenesis of *PHB*	
PHBSDM_R	CTCAAAGCAGCAACAGTC	51.5	Site-directed mutagenesis of *PHB*	
PHBEMS_R1	CTCCACTTGTTTCTTGTGCAATCTA	55.5	Genotyping of *PHBm*	(Liu *et al.*, 2012)
PHB realtime F2	GAGGAGGCCCTAGCAGAGTT	58.5	Genotyping of *PHBm*	
PHBSNP_R	TAACAGCATCATTGAAACCC	50.7	Genotyping of *PHB*	
PHBWtSNP_F	TTTCAGGCTTTGAGACATGTAAGGC	57.5	Genotyping of *PHB*	(Liu *et al.*, 2012)
LBb1.3	ATTTTGCCGATTTCGGAAC	51.5	Genotyping of *phb-13*	SALK Institute
pEGADPHBseq_R	GGAACAGCAAAAGGACTTGC	54.8	Sequencing of *PHB* transgene and *PHB* clones	
pEGADPHBseq_F	CCCATGAAGGTTGCTGAAAT	53.3	Sequencing of *PHB* transgene and *PHB* clones	
pROK-LB	GGAACCACCATCAAACAGGA	55	Genotyping of *PHV* and *phv-11*	
phv-11R	GCCAGCAAATTTAGCAGAGGA	55.7	Genotyping of *PHV* and *phv-11*	(Prigge *et al.*, 2005)
phv-11F	CCCAATGGTCCACTTTCTTCA	55.1	Genotyping of *PHV* and *phv-11*	(Prigge *et al.*, 2005)
Zip851_R	GAACCCACTCAACAGCGGTT	58	Genotyping of *CNA* and *cna-2*	(Prigge *et al.*, 2005)
F5F19_TF	TTAGTTATTCATCTGGAGGGGGTAGTAGG	58.5	Genotyping of *CNA* and *cna-2*	(Prigge *et al.*, 2005)
pD991-LB	TAACGCTGCGGACATCTACA	56.1	Genotyping of *CNA* and *cna-2*	
CNAe18_R	GAGACATATCCCGCCTTGAA	54.3	RT-PCR of *CNA* and *CNA* genotyping	(Prigge *et al.*, 2005)
CNAe16_F	TGATGCTATAATCTGCTGCTCAA	54.2	RT-PCR of *CNA*	(Prigge *et al.*, 2005)

PHVe18_R	TATTCCTGCCGGAAGATTCG	54.6	RT-PCR of *PHV*	(Prigge *et al.*, 2005)
PHVe16_F	TGTGCTGCTCCCTGAAAACT	57	RT-PCR of *PHV*	(Prigge *et al.*, 2005)
PHBnosRT_R	AAGACCGGCAACAGGATTC	55.3	RT-PCR of *PHB* transgene	
PHBnosRT_F	CGAACCTGGTCGTAAAGCTC	55.6	RT-PCR of *PHB* transgene and *PHB* endogenous	
ERECTA2_R	ATCGACGTAGCACGAACCAG	57.1	Genotyping of *ER* and *er-2*	
ERmu5_F	AAGCTTGTGTGTGTCAAAGACC	55.9	Genotyping of *ER* and *er-2*	(Liu *et al.*, 2012)
ERWT5_F	AAGCTTGTGTGTGTCAAAGACA	55.1	Genotyping of *ER* and *er-2*	(Liu *et al.*, 2012)
cna1AS_F	CAAACCGAACCTTGGATCTCGT	57.3	Genotyping of *CNA* and *cna-1* (L*er*)	(Liu *et al.*, 2012)
CNAWtAS_F	CAAACCGAACCTTGGATCTCGC	58.5	Genotyping of *CNA* and *cna-1* (L*er*)	(Liu *et al.*, 2012)
pMYB117_F2	GGCAGTCCACAGCAAAATCGAATATCG	73.7	Genotyping of *LOF1* and *lof1-1*	(Lee e*t al.*, 2009)
pMYB117_R	CCCGGGTGAACCGCTACATCTCCAAGAG	78.4	Genotyping of LOF1 and *lof1-1*	(Lee *et al.*, 2009)
QLOF1_R	GCATCAGCCTCTCCTCTTCTT	54.4	Genotyping of *LOF1* and *lof1-1*	
LBa1	TGGTTCACGTAGTGGGCCATCG	73.0	Genotyping of *LOF1* and *lof1-1*	SALK Institute
ACT2-C	ACTCACCACCACGAACCAG	63.8	RT-PCR of *ACT2*	
ACT2-N	AAAATGGCCGATGGTGAGG	66.9	RT-PCR of *ACT2*	
ET4016mybRTF	TCAAAGAGCTTGTCTCCATT	59	RT-PCR of *LOF1* (*35S:LOF1* plants)	(Lee *et al.*, 2009)
ET4016mybRTR	GAATATTGCATAACGCGTCT	59.2	RT-PCR of *LOF1* (*35S:LOF1* plants) and genotyping of *35S:LOF1* transgene	(Lee e*t al.*, 2009)
35STAIL	GTCGTGCTCCACCATGTTGG	69	Genotyping of *35S:LOF1* transgene	
LOF1RT_R	CCAATTTGTTCAACATTCACG	55.4	RT-PCR of *LOF1* (Paraclade Junction)	
MYB117seq	CCTAACCCTAACCCTAATTACC	60.1	RT-PCR of *LOF1* (Paraclade Junction)	

Table 3.4 Summary of phenotypes in T2 *pPHB:PHB* Col-0 and T2 *pPHB:PHB lof1-1* plants. T2 lines containing a single T-DNA locus according to segregation ratios were chosen after being grown on selective media (ppt). Resistant plants were transplanted to soil. Plants phenotypes were scored at two- and seven-weeks of age. T2 lines were chosen based on T1 plant phenotype and *PHB* transgene and wild-type *PHB* transcript levels. Data in this table was collected from plants grown in a different growth facility than plants described in for subsequent tables. Thus, the data presented here is not directly comparable to subsequent tables.

	***pPHB:PHB* Col-0**	***pPHB:PHB lof1-1***
Decurrent Strand	25.8	58.7
Silique Shape	75.1	80.4
Meristem Fasciation	30.1	43
Radial Rosette Leaf	3.1	8.5
Radial Cauline Leaf	1.3	5.1
Paraclade Connected to Second Order Paraclade by Decurrent Strand	0	28.5
Multiple Cauline Leaves	7	54.9
No Accessory Buds	11	31.9
One Centrally Located Accessory Bud	28.5	3.8
Multiple Accessory Buds	48.7	40.4
Offset Accessory Bud	60.1	64.3
Accessory Bud Grew Out	57.5	24.3
Number of T2 Lines Phenotyped	9	10
Number of Plants Phenotyped	216	240

Table 3.5 Summary of phenotypes in T1 *pPHB:mPHB* transgenic plants in Col-0, *lof1-1*, *phb-13,* and *lof1-1 phb-13* genetic backgrounds. Numbers reflect percentage of plants with given phenotype out of total plants of each genotype. Percentages are rounded to the nearest 0.1%. Plants were sown on soil and sprayed with basta. Basta-resistant plants were genotyped individually to confirm presence of transgene and genetic background. Plants phenotypes were scored at both two- and seven-weeks of age. This dataset uses the same Col-0 wild-type controls as Table 3.6.

	T1 *pPHB:mPHB* Col-0	T1 *pPHB:mPHB lof1-1*	T1 *pPHB:mPHB phb-13*	T1 *pPHB:mPHB lof1-1 phb-13*	Col-0
Decurrent Strand	8.3	32.1	18.2	45.5	9.4
Silique Shape	12.5	25	13.6	18.2	0
Meristem Fasciation	14.6	10.7	18.2	12.1	0
Radial Rosette Leaf	37.5	32.1	27.3	9.1	0
Radial Cauline Leaf	4.9	10.5	5.6	0	0
Paraclade Connected to Second Order Paraclade by Decurrent Strand	0	47.4	0	29.6	0
Multiple Cauline Leaves	19.5	68.4	16.7	7.4	0
Fused Leaf/Leaves	4.2	0	4.5	6.1	0
Small	29.2	35.7	32.2	24.2	0
No Accessory Buds	17	36.8	27.8	37	18.8
One Centrally Located Accessory Bud	46.3	21.1	44.4	44.4	78.1
Multiple Accessory Buds	36.6	47.4	33.3	7.4	0
Offset Accessory Bud	2.4	0	0	3.7	3.1
Accessory Bud Grew Out	0	15.8	11.1	16	0
Number of Plants Phenotyped	48	28	22	32	32

Table 3.6 Summary of phenotypes in *pPHB:PHB phb-13* and *pPHB:PHB lof1-1 phb-13* in T1 generation. Numbers reflect percentage of plants with given phenotype. Percentages are rounded to the nearest 0.1%. Plants were sown on soil and sprayed with basta. Basta-resistant plants were genotyped individually to confirm presence of transgene and genetic background. Plants phenotypes were scored at both two- and seven-weeks of age. This dataset uses the same Col-0 wild-type controls as Table 3.5.

	T1 *pPHB:PHB phb-13*	**T1 *pPHB:PHB lof1-1 phb-13***	**Col-0**
Decurrent Strand	42.1	90.5	9.4
Silique Shape	21.1	23.8	0
Meristem Fasciation	10.5	14.3	0
Radial Rosette Leaf	10.5	9.5	0
Radial Cauline Leaf	0	0	0
Paraclade Connected to Second Order Paraclade by Decurrent Strand	0	30	0
Multiple Cauline Leaves	27.8	5	0
Fused Leaf/Leaves	5.3	0	0
Small	26.3	0	0
No Accessory Buds	16.7	35	18.8
One Centrally Located Accessory Bud	38.9	25	78.1
Multiple Accessory Buds	44.4	30	0
Offset Accessory Bud	5.6	10	3.1
Accessory Bud Grew Out	0	5	0
Number of Plants Phenotyped	19	21	32

Table 3.7 *pPHB:PHB* Col-0 and *pPHB:PHB lof1-1* seedling phenotypes. Percentage of seedlings containing each phenotype out of total seedlings of each genotype. Percentages are rounded to the nearest 0.1%. *lof1-1* mutant seedlings were used as a control. T2 lines were derived from hemizygous T1 plants with one insertion locus. T2 seedlings were grown on non-selective media for 10 days before phenotyping; therefore, it was expected that ~25% of the T2 plants did not have a transgene insertion.

	lof1-1	T1 *pPHB:PHB* Col-0	T2 *pPHB:PHB* *lof1-1*
Not Involving True Leaves			
Cotyledon Defects	0.2	1.1	0.9
Small	0.2	0.5	0.4
Meristem Termination (Pin)	0	0	6.2
Meristem Termination (No Pin)	0	0.3	2.2
Involving True Leaves			
Two Not Radial	99	57.1	36.7
Two Fused	0	2.2	0.9
One Partially Radial	0	0.3	0
One Radial & One Partially Radial	0	2.2	4
Two Partially Radial	0	28.4	42.9
One Not Radial & One Partially Radial	0.4	7.9	4.4
Two Radial	0	0	0.5
Number of Plants Phenotyped	403	366	372

Table 3.8 Phenotypes of T1 *35S:LOF1* plants in Col-0, *lof1-1*, *phb-13,* and *lof1-1 phb-13* genetic backgrounds. Percentage of plants containing each phenotype is given for each genotype. Percentages are rounded to the nearest 0.1%. Plants used for transformation were from the F4 generation derived from the same F1 parent of a cross between *phb-13 er-2* double and *lof1-1* single mutant. Plants with the *35S:LOF1* transgene were selected for by basta spray. Plant populations were also spot genotyped for the *35S:LOF1* transgene and for the genetic background. Plants were observed at two- three- and seven-weeks of age. *35S:LOF1* plants could be analyzed in T1 generation due to silencing of transgene in later generations.

	***35S:LOF1* Col-0**	***35S:LOF1 lof1-1***	***35S:LOF1 phb-13***	***35S:LOF1 lof1-1 phb-13***
No Accessory Buds	77.3	72.5	55.3	61.7
One Centrally Located Accessory Bud	17	21.6	34.2	35
Multiple Accessory Buds	3.4	3.9	7.9	1.7
Offset Accessory Bud	2.3	2	2.6	1.7
Upward Leaf Curling	8	0	0	0
Number of Plants Phenotyped	88	102	114	60

Table 3.9 Mature plant phenotypes of WT, *lof1-1*, *phb-13*, and *lof1-1 phb-13* genotypes. Percentage of plants containing each phenotype is given for each genotype. Percentages are rounded to the nearest 0.1%. Plants were from the F4 generation derived from the same F1 parent of a cross between *phb-13 er-2* double and *lof1-1* single mutant. Plant phenotypes were scored at seven-weeks of age.

	WT	***lof1-1***	***phb-13***	***lof1-1 phb-13***
Phyllotaxy	25	25	27.8	25
Decurrent Strand	16.7	30.6	11.1	47.2
Silique Shape	0	0	0	0
Meristem Fasciation	0	0	0	0
Radial Rosette Leaf	0	0	0	0
Radial Cauline Leaf	0	0	0	0
Paraclade Connected to Second Order Paraclade by Decurrent Strand	0	0	0	5.6
Multiple Cauline Leaves	0	0	0	0
Fused Leaf/Leaves	0	0	0	0
Small	0	0	0	0
No Accessory Buds	50	100	8.3	100
One Centrally Located Accessory Bud	44.4	0	66.6	0
Multiple Accessory Buds	0	0	11.1	0
Offset Accessory Bud	5.6	0	13.9	0
Accessory Bud Grew Out	0	0	2.8	0
Number of Plants Phenotyped	36	36	36	36

Table 3.10 WT, *lof1-1*, *phb-13,* and *lof1-1 phb-13* floral phenotypes. Percentage of flowers containing each phenotype is given for each genotype. Percentages are rounded to the nearest 0.1%. Plants were from the F4 generation derived from the same F1 parent of a cross between *phb-13 er-2* double and *lof1-1* single mutant. Flowers six to ten on the primary inflorescence of each plant were scored. Phenotypes observed at least once per flower were recorded.

	WT	***lof1-1***	***phb-13***	***lof1-1 phb-13***
Wild-type	87.8	86.2	76	73.7
Stamen Fusion	0.6	0	1.7	1.7
Undeveloped Stamen	1.1	2.3	0.6	2.9
Abnormal Stamen Number	0	1.1	6.3	7.4
Stamen/Petal Structure	0	2.9	0	6.3
Sepal Fusion	8.9	8	10.9	9.7
Abnormal Sepal Number	0.6	0	4	0
Other	2.8	0	8	9.1
Number of Flowers Phenotyped	180	175	175	175
Number of Plants Phenotyped	36	35	35	35

Table 3.11 Floral phenotypes in *er-2*, *phb-13 er-2*, *phv-11 er-2*, and *phb-13 phv-11 cna-2 er-2* mutants. Percentage of flowers containing each phenotype is given for each genotype. Percentages are rounded to the nearest 0.1%. Flowers six to ten on the primary inflorescence of each plant were scored when possible. Phenotypes observed at least once per flower were recorded.

	er-2	*phb-13 er-2*	*phv-11 er-2*	*phb-13 phv-11 cna-2 er-2*
Wild-type	82.2	84.4	88	19.4
Petal Polarity	0	1.1	0	6.7
Forked/Fused/Lobed Petal	0.6	0	0	12.2
Abnormal Petal Number	0.6	0.6	0.6	12.8
Stamen/Petal Structure	0	0	0	3.9
Stamen Fusion	0.6	0.6	0	12.8
Undeveloped Stamen	1.1	0.6	1.1	30.6
Abnormal Stamen Number	12.8	11.7	9.1	43.9
Sepal Fusion	2.8	1.7	1.1	18.3
Abnormal Sepal Number	0	0	0	19.4
Number of Flowers Phenotyped	180	180	175	180
Number of Plants Phenotyped	36	36	35	36

Table 3.12 Floral phenotypes of *pPHB:PHB* Col-0 and T2 *pPHB:PHB lof1-1* plants in T2 generation. Percentage of flowers containing each phenotype is given for each genotype. Percentages are rounded to the nearest 0.1%. T2 lines with one insertion site (based on basta-resistance segregation ratios) were selected. T2 lines were also selected based on the severity in phenotype and *PHB* transgene and endogenous *PHB* transcript levels (Figure 3.9; 3.10). Flowers six to ten on the primary inflorescence of each plant were scored when possible. Phenotypes that were observed at least once per flower were recorded.

	Col-0	***pPHB: PHB* Col-0 #1**	***pPHB: PHB* Col-0 #2**	***lof1-1***	***pPHB: PHB lof1-1* #1**	***pPHB: PHB lof1-1* #2**
Wild-type	87.9	60.06	66.7	85	37.8	48.3
Carpel Shape	0	0.6	0	0	0.6	1.7
Abnormal Carpel Number	0	1.1	0	0	2.8	2.2
Radial Petal	0	13.3	10.6	0	28.3	11.7
Trumpet Petal	0	32.8	20	0	36.1	32.8
Forked/Fused/Lobed Petal	0	1.1	2.8	0	5	1.1
Abnorml Petal Number	0	5.6	5	0	3.9	1.1
Stamen/Petal Structure	1.1	2.2	0	1.8	2.2	0
Stamen Fusion	0	2.2	2.8	0.6	5.6	1.1
Undeveloped Stamen	0.6	8.9	2.8	0.6	8.9	2.2
Abnormal Stamen Number	5	13.9	10.6	1.2	18.9	8.3
Sepal Fusion	5	2.2	4.4	8.2	9.4	13.3
Abnormal Sepal Number	0.6	3.8	4.4	0.6	5	0.6
Number of Flowers Phenotyped	180	180	180	170	180	180
Number of Plants Phenotyped	36	36	36	34	36	36

Table 3.13 Mature plant phenotypes of *er-2*, *phb-13 er-2*, *phv-11 er-2*, and *phb-13 phv-11 cna-2 er-2*. Percentage of plants containing each phenotype is given for each genotype. Percentages are rounded to the nearest 0.1%. Plants of each genotype were obtained from stock resource centers or other laboratories. Plant phenotypes were scored at seven-weeks of age.

	er-2	*phb-13 er-2*	*phv-11 er-2*	*phb-13 phv-11 cna-2 er-2*
Phyllotaxy	19.4	27.8	27.8	100
Decurrent Strand	16.7	30.6	19.4	0
Silique Shape	0	0	0	100
Meristem Fasciation	0	0	0	100
Radial Rosette Leaf	0	0	0	0
Radial Cauline Leaf	0	0	0	0
Paraclade Connected to Second Order Paraclade by Decurrent Strand	0	0	0	0
Multiple Cauline Leaves	0	0	0	15.6
Fused Leaf/Leaves	0	0	0	0
Small	0	0	0	11.1
No Accessory Buds	61.1	25	66.7	0
One Centrally Located Accessory Bud	36.1	58.3	33.3	0
Multiple Accessory Buds	0	5.6	0	100
Offset Accessory Bud	2.8	11.1	0	0
Accessory Bud Grew Out	0	0	0	6.3
Number of Plants Phenotyped	36	36	36	32

Table 3.14 Mature plant phenotypes of *cna-2 er-2* (Col) and *cna-1* (L*er*). Percentage of plants containing each phenotype is given for each genotype. Percentages are rounded to the nearest 0.1%. *cna-2 er-2* is in the Col-0 background. *cna-1* is in the L*er* background, which contains the *er-1* mutation. Plants of each genotype were obtained from stock resource centers. Plant phenotypes were scored at seven-weeks of age.

	cna-2 er-2	*cna-1* (L*er*)
Phyllotaxy	0	4.2
Decurrent Strand	0	0
Silique Shape	0	0
Meristem Fasciation	0	0
Paraclade Connected to Second Order Paraclade by Decurrent Strand	0	0
Multiple Cauline Leaves	0	0
Small	0	0
No Accessory Buds	13	20.8
One Centrally Located Accessory Bud	82.6	79.2
Multiple Accessory Buds	4.3	0
Offset Accessory Bud	0	0
Accessory Bud Grew Out	4.3	0
Number of Plants Phenotyped	23	24

Table 3.15 Observations of *phv-11* in the *ER* background. Percentage of plants containing each phenotype is given for each genotype. Percentages are rounded to the nearest 0.1%. Plants were from the F3 generation derived from the same F1 parent of a cross between *phv-11 er-2* double mutant and Col-0. The total number of plants scored for each genotype is given at the bottom of the table. Plant phenotypes were examined at seven-weeks of age.

	WT	***phv-11***
Phyllotaxy	0	3.3
Decurrent Strand	0	0
Silique Shape	0	0
Meristem Fasciation	0	0
Paraclade Connected to Second Order Paraclade by Decurrent Strand	0	0
Multiple Cauline Leaves	12.9	20
Small	0	0
No Accessory Buds	29	46.7
One Centrally Located Accessory Bud	64.5	36.7
Multiple Accessory Buds	3.2	3.3
Offset Accessory Bud	3.2	13.3
Accessory Bud Grew Out	3.2	0
Number of Plants Phenotyped	31	30

Table 3.16 Observations of *lof1-1* in the *er-2* mutant background. Percentage of plants containing each phenotype is given for each genotype. Percentages are rounded to the nearest 0.1%. Plants were from the F4 generation derived from the same F1 parent of a cross between *phb-13 er-2* double and *lof1-1* single mutant. Plant phenotypes were scored at seven-weeks of age.

	er-2	*lof1-1 er-2*
Phyllotaxy	0	0
Decurrent Strand	10.7	0
Silique Shape	0	0
Meristem Fasciation	0	0
Paraclade Connected to Second Order Paraclade by Decurrent Strand	0	3.6
Multiple Cauline Leaves	10.7	5.5
Small	0	0
No Accessory Buds	46.4	94.5
One Centrally Located Accessory Bud	50	3.6
Multiple Accessory Buds	0	1.8
Offset Accessory Bud	3.6	0
Accessory Bud Grew Out	0	0
Number of Plants Phenotyped	28	55

Conclusions

Stem cells in plants are located in the shoot apical meristem (SAM) – a convex structure near the top of the plant. The SAM forms all above ground organs; lateral organs initiate as protrusions from the periphery of the SAM. As cells of the SAM are incorporated into developing organs, they must be replenished (Evans and Barton, 2002; Weigel and Jürgens, 2002). The boundary region separates the developing organs from the SAM and is characterized by cells that are smaller and divide less frequently then surrounding regions (Hussey, 1971).

A number of genes that are specifically expressed in boundary regions have been described, including *LATERAL ORGAN FUSION1* (*LOF1*), which encodes an MYB transcription factor involved in organ separation and meristem formation. *LOF1* is expressed at the base of floral organs, pedicel-stem junctions, the adaxial side of rosette leaf bases, and junctions between the inflorescence meristem and flower primordia. *LOF1* is also expressed in the paraclade junction between the axillary branch and primary stem and between the cauline leaf and axillary branch (Lee *et al.*, 2009). *lof1-1* mutants, that have no detectable *LOF1* expression in the paraclade junction, have a fusion between the axillary branch and cauline leaf, and do not form accessory buds. *LOF1* is partially functionally redundant with the closely related *LATERAL ORGAN FUSION2* (*LOF2*), which has overlapping function in organ separation (Lee *et al.*, 2009).

In this dissertation, we demonstrate that LOF1 interacts with a number of proteins involved in response to abiotic stress. Many LOF1-interacting proteins are predicted to be subcellularly localized to either the chloroplast or mitochondria (Table 1.1). We

hypothesize that LOF1 may function in a protein complex to modulate petiole angle or growth in response to abiotic stress. Alternatively, LOF1 may function to promote or repress accessory bud formation in response to abiotic stress.

Because LOF1 interacted with proteins involved in abiotic-stress response and proteins localized to the plastid or mitochondria, we asked whether LOF1 subcellular localization was altered in response to abiotic stress. Under our growth conditions, LOF1 was localized to the nucleus, which is typical of transcription factors. We did not observe a change in subcellular localization of LOF1-GFP in roots under any of the abiotic stress conditions tested. However, subtle changes in protein distribution may be difficult to detect. In addition, our experiments did not address the potential for plastid-localized proteins to move to the nucleus.

One LOF1-interactor that was isolated multiple times in our screen – WHIRLY3 (WHY3) – is known to have dual localization in both the chloroplast and nucleus (Krause *et al.*, 2005; Grabowski *et al.*, 2008). WHY proteins are known to bind double- and single-stranded DNA. WHY3 is closely related to WHIRLY1 (WHY1) (Desveaux *et al.*, 2000, 2002; Prikryl *et al.*, 2008; Cappadocia *et al.*, 2010, 2012). However, WHY1 did not interact with LOF1 in our experiments (Figure 1.1). The function of WHY1 and WHY3 in the nucleus is thought to be regulation of gene expression (Desveaux *et al.*, 2000, 2002, 2004; Xiong *et al.*, 2009), whereas these proteins are thought to regulate plastid DNA repair mechanisms in the chloroplast (Maréchal *et al.*, 2009). WHY proteins are candidate retrograde signals because of their localization pattern, and WHY3 function appears to be dependent on plastid redox status (Ströher and Dietz, 2008; Krause *et al.*,

2009; Foyer *et al.*, 2014; Guan *et al.*, 2018). We hypothesize that LOF1 and WHY3 interact in the nucleus to regulate gene expression in control of petiole angle, accessory bud formation, or accessory bud outgrowth in response to oxidative stress.

To better understand *LOF1* function at a molecular level, a genetic suppressor of the *lof1-1* mutant was characterized. We found that a dominant mutation in *PHABULOSA* (*PHB*) increased accessory bud number and suppressed the *lof1-1* mutant phenotype. *PHB* encodes an HD-Zip class III transcription factor involved in leaf polarity and meristem formation (McConnell and Barton, 1998; McConnell *et al.*, 2001; Prigge *et al.*, 2005). Dominant, gain-of-function mutations in *PHB* that disrupt the *miRNA 165/166* binding site have been previously described (McConnell *et al.*, 2001; Mallory *et al.*, 2004). The *phb382*/lof1 suppressor* (*lfs-1D*) mutation isolated in this study is predicted to result in a protein truncation within the START domain and does not disrupt the *miRNA 165/166*-binding site (Figure 3.6). To our knowledge, this is the first report of a dominant mutation in an *HD-Zip III* gene that was not within the miRNA-binding site.

Plants transformed with this dominant version of *PHB* (*phb382*/mPHB*) under the *PHB* promoter had an increased number of accessory buds, and this transgene suppressed the *lof1-1* mutant phenotype (Figure 3.4; 3.33). *pPHB:mPHB* plants also exhibited a range of developmental defects, including fused leaves, radial or partially radial leaves, decurrent strands, and floral defects. Surprisingly, plants that were transformed with the wild-type version of *PHB* (*pPHB:PHB*) exhibited the same range of developmental defects, although at a lower frequency. This finding was unexpected, given that *PHB* overexpressing plants appear phenotypically wild-type according to previous reports

(McConnell and Barton, 1998; McConnell *et al.*, 2001). Previous studies have indicated that decurrent strands and organ fusions are boundary-region defects (Aida *et al.*, 1997; Emery *et al.*, 2003; Lee *et al.*, 2009; Bell *et al.*, 2012; Colling *et al.*, 2015), suggesting that *PHB* could function in the boundary region. Not only did plants transformed with *mPHB* or wild-type *PHB* have boundary-related phenotypes, but *LOF1* overexpressing plants were previously reported as having leaves that curl upwards [(Lee *et al.*, 2009); Figure 3.21]. Leaf curling is a phenotype observed when adaxial-abaxial polarity is defective (McConnell and Barton, 1998; Serrano-Cartagena *et al.*, 2000; Fahlgren *et al.*, 2006; Kim *et al.*, 2010; Bou-Torrent *et al.*, 2012). These data suggested the possibility that *LOF1* and *PHB* may regulate one another.

Our experiments revealed that *LOF1* and *PHB* do not regulate one another at the transcriptional level (Figure 3.11). To look for evidence of a genetic interaction between *LOF1* and *PHB*, we examined plant architecture differences between *lof1-1*, *phb-13*, and *lof1-1 phb-13* plants. The *phb-13* allele was previously reported to be a null loss-of-function allele (Prigge *et al.*, 2005), but we determined it may instead be a knock-down allele (Figure 3.11). The *lof1-1 phb-13* double mutant resembled the *lof1-1* single mutant – lacking accessory buds and having fusion between the axillary branches and cauline leaves (Figure 3.12). We found that *phb-13* mutants produced more accessory buds and *lof1-1* mutants produced fewer paraclade junctions than wild-type plants. In *lof1-1 phb-13* plants, the number of paraclade junctions was restored to a wild-type level. These data indicate that *LOF1* promoted formation of paraclade junctions and accessory buds, and *PHB* repressed formation of paraclade junctions and accessory buds.

To determine if other HD-Zip III family members were involved in accessory bud and paraclade junction formation with PHB, mutants of multiple *HD-Zip III* genes were examined. There are five *HD-Zip class III* genes in *Arabidopsis – PHB*, *PHAVOLUTA* (*PHV*), *REVOLUTA* (*REV*), *CORONA* (*CNA*), and *ARABIDOPSIS THALIANA HOMEOBOX8* (*ATHB8*) (Emery *et al.*, 2003). We found that the *phb-13 phv-11 cna-2 er-2* mutant had significantly more accessory buds and paraclade junctions than other genotypes. Because *phb-13 er-2* and *cna-2 er-2* had more accessory buds than *er-2* or *phv-11 er-2* mutants, we determined that *CNA* functions in accessory bud repression with *PHB* but *PHV* may not. In addition, all of the *phb-13 phv-11 cna-2 er-2* mutants exhibited meristem fasciation. Some *pPHB:mPHB* and *pPHB:PHB* plants also had meristem fasciation. Given their similar accessory bud and floral phenotypes, one may speculate that *pPHB:mPHB* and *pPHB:PHB* act in a dominant-negative manner.

PHB, REV, and PHV were previously reported to interact with ARABIDOPSIS THALIANA HOMEOBOX4 (ATHB4) at the protein level (Merelo *et al.*, 2016). Here, we reported that LOF1 interacted with ATHB4 (Figure 1.1). *ATHB4* is involved in the shade avoidance response, cotyledon development, and meristem maintenance (Sorin *et al.*, 2009; Bou-Torrent *et al.*, 2012; Turchi *et al.*, 2013). *ATHB4* and *HOMEOBOX ARABIDOPSIS THALIANA3* (*HAT3*) are paralogs and share many functions (Sessa *et al.*, 2005; Ciarbelli *et al.*, 2008). *HAT3* is a positive regulator of shade avoidance, but ATHB4 is thought of as an integrator of shade avoidance with hormone-related processes (Sorin *et al.,* 2009). The double loss-of-function *athb4 hat3* mutant was reported to have an inactive SAM and cotyledon fusion phenotypes at low frequencies (Turchi *et al.*,

2013). As previously discussed, organ fusions are often indicative of organ boundary defects. Similar to *LOF1* overexpression, overexpression of *ATHB4* or *HAT3* results in upward-curling leaves [(Lee *et al.*, 2009; Bou-Torrent *et al.*, 2012; Turchi *et al.*, 2013); Figure 3.21], indicating these genes may be involved in adaxial-abaxial leaf polarity. When *athb4 hat3 phb-13* triple mutants were examined, the inactive SAM phenotype of *athb4 hat3* was enhanced, suggesting that *ATHB4* and *HAT3* function with *PHB* in SAM maintenance. Interestingly, our evidence suggests that LOF1 did not interact with HAT3 (Figure 1.1), despite 93% amino acid sequence identity between ATHB4 and HAT3 (Ciarbelli *et al.*, 2008).

Because transcription factors act in complexes and HD-Zip III, HD-Zip II, and MYB domain proteins have been determined to interact with other transcription factors previously (Zimmermann *et al.*, 2004; Merelo *et al.*, 2016), LOF1 could act in a complex with ATHB4 and HD-Zip III proteins. This idea is supported by data collected from our experiments as well as previous studies. HD-Zip III transcription factors were previously reported to homodimerize with one another (Sessa *et al.*, 1998; Magnani and Barton, 2011) and to dimerize with other proteins (Wenkel *et al.*, 2007; Kim *et al.*, 2008). Additionally, MYB transcription factors are known to interact with basic helix-loop-helix (bHLH) and WD-repeat family transcription factors for multiple plant processes (Zimmermann *et al.*, 2004; Gonzalez *et al.*, 2008; Rowan *et al.*, 2009). A dominant, gain-of-function mutant, *phb-1D*, produces ectopic meristems surrounding the base of leaves (McConnell and Barton, 1998; McConnell *et al.*, 2001). Plants containing mutations in more than one *HD-Zip III* gene had multiple accessory buds per paraclade junction in this

study (Figure 3.28; 3.29). Therefore, gain-of-function and loss-of-function phenotypes were similar for *HD-Zip III* genes. A possible explanation for this scenario could be that the proteins act in complexes, such that the stoichiometry of the proteins in the complexes is altered by increased or decreased levels of individual proteins [reviewed in (Prelich, 2012)]. This study reveals a complex relationship between LOF1, ATHB4, and HD-Zip class III transcription factors for the regulation of leaf polarity, paraclade junction formation, SAM maintenance, and formation of axillary and accessory meristems (Figure 3.36). Further experiments are necessary to determine how HD-Zip III transcription factors, HD-Zip II transcription factors, and LOF1 accomplish precise regulation of these important plant processes and determine the individual contributions of each protein.

To further characterize the function of *LOF1* on a molecular level, the following experiments should be carried out:

1) Determine how LOF1 and PHB regulate one another and if ATHB4, PHB, other HD-Zip class III transcription factors, and LOF1 interact in a transcription factor complex. ATHB4 and PHB proteins are reported to interact (Merelo *et al.,* 2016). In Chapter 1, we determined that LOF1 and ATHB4 interact, but we did not identify HD-ZipIII proteins as LOF1 interactors in our screen. *PHB* and other *HD-Zip III* genes are larger than average for the *Arabidopsis* genome [Figure 3.6; (Wortman *et al.*, 2003)] and therefore, their full-length cDNAs may be not be present in our yeast two-hybrid libraries, which generally tend to underrepresent larger clones (Kempin *et al.*, 1995). If ATHB4, PHB, and LOF1

interact in a transcription factor complex, the genes regulated by this complex could be investigated.

2) Understand plant architecture traits in high-light, low red:far-red (R:FR) light, and ROS conditions. It is documented that plants grown in high-light conditions for extended periods of time have more branches (Tian *et al.*, 2017). However, it is not known if the branches are from existing accessory and axillary buds or if new buds form in response to high light. Wild-type *Arabidopsis* plants produce fewer buds in rosette-leaf axils in low R:FR light (Finlayson *et al.*, 2010). A similar mechanism may also regulate accessory buds formation, but this possibility has not yet been investigated. Examining plant architecture in the presence of ROS would require either mutants or transgenic plants that have elevated ROS levels without triggering the programmed cell death response. For example, plants that overexpress *REDOX RESPONSIVE TRANSCRIPTION FACTOR1* (*RRTF1*), which encodes a core component of the redox signaling network and is rapidly upregulated in response to abiotic and biotic stresses (Matsuo *et al.*, 2015), could be used to achieve high ROS levels. These experiments would be the first steps in determining if WHY3 and ATHB4 interact with LOF1 in order to promote or repress accessory bud formation under specific abiotic-stress conditions.

3) Additional investigation of a potential role for LOF1 in the plastid due to its interactions with plastid-localized proteins. A version of LOF1 fused to a plastid-transit could be introduced into the *lof1* mutant background (Glaser and Soll, 2004). These plants would allow us to determine phenotypes associated with a plastid-targeted version of LOF1. These plants could additionally be grown in both standard and abiotic-stress

conditions. This approach may require a *lof1* null mutant, which is not yet available and has not been examined. CRISPR technology could be utilized to obtain a *lof1* null mutant.

4) Further exploration of *LOF1* function with *HD-Zip III* genes. Due to time constraints and genetic linkage between *PHB* and *ER* as well as *PHV*, *LOF1*, and *CNA*, the *phb phv er*, *phb cna er*, and *phv cna er* triple mutants were not evaluated for changes in plant architecture. Additionally, double mutants containing *lof1-1* and individual *HD-Zip III* mutations (besides *phb*) could be explored in the future. Examining all of these genotypes would make the contributions of *PHB*, *PHV*, *CNA*, and *LOF1* in shoot architecture clearer.

References

Aida M, Ishida T, Fukaki H, Fujisawa H, Tasaka M. 1997. Genes involved in organ separation in *Arabidopsis*: an analysis of the *cup-shaped cotyledon* mutant. Plant Cell **9**, 841–857.

Bell EM, Lin W, Husbands AY, Yu L, Jaganatha V, Jablonska B, Mangeon A, Neff MM, Girke T, Springer PS. 2012. *Arabidopsis* lateral organ boundaries negatively regulates brassinosteroid accumulation to limit growth in organ boundaries. Proceedings of the National Academy of Sciences USA **109**, 21146–21151.

Bou-Torrent J, Salla-Martret M, Brandt R, Musielak T, Palauqui JC, Martínez-García JF, Wenkel S. 2012. ATHB4 and HAT3, two class II HD-ZIP transcription factors, control leaf development in Arabidopsis. Plant Signaling and Behavior **7**.

Cappadocia L, Maréchal A, Parent JS, Lepage É, Sygusch J, Brisson N. 2010. Crystal structures of DNA-whirly complexes and their role in *Arabidopsis* organelle genome repair. Plant Cell **22**, 1849–1867.

Cappadocia L, Parent JS, Zampini É, Lepage É, Sygusch J, Brisson N. 2012. A conserved lysine residue of plant Whirly proteins is necessary for higher order protein assembly and protection against DNA damage. Nucleic Acids Research **40**, 258–269.

Ciarbelli AR, Ciolfi A, Salvucci S, Ruzza V, Possenti M, Carabelli M, Fruscalzo A, Sessa G, Morelli G, Ruberti I. 2008. The Arabidopsis homeodomain-leucine zipper II gene family: Diversity and redundancy. Plant Molecular Biology **68**, 465–478.

Colling J, Tohge T, De Clercq R, Brunoud G, Vernoux T, Fernie AR, Makunga NP, Goossens A, Pauwels L. 2015. Overexpression of the *Arabidopsis thaliana* signalling peptide TAXIMIN1 affects lateral organ development. Journal of Experimental Botany **66**, 5337–5349.

Desveaux D, Allard J, Brisson N, Sygusch J. 2002. A new family of plant transcription factors displays a novel ssDNA-binding surface. Nature Structural Biology **9**, 512–517.

Desveaux D, Despres C, Joyeux A, Subramaniam R, Brisson N. 2000. PBF-2 is a novel single-stranded DNA binding factor implicated in *PR-10a* gene activation in potato. Plant Cell **12**, 1477–1489.

Desveaux D, Subramaniam R, Després C, Mess JN, Lévesque C, Fobert PR, Dangl JL, Brisson N. 2004. A 'Whirly' transcription factor is required for salicylic acid-dependent disease resistance in *Arabidopsis*. Developmental Cell **6**, 229–240.

Emery JF, Floyd SK, Alvarez J, Eshed Y, Hawker NP, Izhaki A, Baum SF, Bowman JL. 2003. Radial patterning of *Arabidopsis* shoots by class III HD-ZIP and KANADI genes. Current Biology **13**, 1768–1774.

Evans MMS, Barton MK. 2002. Genetics of angiosperm shoot apical meristem development. Annual Review of Plant Physiology and Plant Molecular Biology **48**, 673–701.

Fahlgren N, Montgomery TA, Howell MD, Allen E, Dvorak SK, Alexander AL, Carrington JC. 2006. Regulation of *AUXIN RESPONSE FACTOR3* by *TAS3* ta-siRNA affects developmental timing and patterning in *Arabidopsis*. Current Biology **16**, 939–944.

Finlayson SA, Krishnareddy SR, Kebrom TH, Casal JJ. 2010. Phytochrome regulation of branching in Arabidopsis. Plant Physiology **152**, 1914–1927.

Foyer CH, Karpinska B, Krupinska K. 2014. The functions of WHIRLY1 and REDOXRESPONSIVE TRANSCRIPTION FACTOR 1 in cross tolerance responses in plants: A hypothesis. Philosophical Transactions of the Royal Society **369**, 15–17.

Glaser E, Soll J. 2004. Targeting signals and import machinery of plastids and plant mitochondria. Molecular Biology and Biotechnology of Plant Organelles.385–417.

Gonzalez A, Zhao M, Leavitt JM, Lloyd AM. 2008. Regulation of the anthocyanin biosynthetic pathway by the TTG1/bHLH/Myb transcriptional complex in Arabidopsis seedlings. Plant Journal **53**, 814–827.

Grabowski E, Miao Y, Mulisch M, Krupinska K. 2008. Single-stranded DNA-binding protein Whirly1 in barley leaves is located in plastids and the nucleus of the same cell. Plant Physiology **147**, 1800–1804.

Guan Z, Wang W, Yu X, Lin W, Miao Y. 2018. Comparative proteomic analysis of coregulation of CIPK14 and WHIRLY1/3 mediated pale yellowing of leaves in *Arabidopsis*. International Journal of Molecular Sciences **19**, 1-22.

Hussey G. 1971. Cell division and expansion and resultant tissue tensions in the shoot apex during the formation of a leaf primordium in the tomato. Journal of Experimental Botany **22**, 702–714.

Kempin SA, Savidge B, Yanofsky MF. 1995. Molecular basis of the cauliflower phenotype in Arabidopsis. Science **267**, 522–525.

Kim HS, Kim SJ, Abbasi N, Bressan RA, Yun DJ, Yoo SD, Kwon SY, Choi SB. 2010. The DOF transcription factor Dof5.1 influences leaf axial patterning by promoting *Revoluta* transcription in Arabidopsis. Plant Journal **64**, 524–535.

Kim Y-S, Kim S-G, Lee M, Lee I, Park H-Y, Seo PJ, Jung J-H, Kwon E-J, Suh SW, Paek K-H, Park C-M. 2008. HD-ZIP III activity is modulated by competitive inhibitors via a feedback loop in *Arabidopsis* shoot apical meristem development. Plant Cell **20**, 920–933.

Krause K, Herrmann U, Fuss J, Miao Y, Krupinska K. 2009. Whirly proteins as communicators between plant organelles and the nucleus? Endocytobiosis and Cell Research **19**, 51–62.

Krause K, Kilbienski I, Mulisch M, Rödiger A, Schäfer A, Krupinska K. 2005. DNA-binding proteins of the Whirly family in *Arabidopsis thaliana* are targeted to the organelles. FEBS Letters **579**, 3707–3712.

Lee D-K, Geisler M, Springer PS. 2009. *LATERAL ORGAN FUSION1* and *LATERAL ORGAN FUSION2* function in lateral organ separation and axillary meristem formation in *Arabidopsis*. Development **136**, 2423–2432.

Magnani E, Barton MK. 2011. A Per-ARNT-sim-like sensor domain uniquely regulates the activity of the homeodomain leucine zipper transcription factor REVOLUTA in *Arabidopsis*. Plant Cell **23**, 567–582.

Mallory AC, Dugas D V., Bartel DP, Bartel B. 2004. MicroRNA regulation of NAC-domain targets is required for proper formation and separation of adjacent embryonic, vegatative, and floral organs. Current Biology **14**, 1035–1046.

Maréchal A, Parent J-S, Véronneau-Lafortune F, Joyeux A, Lang BF, Brisson N. 2009. Whirly proteins maintain plastid genome stability in *Arabidopsis*. Proceedings of the National Academy of Sciences USA **106**, 14693–14698.

Matsuo M, Johnson JM, Hieno A, Tokizawa M, Nomoto M, Tada Y, Godfrey R, Obokata J, Sherameti I, Yamamoto YY, Böhmer F-D, Oelmüller R. 2015. High REDOX RESPONSIVE TRANSCRIPTION FACTOR1 levels result in accumulation of reactive oxygen species in *Arabidopsis thaliana* shoots and roots. Molecular Plant **8**, 1253–1273.

McConnell JR, Barton MK. 1998. Leaf polarity and meristem formation in *Arabidopsis*. Development **125**, 2935–2942.

McConnell JR, Emery J, Eshed Y, Bao N, Bowman J, Barton MK. 2001. Role of *PHABULOSA* and *PHAVOLUTA* in determining radial patterning in shoots. Nature **411**, 709–713.

Merelo P, Ram H, Caggiano MP, Ohno C, Ott F, Straub D, Graeff M, Cho SK, Yang SW, Wenkel S, Heisler MG. 2016. Regulation of *MIR165/166* by class II and class III homeodomain leucine zipper proteins establishes leaf polarity. Proceedings of the National Academy of Sciences USA **113**, 11973–11978.

Prelich G. 2012. Gene overexpression: Uses, mechanisms, and interpretation. Genetics **190**, 841–854.

Prigge MJ, Otsuga D, Alonso JM, Ecker JR, Drews GN, Clark SE. 2005. Class III homeodomain-leucine zipper gene family members have overlapping, antagonistic, and distinct roles in Arabidopsis development. Plant Cell **17**, 61–76.

Prikryl J, Watkins KP, Friso G, van Wijk KJ, Barkan A. 2008. A member of the Whirly family is a multifunctional RNA- and DNA-binding protein that is essential for chloroplast biogenesis. Nucleic Acids Research **36**, 5152–5165.

Rowan DD, Cao M, Lin-Wang K, Cooney JM, Jensen DJ, Austin PT, Hunt MB, Norling C, Hellens RP, Schaffer RJ, Allan AC. 2009. Environmental regulation of leaf colour in red *35S:PAP1 Arabidopsis thaliana*. New Phytologist **182**, 102–115.

Serrano-Cartagena J, Candela H, Robles P, Ponce MR, Perez-Perez JM, Piqueras P, Micol JL. 2000. Genetic analysis of *incurvata* mutants reveals three independent genetic operations at work in Arabidopsis leaf morphogenesis. Genetics **156**, 1363–1377.

Sessa G, Carabelli M, Sassi M, Ciolfi A, Possenti M, Mittempergher F, Becker J, Morelli G, Ruberti I. 2005. A dynamic balance between gene activation and repression regulates the shade avoidance response in *Arabidopsis*. Genes & Development **19**, 2811–2815.

Sessa G, Steindler C, Morelli G, Ruberti I. 1998. The *Arabidopsis Athb-8*, *-9* and *-14* genes are members of a small gene family coding for highly related HD-ZIP proteins. Plant Molecular Biology **38**, 609–622.

Sorin C, Salla-Martret M, Bou-Torrent J, Roig-Villanova I, Martínez-García JF. 2009. ATHB4, a regulator of shade avoidance, modulates hormone response in Arabidopsis seedlings. Plant Journal **59**, 266–277.

Ströher E, Dietz KJ. 2008. The dynamic thiol-disulphide redox proteome of the *Arabidopsis thaliana* chloroplast as revealed by differential electrophoretic mobility. Physiologia Plantarum **133**, 566–583.

Tian Y, Sacharz J, Ware MA, Zhang H, Ruban AV. 2017. Effects of periodic photoinhibitory light exposure on physiology and productivity of Arabidopsis plants grown under low light. Journal of Experimental Botany **68**, 4249–4262.

Turchi L, Carabelli M, Ruzza V, Possenti M, Sassi M, Peñalosa A, Sessa G, Salvi S, Forte V, Morelli G, Ruberti I. 2013. *Arabidopsis* HD-Zip II transcription factors control apical embryo development and meristem function. Development **140**, 2118–2129.

Weigel D, Jürgens G. 2002. Stem cells that make stems. Nature **415**, 751–754.

Wenkel S, Emery J, Hou BH, Evans MMS, Barton MK. 2007. A feedback regulatory module formed by LITTLE ZIPPER and HD-ZIPIII genes. Plant Cell **19**, 3379–3390.

Wortman JR, Haas BJ, Hannick LI, Smith RK, Maiti R, Ronning CM, Chan AP, Yu C, Ayele M, Whitelaw CA, White OR, Town CD. 2003. Annotation of the Arabidopsis genome. Plant Physiology **132**, 461–468.

Xiong JY, Lai CX, Qu Z, Yang XY, Qin XH, Liu GQ. 2009. Recruitment of AtWHY1 and AtWHY3 by a distal element upstream of the kinesin gene *AtKP1* to mediate transcriptional repression. Plant Molecular Biology **71**, 437–449.

Zimmermann IM, Heim MA, Weisshaar B, Uhrig JF. 2004. Comprehensive identification of *Arabidopsis thaliana* MYB transcription factors interacting with R/B-like BHLH proteins. Plant Journal **40**, 22–34.